HAW HAMBURG

BACHELOR THESIS

# Redefinition of current display colour spaces based on CIE 2015 colour-matching functions

Submitted: 2nd March 2026

Johannes Grieb

Supervising examiner: Prof. Dr.-Ing. Carolin Liedtke

Second examiner: Dipl.-Ing. (FH) Matthias Wilkens

**HOCHSCHULE FÜR ANGEWANDTE WISSENSCHAFTEN HAMBURG**

Hamburg University of Applied Sciences

Department Media Technology

Finkenau 35

22081 Hamburg

# Abstract

Colour-matching between different modern display technologies does not always yield acceptable results when using CIE 1931 colour-matching functions. For different colour-matching functions, the existing colour spaces used in video technology need to be redefined with different CIE xy chromaticity coordinates. This thesis describes a method for redefining typical colour spaces ITU-R BT.709 and ITU-R BT.2020, based on the CIE 170-2:2015 2° colour-matching functions. The results are a replacement for the existing CIE xy chromaticity coordinates defining the red, green and blue primary colours. The primary colours are redefined by using measurements of CRT displays. The typical D65 white point is defined by the spectrum of daylight. The precision of the resulting colour spaces falls within the range required for reference displays, but can be further improved with additional measured data.

These redefined colour spaces can be used for calibration of modern displays with a spectroradiometer, as long as CIE 2015 based colour-matching functions are implemented in the used software. The selected process for redefinition maintains compatibility for existing content and signal processing.

# Zusammenfassung

Die Farbanpassung zwischen verschiedenen modernen Displaytechnologien führt bei Verwendung der CIE 1931 Spektralwertfunktionen nicht immer zu akzeptablen Ergebnissen. Für andere Spektralwertfunktionen müssen die bestehenden, in der Videotechnologie verwendeten, Farbräume mit unterschiedlichen CIE xy Koordinaten neu definiert werden. Diese Arbeit beschreibt eine Methode zur Neudefinition typischer Farbräume ITU-R BT.709 und ITU-R BT.2020 auf Grundlage der CIE 170-2:2015 2° Spektralwertfunktionen. Die Ergebnisse ersetzen die bestehenden CIE xy Koordinaten, die die Primärfarben Rot, Grün und Blau definieren. Die Primärfarben werden anhand von Messungen an CRT-Bildschirmen neu definiert. Der typische Weißpunkt D65 wird durch das Spektrum des Tageslichts definiert. Die Genauigkeit der resultierenden Farbräume liegt innerhalb des für Referenzbildschirme erforderlichen Bereichs, kann jedoch mit zusätzlichen Messdaten weiter verbessert werden.

Diese neu definierten Farbräume können für die Kalibrierung moderner Displays mit einem Spektrometer verwendet werden, sofern in der verwendeten Software die CIE 2015 basierten Spektralwertfunktionen implementiert sind. Der gewählte Prozess für die neue Definition gewährleistet die Kompatibilität mit bestehenden Inhalten und bestehender Signalverarbeitung.

# Acknowledgements

I wish to acknowledge all the support that made this thesis possible.

Thanks to Michael Finn (NDR) for the first experimental measurements of a Sony BVM CRT and the actual EBU CRT used; thanks to Dylan Owens for sending the US version of the CRT; and thanks to Konica Minolta Sensing Europe for providing the CS-2000 spectroradiometer.

Thanks to everyone who provided data. Lihao Xu needs to be noted here for providing a massive spectral dataset.

Thanks to Leonie Krüger and Katrin Blake for proofreading.

I would like to thank my thesis advisor, Carolin Liedtke, for all the feedback and support.

Last, and most important, thanks to Matthias Wilkens for being a sparring partner and always pushing me to think more than needed.

# Table of contents

# 1. Preface

For accurate prediction of how colours are perceived by the human eye, colour-matching functions (CMFs) are required. A complex spectral light source can be reduced to a three-dimensional value, for example, LMS or XYZ. Due to metamerism, different spectral light sources appear as the same colour to the human eye as long as their three-dimensional reduced values are identical. When different spectral light sources are used to generate a defined colour perception, these CMFs need to be as accurate as possible.

In video technology, especially in display technology, the CIE 1931 2° CMFs are widely used. All colour spaces used in video technology are defined by values based on the CIE 1931 2° standard observer.

As the CIE 1931 2° CMFs do not perfectly match the human eye, the resulting colour rendering for new display technologies is also not perfect, if the display fully complies with existing standards. In some cases, vendors attempt to compensate for this by adding technology-specific offsets to the standard values (e.g., Sony OLED displays).

A colourimeter or spectroradiometer can perfectly match displays as long as they use the same spectral light sources. Therefore, colour matching of CRT displays is easy. Nowadays, multiple display technologies coexist in studios, which can render a spectroradiometer useless for calibration.

With CIE 2015, newer, more accurate, and well-standardized colour-matching functions are available. This thesis examines how existing colour spaces — for example, those defined in ITU-R BT.709 (BT.709) or ITU-R BT.2020 (BT.2020) — can be redefined by using the CIE 2015 based colour-matching functions. One of the main objectives is to remain fully compatible with existing video signals and recorded video. The resulting approach should be easy to implement for modern displays. A more accurate set of colour-matching functions may bring back meaningful results for display calibration with a spectroradiometer.

This thesis will not attempt to determine “the best” set of colour-matching functions. The method used should be transferable to different CMFs.

# 2. Introduction

## 2.1. Colour space

In video technology, a colour space defines a set of three primary colours, red, green and blue, whose combined intensities can be linearly mixed to represent other colours. The primary colours are usually specified as CIE xy chromaticity coordinates and can be shown in the well-known CIE 1931 xy chromaticity diagram. Three colour spaces used in video technology can be seen in Figure 1. In addition to the three colours, a white point is specified. With this white point, the required luminance ratio needed to mix the white point can be calculated.

When a colour is represented by a red, green and blue (RGB) video signal, a corresponding colour space is needed to map the signal to physical colours.

Modern displays or LED Screens (Figure 2) have a native colour space, defined by the light-emitting and filtering elements built in. The native colour space of a display does not need to be equal to the colour space which defines an RGB video signal. For rendering the correct physical colour, a linear transformation matrix is used to obtain the required mix of native colours.

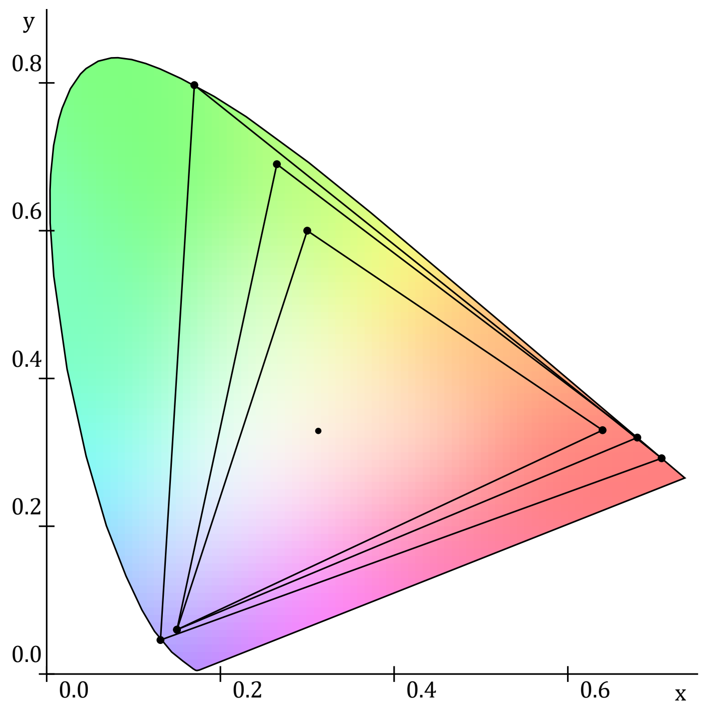


*Figure 1: Typical colour spaces for video technology in CIE 1931 diagram. BT.2020 (largest), DCI-P3, and BT.709 (smallest), including D65 white point. Background colours are only for reference, as no display or print is capable of showing all visible colours inside the specular locus.*

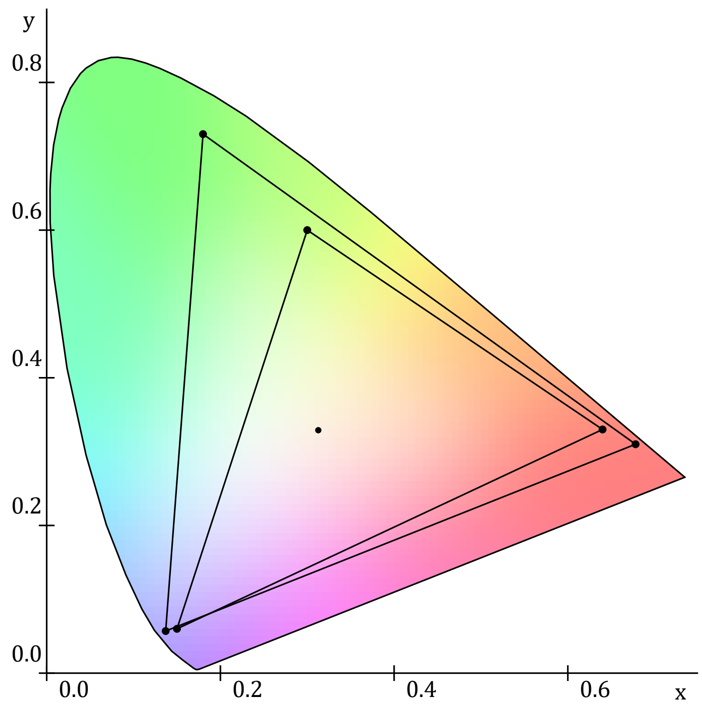


*Figure 2: Native colour space of a typical LED Screen compared to BT.709 (smaller).*

With different linear transformation matrices, a modern display can be switched to accurately show video signals which refer to different colour spaces, without the need to change the actual primary colours.

With physical light sources, as in a display or LED screen, the colours which can be mixed are limited to the inside of the resulting triangle formed by the primary chromaticities in the CIE xy diagram. All colours reproducible with the physical built-in primaries are contained within the display gamut.

For displays or light fixtures with only three colours, it is not possible to mix all visible colours (in theory, an infinite number of primaries is needed [Wyszecki & Stiles, 2000]). However, displays with more than three light sources for extending their native colour space are uncommon at the time of writing, and having more than three primaries introduces additional complexity in calibration and signal processing.

As a display is limited by a colour gamut, this may not be true for all video signals. If a video signal or a file allows negative values for the red, green, and blue channels, as for example with floating point values (often used when processing images on a GPU) or to a certain extent with narrow range video signals [ITU-R BT.1361], colours outside the colour space can be represented as well.

In theory, it is possible to define colour spaces with more than three primary colours. As to Grassmann's first law, described in Section 2.3, three primary chromaticities, and allowing negative values for their representation, are enough to represent all visible colours. With only non-negative values, larger colour spaces, for example, ACES AP0, can be defined (with three primaries) to represent all visible colours.

The term "colour space" is often used to refer to more than just colour primaries and a white point. The OpenColorIO (OCIO) framework, for example, defines everything which is needed for converting images, including transfer functions, as a colour space. This thesis uses the term colour space as primary colours and a white point only, ignoring other parameters needed for a complete interpretation of image or signal data.

## 2.2. Spectral power distribution

A physical light source is defined by the energy emitted for each wavelength in the visible spectrum. The exact spectral power distribution (SPD) fully determines how the luminance and colour of the light source appear to the human eye.

Light sources may be self-illuminating objects or reflectors that modify the SPD of the original light source.

To fully reproduce any given SPD of light sources, an array of ideally sub-nanometre-spaced monochromatic light sources is required. At present, however, no commercially available display technology is capable of synthesizing such arbitrary SPDs with sufficient spectral resolution. Consequently, all current displays approximate target illuminants using a limited number of narrowband or broadband primaries.

## 2.3. Metamerism

As stated in Grassmann's first law, the perceptual appearance of a light source can be determined solely by a three-dimensional value. Consequently, it is neither necessary nor practical to reproduce the exact SPD of light sources in order to achieve an accurate visual match for the human visual system.

Displays can therefore recreate the appearance of diverse light sources and objects by mixing energies of three independent primary colours.

When light sources have different SPDs but appear equal to the human visual system, they are metamer.

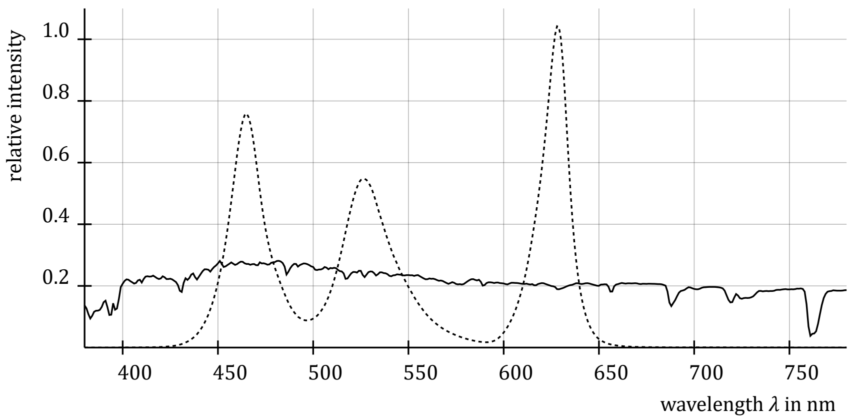


*Figure 3: SPDs of an LED Screen (dashed) and foggy sky in Hamburg (solid), both result in the same visual appearance (D65 white) and are therefore metamer.*

Due to metamerism, it is possible to reduce a physical light source with a complex spectral power distribution to a three-dimensional representation, such as red, green, blue (RGB) or the cone-response-based long, medium, short (LMS) as used for the human visual system. Therefore, within limits, a display does not need to duplicate the physical characteristics of a light source or object. The appearance can be reproduced by the mixture of three primary colourants [Wyszecki & Stiles, 2000, p. 185].

However, this three-dimensional representation is inherently lossy. It is not possible to reconstruct the original SPD from a three-value representation. Multiple different SPDs may map to identical three-value representations, and thus, while metamerism enables colour reproduction, it does not permit spectral reconstruction.

## 2.4. Colour-matching functions

For reducing the SPD of a physical light source to a three-value representation, colour-matching functions (CMFs) are used.

CMFs consist of a set of three spectral sensitivity functions, mostly represented in the form of discrete numbers. These functions, applied to an SPD, produce three values sufficient to describe the appearance of a light source. As soon as two light sources produce the same values, they are metamer and therefore appear identical.

$$
\begin{aligned}
\int_\lambda P_{\text{scene}}(\lambda)\ \bar{r}(\lambda)\ d(\lambda) &= \boldsymbol{R} = \int_\lambda P_{\text{display}}(\lambda)\ \bar{r}(\lambda)\ d(\lambda) \\
\int_\lambda P_{\text{scene}}(\lambda)\ \bar{g}(\lambda)\ d(\lambda) &= \boldsymbol{G} = \int_\lambda P_{\text{display}}(\lambda)\ \bar{g}(\lambda)\ d(\lambda) \\
\int_\lambda P_{\text{scene}}(\lambda)\ \bar{b}(\lambda)\ d(\lambda) &= \boldsymbol{B} = \int_\lambda P_{\text{display}}(\lambda)\ \bar{b}(\lambda)\ d(\lambda)
\end{aligned}
$$

*Equation 1: General equations for CMFs modified for display application. [Wyszecki & Stiles, 2000, p. 184]*

Any visual stimulus, regardless of its actual spectral power distribution $P_{\text{scene}}(\lambda)$, can be reduced to a three-dimensional value $[R, G, B]$ by use of the CMFs. On the display side, a different spectral power distribution $P_{\text{display}}(\lambda)$ is synthesised through additive mixing of the available three primary light sources. As long as the resulting spectral power distribution can be reduced to the same $[R, G, B]$ value, the appearance for the human eye is identical. Two displays with different technologies, such as a CCFL backlight or OLED, may also appear identical if the CMFs result in the same [R,G,B].

Except in cases where the desired chromaticity or luminance exceeds the display's precision, native gamut, or its dynamic range (beyond maximum brightness or below the achievable black level), an accurate match can always be achieved by carefully adjusting the intensities of the primary colours.

In practice, the integration is replaced by summations by using a table of colour-matching properties $\bar{r}(\lambda), \bar{g}(\lambda), \bar{b}(\lambda)$ and the measured discrete values for the SPD of an object or display.

The colour-matching properties $\bar{r}(\lambda), \bar{g}(\lambda), \bar{b}(\lambda)$ used in the CMFs need to precisely match the human visual system under given viewing conditions. While a set of CMFs can transform the SPD to any three-dimensional value represented by a colour space, the CMFs used in video systems defined by CIE typically use $\bar{x}(\lambda), \bar{y}(\lambda), \bar{z}(\lambda)$ properties to transform to the CIE 1931 XYZ tristimulus values. These CIE XYZ tristimulus values separate the luminance of a stimulus, as described in Section 3.1.

There is, however, no single set of CMFs that can accurately model human colour perception across all viewing conditions and individual humans simultaneously. The resulting prediction, if visual stimuli from different display technologies appear identical, can only be as precise as the CMFs employed.

## 2.5. Reasons for new colour spaces

As most, if not all, colour spaces used in video technology are specified by chromaticity coordinates for red, green, blue and white, which refer to the CIE 1931 standard observer CMFs described in Section 3.1. The colour-matching quality achieved with these colour spaces for display calibration can only be as precise as the underlying colour-matching properties.

As early as 1949, Judd described limitations of the CIE 1931 standard observer, particularly for light sources with differences at short wavelengths [Judd, 1949]. Since then, other research has consistently demonstrated inaccuracies.

In some circumstances, “traditional colour-matching functions may completely fail” [Thornton, 1998, p. 403] compared to visual colour-matching. Newer data is also pointing out that the largest error seems to be in a wavelength range of 380 nm to 500 nm and therefore has a larger effect on 6504 K white points, typically used for displays, compared to tungsten sources [Polster, 2013, p. 71].

At the time of writing, however, different colour-matching functions are available that may give better results. For example, the International Commission on Illumination (CIE) published cone-fundamental-based spectral tristimulus values for a 2° field size [CIE 170-2:2015], further referred to as CIE 2015, which can replace the industry standard CIE 1931 2° standard observer CMFs.

As chromaticity coordinates depend on a set of CMFs, any physical colour, defined with the exact spectral power distribution, will therefore result in different chromaticity coordinates for different observers (CMFs).

A fundamental consequence of this dependency is that chromaticity coordinates, which define a colour space, are not absolute physical descriptors but observer-dependent representations and cannot be reused when updating the CMFs.

When colour TVs were introduced, the spectral differences between different displays were very small, as they all used the same principle of generating coloured light. Therefore, colour-matching functions for displays were used to measure colours with weak metamerism, which allows more imperfection for CMFs while still resulting in a good visual match.

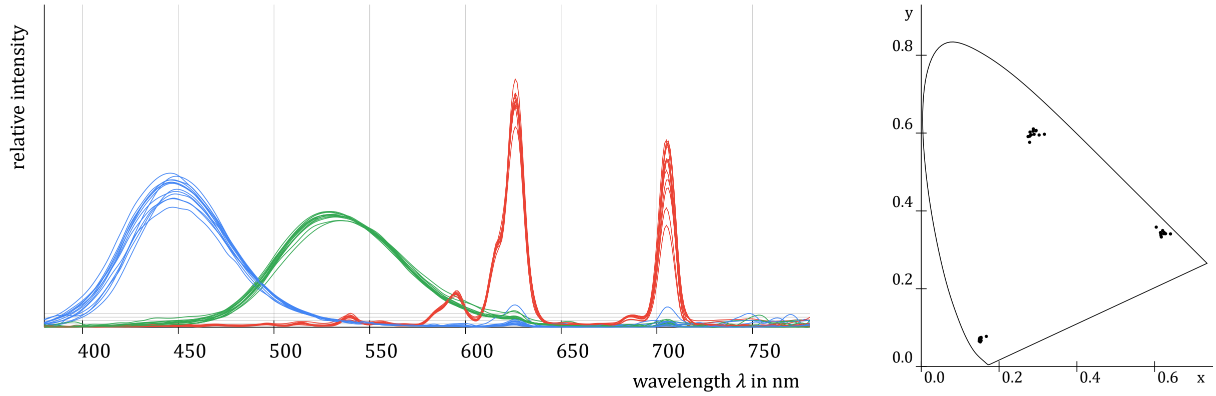


*Figure 4: Different CRT displays measured by Golz and MacLeod (2003).*

The CRT displays in Figure 4 do have different CIE xy chromaticity coordinates, but the SPDs are very similar. Therefore, colour-matching (at least for white) yields good results even with insufficient quality CMFs.

Today, as the existence of CRT TVs fades, there are multiple successor technologies for generating light in displays. The different technologies in modern displays result in larger differences for the spectral power distributions, as seen in Figure 5.

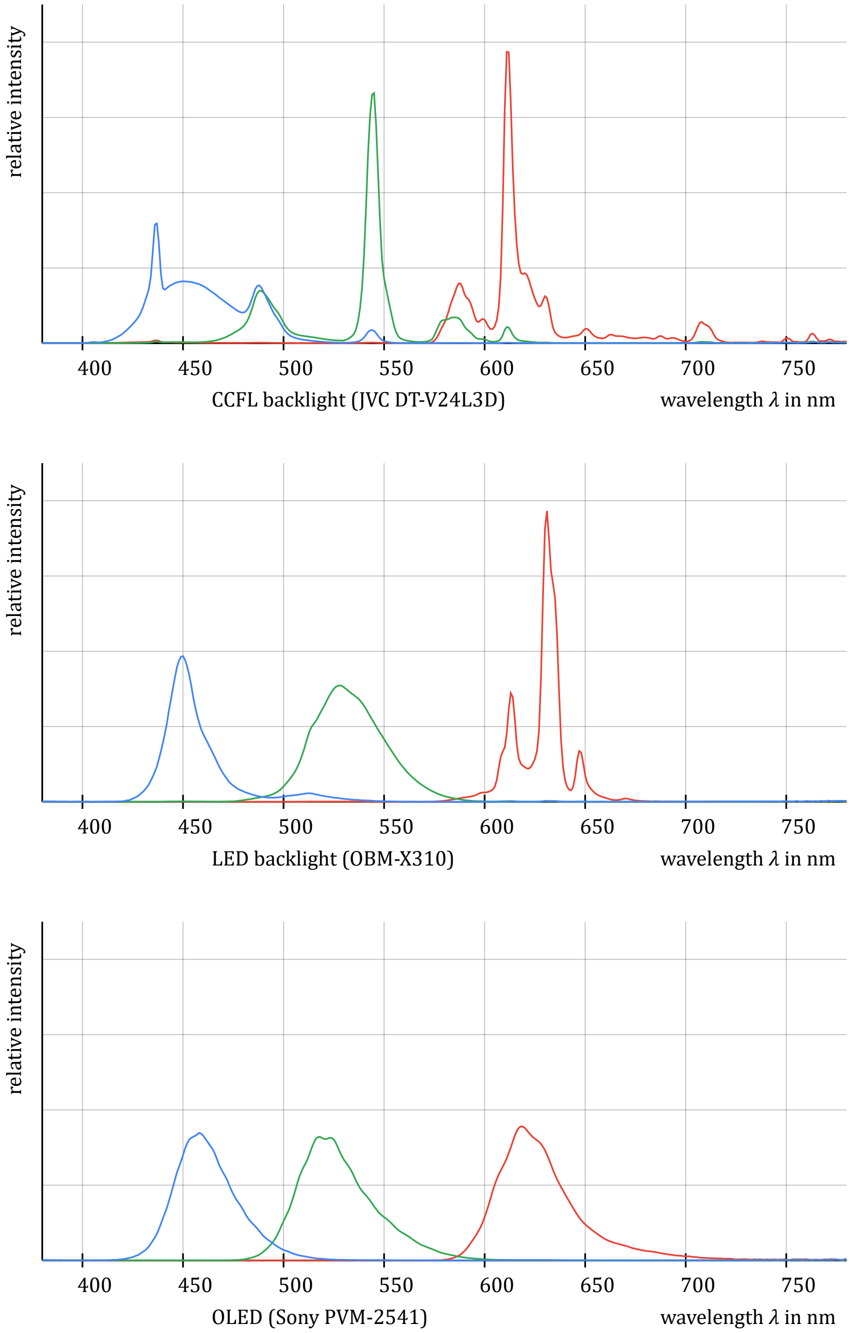


*Figure 5: SPDs of different display technologies.*

These light sources of modern displays can be described as strong metameric. Thornton (1998) describes these errors between visually matched colours and colour-matching by CIE 1931 as more problematic, as soon as there are larger spectral differences.

With all these different display technologies, in some cases directly beneath each other, it is desirable to match all of them as closely as possible by using actual measurement devices.

For the ITU-R BT.2020 colour space, chromaticity coordinates were selected by monochromatic light sources. 467nm for the blue primary colour, 532nm for green, and 630nm for red [ITU-R BT.2246]. The corresponding CIE XYZ values are directly available in the CIE 1931 CMFs properties table. The resulting CIE xy chromaticity coordinates in the CIE diagram are given in the standard documents.

Consequently, the SPDs for the BT.2020 colour space primaries are available. For monochromatic light, the CIE 2015 based XYZ tristimulus values can be read as $\bar{x}(\lambda)$, $\bar{y}(\lambda)$ and $\bar{z}(\lambda)$ from the tables given by CIE (Table 1).

| **Wave-lenght $\boldsymbol{\lambda}$(nm)** | **CIE 2015 2° colour-matching functions** | | | **chromaticity coordinates** | |
|---|---|---|---|---|---|
| | $\bar{x}(\lambda)$ | $\bar{y}(\lambda)$ | $\bar{z}(\lambda)$ | $x(\lambda)$ | $y(\lambda)$ |
| 467 | 2.075619E-01 | 1.155111E-01 | 1.370094E+00 | 0.122588 | 0.0682219 |
| 532 | 2.045085E-01 | 8.783061E-01 | 2.046415E-02 | 0.185364 | 0.796087 |
| 630 | 6.924717E-01 | 2.980865E-01 | 0.000000E+00 | 0.699072 | 0.300928 |

*Table 1: CIE 2015 table reduced to the wavelengths used to define BT.2020.*

In Figure 6, the different resulting chromaticity coordinates are shown. Physically defined light sources yield different chromaticity coordinates. Therefore, keeping the existing chromaticity coordinates for colour spaces and just replacing CMFs will result in wrong colour rendering.

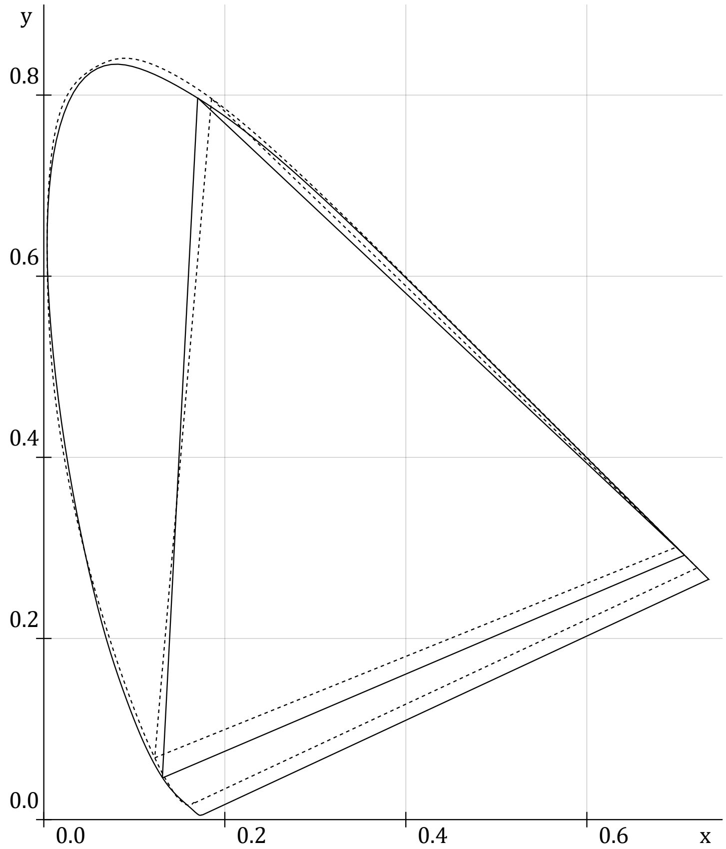


*Figure 6: Comparison of CIE 1931 2° specular locus (solid line) and CIE 2015 2° specular locus (dashed line), including the corresponding monochromatic chromaticity coordinates derived from BT.2020.*

The ITU-R BT.2020 colour space is an example, with SPDs available. In the case of ITU-R BT.709 and Digital Cinema Initiatives - Protocol 3 (DCI-P3), the SPDs are not readily available. For Academy Color Encoding System's Primaries 0 (ACES AP0), it is not possible to create SPDs as the primaries are far beyond the specular locus, and do not, by intention, have a physical representation.

Without the definition of new chromaticity coordinates, usage of the CIE 2015 based CMFs in practice is very limited. For directly calculating a CIE 2015 based chromaticity coordinate, out of a BT.709 based video signal, a redefinition for the primary colours of BT.709 is required.

> *“ With a slight sense of drama we can say that the CIE 1931 standard is broken and no longer sufficient for the new technologies we face today, but luckily there is a potential alternative in the newer, improved CIE 2006 and 2015 standards. This realization is incredibly problematic though as our entire industry is built on the underlying maths of this standard. Moving to a new standard, even if we knew what that standard should be, isn’t a trivial thing. It would require all software and*

> *hardware manufacturers to strip down all the mathematics in their products and essentially start from scratch. "*
>
> [*Metamerism Experts' Day Debrief*, IMAGO, 2025]

One of the conclusions of the Metamerism Experts' Day hosted by Charles Poynton in 2024 is that replacing CIE 1931 in the media industry is like starting from scratch. Therefore, redefined colour spaces should be compatible with existing systems.

This leads to the primary objectives of this thesis for redefining existing colour spaces as follows:

- New chromaticity coordinates should be defined using new (better) colour-matching functions.
- The redefined colour spaces should enable better calibration of displays with different technologies.
- Full compatibility with existing video signals and recorded material should be preserved when using the redefined colour spaces. To ensure implementation simplicity, the new chromaticity coordinates should be deployable on the display side without further changes, neither for products which process or convert colour spaces nor existing cameras.

## 2.6. Assumptions

In this thesis, video signals are simplified as the pure transport of tristimulus colour samples represented as three-dimensional vectors (R, G, B). For simplicity, the effects of finite quantization precision (e.g. 8-bit or 10-bit encoding), non-linear transfer functions, luminance separated signals, and chroma subsampling (4:2:2) are ignored.

Most video transfer systems use a non-linear opto-optical transfer function (OOTF). In some cases, these OOTFs are designed to have an effect on saturation and hue of colours [ITU-R BT.2390], not only contrast. Therefore, an original colour seen in a scene by an ideal camera is not expected to always be equal, when rendered on a display. This complexity is ignored in this thesis. A video system with an ideal camera is seen as linear transport that does not change the contrast appearance or luminance of an image.

Like the human eye, a camera as well has its own CMFs, which are physically built into the beam splitter or filters for the Bayer Pattern. These filters cannot be easily designed to completely match a given set of CMFs. In this thesis, a camera is treated as an ideal camera with a perfect spectral response. This means it copies the used CMFs precisely. This leads to video signals and recorded images with a perfect match for the original scene.

Colour spaces usually refer to a complete system. Both BT.709 and BT.2020 specify luminances for displays. For isolated colour spaces, the luminance of a resulting image is not important and can be normalized. Luminances of the primary colourants are directly tied to the corresponding white point. Changes in how colours appear to the human eye due to different luminance levels are ignored.

While this thesis focuses specifically on broadcast television systems, the mathematical framework and methodology can be transferred to computer displays, cinema applications, studio or event lighting, and other applications relying on high-quality colour reproduction.

# 3. Standard definitions used

## 3.1. CIE 1931 standard colourimetric observer

The industry standard colour-matching functions for colourimetry are defined by the CIE 1931 standard colourimetric observer.

> *“ The data that went into the tristimulus functions was based on measurements by two British researchers in 1929 and 1930: John Guild (of the British National Physics Laboratory) and W. David Wright (of the University of London). Between the two of these researchers, 17 men were recruited to match spectral colors with their two respective colorimeters. ”*
>
> [*Recommended methods for conducting human factors experiments on the subjective evaluation of colour rendition*, Seymour, 2026]

Since 1971, the properties $\bar{x}(\lambda)$, $\bar{y}(\lambda)$ and $\bar{z}(\lambda)$ for the colour-matching functions are available from $\lambda = 360$ nm up to $830$ nm in $1$ nm intervals. These updated tables are linear interpolated and slightly smoothed versions of the original data. The numeric precision of seven figures, in practice, is considered numerically exact even if the experimental data cannot justify this accuracy. [Wyszecki & Stiles, 2000, pp. 131 ff]. The full table can be found in Appendix A.5.

The $\bar{x}(\lambda)$, $\bar{y}(\lambda)$ and $\bar{z}(\lambda)$ properties do not hold direct experimental or measured data. The tables given are derived from experimental data instead. The $\bar{y}(\lambda)$ function given by the CIE 1931 standard observer coincides with the photopic luminous efficiency function $V(\lambda)$ from 1924. This ensures that the resulting Y of the CIE XYZ tristimulus values represents the luminance of a visual stimulus. The separated colour is often presented as a transformed CIE xy chromaticity coordinate. Maths for conversion is available in Equation 24 of Section 7.9.

The CIE 1931 standard observer refers to a 2° field of view. Therefore, it is applicable while concentrating on small image details.

As already introduced in Section 2.5, CIE 1931 is not perfectly suitable to accurately model the human visual system. Especially when applied to narrowband light sources in modern displays (e.g. QD-OLED, LED, or monochromatic laser), deficiencies in the CIE 1931 standard observer colour-matching functions are revealed.

To mitigate these differences in the appearance for white on displays which are calibrated to the same CIE 1931 based xy chromaticity coordinates, display manufacturers implement vendor-specific solutions.

> *" ... when matching colours between a CRT and other flat panel displays such as LCD (especially with LED backlight) or to OLED, viewer perception of the colour match may not agree, even though they are calibrated to the same xy chromaticity values. In the case of OLED, the colour looks greenish compared to CRT. "*
>
> [*Colour Matching Between OLED and CRT White Paper*, SONY, 2013]

Sony, for instance, is applying offsets to the CIE 1931 based xy chromaticity coordinates. For at least one type of display, the offsets are derived from modified colour-matching functions, researched by Judd in 1951 and improved by Vos in 1978. The modification is based on the slightly different $V_M(\lambda)$ adopted as CIE 1988 modified 2° spectral luminous efficiency function. The results were evaluated by Konica Minolta Optics and show a better, but not perfect, visual match. The same process, leading to different offsets by experimenting with different CMFs and empirical data, was repeated for other Sony displays as well [SONY, 2020].

## 3.2. CIE 170-2:2015

In 2006, the CIE published data sets including cone fundamentals $\bar{l}(\lambda)$, $\bar{m}(\lambda)$ and $\bar{s}(\lambda)$, basically colour-matching functions, for a 10° field of view and additionally a 2° field of view. Also provided is physiological data for different fields of view and different ages of the observer [CIE 170-1:2006]. With the data and mathematical framework given, it is possible to derive cone fundamentals $\bar{l}(\lambda)$, $\bar{m}(\lambda)$ and $\bar{s}(\lambda)$ for different viewing conditions. The resulting cone fundamentals model the response of the L-, M- and S-cones of the eye. The ability to represent luminance separated from chromaticity as the CIE 1931 based $\bar{x}(\lambda)$, $\bar{y}(\lambda)$, and $\bar{z}(\lambda)$ CMFs is missing with cone fundamentals.

As the photopic luminous efficiency function $V(\lambda)$ introduced in 1924 and used by the CIE 1931 observer seems not to be suited to model the human visual system, this function is not reused to convert the new cone fundamentals to a colourimetric and photometric $\bar{x}(\lambda)$, $\bar{y}(\lambda)$ and $\bar{z}(\lambda)$ observer.

With CIE 170-2:2015, the International Commission on Illumination published a method to recreate an optimal spectral luminous efficiency function $V_F(\lambda)$ based on the cone fundamentals from CIE 170-1:2006. With $V_F(\lambda)$, the resulting CMFs are given as $\bar{x}_F(\lambda)$, $\bar{y}_F(\lambda)$ and $\bar{z}_F(\lambda)$ spectral tristimulus values for a 2° observer and $\bar{x}_{F,10}(\lambda)$, $\bar{y}_{F,10}(\lambda)$, $\bar{z}_{F,10}(\lambda)$ for a 10° observer. The resulting CIE $X_F Y_F Z_F$ tristimulus values are incompatible with the CIE $XYZ$ values derived by using CIE 1931 standard observer CMFs. Therefore, if two SPDs of light sources are reduced to the same XYZ triplet by using these different CMFs, they are not required to be metamer and may not appear identical to the eye, due to differences in the underlying physiological model.

As the industry-standard colour spaces, used for display applications, are based on a 2° field size, and using data for different field sizes does not always yield better results in experimental colour matching [SONY, 2020], the field size for redefining colour spaces is not changed. The cone-fundamental-based spectral tristimulus values for a 2° field size, as given in CIE 170-2:2015, are used. The full table is in Appendix A.6. To be consistent with the naming convention for CIE 1931, the CIE 170-2:2015 2° CMFs are referred to as CIE 2015 in this thesis.

> *“ The cone fundamentals are grounded on the best experimental colour-matching data collected to date. It is likely that no large database will be collected in the near future. ”*
>
> [*Fundamental Chromaticity Diagram with Physiological Axes - Part 2: Spectral Luminous Efficiency Functions and Chromaticity Diagrams*, CIE 170-2:2015]

While CIE 2015 defines itself as maybe the best CMFs available, this does not imply “perfection”. The CIE 2015 CMFs can still be improved.

With the colour-matching functions 2006-TUIL-2°/10° developed by S. Polster, for example, “it is possible to predict visual colour matches by conducting colour difference evaluations at eight different colour coordinates using nine different spectral power distributions” [Polster, 2013] with smaller errors than with a CIE 170-1:2006 cone-fundamental-based CMFs. However, the test group for verifying the CMFs 2006-TUIL-2°/10° only included people younger than 44 years [Polster, 2013, p. 51]. Considering the age-related changes in lens yellowness, this may be a limitation for general CMFs. For a colour space definition, using a larger dataset which also includes higher ages is desirable.

The mathematical framework used in this thesis will allow the use of other colour-matching functions based on CIE 2015 for different ages or viewing conditions, as well as CMFs like 2006-TUIL-2°, as long as they are available as $\bar{x}(\lambda)$, $\bar{y}(\lambda)$ and $\bar{z}(\lambda)$ with $\bar{y}(\lambda)$ representing the luminance.

This thesis does not claim to use the best colour-matching functions. A well-accepted standard, with the option to adjust for different viewing conditions, is therefore used to describe the process of redefining colour spaces.

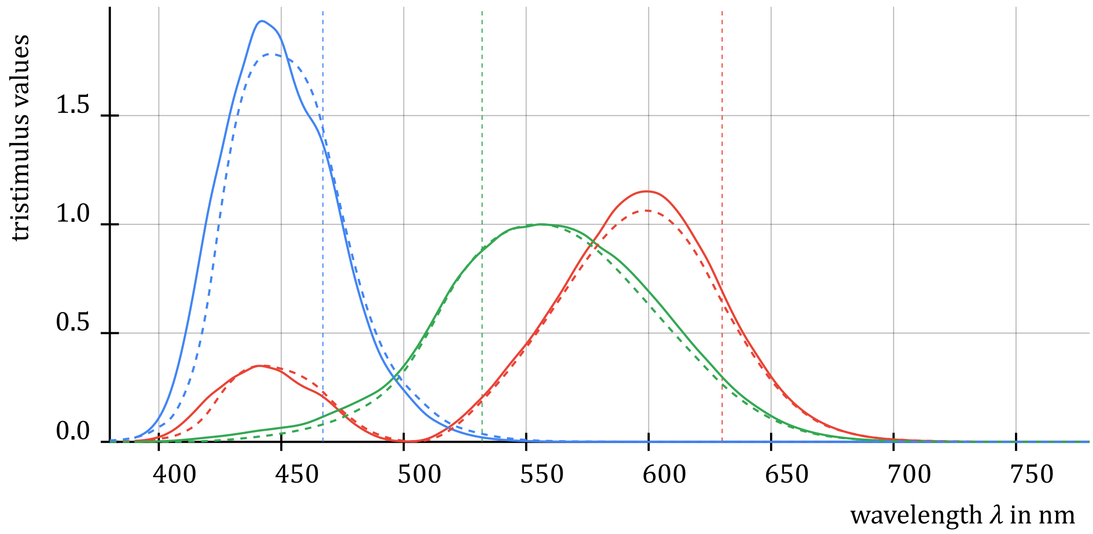


*Figure 7: CIE 1931 standard observer $\bar{x}(\lambda)$ (blue), $\bar{y}(\lambda)$ (green) and $\bar{z}(\lambda)$ (red) colour-matching functions (dashed), compared to CIE 2015 2° $\bar{x}_F(\lambda)$, $\bar{y}_F(\lambda)$ and $\bar{z}_F(\lambda)$ (solid).*

On Barco RGB-Laser projectors for cinema applications, calibration of the white point based on CIE 1931 does not result in a neutral white. With monochromatic lasers optimized for BT.2020, marked as dashed, coloured lines in Figure 7, the effect of the blue and red lasers on different $Y$ and $Y_F$ responses is obvious. In practice, this leads to a greenish white after calibration with the CIE 1931 standard observer compared to CIE 2015 2° CMFs.

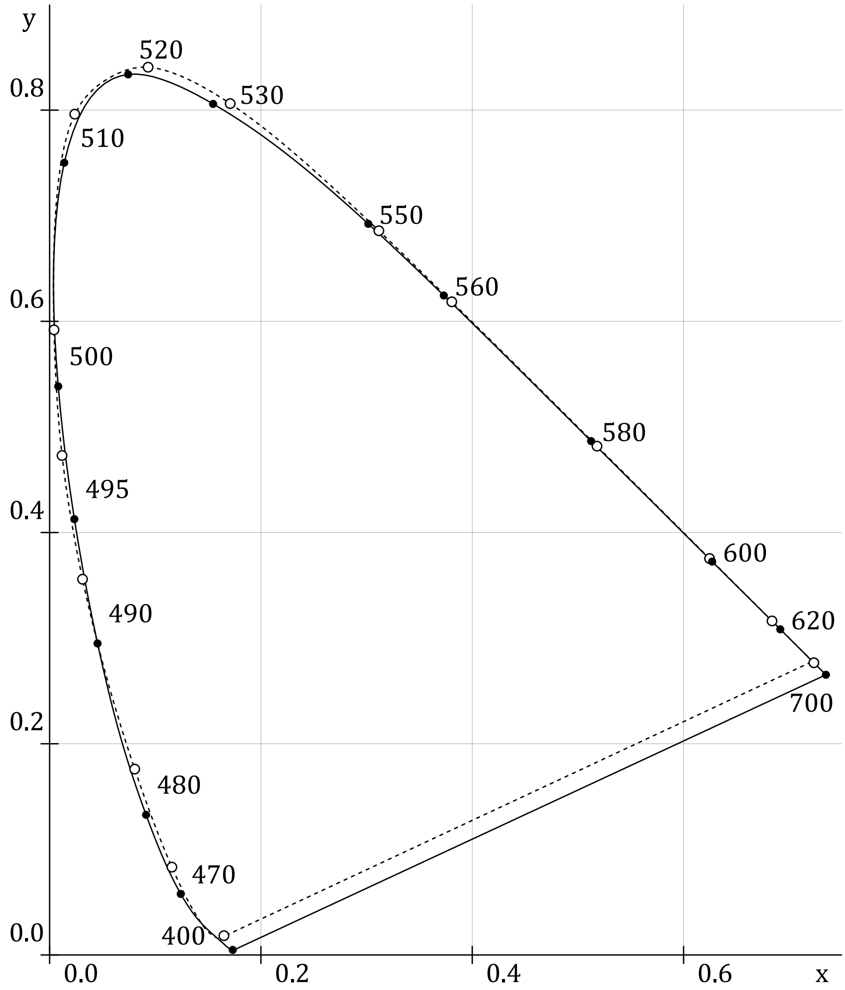


*Figure 8: CIE 1931 2° specular locus (solid) and CIE 2015 2° specular locus (dashed)*

Both CIE 1931 and CIE 2015 CMFs can be used to get CIE xy chromaticity coordinates. In Figure 8, the outer, curved line in the CIE xy diagram is called the specular locus. This line represents monochromatic light. Both areas (CIE 1931 and CIE 2015 2°) contain all visible colours. None of the representations is missing colours. The edges of the visible area are just represented with different, incompatible xy coordinates.

### 3.2.1. The rationale for the 2° observer

The 2° observer specified in CIE 2015 is used mainly because the existing colour spaces are also based on a 2° field of view, even though a normal television under ideal viewing conditions has a larger field of view. An HD video signal with a 1920 pixel width, for example, can result in a 32° horizontal field of view [Poynton, 2012, p. 101].

An approximately 1.4° field of view corresponds to the foveola (fovea centralis) with the sharpest vision under daylight conditions [Wyszecki & Stiles, 2000, p. 89]. Therefore, while focusing on small image details, a small field of view is reasonable.

Admesy, a spectroradiometer vendor, comes to the same conclusion. For display applications, regardless of which CMFs are used, the 2° observer is applicable.

> *“ Now the practical question arises which standard observer to choose for display applications? One could think that the 10° observer would be the better choice, because a display will in most cases be viewed under an angle which is larger than 4°. But when we remember that the viewing angle of the color stimuli as such is determining, we find that the 2° observer can be the closer fit, for example when we view a photo with detailed elements. For that reason the ICDM, the International Committee for Display Metrology, part of SID’s Definitions and Standards Committee, bases all display metrology on the CIE 1931 2° color-matching functions [Chapter 21.2.2, IDMS version 1.2]. ”*
>
> [*Measure How We See - The Way to Perfect Display Colors*, Admesy, 2024]

For large venue events with LED screens as background, a 10° observer, designed to better model peripheral retinal response, might be more appropriate. However, a larger field of view (outside the fovea, approx. 5°) seems to require more attention. The concurrent usage of one set of CMFs for small details and one for large area backgrounds at the same time may be needed [Polster, 2013, p. 97].

As to CIE 170-1:2006 physiological data, the effect of different observers’ fields may be larger for younger persons [Fairchild, 2005, pp. 339 f ].

## 3.3. CIE Illuminant Series D

The majority of video and display colour spaces, including BT.709 and BT.2020, define CIE standard illuminant D65 as their white point. The correlated colour temperature of D65 is 6504 K. For D65, an exact spectral power distribution is given. With CIE 1931 CMFs, this SPD results in chromaticity coordinates $x = 0.312713$ and $y = 0.329016$.

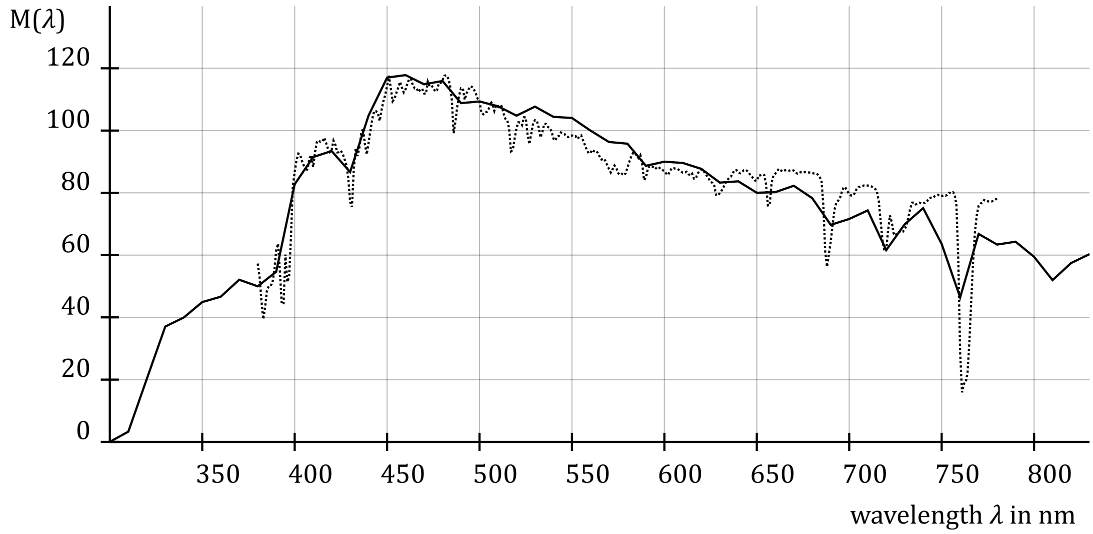


*Figure 9: Normalized CIE standard illuminant D65 spectral power distribution, compared to measured slightly cloudy sky (Hamburg, December 2025, dotted) with the same CIE 1931 xy chromaticity coordinates.*

The SPD shown in Figure 9 is defined based on measurements of the sky at different times of day. A technical definition for white or neutral grey, concerning the human eye, is only possible relative to the viewing conditions and adjustment of the eye. As the human visual system is trained, by near every day practice, to accept normal daylight as neutral, an SPD matching this condition is desirable.

The original CIE dataset for D65 is defined in 10 nm intervals. Even if Sprague interpolation (fifth-order polynomial interpolation described in CIE 167:2005) is recommended for measured SPDs by CIE 015:2018, the dataset for D65 given in the same document is linear interpolated from 10 nm to 5 nm intervals. Therefore, linear interpolation was used to get a 1 nm spaced table.

The exact SPD can be found in Appendix A.4 as $S_{D65}(\lambda)$.

With this dataset, the D65 white point can be recalculated for CIE 2015 based CMFs. As discussed in Section 7.2, four significant figures are accurate enough to specify a white point for video and display applications. This corresponds to the numbers given in ITU colour space standards. The recalculated CIE xy chromaticity coordinates are given in Table 2.

| CMFs | x | y |
|---|---|---|
| CIE 1931 2° | 0.3127 | 0.3290 |
| CIE 2015 2° | 0.3135 | 0.3308 |

*Table 2: D65 white point based on CIE 2015 2° and CIE 1931 2°*

The accuracy of modern spectroradiometers has increased over time. Daylight varies slightly depending on dust, clouds, and time of day. Nevertheless, the SPD is seen as numerically accurate. Therefore, the CIE xy chromaticity coordinates can be seen as accurate as well.

There are colour spaces which do not use CIE D65 as a white point. As long as a colour temperature for a D series daylight illuminant is referenced, the spectral power distribution can be calculated. The mathematical process is described in Section 7.10.

Chromaticity coordinates for white points that are not referred to the CIE illuminant series D can be calculated using the same method as long as an SPD is defined. As illuminant A or tungsten light, defined white points are not typical for displays under normal viewing conditions, numbers are not elaborated here.

## 3.4. BT.709, BT.2020 and DCI-P3

While both ITU-R BT.709 and ITU-R BT.2020 incorporate many specifications, including colour spaces, transfer curves, resolutions and more, this thesis focuses exclusively on their chromaticity definitions.

Even if modern SDI signals are defined with a Colour VANC packet [ST 2048-1:2024], enabling arbitrary colour spaces and logarithmic transfer curves, implementation in non-cinematography products is rare. The vast majority of professional broadcast equipment relies on the simple SDI payload identifiers, which can only distinguish between a BT.709 or BT.2020 colour space [ST 2082-10:2018]. In case of HDMI, the built-in colour spaces are also BT.2020 and BT.709 [HDMI 2.0]. HDMI adds sRGB, the difference is the transfer curve, not the colour space primary values, compared to BT.709.

BT.601 is seen as legacy for signals, even if crucial for redefinition in Section 4.2. The OpenColorIO (OCIO) configuration for ACES workflows lists more than 20 distinct colour spaces for cameras and displays [OCIO, 2025]. They are available during a production workflow, but as they are not typically available for video signals, these colour spaces are seen as exceptions rather than targets for direct redefinition.

A notable exception is the Digital Cinema Initiatives - Protocol 3 (DCI-P3), while not a typical colour space for encoding RGB data for video signals, this colour space is significant when it comes to displays. The DCI-P3 colour space defines the possible colour volume for cinema projectors, even though the triplet of code values $(CV_{X''}, CV_{Y''}, CV_{Z''})$ used in a modern HDR DCDM image can exceed this colour volume by far[DCI HDRD, 2024]. Compared to BT.709 and BT.2020, DCI-P3 can be seen as a colour space which defines display capabilities and is not typically used for actually interpreting a video signal.

## 3.5. Required precision of colour spaces

Different colour spaces use different numbers of significant figures for the CIE xy chromaticity coordinates given in the standards. Figuring out the accuracy of the underlying data and calculating the error may be impossible or frustrating because errors can accumulate. As it is desirable to have numerical precision and ignore uncertainties for all further calculations, it may be more helpful to analyse the desired precision of a colour space.

A future industry standard may be $IC_tC_p$ encoded video signals with 12-bit quantization and the perceptual quantizer (PQ) as the electro-optical transfer function (EOTF). This system ensures that no code value change is above the visual threshold when analysed with $\Delta E2000$ [Dolby, 2020]. For distinguishing between colours of a 12-bit $IC_tC_p$ video signal in the CIE xy chromaticity diagram, x and y coordinates need to have a precision within ±0.0002. The maths used, and a table for different colours, is given in Section 7.2.

Spectroradiometers with this precision are not broadly available. Therefore, this precision is desired for calculations, but cannot be reproduced while matching displays. As a class 1 reference display is required to be within $\Delta E^*_{uv}$ smaller than 4 of the defined colour space [EBU Tech 3320], with a well-established uncertainty of ±0.002 or better, a normal spectroradiometer is accurate enough.

# 4. Redefinition

## 4.1. Existing workflows

As the limitations of CIE 1931 are well known to the industry, vendors of displays, colourimeters and spectroradiometers try to mitigate these issues. The offsets Sony implements with their products, described in Section 3.1, is one approach to adjust the white points (not done for primary colours) of displays for a better visual match. In the case of Sony reference displays, verification is based on a visual evaluation.

Assuming there is a set of CMFs perfectly modelling the eye, it is valid to measure red, green, blue and white of one display with a spectroradiometer, then transfer the resulting colour space to a different display with different SPDs and match the first display measured. This workflow is done in practice. All displays of one studio are matched to one reference display. The use of different CMFs for calibration is possible as long as the SPD of the reference display is known.

## 4.2. Redefinition of ITU-R BT.709 based on CIE 2015 2° CMFs

The colour space defined in ITU-R BT.709 (Table 3) may be the most used colour space in television and video applications. The three chromaticity coordinates of the primaries defined in the standard are based on the CIE 1931 standard observer CMFs. There is a direct definition for x and y. The luminance of each primary colour can be calculated by the specified white point. The maths for calculating the required luminance of each primary is described in Section 7.7 and Section 7.8.

For computer displays, one of the most used colour spaces is sRGB. The IEC 61966-2-1 standard, which defines sRGB, uses CIE 1931 based primary colours as well. They are defined with the same values as the ITU-R BT.709 (BT.709) colour space. They can be seen as equal and interchangeable. Therefore, the redefined BT.709 will also be valid for sRGB. (Only the colour space matches, the EOTF does not match).

| Colour | x | y | Luminance |
|---|---|---|---|
| Red | 0.640 | 0.330 | 0.2126 |
| Green | 0.300 | 0.600 | 0.7152 |
| Blue | 0.150 | 0.060 | 0.07219 |
| White (D65) | 0.3127 | 0.3290 | 1.0 |

*Table 3: CIE 1931 based ITU-R BT.709 and sRGB colour space definition*

The ITU document presents the chromaticity coordinates with three significant figures, while white is presented with four figures. The required luminance for white is calculated and also specified in the standard as formulae for calculating luminance for a chroma-separated signal. Consequently, the numbers can be found in the conversion matrix for converting linear RGB to the XYZ Colour space, where Y is the luminance.

The luminance for white is defined in normalized form here and can be translated to a maximum screen brightness of 100 cd/m$^2$ for a class 1 display, 200 cd/m$^2$ for domestic viewing conditions [EBU Tech 3320], or 80 cd/m$^2$ for sRGB [IEC 61966-2-1].

The numbers provided for the white point are not just CIE 1931 chromaticity coordinates. They refer to the CIE standard illuminant D65 [ITU-R BT.2035], which is well-defined with an SPD. A full spectral dataset [CIE D65] for the white point is given with the ISO/CIE 11664-2:2022 standard. Therefore, a redefinition of the white point based on CIE 2015 2° CMFs can be done. The resulting chromaticity coordinates are presented in Table 2 from Section 3.3. The numbers given for the primary colours, however, are reduced to a three-dimensional value (xy chromaticity coordinate and calculated luminance). For redefinition with new colour-matching functions, the spectral power distributions of the primary colours are needed.

The BT.709 colour space was first defined in 1990 and published as CCIR Rec. 709, today known as ITU-R BT.709. The chromaticities were derived from the colours defined earlier by EBU and SMPTE. The red and blue primary colours are taken from EBU Tech 3213-E standard, further referred to as EBU colours. The green primary colour is a mathematical average of the EBU green and the green which is defined in SMPTE RP 145, further named SMPTE colours [Poynton, 2012, p. 290].

The CIE 1931 based chromaticity coordinates given for the EBU colours, as well as the SMPTE colours, are a result of the colourimetric characteristics of the light-emitting phosphors available in 1970.

The SMPTE and EBU documents do not define a spectral distribution. Only the reduced CIE 1931 2° standard observer-based chromaticity coordinates are defined.

The best sources for the SPDs are therefore based on the SMPTE and EBU phosphors used in reference cathode-ray tube (CRT) displays from 1990 as sources for red, green and blue.

### 4.2.1. Measuring CRT phosphor SPDs

In CRT displays, the chromaticities of the red, green, and blue primaries are determined by the spectral emission characteristics of the phosphor materials deposited on the screen's inner surface. The expected CIE 1931 xy coordinates of these emissions are well documented in the industry standards EBU Tech 3213-E and SMPTE RP 145. The underlying SPDs, which define the physical light output, have never been standardized.

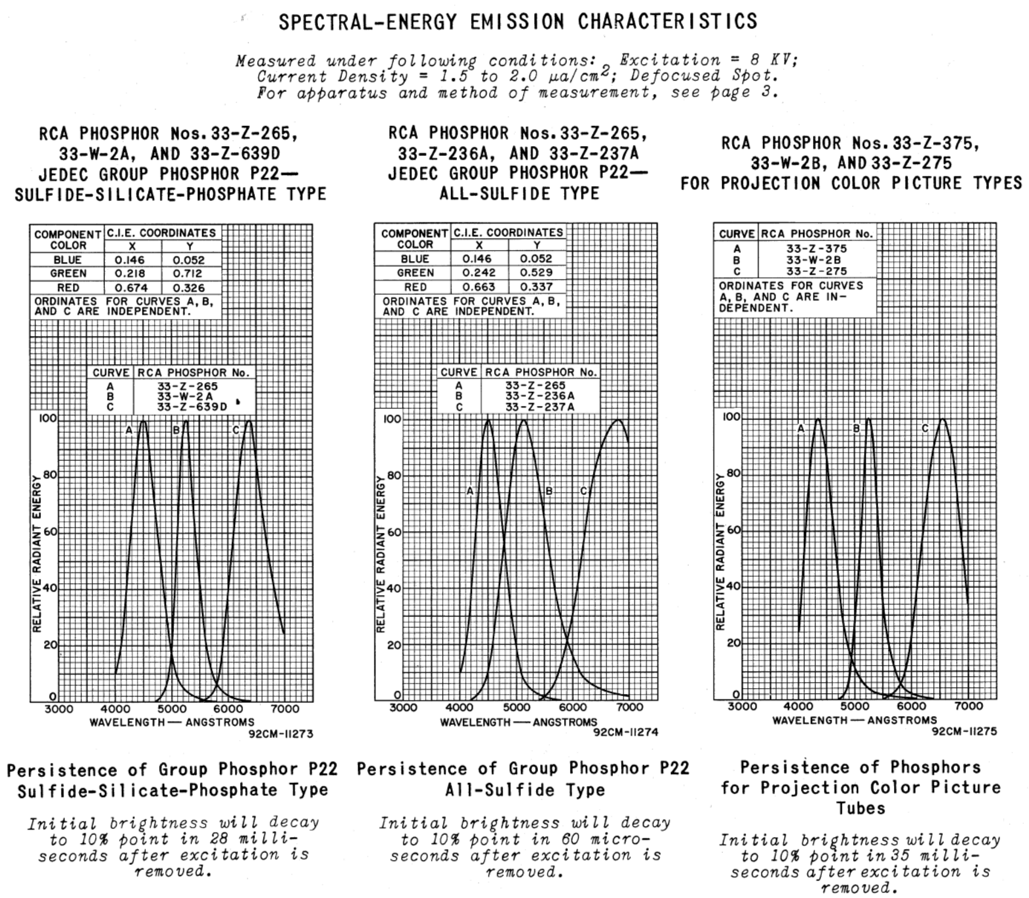


*Figure 10: Example datasheet for different spectral emissions for different phosphors used in CRT displays [RCA TPM-1508A, 1995].*

The used material is sometimes referred to as "P22 phosphors". As seen in Figure 10, the Radio Corporation of America listed multiple versions of P22 phosphors.

Public, high-quality data for exact spectral power distributions of CRT displays seems to be rare. The graphs given in some datasheets do not comply with the CIE xy chromaticity coordinates, which are produced when these phosphors are used for coating glass of a CRT. Measurement of 15 different CRT displays was analysed by Golz and MacLeod (2003). The available dataset yields CIE xy chromaticity coordinates within the range of SMPTE and EBU colours. A clear definition of which phosphors are used and what standards are followed is only available for some of them.

In the absence of any publicly available, traceable SPDs from reference CRT displays, the spectral emissions of one reference-grade CRT display representative of each standard (SMPTE and EBU) have been measured.

The Sony BVM-20F1E was chosen as the reference for EBU colours. One of these displays was available with less than 19 000 hours of operation at NDR in Hamburg. This type of display was long used as a reference display in the broadcast industry. The manual [SONY, 1995] confirms that the EBU version complies with EBU Tech 3213-E within ±0.005 for the CIE 1931 based chromaticity coordinates.

For measuring two most similar displays under equal conditions, a Sony BVM-20F1U was chosen. As they were not typically sold in Europe, a display from the USA was sent to Hamburg. The CRT inside this display has a runtime of approximately 21 000 hours.

The spectral power distributions of the primary colours were measured with a CS-2000 spectroradiometer from Konica Minolta (5nm spectral bandwidth).

Especially for the narrow spectral lines of the red phosphor, results were verified with a JETI specbos 2501-HiRes (2nm spectral bandwidth). The results are within the tolerance of the devices.

Konica Minolta claims an accuracy of ±0.0015 / ±0.001 for the resulting x / y chromaticity coordinates while measuring an illuminant A. There is no detailed information on the accuracy achievable with more complex spectral sources. Simulated errors to the measured data (spectral shift of 0.3 nm, slight variation in intensity for some spectral areas) resulted in errors which are below the uncertainty of the datasheet.

The accuracy for luminance is given with ±2% for an illuminant A at 100 cd/m$^2$. As all the resulting luminances for the primary colours are normalised to a white point, exact luminance measurements are not required in this case.

A CRT flickers, this means the light output is not constant over time, as seen in Figure 11. A spectroradiometer with an integration time below or near the frame rate may not see the same

SPD effect as the human eye. The integration time was set to a fixed value (40 000µs in case of the EBU CRT, 33 333µs for the SMPTE CRT). As the repeatability while using single measurements and a trigger signal synchronized to the light output was not within the expected range, 100 measurements were taken and averaged.

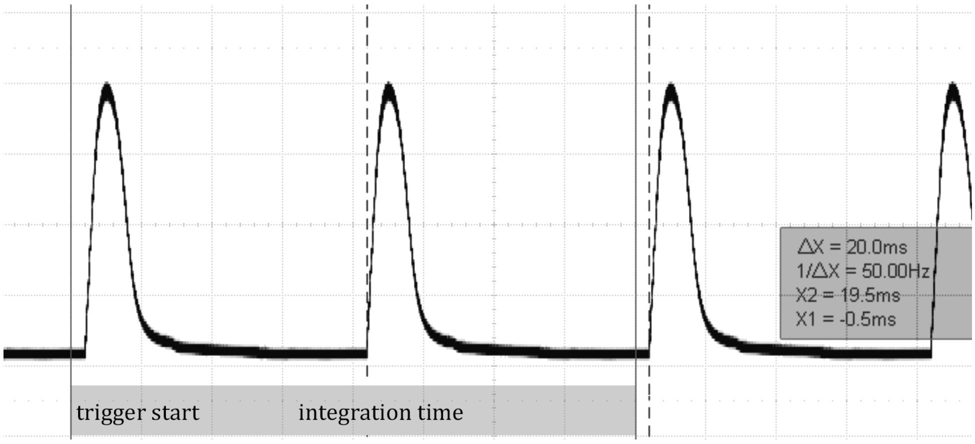


*Figure 11: Luminance of a CRT (Sony BVM-20F1E, white) over time, measured with a photodiode.*

The short integration time of only two fields was needed to prevent overexposure. As the red phosphor has most of its energy in narrow spectral peaks, single pixels of the line sensor in a spectroradiometer reach their limits, while the overall luminance is well beyond the maximum specified (illuminant A) for the spectroradiometer.

For the EBU CRT display, a BKM-21D SDI Multi Decoder card was used for signal input. The SMPTE version was equipped with a BKM-20D SDI Input board. The SDI signal was generated as a 525i/29.97 SDI video signal for the SMPTE CRT, and 625i/25 for the EBU CRT display.

As the displays can turn off single primary colours, a full area 100% white video signal, calibrated to 100 cd/m$^2$ and a D65 white point (CIE 1931), was used for all measurements.

Measurement was done with a controlled ambient temperature between 21°C and 23°C. Humidity was between 40% and 50%. The warm-up time for the CRTs was at least 45 minutes.

Both displays are measured with a luminance decay from the middle of the screen to the edges, as well as slight colour shifts.

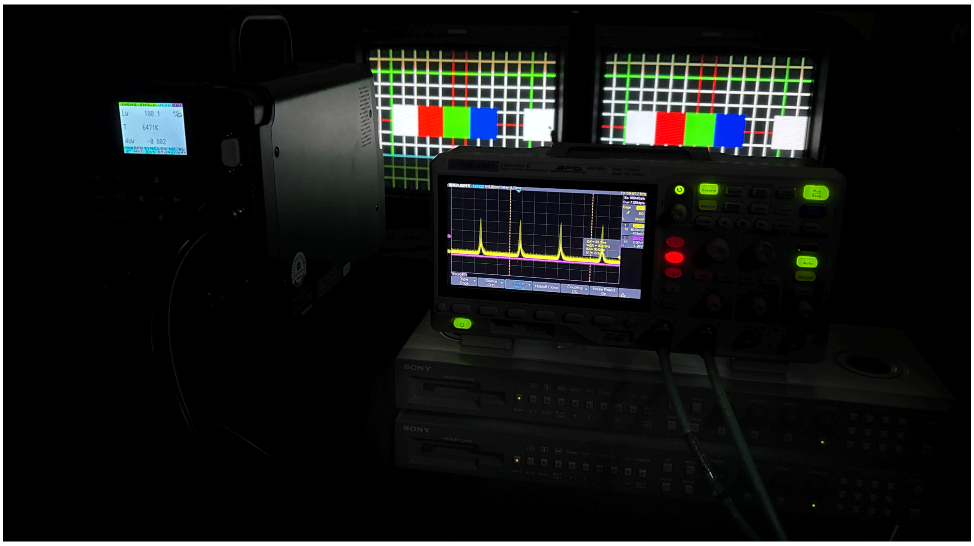

*Figure 12: Alignment setup for measuring CRT displays, locking the spectroradiometer to the light output is done with a photodiode and an Oscilloscope.*

The measured SPDs are presented in Figure 13 and Figure 14. A table with detailed data can be found in Appendix A.3.

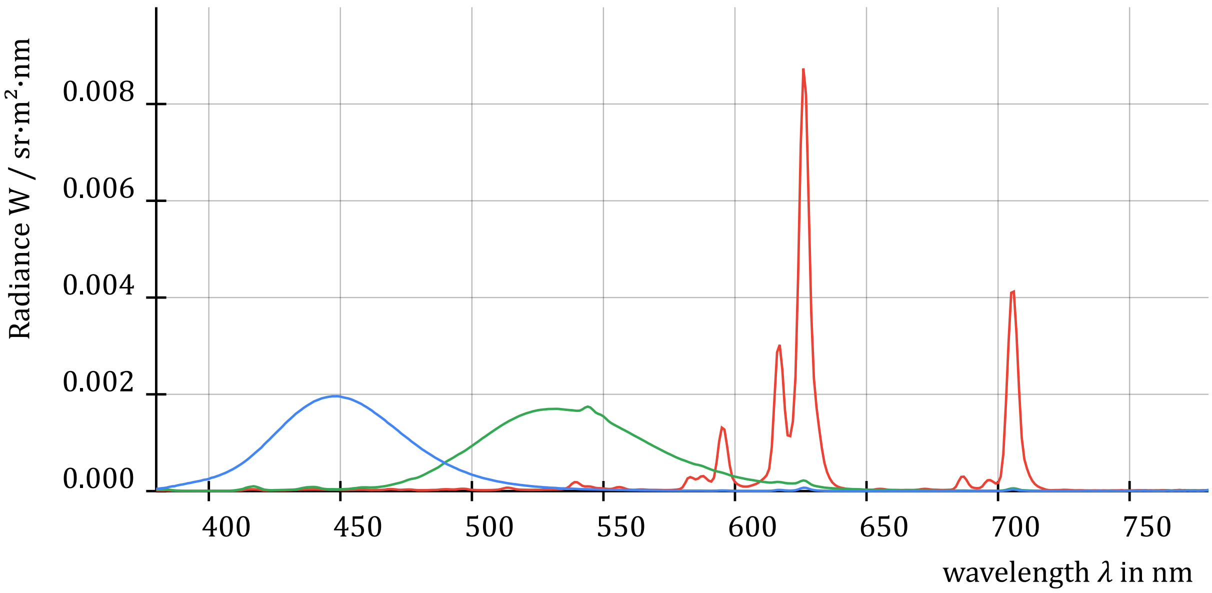


*Figure 13: SPDs of EBU colours from Sony BVM-20F1E.*

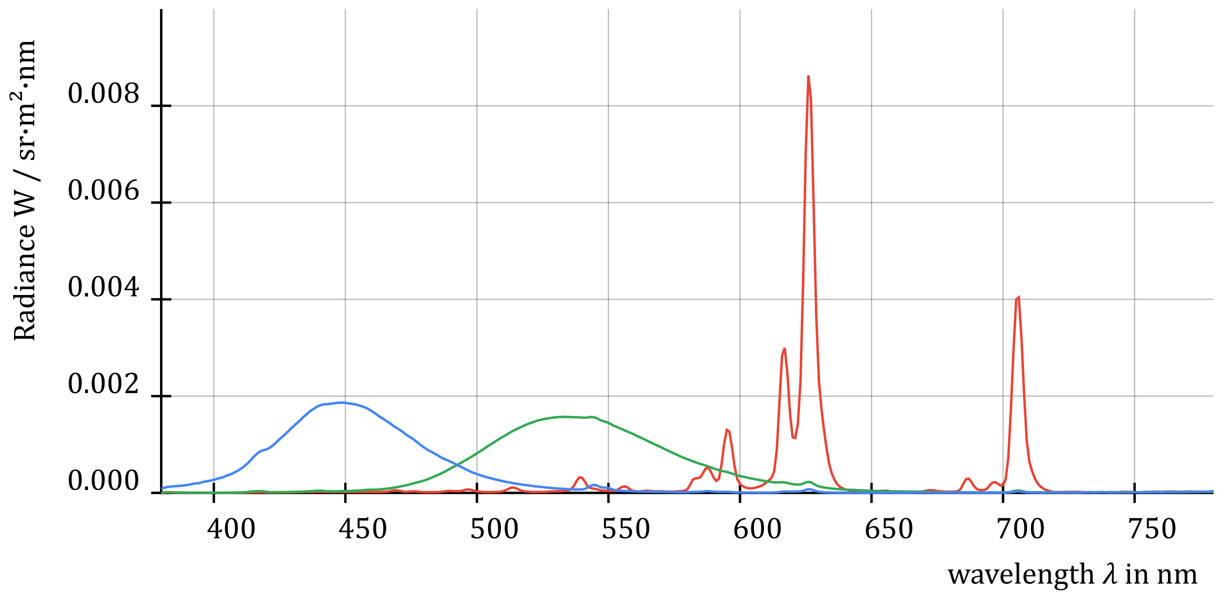


*Figure 14: SPDs of SMPTE colours from Sony BVM-20F1U.*

The red peaks are slightly visible as crosstalk in the SPDs of the other colours. This is also described by Golz and MacLeod (2003). As this seems to be the actual-seen colour for an observer, the data is left as is. The measurements used for redefining BT.709 are taken from the middle of the screen. This ensures that the resulting colour space best reproduces the visual colours seen on these CRT displays.

The SPDs used to specify the red and blue colours for a BT.709 based on CIE 2015 2° CMFs are directly taken from the measurements of the BVM-20F1E display (EBU colours). The green is a mix of the EBU and SMPTE green measured from BVM-20F1U. The difference is shown in Figure 15.

The mix for the green SPD is done by averaging the energy for each wavelength, after normalization to the same overall luminance for the EBU and SMPTE green. The luminance is calculated with CIE 1931 2° observer CMFs. The normalization is not done with CIE xy chromaticity coordinates. Doing so will lead to a reduction to a three-dimensional value without keeping a single SPD. Without this SPD, it is not possible to transfer this concept of redefining a colour space to other CMFs.

$$\beta = \frac{Y_{\mathrm{EBU}}}{Y_{\mathrm{SMPTE}}}$$

$$P_{\mathrm{BT.709}_{\mathrm{green}}}(\lambda) = P_{\mathrm{EBU}_{\mathrm{green}}}(\lambda) + \beta P_{\mathrm{SMPTE}_{\mathrm{green}}}(\lambda)$$

*Equation 2: Averaging SMPTE and EBU green with normalization.*

The normalisation factor for the measurements is $\beta = 1.0403$

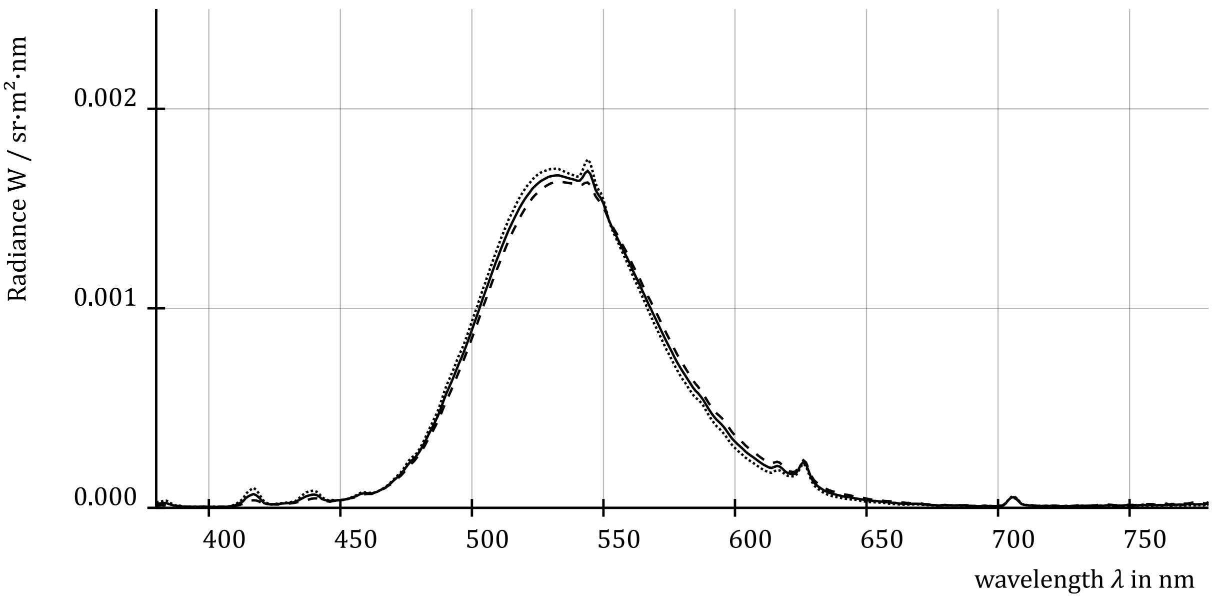


*Figure 15: EBU green (dotted) and SMPTE green (dashed), compared to the resulting average (solid).*

With these spectral power distributions, real physical colours are now available, which can serve as a basis for redefining the BT.709 colour space based on CIE 2015 2° colour-matching functions. The following equations are used to calculate the CIE xy chromaticity coordinates. The same set of equations is valid for CIE 1931 as well as CIE 2015.

$$X_F = \sum_{\lambda=380nm}^{780nm} \bar{x}_F(\lambda)P(\lambda)$$

$$Y_F = \sum_{\lambda=380nm}^{780nm} \bar{y}_F(\lambda)P(\lambda)$$

$$Z_F = \sum_{\lambda=380nm}^{780nm} \bar{z}_F(\lambda)P(\lambda)$$

*Equation 3: Calculation of the CIE $X_F Y_F Z_F$ tristimulus values.*

With discrete values at 1nm steps for the CMFs and the primary colour SPDs, a summation can be used with $\lambda$ in the range of 380nm to 780nm, $\bar{x}_F, \bar{y}_F, \bar{z}_F$ are available with CIE 170-2:2015 2° cone-fundamental based CMFs (Appendix A.6), $P(\lambda)$ is the measured energy for the phosphor or the luminance of the D65 standard illuminant (in case of white) at a given wavelength. The CIE xy chromaticity coordinates are then calculated with Equation 4.

$$x_F = \frac{X_F}{X_F + Y_F + Z_F}$$

$$y_F = \frac{Y_F}{X_F + Y_F + Z_F}$$

*Equation 4: Calculation of the CIE chromaticity coordinates.*

A full table with the data for the spectral power distributions of the redefined colour space, as shown in Figure 16, can be found in Appendix A.3.

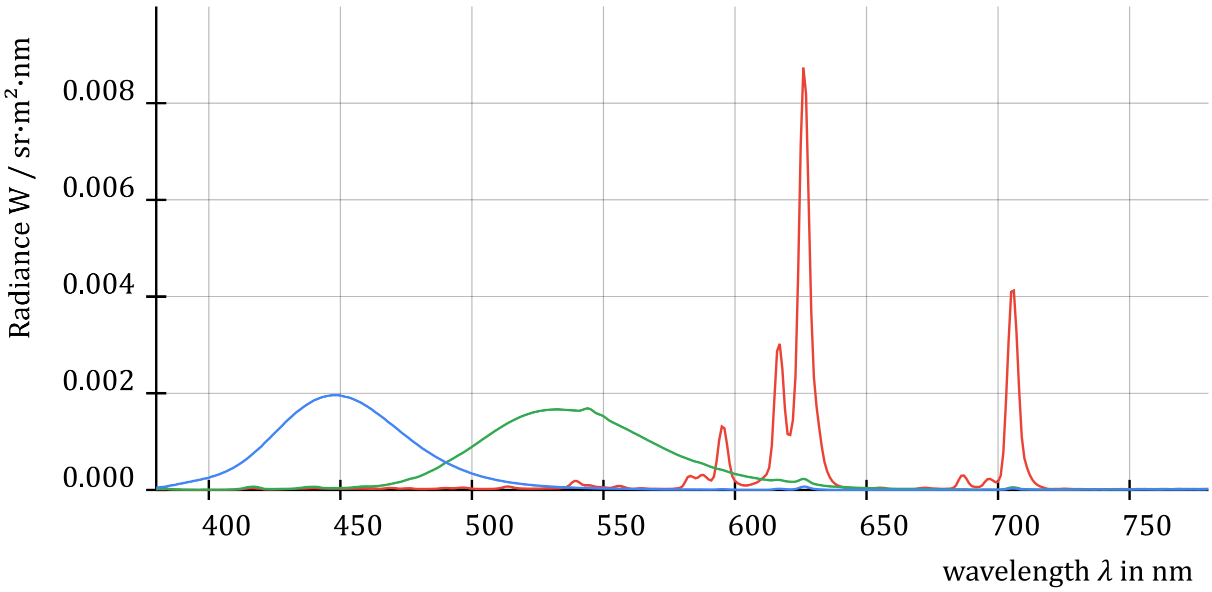


*Figure 16: SPDs of the resulting BT.709 colours, mixed from Sony BVM-20F1E and BVM-20F1U.*

The luminance given in Table 4 is not calculated from the measured SPDs. The given value is the relative luminance required to mix D65 white. When the colour of the primaries is slightly altered, the luminance required to reach white changes accordingly. The maths for calculating required luminances is given in Section 7.8.

| Primary colour | ITU-R BT.709 (BT.709) based on CIE 2015 2° | | |
|---|---|---|---|
| | x | y | Luminance |
| Red | 0.6345 | 0.3369 | 0.2211 |
| Green | 0.3126 | 0.6012 | 0.6927 |
| Blue | 0.1407 | 0.07094 | 0.08614 |
| White | 0.3135 | 0.3308 | 1.0 |

*Table 4: CIE chromaticity coordinates for ITU-R BT.709 (BT.709) based on CIE 2015 2° CMF. White point is defined as CIE D65 daylight illuminant. Luminance for White is normalized to 1, the Luminance for the colours is calculated with the white point.*

The resulting colour space can be used for calibration of displays with CIE 2015 2° colour-matching functions. The result will match the colours of a BT.709 reference CRT display within the limits of CMFs. To be precise, a theoretical BT.709 CRT display. Even a newer BVM-D24E1WU/E CRT separates in SMPTE and EBU phosphors. The supported BT.709 colour space is implemented by linear matrix processing introduced with HD support [SONY, 1999].

### 4.2.2. Precision of the resulting colour space

For evaluating the deviation of the measured SPDs against the definition of the BT.709 standard, the resulting CIE 1931 standard observer based chromaticity coordinates are presented in Table 4. They are compared to the standards defined chromaticity coordinates, and the deviation is given as $\Delta E*_{\mathrm{uv}}$. The maths for calculating $\Delta E*_{\mathrm{uv}}$ is given in Section 7.6.

$\Delta E*_{\mathrm{uv}}$ is used for defining display accuracy in ITU standards. It is not suitable for precise colour deviations across different luminances. As the luminance is normalized here, the deviation of the luminance is ignored and $\Delta E*_{\mathrm{uv}}$ can be used. CIEDE2000 is given as additional deviation for convenience. Calculation of CIEDE2000 is done with the JavaScript implementation by Leonard (2026).

| Primary colour | x | | y | | Error | |
|---|---|---|---|---|---|---|
| | CRT 1931 | Target | CRT 1931 | Target | CIEDE2000 | $\Delta E^*_{\mathrm{uv}}$ |
| Red | 0.6381 | 0.640 | 0.3317 | 0.330 | 0.33 | 1.8 |
| Green EBU | 0.2918 | 0.290 | 0.6021 | 0.600 | 0.35 | 1.0 |
| Green SMPTE | 0.3087 | 0.310 | 0.5985 | 0.595 | 0.25 | 1.1 |
| Green 709 | 0.3003 | 0.300 | 0.6003 | 0.600 | 0.05 | 0.19 |
| Blue | 0.1502 | 0.150 | 0.05802 | 0.060 | 0.72 | 0.99 |

*Table 5: CIE chromaticity coordinates, comparison of ITU-R BT.709 (BT.709) reference values with measured CRT values.*

A class 1 or grade 1 display needs to comply with ITU-R BT.709 (BT.709) standard chromaticity coordinates within $\Delta E^*_{\mathrm{uv}}$ smaller than 4 [EBU Tech 3320].

The CIE chromaticity coordinates of the displays measured with the Konica Minolta CS-2000 are well within the tolerances in the datasheet and within the limits for a class 1 display, even after considering the uncertainty of the spectroradiometer. There was only one display available of each type. Therefore, it is unknown how representative the offset to BT.709 is when measured with a modern spectroradiometer.

As rounding the CIE xy chromaticity coordinates will lead to an offset between the SPDs and the redefined colour space, the numbers presented here and used for further calculations are given with 4 significant figures, even if they hold an uncertainty of ±0.0015 / ±0.001. While no detailed data for the uncertainty of the measured spectral data is available, it is not desirable to reduce the precision of the SPDs. The white point of the redefined BT.709 colour space is considered fully accurate, as it is based on the SPD defined by CIE standards.

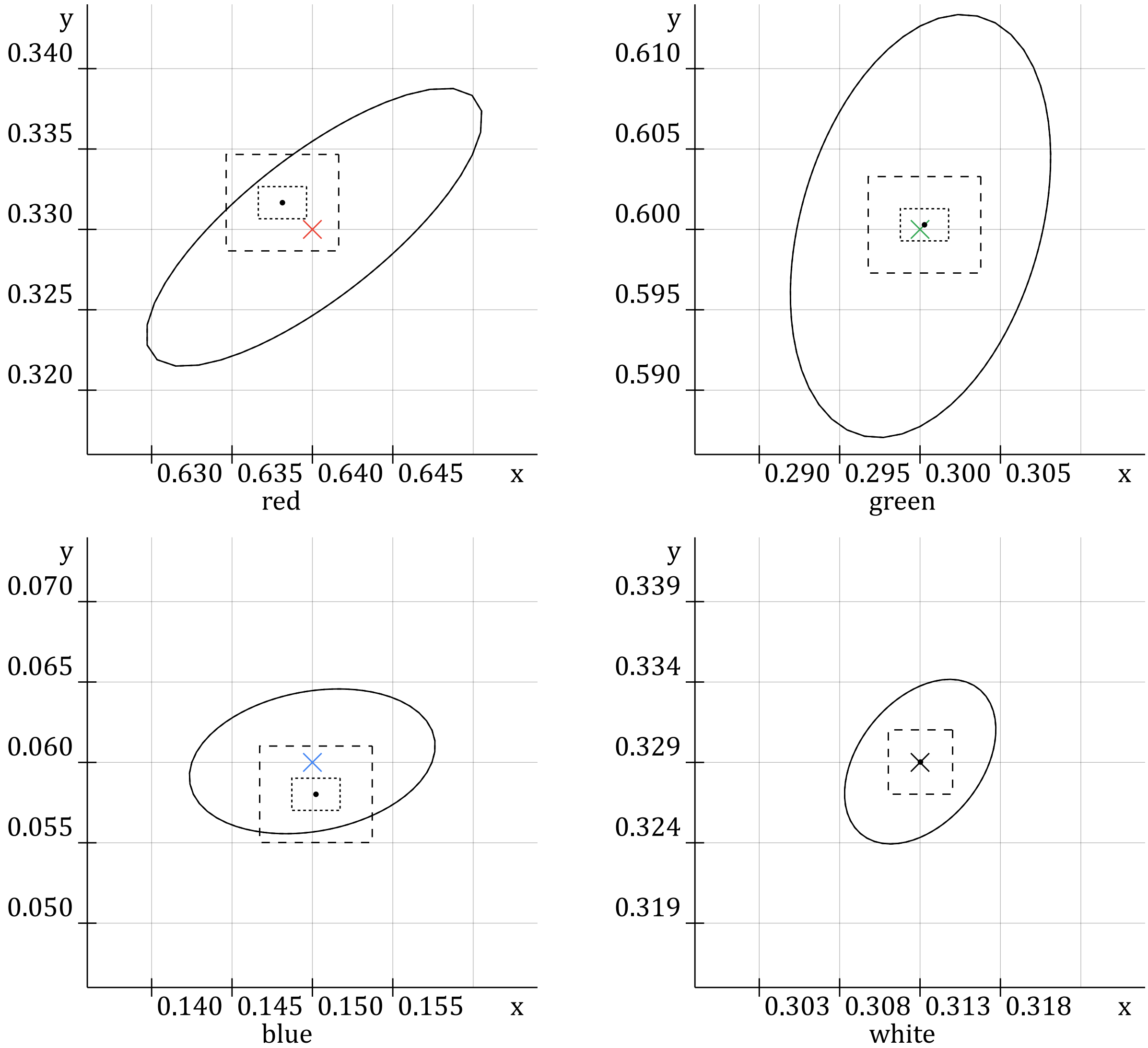


*Figure 17: Enlarged CIE 1931 xy chromaticity diagram for red, green and blue. The measured results (point), the corresponding probe uncertainty (inner dotted square) and the resulting uncertainty for a display calibrated within ±0.002 for xy (outer dashed square) are compared to the ITU-R BT.709 (BT.709) primaries (cross) and the required precision of $\Delta E^*_{\text{uv}} < 4$ (solid ellipsis).*

The requirement for a class 1 display to reproduce skin tones is defined with a deviation of $\Delta E^*_{\text{uv}}$ smaller than 2.6 [EBU Tech 3320]. EBU Tech 3273-E defines one skin tone with $Y = 0.4404, u' = 0.2221, v' = 0.4884$. For creating the skin tone with BT.709 primaries, a linear mix of $R = 0.6073, G = 0.4041, B = 0.3084$ is required. When this colour is mixed with the measured (and averaged for green) colours, the resulting skin tone can be rendered precisely.

The measured displays comply with this standard. For calibrating a display based on the redefined colour space, the uncertainty of a spectroradiometer should be very low. The worst-case error while using typical spectroradiometers can be seen in Figure 17.

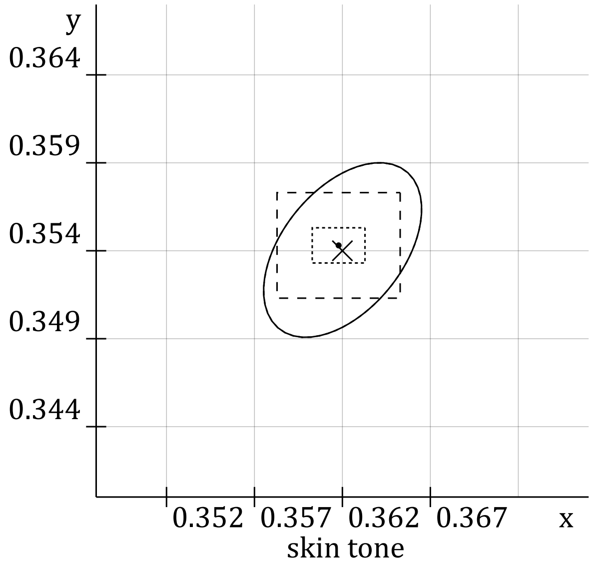


*Figure 18: Enlarged CIE 1931 xy chromaticity diagram for skin tone defined in EBU Tech 3273-E. The measured results (point), the corresponding probe uncertainty (inner dotted square) and the resulting uncertainty for a display calibrated within ±0.002 for xy (outer dashed square) are compared to the ITU-R BT.709 (BT.709) primaries (cross) and the required precision of* $\Delta E^*_{\mathrm{uv}} < 2.6$ *(solid ellipsis).*

The resulting match between the measured SPDs and the existing BT.709 colour space, when adding up the errors from the CS-2000 and a spectroradiometer used to calibrate a display (for example, ±0.002 for xy coordinates), is not within the limits to fully comply with class 1 displays. As seen in Figure 18, the added errors of two spectroradiometers exceed the requirements, even if the simulated display could achieve this colour with near-perfection.

### 4.2.3. Simplification of the measured SPDs

While the Blue and green phosphors of a CRT do have very simple and wide spectral power distributions, the red phosphor of CRT displays shows narrow peaks and can be described as more complex. It may be desirable to simplify the shape of the red SPD.

A change to the spectral data will need a verification method which is more accurate than the existing CMFs. Furthermore, the changed SPD needs to visually match the original CRT display colour for all observers. Otherwise, the resulting SPD cannot be used as a general physical source for redefining a colour space with different CMFs for different viewing conditions or further optimization.

Simplifying the red spectral power distribution will need a compromise and a visual verification. Even if desirable, this is not part of this thesis.

## 4.3. Redefinition of ITU-R BT.2020 based on CIE 2015 2° CMFs

The colour space defined in ITU-R BT.2020 is derived from monochromatic light sources at 630 nm for red, 532 nm for green and 467 nm for blue. The white point is defined as D65, consistent with BT.709. The definition for the chromaticity coordinates in the standard is based on the CIE 1931 2° standard observer.

| **Colour** | **x** | **y** | **Luminance** | **monochromatic $\lambda$** |
|---|---|---|---|---|
| Red | 0.708 | 0.292 | 0.2627 | 630nm |
| Green | 0.170 | 0.797 | 0.6780 | 532nm |
| Blue | 0.131 | 0.046 | 0.05930 | 467nm |
| White (D65) | 0.3127 | 0.3290 | 1.000 | - |

*Table 6: CIE 1931 based ITU-R BT.2020 colour space definition*

Redefining the ITU-R BT.2020 colour space by reading the CIE 2015 2° $X_F Y_F Z_F$ values and transforming them to CIE xy chromaticity coordinates would result in a new colour space based on monochromatic light, with the same spectral power distributions, visually identical (primary colours only) to CIE 1931 based BT.2020.

One of the objectives while defining a wider colour space than BT.709, covering all real surface colours, was to use physically possible primary colours and not imaginary colours (which would allow even larger colour spaces). For red, there have been two different approaches. Selecting a monochromatic light which can be reproduced with a laser, which is simple to manufacture (635nm), was one of the approaches. The other approach is to select a monochromatic light on the equi-hue line of the red of an existing display technology at this time (625nm). A compromise at 630nm was selected because the equi-hue line of the 630 nm based red primary can be reached by laser and LED-backlit display technology with a near-invisible colour difference as to CIELAB $\Delta$E [ITU-R BT.2246].

Introducing a colour space, defined on the same monochromatic light sources, using chromaticity coordinates with respect to CIE 2015 2° CMFs, will break the existing relation between BT.709 and BT.2020, as given by a colour space transformation matrix in ITU-R BT.2087.

This transformation matrix is the base for converting BT.2020 video signals to other colour spaces and vice versa. Such a definition is also required to convert signals for displays without native BT.2020 primary colours. Therefore, a video signal based on BT.2020 defined with CIE 1931 will be incompatible with the BT.2020 colour space defined with CIE 2015 2° and monochromatic light sources.

As not all displays are wide-gamut (e.g. BT.2020) capable, content from different colour spaces often needs to be mapped to BT.709. Colours inside the BT.709 colour space, for example, skin tones shall be visually identical on displays with different capabilities.

With existing products having a transformation matrix already built in, and existing content already converted between wide-colour gamut (BT.2020) and standard colour gamut (BT.709) and vice versa, having a new transformation matrix will result in incompatibilities, basically “starting over again” [IMAGO, 2025].

As compatibility is one of the main objectives for a smooth upgrade path, breaking existing colour space mappings is not desirable. All modern displays can, and are required to, do a simple linear matrix transformation. It is not important to match real colours with the primaries given in a colour space. Therefore, one initial idea behind BT.2020 to select a primary colour which is related to the native colours of a display is not important for modern technology.

Today, the intent of ITU-R BT.2020 can be seen more as a large transport container to best cover the Pointer’s Gamut. Using the existing linear matrix-based maths to convert from the redefined BT.709 to a CIE 2015 2° based BT.2020 seems to be reasonable and complies with the requirement defined on page 19.

For the redefinition of BT.2020, the already redefined BT.709 (Section 4.2) is transformed by the matrix given in ITU-R BT.2087. This ensures compatibility with existing products. As long as a display is calibrated to show colours of BT.709 content as expected, existing BT.2020 signals can also be shown as expected.

The colour space transformation matrix presented in ITU-R BT.2087 can be calculated and will give highly precise numbers. Even if in some cases these highly accurate numbers are required (e.g. to have accurate round-trips of signals), the rounded numbers given in ITU-R BT.2087 are often seen in implementations for colour space conversion.

For preserving the exact relation between BT.709 and BT.2020, a calculated transformation matrix is used to reach higher precision (see Section 7.7 for maths). Content conversion using the less precise matrix from standard documents will result in the same relation for rounding errors for both the original BT.2020 and the redefined BT.2020 colour spaces.

$$\begin{bmatrix} R_{\mathrm{BT.2020}} \\ G_{\mathrm{BT.2020}} \\ B_{\mathrm{BT.2020}} \end{bmatrix} = \begin{bmatrix} 0.6274039 & 0.3292830 & 0.0433131 \\ 0.0690973 & 0.9195404 & 0.0113623 \\ 0.0163914 & 0.0880133 & 0.8955953 \end{bmatrix} \begin{bmatrix} R_{\mathrm{BT.709}} \\ G_{\mathrm{BT.709}} \\ B_{\mathrm{BT.709}} \end{bmatrix}$$

*Equation 5: Exact colour space conversion Matrix for converting BT.709 to BT.2020.*

The matrix in Equation 5 shows the exact relation between the existing BT.709 and BT.2020 colour spaces. With the inverse of this matrix, this relation is bidirectional. The maths for converting one colour space to another using a transformation matrix can be implemented by linear mixing of CIE XYZ tristimulus values, as described in Section 7.9.

The resulting colour space does not correspond to any monochromatic light sources. As seen in Figure 19, the green and blue primaries for ITU-R BT.2020 are not even within the specular locus. As there are already colour spaces that use impossible, or imaginary colours like ACES AP0, this should not be a problem. It will just not be possible to reach 100% of this colour space, or to build a display with native BT.2020 primaries.

| **Primary** | $x_{\mathrm{CIE\ 2015\ 2°}}$ | $y_{\mathrm{CIE\ 2015\ 2°}}$ | **Luminance** |
|---|---|---|---|
| Red | 0.6963 | 0.6963 | 0.2793 |
| Green | 0.1831 | 0.1831 | 0.6462 |
| Blue | 0.1213 | 0.1213 | 0.07448 |
| White (D65) | 0.3135 | 0.3135 | 1.000 |

*Table 7: Redefined ITU-R BT.2020 (BT.2020) based on CIE 2015 2° CMFs (BT.2020$_{\mathrm{CIE\ 2015\ 2°}}$) with Luminances*

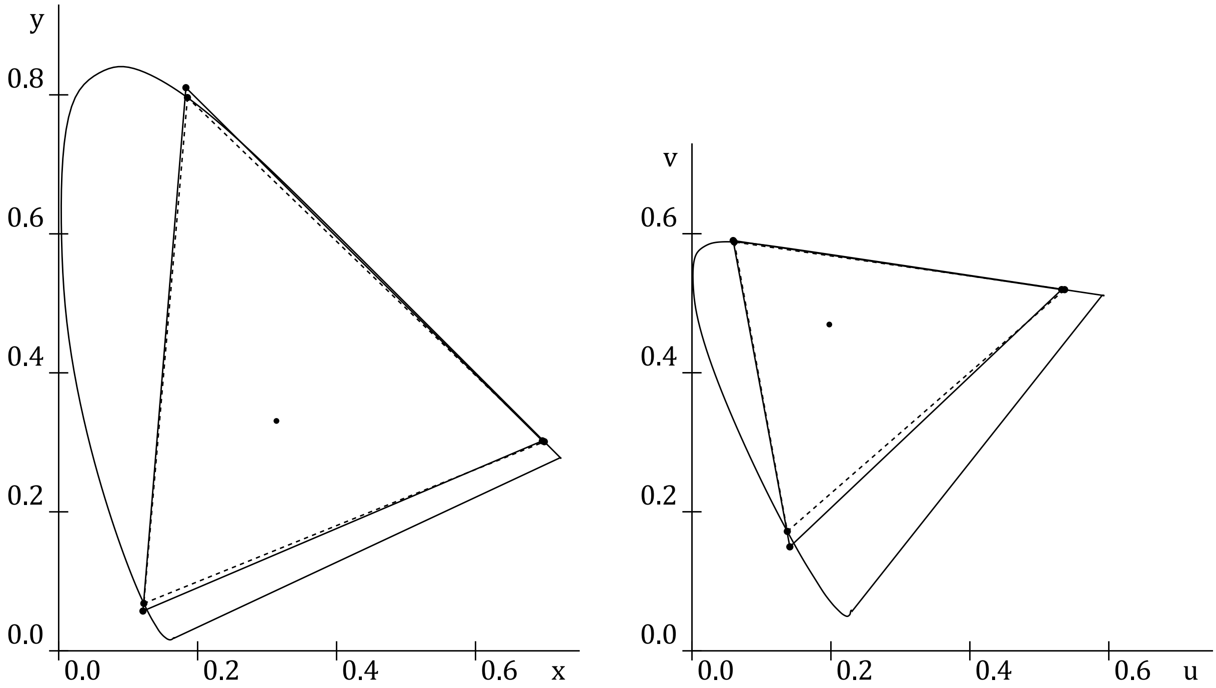


*Figure 19: Redefined ITU-R BT.2020 in CIE xy and CIE uv 1976 diagram, compared to monochromatic light sources as defined in the original BT.2020 colour space (dashed line).*

This approach has a significant impact on video signals, which shall represent monochromatic laser light. As long as DCI-P3 is used as the mastering gamut, as described in ITU-R BT.2407, these extremely saturated monochromatic colours will not be within a BT.2020 video signal. All colours which are inside BT.709 (skin tone, a lot of Pointer's gamut) will be displayed with the same accuracy as the redefined BT.709 colour space.

## 4.4. Redefinition of DCI-P3 D65 based on CIE 2015 2° CMFs

The DCI-P3 colour space (Table 8), created by Digital Cinema Initiatives (DCI), defines the required colour volume for a modern cinema projector. In addition to the BT.709 primaries, the HDR-Addendum created by DCI defines the primary chromaticity coordinates from DCI-P3 as test colours that must be within a certain precision for a certified product [DCI HDRD, 2024].

| Colour | x | y | Luminance |
|---|---|---|---|
| Red | 0.680 | 0.320 | 0.2290 |
| Green | 0.265 | 0.690 | 0.6917 |
| Blue | 0.150 | 0.060 | 0.07929 |
| White (D65) | 0.3127 | 0.3290 | 1.000 |

*Table 8: CIE 1931 based DCI-P3 colour space definition with D65 white point*

For display use, the DCI-P3 colour space is combined with the same D65 white point as BT.709 and BT.2020.

As already described in Section 4.3, colour spaces, which can be derived from BT.709, can be redefined in a compatible way with the existing transformation matrices. A redefinition of DCI-P3 can be done in the same way as described for BT.2020 in Section 4.3.

The Matrix for conversion from BT.709 RGB video signals to DCI-P3 RGB signals is given in Equation 6 and can be calculated as described in Section 7.7.

$$\begin{bmatrix} R_{\text{DCI-P3}} \\ G_{\text{DCI-P3}} \\ B_{\text{DCI-P3}} \end{bmatrix} = \begin{bmatrix} 0.8224620 & 0.1775380 & 0.0 \\ 0.0331942 & 0.9668058 & 0.0 \\ 0.0170826 & 0.0723974 & 0.9105199 \end{bmatrix} \begin{bmatrix} R_{\text{BT.709}} \\ G_{\text{BT.709}} \\ B_{\text{BT.709}} \end{bmatrix}$$

*Equation 6: Conversion matrix from ITU-R BT.709 to DCI-P3 D65*

This matrix can be used to convert the already redefined BT.709 colour space from Section 4.2 to a new DCI-P3 colour space.

| **Primary** | $x_{\mathrm{CIE\ 2015\ 2°}}$ | $y_{\mathrm{CIE\ 2015\ 2°}}$ | **Luminance** |
|---|---|---|---|
| Red | 0.6719 | 0.3280 | 0.2400 |
| Green | 0.2801 | 0.6949 | 0.6653 |
| Blue | 0.1407 | 0.07094 | 0.09461 |
| White (D65) | 0.3135 | 0.3308 | 1.000 |

*Table 9: CIE 2015 based DCI-P3 colour space definition with D65 white point.*

A modern RGB laser cinema projector, in theory, can show the new, redefined DCI-P3 colour space completely. In practice, the slight crosstalk between the primary colours due to contrast limits results in a slight trade-off for blue and red. These limitations as seen in Figure 20, while not critical in practice, in some cases do not allow full certifications for some products (cannot show 100% of the colour space).

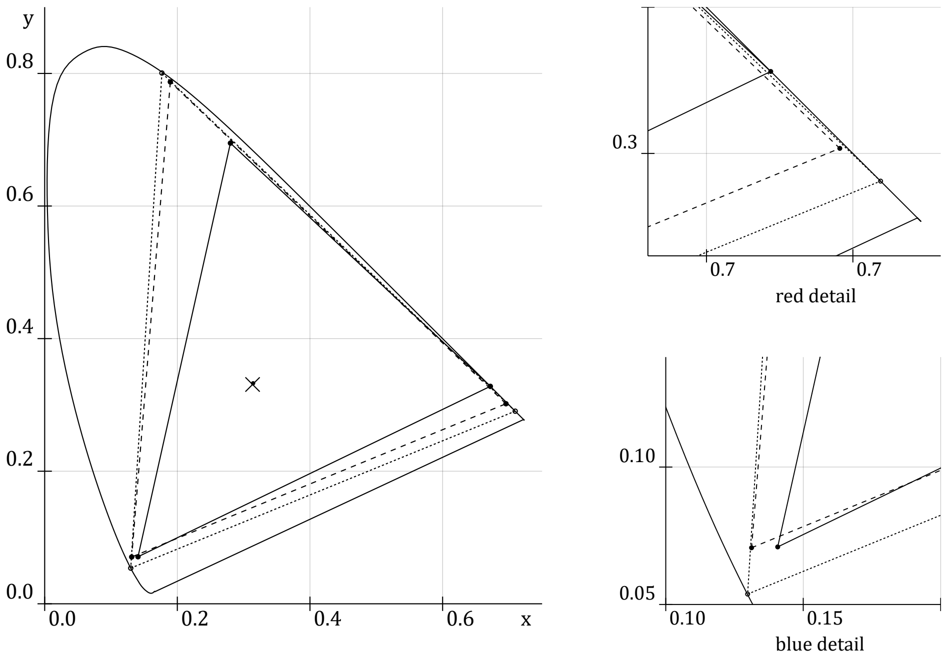


*Figure 20: CIE 2015 based DCI-P3 colour space (solid line) with D65 white point, compared to separated RGB laser primaries (dotted, outside line) and practical RGB laser primaries of a real projector (dashed line).*

The spectral power distributions for the primaries of an RGB laser projector are, in practice, not comparable to real monochromatic light. The CIE xy chromaticity coordinates remain extremely close to the specular locus when red, green, or blue are evaluated separately. Because all primary colours of the projector need to be turned on all the time, the limited contrast ratio leads to crosstalk (Figure 21) between colours, which is visible as slight desaturation.

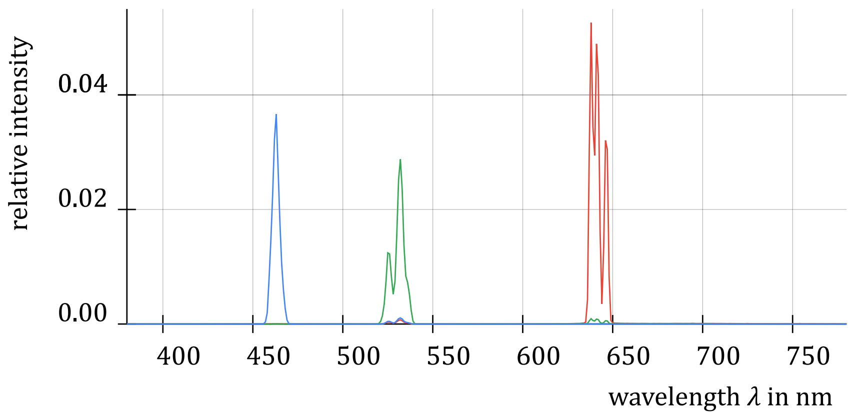


*Figure 21: SPDs of an RGB laser projector (Barco Nerthus), measured with 2nm spectral bandwidth*

The same simulation can be done for CIE 1931. While slightly running into limits for red, the same RGB laser projector is not running into limits for the CIE 1931 based DCI-P3 blue. Evaluations for colour gamut coverage need to be redone while using the redefined DCI-P3. The requirements in the DCI specification for primary colour accuracy may not be met with this redefined colour space for an RGB laser projector.

### 4.4.1. DCI-P3 based on synthetic SPDs

At the ICC Expert Day in Vienna (2025), another method for redefining a colour space was presented. By "using Optimal Spectral Stimuli" [Pruitt *et al.*, 2025], a display colour space is defined. For compatibility, DCI-P3 can be defined based on such synthetic SPDs. All other colour spaces can then be derived with the already existing colour space transformation matrices.

| **Primary colour** | **$x_{\text{CIE 2015 2°}}$** | | **$y_{\text{CIE 2015 2°}}$** | | **Error** | |
|---|---|---|---|---|---|---|
| | **this thesis** | **Pruitt et al.** | **this thesis** | **Pruitt et al.** | **CIEDE2000** | **$\Delta E^*_{\text{uv}}$** |
| Red | 0.6719 | 0.6730 | 0.3280 | 0.3270 | 0.20 | 1.3 |
| Green | 0.2801 | 0.2784 | 0.6949 | 0.6895 | 0.94 | 1.5 |
| Blue | 0.1407 | 0.1409 | 0.07094 | 0.0736 | 0.97 | 0.91 |
| White (D65) | 0.3135 | 0.3135 | 0.3308 | 0.3308 | 0.00 | 0.0 |

*Table 10: Comparison of two different approaches for redefining DCI-P3. The differences $\Delta E^*_{\text{uv}}$ and CIEDE2000 are calculated with the required luminances to mix the defined white point.*

Compared to the redefined DCI-P3 from this thesis, the redefinition proposed at ICC Expert Day by Pruitt *et al.* (2025) a slight difference (see Table 10) will be visible. Despite two different approaches, the results are still in the range of $\Delta E^*_{\text{uv}} > 2.6$ required for class 1 displays (skin tone only).

## 4.5. Other colour spaces

In practice, there are more than just these three colour spaces. Especially considering cameras, some vendors bring their own colour spaces. For example, Sony S-Gamut in multiple versions [SONY, 2014] or ARRI Wide Gamut [ARRI, 2025]. All these different colour spaces at some point need to be converted to a typical colour space for video signals or distribution systems.

As long as a colour space is defined in CIE 1931 xy chromaticity coordinates, a transformation matrix for CIE 1931 based colour spaces can be calculated, and the process, as used for BT.2020 and DCI-P3, is applicable.

# 5. Summary of the resulting colour spaces

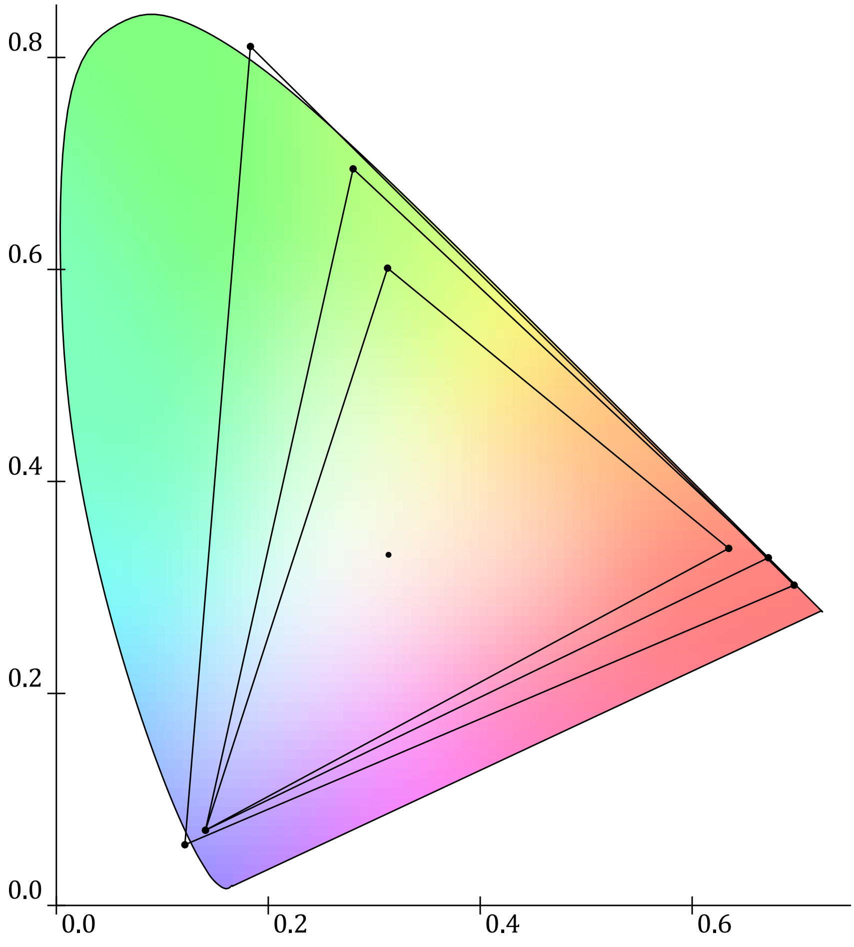


*Figure 22: CIE xy diagram of redefined colour spaces based on CIE 2015 2°*

| BT.709 | $x_{CIE\ 2015\ 2°}$ | $y_{CIE\ 2015\ 2°}$ | Luminance |
|---|---|---|---|
| Red | 0.6345 | 0.3369 | 0.2211 |
| Green | 0.3126 | 0.6012 | 0.6927 |
| Blue | 0.1407 | 0.07094 | 0.08614 |
| White (D65) | 0.3135 | 0.3308 | 1.0 |

*Table 11: CIE 2015 2° based ITU-R BT.709 and sRGB colour space definition.*

| DCI-P3 | $x_{CIE\ 2015\ 2°}$ | $y_{CIE\ 2015\ 2°}$ | Luminance |
|---|---|---|---|
| Red | 0.6719 | 0.3280 | 0.2400 |
| Green | 0.2801 | 0.6949 | 0.6653 |
| Blue | 0.1407 | 0.07094 | 0.09461 |
| White (D65) | 0.3135 | 0.3308 | 1.0 |

*Table 12: CIE 2015 2° based DCI-P3 (D65) colour space definition.*

| BT.2020 | $x_{CIE\ 2015\ 2°}$ | $y_{CIE\ 2015\ 2°}$ | Luminance |
|---|---|---|---|
| Red | 0.6963 | 0.3022 | 0.2793 |
| Green | 0.1831 | 0.8104 | 0.6462 |
| Blue | 0.1213 | 0.05724 | 0.07448 |
| White (D65) | 0.3135 | 0.3308 | 1.0 |

*Table 13: CIE 2015 2° based ITU-R BT.2020 colour space definition.*

## 5.1. Usage

For calibrating displays to absolute colour space primaries, it is important to check the display's capabilities first. Some, even modern wide-colour-gamut-capable displays, may not fully reproduce all defined primaries for a given colour space. LED screens, for example, often have 470 nm as their dominant blue wavelength. With such LEDs, it is impossible to accurately render BT.709 blue.

As a consequence, a display should be verified with slightly desaturated colours within the display gamut. For the DCI specification for projectors and LED screens, there are test signals with an absolutely defined CIE xy chromaticity coordinate. When generating such pairs of defined video signals and the CIE xy colour output of a display, the display's gamma needs to be taken into account.

Measuring and validating desaturated colours is extremely crucial for the redefined BT.2020, as the primary targets cannot be reached by any display.

# 6. Limits for redefined colour spaces

## 6.1. Colour changes due to gamma changes

Achieving a visual match for actual image content on multiple display technologies is more than just matching four colours (red, green, blue and white). A precise match of transfer functions (for example, gamma or PQ), black levels and white luminance is required. As already mentioned in Section 2.6, changing the opto-optical transfer functions of a system will lead to changes for some colours.

A redefined colour space on its own cannot help recreate the look of old CRT displays.

With modern OLED displays, low black levels seem desirable for high-contrast images. These effective changes in the EOTF also result in a changed colour appearance. Therefore, a redefined colour space, based on perfect CMFs, on its own, cannot guarantee an overall visual match.

## 6.2. Quality of CMFs

As the CIE 1931 CMFs are known to be imperfect, the CIE 2015 CMFs are not known to give perfect results in all circumstances. In the author's experience, the overall colour matching quality of the new CMFs is better, but with large differences for the blue primary colour, the results still seem inaccurate (simulated by ETC S4 Lustre X8, blue replaced by indigo). These observations are inline with the observations by Polster (2013) and Ko *et al.* (2023).

One of the reasons for this inaccuracy in the results is the difference between human individuals; age has a large influence [Bieske *et al.*, 2017]. For perfect results, it may be required to use a personal or age-optimised set of CMFs. While using a spectroradiometer, this is possible in theory, limitations in practice are obvious: A display calibrated for one human individual may produce wrong colours for someone else. For a general usable colour space, CMFs based on a large test group are needed to keep the average error low.

## 6.3. Redefined BT.2020 chromaticity coordinates outside the specular locus

The resulting redefined BT.2020 colour space is outside the specular locus. Consequently, it is not possible to reach 100% of the redefined BT.2020 colour space with lasers or with three light sources available at the moment. As BT.2020 at the time of writing, is often not used and only filled with colours that are contained in DCI-P3 [ITU-R BT.2407]. The impact of a colour space with imaginary colours is small. All modern displays (RGB Laser Projectors included) need a linear matrix which can be adjusted to convert different colour spaces in video signals to their own native colour space. The same process that is used to convert the existing BT.2020 signals to a BT.709 capable display can be used to convert the redefined BT.2020 colour space to the native RGB laser projector colour space.

A conversion from a larger to a smaller colour space may lead to negative RGB values for the display output. This is already the case in normal state-of-the-art video technology and is often solved by just clipping the negative values, consequently resulting in hue shifts. For example, converting a DCI-P3 primary red with 1 cd/m$^2$ to BT.709 will result in 1.22 cd/m$^2$ BT.709 red and −0.22 cd/m$^2$ green. As a display cannot reduce light below 0 cd/m$^2$, the most simple approach is to ignore negative values and show a pure, brighter BT.709 red instead.

Compared to a BT.2020 or DCI-P3 red, the BT.709 red appears orange. This problem already exists in state-of-the-art video technology and is not solved by redefined colour spaces. However, colour appearance models for mapping different colour gamuts can be improved by using an optimized $V_F(\lambda)$ function.

## 6.4. Luminance separated signals

When video signals are transmitted over cables, the chroma resolution is often reduced. For example, the SDI signal typically reduces the horizontal resolution for the chroma components Cb and Cr by a factor of two.

The matrix used for chroma separation is directly derived from the colour primaries of the colour space. With the change of the CMFs and consequently, the change of the colour space chromaticity coordinates, a new matrix for converting to chroma-separated signals is required.

As the existing matrix is based on an imperfect $V(\lambda)$, the resulting Y'CbCr signals already hold some crosstalk between chroma and luminance. With this crosstalk, a small part of the luminance is encoded in the chroma components. If chroma resolution is reduced, this also leads to a slightly reduced resolution for luminance.

Adding redefined luminance separation matrices to the colour spaces redefined based on CIE 2015 2° CMFs is possible, but adoption will be extremely slow. For being compatible with existing video signals and old hardware, and as there is little space for signalling required metadata in SDI, it is crucial not to change the luminance separation matrices already implemented.

## 6.5. Displays with white point adjustment only

While Sony is only implementing offsets for the white point [SONY, 2013], the redefined colour spaces are also changing the primary colours. If a display does not have the possibility for adjusting the linear matrix used for colour space processing, an external processing unit is needed for calibration. Compared to internal image processing, this can lead to reduced image quality, especially while using 8-bit video signals.

## 6.6. Visually corrected or graded content

Content which is graded and colour corrected, for example, by just empirically and visually adjusting white, may have a correction built in if graded on a display calibrated strictly with the use of CIE 1931 (greenish white on display leads to a magenta offset in content).

Content with such a visual correction, without technical white, will be shown with an undesired visual offset on a display which is calibrated by using different CMFs.

# 7. Maths

## 7.1. Precision of numbers, verification of maths

Most of the maths in this thesis is run with Node.js version 24.13.1 using 64-bit floating-point precision (IEEE 754). Interim results given in the text are rounded to a useful precision. However, whenever possible, the exact result in 64-bit floating-point is used for further calculations. In some cases, it is very important to maintain the highest possible precision in image processing, especially when multiple round-trip calculations are required, even if a measured number cannot be considered precise at all.

As 64-bit floating-point itself introduces errors at each processing step (steps are only visible while analysing assembler code), the precision of the results needs some investigation [ECMA-262, 2025]. The largest error in floating point is introduced while adding (or subtracting) a very large number to a very small number. None of the used maths should introduce such large errors. None of the maths uses long cascaded loops for generating numbers.

As all the values for CMFs, SPDs or colour spaces are given with 8-figure precision or less, the resulting precision of 64-bit floating point used in Node.js is therefore seen as acceptable (15-figure precision reduced by multiplications and additions).

Most of the maths implemented and used in this thesis was tested by recalculating values defined in standard documents. If not possible, results or source code were compared to the open-source Python “Colour Science” implementation [Colour, 2025].

## 7.2. Estimating the required precision for xy chromaticity coordinates

Following the theory that an $IC_tC_p$ based video signal with 12-bit quantization and the perceptual quantizer (PQ) as electro-optical transfer function (EOTF) is precise enough for indistinguishable stimuli on a perfect display, changes in such a video signal can be used to get the required precision for CIE xy chromaticity coordinates.

In Table 14, the BT.2020 primary colours and white are encoded as an $IC_tC_p$ video signal, slightly changed and a difference for CIE xy chromaticity coordinates is given.

| | $IC_tC_p$ signal | | | chromaticity coordinate | | difference | |
|---|---|---|---|---|---|---|---|
| | I | $C_t$ | $C_p$ | x | y | Δx | Δy |
| **White** | **2081** | **2048** | **2048** | **0.312700** | **0.329000** | | |
| | 2081 | 2049 | 2048 | 0.312620 | 0.328772 | 0.000080 | 0.000228 |
| | 2081 | 2048 | 2049 | 0.312972 | 0.329007 | -0.000272 | -0.000007 |
| | 2081 | 2049 | 2049 | 0.312892 | 0.328779 | -0.000192 | 0.000221 |
| | 2081 | 2047 | 2047 | 0.312508 | 0.329221 | 0.000192 | -0.000221 |
| | 2081 | 2047 | 2048 | 0.312780 | 0.329228 | -0.000080 | -0.000228 |
| | 2081 | 2048 | 2047 | 0.312428 | 0.328993 | 0.000272 | 0.000007 |
| **Red** | **1563** | **1588** | **3570** | **0.708000** | **0.292000** | | |
| | 1563 | 1589 | 3570 | 0.708001 | 0.291941 | -0.000001 | 0.000059 |
| | 1563 | 1588 | 3571 | 0.708163 | 0.291893 | -0.000163 | 0.000107 |
| | 1563 | 1589 | 3571 | 0.708127 | 0.291859 | -0.000127 | 0.000141 |
| | 1563 | 1587 | 3569 | 0.707949 | 0.292090 | 0.000051 | -0.000090 |
| | 1563 | 1587 | 3570 | 0.708074 | 0.292008 | -0.000074 | -0.000008 |
| | 1563 | 1588 | 3569 | 0.707912 | 0.292056 | 0.000088 | -0.000056 |
| **Green** | **1884** | **461** | **1603** | **0.170000** | **0.797000** | | |
| | 1884 | 462 | 1603 | 0.170175 | 0.796649 | -0.000175 | 0.000351 |
| | 1884 | 461 | 1604 | 0.170710 | 0.796418 | -0.000710 | 0.000582 |
| | 1884 | 462 | 1604 | 0.170751 | 0.796195 | -0.000751 | 0.000805 |
| | 1884 | 460 | 1602 | 0.169516 | 0.797551 | 0.000484 | -0.000551 |
| | 1884 | 460 | 1603 | 0.170093 | 0.797095 | -0.000093 | -0.000095 |
| | 1884 | 461 | 1602 | 0.169557 | 0.797327 | 0.000443 | -0.000327 |
| **Blue** | **1177** | **3078** | **1163** | **0.131000** | **0.046000** | | |
| | 1177 | 3079 | 1163 | 0.131024 | 0.045880 | -0.000024 | 0.000120 |
| | 1177 | 3078 | 1164 | 0.131042 | 0.046027 | -0.000042 | -0.000027 |
| | 1177 | 3079 | 1164 | 0.131076 | 0.045923 | -0.000076 | 0.000077 |
| | 1177 | 3077 | 1162 | 0.130904 | 0.046046 | 0.000096 | -0.000046 |
| | 1177 | 3077 | 1163 | 0.130956 | 0.046089 | 0.000044 | -0.000089 |
| | 1177 | 3078 | 1162 | 0.130938 | 0.045942 | 0.000062 | 0.000058 |

*Table 14: Resulting CIE 1931 chromaticity coordinate differences for indistinguishable colour changes in an ICtCp, 12-bit, full range, PQ video signal.*

In general, changes below ±0.0002 for $\Delta$x or $\Delta$y can be seen as indistinguishable. This is also true for a D65 white point, which sometimes is given with 6-figure precision. For a colour space definition, 4 figures of precision is desirable. While this precision is outside the range of uncertainty of modern spectroradiometers, defining a colour space with this precision ensures a numerical difference to the next visible different stimuli on a modern display.

Green is overrepresented in the CIE diagram compared to $IC_tC_p$, which explains the larger tolerable difference for green.

While investigating Dolby and ITU-R BT.2390 documents, 11.5 bits are enough for indistinguishable colour differences. For luminance changes only, 11 bits of precision when encoded with PQ is enough to outperform the human eye's contrast sensitivity as calculated by Barten (1999). With 11 bits of signal precision, the required colour space still needs to be precise within ±0.0004 for $\Delta$ x or $\Delta$y.

### 7.2.1. Encoding BT.2020 RGB to $IC_tC_p$ with PQ

The maths for generating $IC_tC_p$ video signal values from BT.2020 RGB equations are given by ITU-R BT.2100 documents. For processing the required CIE xy chromaticity coordinate precision, rounded 12-bit $IC_tC_p$ values are required. The modification is included in Equation 7.

The maths and numbers given in BT.2100 and corresponding white papers by Dolby, concerning PQ and LMS conversions, are often given as integer multiplication and bit-shift based divisions (divide by power of two) for FPGA implementation with 12-bit precision. The numbers given by standard documents are presented here, numbers which are calculated, rounded and used with floating point will have slightly different rounding errors (binary compared to decimal rounded values).

$$M_{\text{BT.2020 to LMS BT.2100}} = \begin{bmatrix} \frac{1688}{4096} & \frac{2146}{4096} & \frac{262}{4096} \\ \frac{683}{4096} & \frac{2951}{4096} & \frac{462}{4096} \\ \frac{99}{4096} & \frac{309}{4096} & \frac{3688}{4096} \end{bmatrix}$$

$$M_{\text{L'M'S' to ICtCp BT.2100}} = \begin{bmatrix} 0.5 & 0.5 & 0 \\ \frac{6610}{4096} & -\frac{13613}{4096} & \frac{7003}{4096} \\ \frac{17933}{4096} & -\frac{17390}{4096} & -\frac{543}{4096} \end{bmatrix}$$

*Conversion matrices used in ITU-R BT.2100.*

$$\begin{bmatrix} L \\ M \\ S \end{bmatrix} = M_{\text{BT.2020 to LMS BT.2100}} \begin{bmatrix} R \\ G \\ B \end{bmatrix}$$

*R,G,B in the range of 0.0 for black,*

*1.0 for diffuse white defined with 100 cd/m²*

*and 100.0 as peak white of 10 000 cd/m² by PQ.*

$$\begin{bmatrix} L' \\ M' \\ S' \end{bmatrix} = \begin{bmatrix} EOTF^{-1}(L) \\ EOTF^{-1}(M) \\ EOTF^{-1}(S) \end{bmatrix}$$

$$\begin{bmatrix} I \\ C_t \\ C_p \end{bmatrix} = M_{\text{L'M'S' to ICtCp BT.2100}} \begin{bmatrix} L' \\ M' \\ S' \end{bmatrix}$$

*The resulting I value is scaled to [0,1], where 0.508 represents diffuse white. Ct and Cp values are scaled to [−0.5, +0.5] while 0.0 corresponds to neutral grey. The matrix for calculating ICtCp values also introduces a rotation for basic compatibility with Y'CbCr signals.*

$$\begin{bmatrix} I_{\text{12-bit}} \\ C_{t\ \text{12-bit}} \\ C_{p\ \text{12-bit}} \end{bmatrix} = \begin{bmatrix} 4095I \\ (4095C_t) + 2048 \\ (4095C_p) + 2048 \end{bmatrix}$$

*Equation 7: BT.2020 RGB to ICtCp 12-bit conversion.*

$$[M_{\text{BT.2020 to LMS BT.2100}}]^{-1} = \begin{bmatrix} 3.4366 & -2.5065 & 0.069854 \\ -0.79133 & 1.9836 & -0.19227 \\ -0.025950 & -0.098914 & 1.1249 \end{bmatrix}$$

$$[M_{\text{L'M'S' to ICtCp BT.2100}}]^{-1} = \begin{bmatrix} 1 & 0.0086090 & 0.11103 \\ 1 & -0.0086090 & -0.11103 \\ 1 & 0.56003 & -0.32063 \end{bmatrix}$$

*Equation 8: Inverse matrices used for inverting maths given in BT.2100.*

$$\begin{bmatrix} I \\ C_t \\ C_p \end{bmatrix} = \begin{bmatrix} \frac{I_{\text{12-bit}}}{4095} \\ \frac{(C_{t\ \text{12-bit}})-2048}{4095} \\ \frac{(C_{p\ \text{12-bit}})-2048}{4095} \end{bmatrix}$$

$$\begin{bmatrix} L' \\ M' \\ S' \end{bmatrix} = \left[M_{\text{L'M'S' to ICtCp BT.2100}}\right]^{-1} \begin{bmatrix} I \\ C_t \\ C_p \end{bmatrix}$$

$$\begin{bmatrix} L \\ M \\ S \end{bmatrix} = \begin{bmatrix} EOTF(L') \\ EOTF(M') \\ EOTF(S') \end{bmatrix}$$

$$\begin{bmatrix} R \\ G \\ B \end{bmatrix} = \left[M_{\text{BT.2020 to LMS BT.2100}}\right]^{-1} \begin{bmatrix} L \\ M \\ S \end{bmatrix}$$

*Equation 9: ICtCp 12-bit conversion to BT.2020 RGB, inverting Equation 7.*

$$E = EOTF(E') = \left( \frac{\max\left(\left(E'^{\frac{1}{m_2}} - c_1\right), 0\right)}{c_2 - c_3^{\frac{1}{m_2}}} \right)^{\frac{1}{m_1}}$$

*$E$ is the intensity of linear light in the range [0,1] where 1.0 corresponds to a luminance of 10 000 cd/m$^2$. $E'$ is the non-linear representation in the range [0,1]. The constants are defined with:*

$$m_1 = \frac{2610}{16384} = 0.1593017578125$$

$$m_2 = \frac{2523}{4096} \cdot 128 = 78.84375$$

$$c_1 = \frac{3424}{4096} = 0.8359375 = c_3 - c_2 + 1$$

$$c_2 = \frac{2413}{4096} \cdot 32 = 18.8515625$$

$$c_3 = \frac{2392}{4096} \cdot 32 = 18.6875$$

*Equation 10: PQ EOTF as defined in ITU-R BT.2100*

$$E' = EOTF^{-1}(E) = \left(\frac{c_1 + c_2 E^{m_1}}{1 + c_3 E^{m_1}}\right)^{m}_{2})$$

*with the constants $m_1, m_2, c_1, c_2, c_3$ defined in Equation 10*

*Equation 11: PQ EOTF^-1 as defined in BT.2100, inverting Equation 10*

## 7.3. Colour matching functions

The most general form of colour-matching functions can be expressed as in Equation 12. $X, Y$ and $Z$ is a three-dimensional value as required for Grassmann's first law.

$$X = \int_\lambda \bar{x}(\lambda) P(\lambda) d(\lambda)$$

$$Y = \int_\lambda \bar{y}(\lambda) P(\lambda) d(\lambda)$$

$$Z = \int_\lambda \bar{z}(\lambda) P(\lambda) d(\lambda)$$

*Equation 12: General form of colour-matching functions*

The mathematical framework around the CIE 1931 standard observer can be reused for other colour-matching functions, such as the CIE 2015 based ones. The CIE standards use the $F$ indices to distinguish between CIE 1931 and CIE 2015. For simplicity, the indices are removed here. The maths can be used for both standards.

A set of three colour-matching functions can be generated to result in $L, M, S$ cone-based values or directly result in BT.2020 or BT.709 based $R, G, B$ values by linear transformation. In practice, the CIE XYZ tristimulus values are used, where Y represents the luminance of stimuli. The functions $\bar{x}(\lambda), \bar{y}(\lambda)$ and $\bar{z}(\lambda)$ are given as a table with 1nm intervals. The $P(\lambda)$ can be a measured SPD also given in 1 nm intervals. Therefore, the integral can be replaced by a summation.

$$X = K_m \sum_\lambda \bar{x}(\lambda) P(\lambda)$$

$$Y = K_m \sum_\lambda \bar{y}(\lambda) P(\lambda)$$

$$Z = K_m \sum_\lambda \bar{z}(\lambda) P(\lambda)$$

*Equation 13: Summation form of colour-matching functions.*

The tables for the CIE 2015 colour-matching functions are given between 390 nm and 830 nm. CIE 1931 is defined between 380 nm and 780 nm. The SPDs for CIE standard illuminants are given in the range 300 nm to 780 nm. The D series can be calculated up to 830 nm. Measured results from Konica Minolta CS-2000, as well as values from JETI specbos 2501-HiRes spectroradiometers, are in the range from 380 to 780 nm. Output from the devices is taken in 1 nm intervals.

The different shapes of the tables are corrected by adding zero values for missing wavelengths. Interpolation for the CIE illuminant series D is done linearly. Tables for the used CMFs can be found in Appendix A.5 and Appendix A.6.

When calculating the luminance of a measured SPD, the photopic luminous efficacy scaling factor $K_m$ needs to be used. This value is often given as $K(\lambda_d) = 683\frac{lm}{W}$. As all luminances of the measured values are normalized in this thesis, the approximation could be used for both CIE 1931 and CIE 2015. This value has no effect on the the CIE chromaticity coordinates.

The precise value in the case of CIE 1931 is given as $K_m = 683.002\frac{lm}{W}$ .

The CIE 2015 based $V_F(\lambda)$ is scaled to unity peak (value of 1.0) at $556.1nm$ [CIE 170-2:2015] compared to the original $V(\lambda)$, which peaks at $555nm$. The expected unity peak for $K_m = 683\frac{lm}{W}$ is at $540\ THz$, which corresponds to $\lambda_d = 555.016nm$ in air [Wyszecki & Stiles, 2000].

With linear scaling, $V_F(\lambda)$ equals $0.999535872$ at $\lambda_d$ .

$$K_{m\ CIE2015\ 2^\circ} = \frac{K(\lambda_d)}{V_F(\lambda_d)} = 683.317\frac{lm}{W}$$

When calculating luminances in $\frac{cd}{m^2}$ with CIE 2015 2° the new $K_{m\ CIE2015\ 2^\circ}$ needs to be used.

## 7.4. CIE XYZ to CIE xy and CIE 1976 u'v' chromaticity coordinates

$$x = \frac{X}{X+Y+Z}$$

$$y = \frac{Y}{X+Y+Z}$$

$$L = Y \text{ (luminance)}$$

*Equation 14: Calculation of the CIE xy chromaticity coordinates [Wyszecki & Stiles, 2000, p. 156].*

$$u' = \frac{4x}{-2x + 12y + 3}$$

$$v' = \frac{6y}{-2x + 12y + 3}$$

*Equation 15: Calculation of the CIE 1976 u'v' [Wyszecki & Stiles, 2000, p.165].*

## 7.5. Calculating the CIE 1976 L*u*v* (CIELUV) uniform colour space

With $u'$ and $v'$ from Equation 15, the CIELUV uniform colour space can be calculated.

$$L_{a/n}* = \begin{cases} 116\left(\frac{Y_a}{Y_n}\right)^{\frac{1}{3}} - 16 & \text{for} \quad \frac{Y_a}{Y_n} > \frac{216}{24389} \\ \frac{24389}{27}\left(\frac{Y_a}{Y_n}\right) & \text{for} \quad \frac{Y_a}{Y_n} \leq \frac{216}{24389} \end{cases}$$

$$u_a* = 13\ L_{a/n}*\ (u'_a - u'_n)$$
$$v_a* = 13\ L_{a/n}*\ (v'_a - v'_n)$$

*Equation 16: Calculation of the CIE 1976 L*u*v* colour space.*

$Y_n$, $u'_n$ and $v'_n$ refer to the reference white point. In case of CIE 1931 and display applications, the chromaticity coordinates $u'_{D65} = 0.1978$ and $v'_{D65} = 0.4683$ can be used. For a class 1 or grade 1 display $Y_n = 100cd/m^2$ is used. The normalized luminance values in this thesis are scaled to $Y_n = 100cd/m^2$ when used in the CIELUV maths.

## 7.6. Calculating $\Delta E*_{uv}$

$\Delta E*_{uv}$ is a simple method for calculating colour differences used in EBU Tech 3320.

$$\Delta L* = L_1* - L_2*$$
$$\Delta u* = u_1* - u_2*$$
$$\Delta v* = v_1* - v_2*$$

$$\Delta E*_{uv} = \sqrt{\Delta L*^2 + \Delta u*^2 + \Delta v*^2}$$

*Equation 17: Calculation of the CIE 1976 L*u*v* based $\Delta E*_{uv}$.*

$L_1*, u_1*, v_1*$ and $L_2*, u_2*, v_2*$ are two colours with respect to the same white point calculated by Equation 16.

## 7.7. Calculating an RGB to XYZ matrix

For the conversion of colour spaces, the transformation matrix which is used for RGB to XYZ conversion is most useful. Sometimes this matrix is given in standard documents. For example, ITU-R BT.2390 gives two broadly used conversion matrices. Each of these matrices allows bidirectional conversion by using the inverse matrix.

$$\begin{aligned} M_{\text{XYZ to BT.2020}} &= \begin{bmatrix} 1.717 & -0.356 & -0.253 \\ -0.667 & 1.515 & 0.016 \\ 0.018 & -0.043 & 0.942 \end{bmatrix} \\ M_{\text{BT.2020 to XYZ}} &= \left[M_{\text{XYZ to BT.2020}}\right]^{-1} \end{aligned}$$

$$\begin{aligned} M_{\text{XYZ to LMS}} &= \begin{bmatrix} 0.359 & 0.696 & -0.036 \\ -0.192 & 1.100 & 0.075 \\ 0.007 & 0.075 & 0.843 \end{bmatrix} \\ M_{\text{LMS to XYZ}} &= \left[M_{\text{XYZ to LMS}}\right]^{-1} \end{aligned}$$

*Equation 18: Example conversion matrices*

These matrices are taken directly from the standards. In the case of the $M_{\text{XYZ to LMS}}$, the value $0.007$ has a questionable precision of only one figure. As these matrices in standard documents may be implemented in products, it is desirable to implement colour space transformation with the same rounding errors as decided by the standard committee. For a round-trip between colour spaces, a precise version of at least the inverse matrix should be used.

For direct colour space conversion, it is possible to combine two matrices. If the matrices are based on colour spaces with different white points, a chromatic adaptation algorithm must be used (see Section 8.2).

$$M_{\text{BT.2020 to LMS}} = M_{XYZ\ to\ LMS} \cdot \left[M_{XYZ\ to\ BT.2020}\right]^{-1}$$

*Equation 19: Combination of two matrices*

In a general form, a transformation matrix between two colour spaces $(ca)$ and $(cb)$ can be calculated by combining the matrices used for conversion to XYZ.

$$M_{ca\ to\ cb} = \left[M_{cb\ to\ XYZ}\right]^{-1} \cdot M_{ca\ to\ XYZ}$$

*Equation 20: Combination of two matrices*

For all colour spaces given in CIE xy chromaticity coordinates for primary colours and white, a transformation matrix can be calculated.

The maths presented here are available in a simple but slightly incomplete form on the website of Lindbloom (2017), a well-proven source for colour maths. The equations presented here have been implemented and verified for use in production systems by the author of this thesis. The numbers given in the standard documents can all be reproduced with these equations. It also corresponds to the maths given by Poynton (2012), p. 306.

$$M_{\text{RGB to XYZ}} = \begin{bmatrix} S_r \cdot X_r & S_g \cdot X_g & S_b \cdot X_b \\ S_r \cdot Y_r & S_g \cdot Y_g & S_b \cdot Y_b \\ S_r \cdot Z_r & S_g \cdot Z_g & S_b \cdot Z_b \end{bmatrix}$$

$$\begin{bmatrix} S_r \\ S_g \\ S_b \end{bmatrix} = \begin{bmatrix} X_r & X_g & X_b \\ Y_r & Y_g & Y_b \\ Z_r & Z_g & Z_b \end{bmatrix}^{-1} \cdot \begin{bmatrix} X_w \\ Y_w \\ Z_w \end{bmatrix}$$

$$X_r = \frac{x_r}{y_r} \qquad X_g = \frac{x_g}{y_g} \qquad X_b = \frac{x_b}{y_b} \qquad X_w = \frac{x_w}{y_w}$$

$$Y_r = Y_g = Y_b = Y_w = 1$$

$$Z_r = \frac{1 - x_r - y_r}{y_r} \qquad Z_g = \frac{1 - x_g - y_g}{y_g} \qquad Z_b = \frac{1 - x_b - y_b}{y_b} \qquad Z_w = \frac{1 - x_w - y_w}{y_w}$$

*Equation 21: Calculating RGB to XYZ transformation matrix.*

## 7.8. Calculating required luminance for target white point

$$\begin{bmatrix} X \\ Y \\ Z \end{bmatrix} = \begin{bmatrix} 0.4123908 & 0.3575843 & 0.1804808 \\ 0.2126390 & 0.7151687 & 0.0721923 \\ 0.0193308 & 0.1191948 & 0.9505322 \end{bmatrix} \begin{bmatrix} R_{BT.709} \\ G_{BT.709} \\ B_{BT.709} \end{bmatrix}$$

*Equation 22: BT.709 conversion matrix for converting RGB to XYZ*

As seen in Equation 22, the luminance $Y$ of the CIE XYZ tristimulus value consists of $0.2126390 \cdot R + 0.7151687 \cdot G + 0.0721923 \cdot B$. An RGB signal of [1,1,1] will result in CIE XYZ values for the D65 white point with $Y = 1$.

For all colour spaces, the $M_{\text{colour space to XYZ}}$ matrix includes how much relative luminance is required of each primary colour to produce the defined white point.

These values can also be seen in the maths for luminance separated signals in ITU-R BT.709.

## 7.9. Converting colour spaces based on a transformation matrix

A transformation matrix for conversion between two colour spaces defines the relative luminance needed for the red, green and blue primaries of one colour space, for creating a colour of another colour space.

$$\begin{bmatrix} R_{BT.709} \\ G_{BT.709} \\ B_{BT.709} \end{bmatrix} = \begin{bmatrix} 1.6604910 & \text{-}0.5876411 & \text{-}0.0728499 \\ \text{-}0.1245505 & 1.1328999 & \text{-}0.0083494 \\ \text{-}0.0181508 & \text{-}0.1005789 & 1.1187297 \end{bmatrix} \begin{bmatrix} R_{BT.2020} \\ G_{BT.2020} \\ B_{BT.2020} \end{bmatrix}$$

*Equation 23: BT.2020 to BT.709 conversion matrix*

The matrix given in Equation 23 defines that a BT.2020 native red will result in a linear BT.709 video signal of $R = 1.6604910, B = \text{-}0.5876411, G = \text{-}0.0728499$. The conclusion is, with BT.709 primary colours, a BT.2020 red can be mixed by adding negative luminances of BT.709 blue and BT.709 green to the native BT.709 red. While it is physically impossible to turn on a light source with a negative luminance, this theoretical concept can be used to mix CIE xy chromaticity coordinates.

Calculating a colour space $(cb)$ based on a colour space $(ca)$ is done with the Matrix $M_{ca\ to\ cb}$, the inverse of the intuitive selected $M_{cb\ to\ ca}$.

Mixing CIE xy chromaticity coordinates can be done by additive mixing of their corresponding CIE XYZ tristimulus values.

$$
\begin{aligned}
X &= \frac{x}{y}L \\
Y &= L \text{ (luminance)} \\
Z &= \frac{1-x-y}{y}L
\end{aligned}
$$

$$
\begin{aligned}
x &= \frac{X}{X+Y+Z} \\
y &= \frac{Y}{X+Y+Z} \\
L &= Y \text{ (luminance)}
\end{aligned}
$$

*Equation 24: Equations for round trip between CIE XYZ and CIE xy, including luminance.*

With the conversion maths given in Equation 24, general and simplified equations for mixing colours can be created. If the white point of the colour space does not change, no calculation is needed for the CIE xy chromaticity coordinates of white. However, the luminance of the primaries required to create white is needed.

$$x_{Rcb} = \frac{\frac{x_{Rca}}{y_{Rca}} L_{Rca} M_{11} + \frac{x_{Gca}}{y_{Gca}} L_{Gca} M_{12} + \frac{x_{Bca}}{y_{Bca}} L_{Bca} M_{13}}{\frac{M_{11}}{y_{Rca}} + \frac{M_{12}}{y_{Gca}} + \frac{M_{13}}{y_{Bca}}}$$

$$y_{Rcb} = \frac{L_{Rca} M_{11} + L_{Gca} M_{12} + L_{Bca} M_{13}}{\frac{M_{11}}{y_{Rca}} + \frac{M_{12}}{y_{Gca}} + \frac{M_{13}}{y_{Bca}}}$$

$$L_{Rcb} = M_{11} L_{Rca} + M_{12} L_{Gca} + M_{13} L_{Bca}$$

$$x_{Gcb} = \frac{\frac{x_{Rca}}{y_{Rca}} L_{Rca} M_{21} + \frac{x_{Gca}}{y_{Gca}} L_{Gca} M_{22} + \frac{x_{Bca}}{y_{Bca}} L_{Bca} M_{23}}{L_{Rca} \frac{M_{21}}{y_{Rca}} + L_{Gca} \frac{M_{22}}{y_{Gca}} + L_{Bca} \frac{M_{23}}{y_{Bca}}}$$

$$y_{Gcb} = \frac{L_{Rca} M_{21} + L_{Gca} M_{22} + L_{Bca} M_{23}}{L_{Rca} \frac{M_{21}}{y_{Rca}} + L_{Gca} \frac{M_{22}}{y_{Gca}} + L_{Bca} \frac{M_{23}}{y_{Bca}}}$$

$$L_{Gcb} = M_{21} L_{Rca} + L_{Gca} M_{22} L_{Gca} + L_{Bca} M_{23} L_{Bca}$$

$$x_{Bcb} = \frac{\frac{x_{Rca}}{y_{Rca}} L_{Rca} M_{31} + \frac{x_{Gca}}{y_{Gca}} L_{Gca} M_{32} + \frac{x_{Bca}}{y_{Bca}} L_{Gca} M_{33}}{L_{Rca} \frac{M_{31}}{y_{Rca}} + L_{Gca} \frac{M_{32}}{y_{Gca}} + L_{Gca} \frac{M_{33}}{y_{Bca}}}$$

$$y_{Bcb} = \frac{L_{Rca} M_{31} + L_{Gca} M_{32} + L_{Gca} M_{33}}{L_{Rca} \frac{M_{31}}{y_{Rca}} + L_{Gca} \frac{M_{32}}{y_{Gca}} + L_{Gca} \frac{M_{33}}{y_{Bca}}}$$

$$L_{Bcb} = L_{Rca} M_{31} L_{Rca} + L_{Gca} M_{32} L_{Gca} + L_{Gca} M_{33} L_{Bca}$$

*with the transformation matrix*

$$\begin{bmatrix} R_{ca} \\ G_{ca} \\ B_{ca} \end{bmatrix} = \begin{bmatrix} M_{11} & M_{12} & M_{13} \\ M_{21} & M_{22} & M_{23} \\ M_{31} & M_{32} & M_{33} \end{bmatrix} \begin{bmatrix} R_{cb} \\ G_{cb} \\ B_{cb} \end{bmatrix}$$

*Equation 25: Maths for mixing three CIE xy chromaticity coordinates based on a colour space transformation matrix.*

## 7.10. Calculating CIE Illuminant Series D SPDs

The exact physical colour for a CIE illuminant series D light, with a given colour temperature $T_C$ in the range [4000 K, 25000 K], is defined by a linear combination of spectral power distributions.

$$S_{D(\lambda)} = S_0(\lambda) + M_1 S_1(\lambda) + M_2 S_2(\lambda)$$

*with*

$$M_1 = \frac{-1.3515 - 1.7703 x_D + 5.9114 y_D}{0.0241 + 0.2562 x_D - 0.7341 y_D}$$

$$M_2 = \frac{0.0300 - 31.4424 x_D + 30.0717 y_D}{0.0241 + 0.2562 x_D - 0.7341 y_D}$$

$$y_D = -3.000 x_D^2 + 2.870 x_D - 0.275$$

$$x_D = \begin{cases} -4.6070 \frac{10^9}{T_C^3} + 2.9678 \frac{10^6}{T_C^2} + 0.09911 \frac{10^3}{T_C} + 0.244063 & \text{for} \quad 4000K \leq T_C \leq 7000K \\ -2.0064 \frac{10^9}{T_C^3} + 1.9018 \frac{10^6}{T_C^2} + 0.24748 \frac{10^3}{T_C} + 0.237040 & \text{for} \quad 7000K < T_C \leq 25000K \end{cases}$$

*Equation 26: Calculating the CIE Illuminant Series D SPD [Wyszecki & Stiles, 2000, p. 146]*

$S_D(\lambda)$ is the spectral power distribution for the D series white point.

$S_0(\lambda)$ is the mean of all daylight distributions with the two most important eigenvectors $S_1(\lambda)$ and $S_2(\lambda)$ [Wyszecki & Stiles, 2000, p. 147].

$x_D$ and $y_D$ are the CIE 1931 2° chromaticity coordinates of the resulting white point.

For a $T_C$ of 6504 K, the intermediate values are:

$$\begin{aligned} M_{1_{D65}} &= \text{-}0.294470 \\ M_{2_{D65}} &= \text{-}0.689214 \\ x_{D65} &= 0.312714 \\ y_{D65} &= 0.329119 \end{aligned}$$

The values for the SPD $S_{D65}(\lambda)$ for 6504 K can be found in Appendix A.4.

## 7.11. Calculate the correlated colour temperature for an arbitrary SPD

When measuring light, the correlated colour temperature (CCT) and a deviation $\Delta uv$ for a stimulus are often needed.

This process is, in practice, often done by a lookup table. One method is described by Robertson (1968). A table with CIE 2015 2° based colour temperatures and data for the isotemperature lines is given in Table 15. As the 31 entries from the original table lead to a maximum error of 151.7 K, the updated table is given in 10% steps. In case of CIE 1931 this will lead to a smaller maximum error somewhere below 18 K, [Baxter, Royer & Smet, 2024]. The maximum error is not recomputed for CIE 2015 2°. For greater precision, a higher-resolution table needs to be computed.

$$u_s = \frac{4x}{12y - 2x + 3}$$

$$v_s = \frac{6y}{12y - 2x + 3}$$

$$d_i = \frac{(v_s - v_i) - t_i(u_s - u_i)}{(1 + t_i^2)^{\frac{1}{2}}}$$

$$T_c = \left[\frac{1}{T_j} + \frac{d_j}{d_j + d_{j+1}}\left(\frac{1}{T_{j+1}} - \frac{1}{T_j}\right)\right]^{-1}$$

*Equation 27: Interpolation for correlated colour temperatures and isotemperature lines.*

The interpolation is done by the equations in Equation 27. For a CIE 1960 UCS $(u_s, v_s)$ chromaticity coordinate, computed from CIE 2015 2° based xy chromaticity coordinates, the distances $d_i$ to all isotemperature lines are computed. The chromaticity point $(u_s, v_s)$ lies between the adjacent lines $i = j$ and $i = j + 1$, if the ratio $\frac{d_j}{d_{j+1}}$ is negative.

| $i$ | Tempera-ture T (K) | CIE 1960 UCS chromaticity coordinate based on CIE2015 2° CMFs | | Slope $t_T(u,v)$ | CIE 2015 2° chromaticity coordinate | |
|---|---|---|---|---|---|---|
| | | $u_T$ | $v_T$ | | $x_T$ | $y_T$ |
| 1 | 100000 | 0.17700 | 0.26469 | -0.31659 | 0.23743 | 0.23671 |
| 2 | 90000 | 0.17709 | 0.26497 | -0.31801 | 0.23777 | 0.23718 |
| 3 | 81000 | 0.17719 | 0.26529 | -0.31961 | 0.23815 | 0.23771 |
| 4 | 72900 | 0.17730 | 0.26564 | -0.32145 | 0.23858 | 0.23830 |
| 5 | 65610 | 0.17743 | 0.26604 | -0.32354 | 0.23906 | 0.23897 |
| 6 | 59049 | 0.17757 | 0.26649 | -0.32594 | 0.23961 | 0.23973 |
| 7 | 53144 | 0.17774 | 0.26699 | -0.32869 | 0.24023 | 0.24058 |
| 8 | 47830 | 0.17792 | 0.26755 | -0.33186 | 0.24094 | 0.24154 |
| 9 | 43047 | 0.17814 | 0.26819 | -0.33552 | 0.24173 | 0.24262 |
| 10 | 38742 | 0.17838 | 0.26891 | -0.33975 | 0.24264 | 0.24386 |
| 11 | 34868 | 0.17866 | 0.26972 | -0.34466 | 0.24368 | 0.24525 |
| 12 | 31381 | 0.17898 | 0.27064 | -0.35037 | 0.24486 | 0.24684 |
| 13 | 28243 | 0.17935 | 0.27168 | -0.35703 | 0.24621 | 0.24865 |
| 14 | 25419 | 0.17977 | 0.27286 | -0.36483 | 0.24777 | 0.25071 |
| 15 | 22877 | 0.18026 | 0.27419 | -0.37399 | 0.24955 | 0.25306 |
| 16 | 20589 | 0.18083 | 0.27570 | -0.38478 | 0.25162 | 0.25574 |

| $i$ | Tempera-ture T (K) | CIE 1960 UCS chromaticity coordinate based on CIE2015 2° CMFs | | Slope $t_T(u,v)$ | CIE 2015 2° chromaticity coordinate | |
|---|---|---|---|---|---|---|
| | | $u_T$ | $v_T$ | | $x_T$ | $y_T$ |
| 17 | 18530 | 0.18150 | 0.27741 | -0.39752 | 0.25400 | 0.25881 |
| 18 | 16677 | 0.18229 | 0.27934 | -0.41261 | 0.25676 | 0.26231 |
| 19 | 15009 | 0.18321 | 0.28153 | -0.43054 | 0.25997 | 0.26632 |
| 20 | 13509 | 0.18429 | 0.28399 | -0.45190 | 0.26369 | 0.27090 |
| 21 | 12158 | 0.18558 | 0.28676 | -0.47742 | 0.26804 | 0.27612 |
| 22 | 10942 | 0.18711 | 0.28986 | -0.50801 | 0.27310 | 0.28205 |
| 23 | 9848 | 0.18892 | 0.29331 | -0.54478 | 0.27900 | 0.28877 |
| 24 | 8863 | 0.19108 | 0.29712 | -0.58913 | 0.28587 | 0.29634 |
| 25 | 7977 | 0.19365 | 0.30129 | -0.64284 | 0.29386 | 0.30481 |
| 26 | 7179 | 0.19671 | 0.30583 | -0.70820 | 0.30313 | 0.31418 |
| 27 | 6461 | 0.20034 | 0.31069 | -0.78822 | 0.31382 | 0.32444 |
| 28 | 5815 | 0.20464 | 0.31582 | -0.88700 | 0.32608 | 0.33550 |
| 29 | 5233 | 0.20970 | 0.32117 | -1.01021 | 0.34004 | 0.34720 |
| 30 | 4710 | 0.21562 | 0.32663 | -1.16600 | 0.35578 | 0.35929 |
| 31 | 4239 | 0.22253 | 0.33210 | -1.36646 | 0.37332 | 0.37143 |
| 32 | 3815 | 0.23050 | 0.33745 | -1.63027 | 0.39259 | 0.38316 |
| 33 | 3434 | 0.23965 | 0.34254 | -1.98751 | 0.41343 | 0.39395 |
| 34 | 3090 | 0.25005 | 0.34723 | -2.48935 | 0.43556 | 0.40321 |
| 35 | 2781 | 0.26178 | 0.35138 | -3.22922 | 0.45857 | 0.41036 |
| 36 | 2503 | 0.27487 | 0.35487 | -4.39539 | 0.48201 | 0.41487 |
| 37 | 2253 | 0.28934 | 0.35762 | -6.42665 | 0.50535 | 0.41640 |
| 38 | 2028 | 0.30520 | 0.35958 | -10.62302 | 0.52811 | 0.41481 |
| 39 | 1825 | 0.32239 | 0.36074 | -23.23472 | 0.54988 | 0.41021 |
| 40 | 1642 | 0.34082 | 0.36114 | -522.71450 | 0.57040 | 0.40293 |
| 41 | 1478 | 0.36039 | 0.36085 | 33.33545 | 0.58951 | 0.39350 |
| 42 | 1330 | 0.38093 | 0.35997 | 18.59671 | 0.60719 | 0.38252 |
| 43 | 1197 | 0.40223 | 0.35863 | 14.14022 | 0.62348 | 0.37061 |
| 44 | 1078 | 0.42401 | 0.35696 | 12.15882 | 0.63845 | 0.35833 |

*Table 15: Correlated colour temperatures and isotemperature lines based on CIE 2015 for Interpolation*

A high-resolution dataset with 1% steps is available at: https://github.com/3dmedium/display_calibration_tool/tree/79833b1/datasets/isotemperature_lines

# 8. Further research and missing pieces

## 8.1. Practical quality of the results

This thesis focuses on the concept of redefining a colour space, not on the quality of the colour-matching functions used. As to the experience of the author, the quality of the results when calibrating different display types seems to be better, though not perfect. The overall quality for different displays and different human observers needs to be researched. The process can be repeated for the blue modifications to the CIE 2006 cone fundamentals, proposed by Polster (2013) or Ko *et al.* (2023).

## 8.2. White point change of a colour space

In this thesis, the maths for calculating colour temperature and $\Delta uv$ offset based on a CIE 2015 2° xy chromaticity coordinate is given for convenience. As all the redefined colour spaces use D65 as the white point, there is no need to map colours between different white points. For cinema applications, however, more than one white point needs to be considered. ACES AP0, for example, is defined with a white point of approximately 6000 K [ST 2065-1:2021]. The ACES workflow implemented in OpenColorIO configurations uses the Python colour library for generating chromatic adaptation transformation with the Bradford-Matrix [OCIO, 2025, utilities.py line 89 ff], when converting colours from ACES AP0 white point to D65 white points. The Bradford transformation is a modern version of the von Kries transformation and uses “optimized” cone responsivities [Fairchild, 2005, p. 180]. Since the Bradford Method was already described in 1998, the cone responsivities given with CIE 2015 CMFs were not available at this time. The maths done for the transformation matrix can be redone with updated cone responsivities.

## 8.3. Pointer’s Gamut

The Pointer’s Gamut contains the colours of real objects. As this gamut is available as CIE 1931 based xy chromaticity coordinates, a simple transfer to CIE 2015 2° CMFs is not possible. Thanks to Xu *et al.* (2025), a set of more than 100 000 SPDs for the reflection of real objects is available.

This set can be used to recreate a gamut for real surface colours.

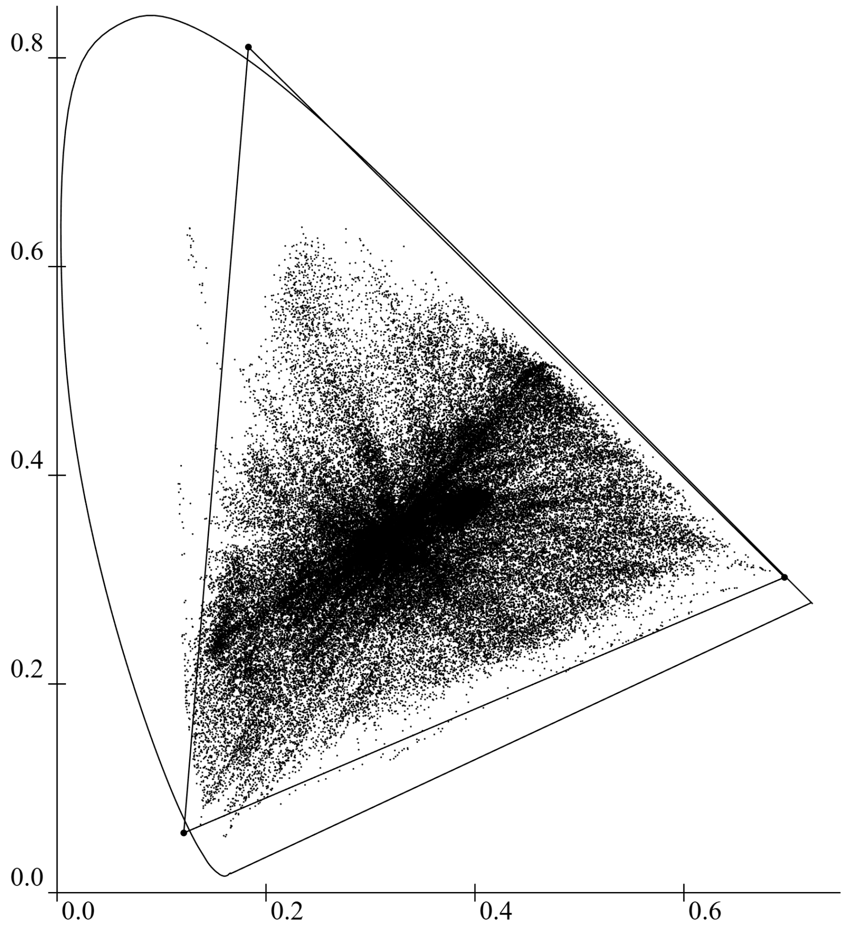


*Figure 23: Real surface colours as CIE 2015 2° chromaticity coordinates under D65 light. [*Construction of the Real Surface Color Gamut*, Xu* et al.*, 2025]*

The area for the real surface gamut changes under different lights. As video signals are normalized to the D65 white point in most cases, the CIE 2015 based xy chromaticity coordinates for the reflecting objects are calculated with a D65 light source. As seen in Figure 23, the redefined BT.2020 colour space does not include all real surface colours.

## 8.4. More than three primaries

ITU-R BT.2246 lists some approaches to expand the colour gamut of image systems. A short notice of a system with more than three primaries is classified as a "completely different system".

As there is no single set of CMFs which fits all viewing conditions and age groups, for a perfect reproduction of the visual appearance of colours, it may be required to capture and transmit the detailed SPD of a light source, and in the case of television broadcast, a full scene in high resolution. For making use of these captured SPDs, a display also needs to be able to precisely reproduce the SPD for each pixel. It is possible at the time of writing to buy cameras which can capture spectral data for low-resolution images [Specim, 2026], but rebuilding the SPD is not yet possible for a display product. With Quantum Dot (QD) technology, it is possible to create narrow spectral light sources with a 10 nm interval [PlasmaChem, 2024]. Therefore, this technology may be suitable to model the SPD for each pixel of a display with 6 or more primary colours.

The required precision in spectral reconstruction, and therefore the required number of primary colours, to overcome the colour-matching limits of traditional displays, seems to be little researched.

## 8.5. Integration with spectroradiometers, adaptation to other CMFs

At the time of writing, the integration of the CIE 170-2:2015 colour-matching functions was not available in all spectroradiometer software solutions. As long as the SPD for measurements is available, for example via SDK or API access, every spectroradiometer can be used for working with arbitrary CMFs. For transferring the results to different CMFs, the spectral data for the CRT displays is available at:

https://github.com/3dmedium/display_calibration_tool

# 9. Conclusion

As there is no set of colour-matching functions that perfectly models all individual human visual systems, a colour space defined by CIE xy chromaticity coordinates and usage of three-value-based video signals will not lead to a perfect colour match of all display technologies and transfer of scene light to display light in all circumstances.

Using different colour spaces, based on optimized colour-matching functions, however, can lead to better display matching results and is easy to implement for existing video systems. A changed display calibration (ideal with access to the linear matrix of a display) is enough for changing CMFs. The redefined colour spaces can be implemented in display calibration software as long as a spectroradiometer is used. A tristimulus colourimeter is only suitable if it implements the requested CMFs in hardware.

For further work, a single colour space should be defined based on the spectral power distributions of physical light sources. For example, the redefined BT.709 based on CRT phosphors, consolidating the "immovable legacy effect of the CRT" [EBU Tech 3320]. All other colour spaces which need to be converted should be derived from this single physical source. The SPDs of CRT phosphors are available in a technical way, SPDs which better match the typical shape of LED lights or QD-OLED sources, especially for red, may be introduced by a visual match to the CRT phosphors to maintain compatibility with existing recorded video.

Using CRT phosphors as the source for defining the modern BT.2020 wide colour gamut seems to be counterintuitive, but may be the most accurate and backwards-compatible way to update display colour-matching.

Using different colour-matching functions for more than display calibration, for example, luminance separation for chroma subsampled SDI signals, will lead to incompatibilities. Even with IP-based ST-2110 video signals and basically endless space for metadata in SDP files, different colour spaces still need hardware support of the changed luminance separation matrix in every single device. This will basically break backwards compatibility. The minor crosstalk error resulting from a matrix based on an imperfect colour space can be ignored compared to the compatibility drawbacks introduced with new video signal standards.

While colour-matching functions will always be limited by the differences between individual humans, recreating the original spectral power distributions of a light source can result in a perfect visual match. This will need an update for all involved technology, starting with a spectral-based camera, transfer and encoding of an SPD for each pixel, and a display with more than 3 primary colours.

# Bibliography


[Admesy, 2024] *Measure How We See - The Way to Perfect Display Colors*, Admesy, 2024. Available at: https://static.admesy.com/assets/PDF/Admesy-White-Paper-Perfect-Display-Color-Matching.pdf (Accessed: January 10, 2026)

[ARRI, 2025] *ARRI LogC4 Logarithmic Color Space SPECIFICATION*, ARRI, 2025. Available at: https://www.arri.com/resource/blob/278790/dc29f7399c1dc9553d329e27f1409a89/2022-05-arri-logc4-specification-data.pdf

[Barten, 1999] Barten, P.G.J., *Contrast sensitivity of the human eye and its effects on image quality*, Institute for Perception Research, Eindhoven, 1999. Available at: https://doi.org/10.6100/IR523072

[Baxter, Royer & Smet, 2024] Baxter, D.B., Royer, M. and Smet, K., *Modifications of the Robertson Method for Calculating Correlated Color Temperature to Improve Accuracy and Speed*, *The Journal of the Illuminating Engineering Society*, 2024, 20(1), pp. 55–66. Available at: https://doi.org/10.1080/15502724.2023.2166060

[Bieske *et al.*, 2017] Bieske, K. *et al.*, *Testing Colour-Matching Functions - Perception of Luminous Colour Differences of white LEDs in Relation to Ambient Luminous Colour and Age of Observers*, Lux Europa, 2017

[CIE 015:2018] *Colorimetry, 4th Edition*, International Commission on Illumination (CIE), 2018, ISBN: 978-3-902842-13-8. Available at: https://doi.org/10.25039/TR.015.2018

[CIE 170-1:2006] *Fundamental Chromaticity Diagram with Physiological Axes - Part 1*, International Commission on Illumination (CIE), 2006, ISBN: 978-3-901906-46-6

[CIE 170-2:2015] *Fundamental Chromaticity Diagram with Physiological Axes - Part 2: Spectral Luminous Efficiency Functions and Chromaticity Diagrams*, International Commission on Illumination (CIE), 2015, ISBN: 978-3-902842-06-0

[CIE 1931] *CIE 1931 colour-matching functions, 2 degree observer*, International Commission on Illumination (CIE), 2019. Available at: https://doi.org/10.25039/CIE.DS.xvudnb9b

[CIE 2015] *CIE cone-fundamental-based spectral tristimulus values for 2 degree field size*, International Commission on Illumination (CIE), 2015. Available at: https://doi.org/10.25039/CIE.DS.548rw69q

[CIE D65] *CIE standard illuminant D65*, International Commission on Illumination (CIE), 2019. Available at: https://doi.org/10.25039/CIE.DS.hjfjmt59

[Colour, 2025] *Github, colour-science / colour*, Colour Science & Digital Imaging, 2025. Available at: https://github.com/colour-science/colour (Accessed: January 17, 2026)

[DCI HDRD, 2024] *High Dynamic Range D-Cinema Addendum*, Digital Cinema Initiatives, LLC, Member Representative Committee, 2024. Available at: https://documents.dcimovies.com/HDR-Addendum/release/1.2.1 (Accessed: January 21, 2026)

[Dolby, 2020] *ICtCp Dolby White paper*, Dolby, 2020. Available at: https://professional.dolby.com/siteassets/pdfs/ictcp_dolbywhitepaper_v071.pdf

[EBU Tech 3213-E] *E.B.U. STANDARD FOR CHROMATICITY TOLERANCES FOR STUDIO MONITORS*, European Broadcasting Union (EBU), 1975

[EBU Tech 3273-E] *Methods of measurement of the colorimetric performance of studio monitors*, European Broadcasting Union (EBU), 1993

[EBU Tech 3320] *USER REQUIREMENTS FOR VIDEO MONITORS IN TELEVISION PRODUCTION*, European Broadcasting Union (EBU), 2019

[ECMA-262, 2025] *ECMAScript® 2025 Language Specification*, Ecma International, 2025

[Fairchild, 2005] Fairchild, M.D., *Color Appearance Models*. Second Edition, John Wiley & Sons, 2005, ISBN: 978-0470012161

[Golz & MacLeod, 2003] Golz, J. and MacLeod, D.I.A., *Colorimetry for CRT displays*, *Journal of the Optical Society of America A*, 2003, 20(5), pp. 769–781. Available at: https://doi.org/10.1364/JOSAA.20.000769

[HDMI 2.0] *High-Definition Multimedia Interface Specification Version 2.0*, HDMI Forum, 2013

[IEC 61966-2-1] *IEC 61966-2-1:1999 Multimedia systems and equipment - Colour measurement and management - Part 2-1: Colour management - Default RGB colour space - sRGB*. 1st ed, 1999

[IMAGO, 2025] *Metamerism Experts' Day Debrief*, International federation of cinematographers, 2025. Available at: https://imago.org/committees/technical/metamerism-experts-day-debrief/ (Accessed: December 24, 2025)

[ISO/CIE 11664-2:2022] *ISO/CIE 11664-2:2022 Colorimetry Part 2: CIE standard illuminants*, International Commission on Illumination (CIE), 2022

[ITU-R BT.1361] *Rec. ITU-R BT.1361 Worldwide unified colorimetry and related characteristics of future television and imaging systems*, International Telecomunication Union (ITU), 2002

[ITU-R BT.2020] *Recommendation ITU-R BT.2020-2 Parameter values for ultra-high definition television systems for production and international pro-*

*gramme exchange*, International Telecomunication Union (ITU), 2015

[ITU-R BT.2035] *Recommendation ITU-R BT.2035 A reference viewing environment for evaluation of HDTV program material or completed programmes*, International Telecomunication Union (ITU), 2013

[ITU-R BT.2087] *Recommendation ITU-R BT.2087-0 Colour conversion from Recommendation ITU-R BT.709 to Recommendation ITU-R BT.2020*, International Telecomunication Union (ITU), 2015

[ITU-R BT.2100] *Image parameter values for high dynamic range television for use in production and international programme exchange*, International Telecomunication Union (ITU), 2015

[ITU-R BT.2246] *Report ITU-R BT.2246-9 The present state of ultra-high definition television*, International Telecomunication Union (ITU), 2025

[ITU-R BT.2390] *Report ITU-R BT.2390-12 High dynamic range television for production and international programme exchange*, International Telecomunication Union (ITU), 2015

[ITU-R BT.2407] *Report ITU-R BT.2407-0 Colour gamut conversion from Recommendation ITU-R BT.2020 to Recommendation ITU-R BT.709*, International Telecomunication Union (ITU), 2017

[ITU-R BT.709] *Recommendation ITU-R BT.709-6 Parameter values for the HDTV standards for production and international programme exchange*, International Telecomunication Union (ITU), 2015

[Judd, 1949] Judd, D., *A Comparison of Direct Colorimetry of Titanium Pigments With Their Indirect Colorimetry Based on Spectrophotometry and a Standard Observer*, *Journal of the Optical Society of America*, 1949, 43(11), pp. 945–950. Available at: https://doi.org/10.1364/JOSA.39.000945

[Ko *et al.*, 2023] Ko, M. *et al.*, *Reducing the CIE colorimetric matching failure on wide color gamut displays*, *Optics Express*, 2023, 31(4), pp. 5670–5686. Available at: https://doi.org/10.1364/OE.480001

[Leonard, 2026] Leonard, M., *Github, The CIEDE2000 (ΔE00) Color Difference Formula*, 2026. Available at: https://github.com/michel-leonard/ciede2000-color-matching (Accessed: January 10, 2026)

[Lindbloom, 2017] Lindbloom, B., *Computing RGB-to-XYZ and XYZ-to-RGB matrices*, 2017. Available at: http://brucelindbloom.com/index.html?LContinuity.html (Accessed: January 18, 2026)

[OCIO, 2025] *Github, OpenColorIO-Config-ACES*, AcademySoftwareFoundation, 2025. Available at: https://github.com/AcademySoftwareFoundation/OpenColorIO-Config-ACES/releases/tag/v4.0.0 (Accessed: January 9, 2026)

[PlasmaChem, 2024] *Nanomaterials and related products, catalogue & price-list*, PlasmaChem GmbH, 2024

[Polster, 2013] Polster, S., *Neue Spektralwertfunktionen für die korrekteBewertung von LED-Spektren und Einführung eines Metamerie-Index für Beobachterfeldgrößenabhängigkeit*, 2013, ISBN: 978-3-86247-473-8

[Poynton, 2012] Poynton, C., *Digital Video and HD: Algorithms and Interfaces*. second edition, Morgan Kaufmann, 2012, ISBN: 978-0-12-391926-7. Available at: https://doi.org/10.1016/C2010-0-68987-5

[Pruitt *et al.*, 2025] Pruitt, T. *et al.*, *Towards Standardization for Display Color Consistency*, ICC Expert Day, 2025. Available at: https://www.color.org/events/vienna/7.Peyvandi_etal_ICCExpertDay_ViennaJuly2025.pdf (Accessed: February 19, 2026)

[RCA TPM-1508A, 1995] *RCA PHOSPHORS for Cathode-Ray Tubes, Black-and-White and Color Ricture Tubes, and Other Applications*, Radio Corporation of America, 1995

[Robertson, 1968] Robertson, A.R., *Computation of Correlated Color Temperature and Distribution Temperature*, *Journal of the Optical Society of America*, 1968, 58(11), pp. 1528–1535. Available at: https://doi.org/10.1364/JOSA.58.001528

[Seymour, 2026] Seymour, J., *Recommended methods for conducting human factors experiments on the subjective evaluation of colour rendition*, *Color Research & Application*, 2026, 51(1). Available at: https://doi.org/10.1002/col.70032

[SMPTE RP 145] *RP 145-2004 SMPTE C Color Monitor Colorimetry*, THE SOCIETY OF MOTION PICTURE AND TELEVISION ENGINEERS (SMPTE), 2004

[SONY, 1995] *SONY Trinitron color video monitor manual (BVM-20F1U/E)*, SONY, 1995

[SONY, 1999] *SONY Trinitron color video monitor operation manual (BVM-D24E1WU/E)*, SONY, 1999

[SONY, 2013] *Colour Matching Between OLED and CRT White Paper*, SONY, 2013. Available at: https://pro.sony/s3/2021/01/22153606/ColourMatching_Between_OLED_and_CRT_E.pdf

[SONY, 2014] *Technical Summary for S-Gamut3.Cine/S-Log3 and S-Gamut3/S-Log3*, SONY, 2014. Available at: https://pro.sony/s3/cms-static-content/uploadfile/06/1237494271406.pdf

[SONY, 2020] *Colour Matching Between BVM-HX310 and BVM-X300*, SONY, 2020. Available at: https://pro.sony/s3/2021/01/08115713/HX310_X300_Colormatching_v102_220208_E.pdf

[Specim, 2026] *SPECIM FX10 Technical Datasheet*, specim, 2026. Available at: https://www.specim.com/wp-content/uploads/2024/06/Specim-FX10-Technical-Datasheet-08.pdf (Accessed: January 10, 2026)

[ST 2048-1:2024] *ST 2048-1:2024 2048 x 1080 and 4096 x 2160 Digital Cinematography Production Image Formats FS/709*, Society of Motion Picture and Television Engineers (SMPTE), 2024

[ST 2065-1:2021] *ST 2065-1:2021 Academy Color Encoding Specification (ACES)*, Society of Motion Picture and Television Engineers (SMPTE), 2020

[ST 2082-10:2018] *ST 2082-10:2018 2160-line and 1080-line Source Image and Ancillary Data Mapping for 12G-SDI*, Society of Motion Picture and Television Engineers (SMPTE), 2018

[Thornton, 1998] Thornton, W.A., *How strong metamerism disturbs color spaces*, *Color Research & Application*, 1998, 23(6), pp. 402–207. Available at: https://doi.org/10.1002/(SICI)1520-6378(199812)23:6<402::AID-COL8>3.0.CO;2-X

[Wyszecki & Stiles, 2000] Wyszecki, G. and Stiles, W.S., *Color Science Concepts and Methods, Quantitative Data and Formulae*. Second Edition, John Wiley & Sons, 2000, ISBN: 978-0-471-39918-6

[Xu *et al.*, 2025] Xu, L. *et al.*, *Construction of the Real Surface Color Gamut*, *Color Research & Application*, 2025, 50(6), pp. 701–710. Available at: https://doi.org/10.1002/col.70004

# List of Abbreviations

| | |
|---|---|
| ACES | Academy Color Encoding System |
| ACES AP0 | Academy Color Encoding System's Primaries 0 |
| BT.2020 | ITU-R BT.2020 |
| BT.709 | ITU-R BT.709 |
| CCFL | cold cathode fluorescent lamp |
| CCIR | Comité Consultatif International des Radiocommunications |
| CCT | correlated colour temperature |
| CIE | International Commission on Illumination |
| CMF | colour-matching function |
| CRT | cathode-ray tube |
| D65 | CIE standard illuminant D series with 6504 K |
| DCDM | Digital Cinema Distribution Master |
| DCI | Digital Cinema Initiatives |
| DCI-P3 | Digital Cinema Initiatives - Protocol 3 |
| EOTF | electro-optical transfer function |
| FPGA | field programmable gate array |
| HDR | high dynamic range |
| LED | light-emitting diode |
| LMS | long, medium, short |
| NDR | Norddeutscher Rundfunk |
| OCIO | OpenColorIO |
| OLED | organic light-emitting diode |
| OOTF | opto-optical transfer function |
| PQ | perceptual quantizer |
| QD | Quantum Dot |
| QD-OLED | Quantum Dot organic light emitting diode |
| RGB | red, green, blue |

| | |
|---|---|
| SDI | Serial Digital Interface |
| SDP | session description protocol |
| SPD | spectral power distribution |
| TV | Television |
| VANC | vertical ancillary data |

# List of figures

# List of tables

# List of equations

# Appendix

## A.1. Spectral radiant power distribution of a Sony BVM-20E1U (SMPTE phosphor)

$\lambda = 380$ nm to 780 nm at 1 nm interval, measured with Konica Minolta CS-2000 spectroradiometer.

Data is available at: https://github.com/3dmedium/display_calibration_tool/tree/79833b1/datasets/display_primaries/crt_displays

Data is averaged from 100 measurements, 33.333 ms integration time for each.

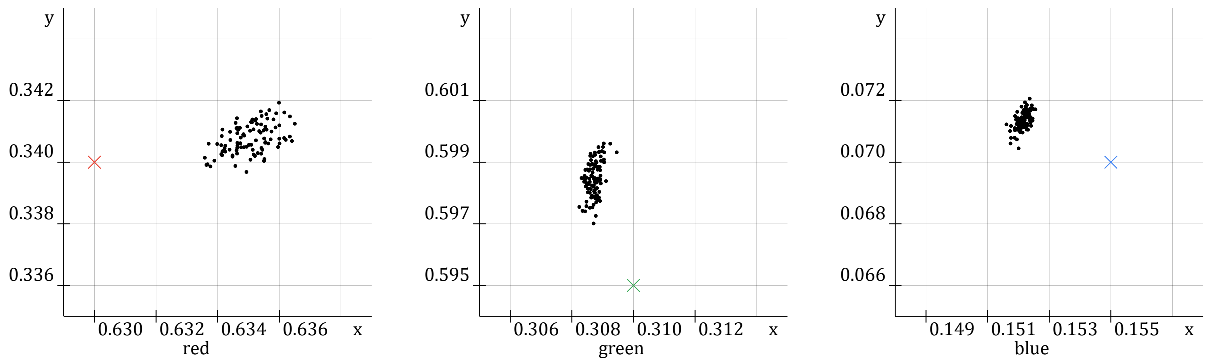


*Figure 24: Deviation of the single measurements in CIE 1931 xy chromaticity diagram, SMPTE phosphors.*

| **Colour** | **x** | | **y** | |
|---|---|---|---|---|
| | $\bar{x}$ | $\sigma_x$ | $\bar{y}$ | $\sigma_y$ |
| Red | 0.63505 | 0.00069 | 0.34076 | 0.00048 |
| Green | 0.30872 | 0.00021 | 0.59848 | 0.00057 |
| Blue | 0.15216 | 0.00019 | 0.071364 | 0.00029 |

*Table 16: Averaged chromaticity coordinates and standard deviation, SMPTE phosphors.*

| Wavelenght $\lambda(\mathrm{nm})$ | Primary colourants of the CRT (SMPTE phosphor) | | |
|---|---|---|---|
| | **red** | **green** | **blue** |
| 380.000 | 0.00000736408 | 0.00000942620 | 0.0000864974 |
| 381.000 | 0.00000608050 | 0.0000119623 | 0.000102517 |
| 382.000 | 0.00000807373 | 0.0000135567 | 0.000118546 |
| 383.000 | 0.00000766130 | 0.0000122739 | 0.000127326 |
| 384.000 | 0.0000101456 | 0.00000998169 | 0.000132151 |
| 385.000 | 0.00000683804 | 0.00000924733 | 0.000137535 |
| 386.000 | 0.00000739836 | 0.00000888873 | 0.000140316 |
| 387.000 | 0.00000641331 | 0.00000602307 | 0.000147018 |
| 388.000 | 0.00000606444 | 0.00000725604 | 0.000148905 |
| 389.000 | 0.00000567324 | 0.00000833711 | 0.000158329 |
| 390.000 | 0.00000458105 | 0.00000495192 | 0.000162354 |
| 391.000 | 0.00000406524 | 0.00000477075 | 0.000174785 |
| 392.000 | 0.00000470962 | 0.00000585912 | 0.000186853 |
| 393.000 | 0.00000599146 | 0.00000427269 | 0.000196285 |
| 394.000 | 0.00000466153 | 0.00000513234 | 0.000198785 |
| 395.000 | 0.00000377940 | 0.00000498516 | 0.000209299 |
| 396.000 | 0.00000441394 | 0.00000398064 | 0.000227084 |
| 397.000 | 0.00000548051 | 0.00000521231 | 0.000237821 |
| 398.000 | 0.00000524794 | 0.00000474104 | 0.000247320 |
| 399.000 | 0.00000377547 | 0.00000545257 | 0.000257486 |
| 400.000 | 0.00000370669 | 0.00000650437 | 0.000272967 |
| 401.000 | 0.00000535109 | 0.00000471408 | 0.000284940 |
| 402.000 | 0.00000442950 | 0.00000320208 | 0.000303929 |
| 403.000 | 0.00000443679 | 0.00000370740 | 0.000315431 |
| 404.000 | 0.00000413230 | 0.00000460349 | 0.000335347 |
| 405.000 | 0.00000329390 | 0.00000559368 | 0.000357736 |
| 406.000 | 0.00000516796 | 0.00000501148 | 0.000376369 |
| 407.000 | 0.00000391310 | 0.00000524753 | 0.000398757 |
| 408.000 | 0.00000508460 | 0.00000701156 | 0.000426577 |
| 409.000 | 0.00000598721 | 0.00000779971 | 0.000455603 |
| 410.000 | 0.00000654006 | 0.00000843125 | 0.000488735 |
| 411.000 | 0.00000578693 | 0.0000117882 | 0.000524920 |
| 412.000 | 0.00000714783 | 0.0000153803 | 0.000571860 |
| 413.000 | 0.00000912550 | 0.0000195267 | 0.000619866 |
| 414.000 | 0.0000106734 | 0.0000266238 | 0.000678127 |
| 415.000 | 0.0000124684 | 0.0000317169 | 0.000736855 |
| 416.000 | 0.0000132724 | 0.0000353510 | 0.000788005 |
| 417.000 | 0.0000125547 | 0.0000363956 | 0.000836869 |
| 418.000 | 0.0000150808 | 0.0000352302 | 0.000865185 |
| 419.000 | 0.0000123998 | 0.0000314653 | 0.000884457 |
| 420.000 | 0.0000103768 | 0.0000239135 | 0.000899170 |
| 421.000 | 0.00000890959 | 0.0000150018 | 0.000925505 |
| 422.000 | 0.00000895406 | 0.0000139091 | 0.000960312 |
| 423.000 | 0.00000991096 | 0.0000161018 | 0.00100887 |

| Wavelenght $\lambda(\mathrm{nm})$ | Primary colourants of the CRT (SMPTE phosphor) | | |
|---|---|---|---|
| | **red** | **green** | **blue** |
| 424.000 | 0.00000908047 | 0.0000170325 | 0.00105768 |
| 425.000 | 0.0000116843 | 0.0000162380 | 0.00111020 |
| 426.000 | 0.0000120019 | 0.0000156443 | 0.00115815 |
| 427.000 | 0.0000101356 | 0.0000170220 | 0.00120505 |
| 428.000 | 0.0000122006 | 0.0000190431 | 0.00125720 |
| 429.000 | 0.0000117915 | 0.0000194780 | 0.00131402 |
| 430.000 | 0.0000134281 | 0.0000196438 | 0.00136182 |
| 431.000 | 0.0000154700 | 0.0000212694 | 0.00141378 |
| 432.000 | 0.0000164700 | 0.0000229480 | 0.00145932 |
| 433.000 | 0.0000166366 | 0.0000249378 | 0.00151202 |
| 434.000 | 0.0000178658 | 0.0000281687 | 0.00156584 |
| 435.000 | 0.0000218572 | 0.0000301310 | 0.00161226 |
| 436.000 | 0.0000206546 | 0.0000332420 | 0.00166240 |
| 437.000 | 0.0000209938 | 0.0000365549 | 0.00170568 |
| 438.000 | 0.0000212629 | 0.0000400556 | 0.00173849 |
| 439.000 | 0.0000226022 | 0.0000438949 | 0.00177458 |
| 440.000 | 0.0000228753 | 0.0000454150 | 0.00180237 |
| 441.000 | 0.0000231569 | 0.0000456280 | 0.00181814 |
| 442.000 | 0.0000212062 | 0.0000416388 | 0.00183261 |
| 443.000 | 0.0000207246 | 0.0000343503 | 0.00183477 |
| 444.000 | 0.0000207121 | 0.0000326956 | 0.00183751 |
| 445.000 | 0.0000212684 | 0.0000317441 | 0.00184701 |
| 446.000 | 0.0000194327 | 0.0000296307 | 0.00185328 |
| 447.000 | 0.0000205186 | 0.0000321751 | 0.00186148 |
| 448.000 | 0.0000202336 | 0.0000344354 | 0.00186490 |
| 449.000 | 0.0000202786 | 0.0000364739 | 0.00186474 |
| 450.000 | 0.0000199498 | 0.0000362425 | 0.00186261 |
| 451.000 | 0.0000201013 | 0.0000385584 | 0.00185088 |
| 452.000 | 0.0000196461 | 0.0000407643 | 0.00184238 |
| 453.000 | 0.0000197934 | 0.0000439359 | 0.00183667 |
| 454.000 | 0.0000188568 | 0.0000467168 | 0.00182711 |
| 455.000 | 0.0000200228 | 0.0000489486 | 0.00181025 |
| 456.000 | 0.0000200250 | 0.0000521161 | 0.00179358 |
| 457.000 | 0.0000200766 | 0.0000573908 | 0.00177475 |
| 458.000 | 0.0000199305 | 0.0000632133 | 0.00175522 |
| 459.000 | 0.0000197576 | 0.0000645151 | 0.00172238 |
| 460.000 | 0.0000195943 | 0.0000669403 | 0.00169030 |
| 461.000 | 0.0000189241 | 0.0000670536 | 0.00165441 |
| 462.000 | 0.0000185394 | 0.0000670628 | 0.00161795 |
| 463.000 | 0.0000191718 | 0.0000725931 | 0.00157591 |
| 464.000 | 0.0000201861 | 0.0000763523 | 0.00154392 |
| 465.000 | 0.0000221976 | 0.0000837986 | 0.00150800 |
| 466.000 | 0.0000263892 | 0.0000893292 | 0.00147234 |
| 467.000 | 0.0000357697 | 0.0000950333 | 0.00143854 |

| Wavelenght $\lambda(\mathrm{nm})$ | Primary colourants of the CRT (SMPTE phosphor) | | |
|---|---|---|---|
| | red | green | blue |
| 468.000 | 0.0000481642 | 0.000105105 | 0.00139492 |
| 469.000 | 0.0000547653 | 0.000111977 | 0.00135969 |
| 470.000 | 0.0000505479 | 0.000124063 | 0.00132675 |
| 471.000 | 0.0000404601 | 0.000133688 | 0.00128988 |
| 472.000 | 0.0000265769 | 0.000144493 | 0.00125156 |
| 473.000 | 0.0000211784 | 0.000154621 | 0.00120796 |
| 474.000 | 0.0000245530 | 0.000168672 | 0.00117212 |
| 475.000 | 0.0000294307 | 0.000184326 | 0.00113969 |
| 476.000 | 0.0000306978 | 0.000197847 | 0.00110400 |
| 477.000 | 0.0000279686 | 0.000212627 | 0.00105898 |
| 478.000 | 0.0000220283 | 0.000224151 | 0.00101529 |
| 479.000 | 0.0000191794 | 0.000240617 | 0.000973097 |
| 480.000 | 0.0000162551 | 0.000256885 | 0.000936983 |
| 481.000 | 0.0000154172 | 0.000276095 | 0.000896922 |
| 482.000 | 0.0000154532 | 0.000297525 | 0.000868309 |
| 483.000 | 0.0000158244 | 0.000321419 | 0.000838595 |
| 484.000 | 0.0000163206 | 0.000344407 | 0.000810139 |
| 485.000 | 0.0000163412 | 0.000366069 | 0.000779115 |
| 486.000 | 0.0000189337 | 0.000391070 | 0.000745584 |
| 487.000 | 0.0000253426 | 0.000416172 | 0.000714481 |
| 488.000 | 0.0000329496 | 0.000444436 | 0.000690503 |
| 489.000 | 0.0000401882 | 0.000476330 | 0.000670838 |
| 490.000 | 0.0000410631 | 0.000506881 | 0.000644042 |
| 491.000 | 0.0000375871 | 0.000534604 | 0.000619508 |
| 492.000 | 0.0000352067 | 0.000562737 | 0.000589055 |
| 493.000 | 0.0000343020 | 0.000592121 | 0.000560921 |
| 494.000 | 0.0000389210 | 0.000623016 | 0.000538975 |
| 495.000 | 0.0000549788 | 0.000653847 | 0.000509726 |
| 496.000 | 0.0000680204 | 0.000684151 | 0.000481362 |
| 497.000 | 0.0000711205 | 0.000716878 | 0.000455213 |
| 498.000 | 0.0000615268 | 0.000749545 | 0.000430733 |
| 499.000 | 0.0000444173 | 0.000781789 | 0.000407516 |
| 500.000 | 0.0000316174 | 0.000817200 | 0.000388617 |
| 501.000 | 0.0000253634 | 0.000851317 | 0.000370790 |
| 502.000 | 0.0000197698 | 0.000886677 | 0.000353588 |
| 503.000 | 0.0000169113 | 0.000922648 | 0.000336939 |
| 504.000 | 0.0000157869 | 0.000959460 | 0.000318934 |
| 505.000 | 0.0000151873 | 0.000993760 | 0.000306105 |
| 506.000 | 0.0000168119 | 0.00102759 | 0.000292097 |
| 507.000 | 0.0000179037 | 0.00106321 | 0.000278086 |
| 508.000 | 0.0000201616 | 0.00109840 | 0.000265794 |
| 509.000 | 0.0000254648 | 0.00113281 | 0.000252146 |
| 510.000 | 0.0000355801 | 0.00116398 | 0.000240990 |
| 511.000 | 0.0000570285 | 0.00119635 | 0.000228385 |

| Wavelenght $\lambda(\mathrm{nm})$ | Primary colourants of the CRT (SMPTE phosphor) | | |
|---|---|---|---|
| | **red** | **green** | **blue** |
| 512.000 | 0.0000825268 | 0.00122670 | 0.000219572 |
| 513.000 | 0.000108936 | 0.00125910 | 0.000209093 |
| 514.000 | 0.000109445 | 0.00128801 | 0.000197996 |
| 515.000 | 0.0000939800 | 0.00131615 | 0.000189000 |
| 516.000 | 0.0000668773 | 0.00134307 | 0.000180985 |
| 517.000 | 0.0000443108 | 0.00136681 | 0.000173425 |
| 518.000 | 0.0000315610 | 0.00139309 | 0.000165327 |
| 519.000 | 0.0000269975 | 0.00141601 | 0.000158214 |
| 520.000 | 0.0000235239 | 0.00143730 | 0.000150503 |
| 521.000 | 0.0000194137 | 0.00145540 | 0.000143983 |
| 522.000 | 0.0000181655 | 0.00147396 | 0.000135622 |
| 523.000 | 0.0000195197 | 0.00149292 | 0.000130955 |
| 524.000 | 0.0000196798 | 0.00150671 | 0.000124491 |
| 525.000 | 0.0000202247 | 0.00151835 | 0.000119667 |
| 526.000 | 0.0000208930 | 0.00153125 | 0.000111949 |
| 527.000 | 0.0000252403 | 0.00153982 | 0.000107763 |
| 528.000 | 0.0000287335 | 0.00154917 | 0.000102647 |
| 529.000 | 0.0000316629 | 0.00155668 | 0.0000977945 |
| 530.000 | 0.0000330799 | 0.00156316 | 0.0000945902 |
| 531.000 | 0.0000320140 | 0.00156692 | 0.0000886633 |
| 532.000 | 0.0000344221 | 0.00156884 | 0.0000871591 |
| 533.000 | 0.0000386421 | 0.00157089 | 0.0000828680 |
| 534.000 | 0.0000441620 | 0.00157035 | 0.0000802012 |
| 535.000 | 0.0000557491 | 0.00156844 | 0.0000759542 |
| 536.000 | 0.0000832122 | 0.00156656 | 0.0000726350 |
| 537.000 | 0.000154172 | 0.00156458 | 0.0000714424 |
| 538.000 | 0.000256911 | 0.00156268 | 0.0000707973 |
| 539.000 | 0.000322191 | 0.00156178 | 0.0000703775 |
| 540.000 | 0.000311057 | 0.00155573 | 0.0000723500 |
| 541.000 | 0.000236686 | 0.00155409 | 0.0000818212 |
| 542.000 | 0.000144632 | 0.00155700 | 0.000105595 |
| 543.000 | 0.000103110 | 0.00156568 | 0.000139190 |
| 544.000 | 0.0000902750 | 0.00156713 | 0.000163822 |
| 545.000 | 0.0000831039 | 0.00155516 | 0.000162773 |
| 546.000 | 0.0000689564 | 0.00152987 | 0.000141962 |
| 547.000 | 0.0000534052 | 0.00150154 | 0.000118405 |
| 548.000 | 0.0000486078 | 0.00148395 | 0.000111392 |
| 549.000 | 0.0000447562 | 0.00146763 | 0.000108426 |
| 550.000 | 0.0000421993 | 0.00144705 | 0.000101169 |
| 551.000 | 0.0000426498 | 0.00141993 | 0.0000852674 |
| 552.000 | 0.0000431883 | 0.00138790 | 0.0000637639 |
| 553.000 | 0.0000534199 | 0.00136681 | 0.0000507073 |
| 554.000 | 0.0000834580 | 0.00134297 | 0.0000451740 |
| 555.000 | 0.000120337 | 0.00132149 | 0.0000427478 |

| Wavelenght $\lambda(\mathrm{nm})$ | Primary colourants of the CRT (SMPTE phosphor) | | |
|---|---|---|---|
| | **red** | **green** | **blue** |
| 556.000 | 0.000134076 | 0.00129568 | 0.0000397224 |
| 557.000 | 0.000120170 | 0.00127248 | 0.0000372160 |
| 558.000 | 0.0000827366 | 0.00124988 | 0.0000353440 |
| 559.000 | 0.0000492128 | 0.00122723 | 0.0000327971 |
| 560.000 | 0.0000346717 | 0.00120049 | 0.0000301896 |
| 561.000 | 0.0000293588 | 0.00117302 | 0.0000289418 |
| 562.000 | 0.0000307789 | 0.00114835 | 0.0000280112 |
| 563.000 | 0.0000386649 | 0.00112367 | 0.0000265428 |
| 564.000 | 0.0000437106 | 0.00109819 | 0.0000249108 |
| 565.000 | 0.0000447013 | 0.00107002 | 0.0000248454 |
| 566.000 | 0.0000404046 | 0.00104518 | 0.0000236846 |
| 567.000 | 0.0000346360 | 0.00101764 | 0.0000231217 |
| 568.000 | 0.0000315689 | 0.000993694 | 0.0000229468 |
| 569.000 | 0.0000318858 | 0.000967805 | 0.0000212128 |
| 570.000 | 0.0000332508 | 0.000942854 | 0.0000221762 |
| 571.000 | 0.0000310548 | 0.000916607 | 0.0000194793 |
| 572.000 | 0.0000270356 | 0.000889710 | 0.0000190962 |
| 573.000 | 0.0000241416 | 0.000864101 | 0.0000186044 |
| 574.000 | 0.0000237807 | 0.000838678 | 0.0000177754 |
| 575.000 | 0.0000264920 | 0.000813790 | 0.0000164450 |
| 576.000 | 0.0000291869 | 0.000789934 | 0.0000158500 |
| 577.000 | 0.0000348819 | 0.000763717 | 0.0000141761 |
| 578.000 | 0.0000385526 | 0.000739426 | 0.0000143966 |
| 579.000 | 0.0000468647 | 0.000718228 | 0.0000141042 |
| 580.000 | 0.0000757717 | 0.000696716 | 0.0000146509 |
| 581.000 | 0.000160515 | 0.000675668 | 0.0000179617 |
| 582.000 | 0.000267992 | 0.000655359 | 0.0000196098 |
| 583.000 | 0.000301017 | 0.000635766 | 0.0000215078 |
| 584.000 | 0.000302167 | 0.000614974 | 0.0000228347 |
| 585.000 | 0.000326352 | 0.000597162 | 0.0000245095 |
| 586.000 | 0.000413549 | 0.000582981 | 0.0000291566 |
| 587.000 | 0.000507268 | 0.000564424 | 0.0000355596 |
| 588.000 | 0.000523803 | 0.000546409 | 0.0000364261 |
| 589.000 | 0.000430313 | 0.000525656 | 0.0000310729 |
| 590.000 | 0.000316823 | 0.000505027 | 0.0000268403 |
| 591.000 | 0.000248213 | 0.000486520 | 0.0000250991 |
| 592.000 | 0.000290442 | 0.000470264 | 0.0000220998 |
| 593.000 | 0.000589411 | 0.000455334 | 0.0000209275 |
| 594.000 | 0.00102396 | 0.000444445 | 0.0000214092 |
| 595.000 | 0.00130204 | 0.000432168 | 0.0000215082 |
| 596.000 | 0.00126301 | 0.000417495 | 0.0000199684 |
| 597.000 | 0.000928700 | 0.000398815 | 0.0000151845 |
| 598.000 | 0.000533422 | 0.000380994 | 0.0000115791 |
| 599.000 | 0.000279948 | 0.000362975 | 0.0000101182 |

| Wavelenght $\lambda(\mathrm{nm})$ | Primary colourants of the CRT (SMPTE phosphor) | | |
|---|---|---|---|
| | **red** | **green** | **blue** |
| 600.000 | 0.000183476 | 0.000349702 | 0.00000998607 |
| 601.000 | 0.000141091 | 0.000337156 | 0.00000878084 |
| 602.000 | 0.000112426 | 0.000325986 | 0.00000744104 |
| 603.000 | 0.0000969454 | 0.000313521 | 0.00000734248 |
| 604.000 | 0.0000928907 | 0.000300370 | 0.00000705610 |
| 605.000 | 0.0000962308 | 0.000289476 | 0.00000826856 |
| 606.000 | 0.000108146 | 0.000279740 | 0.00000702659 |
| 607.000 | 0.000125957 | 0.000270686 | 0.00000732268 |
| 608.000 | 0.000144339 | 0.000260407 | 0.00000730093 |
| 609.000 | 0.000173418 | 0.000249887 | 0.00000707494 |
| 610.000 | 0.000214500 | 0.000240857 | 0.00000722691 |
| 611.000 | 0.000259269 | 0.000232007 | 0.00000700478 |
| 612.000 | 0.000315052 | 0.000225076 | 0.00000777314 |
| 613.000 | 0.000443416 | 0.000218487 | 0.00000837482 |
| 614.000 | 0.000889942 | 0.000214961 | 0.0000113349 |
| 615.000 | 0.00187367 | 0.000218372 | 0.0000173603 |
| 616.000 | 0.00283887 | 0.000221842 | 0.0000259682 |
| 617.000 | 0.00299529 | 0.000217394 | 0.0000281640 |
| 618.000 | 0.00248828 | 0.000205689 | 0.0000275549 |
| 619.000 | 0.00166235 | 0.000190753 | 0.0000260930 |
| 620.000 | 0.00115070 | 0.000181483 | 0.0000256789 |
| 621.000 | 0.00113266 | 0.000175141 | 0.0000275394 |
| 622.000 | 0.00141959 | 0.000172557 | 0.0000296094 |
| 623.000 | 0.00230320 | 0.000175041 | 0.0000325641 |
| 624.000 | 0.00434042 | 0.000190893 | 0.0000449493 |
| 625.000 | 0.00703657 | 0.000215535 | 0.0000627351 |
| 626.000 | 0.00862823 | 0.000229323 | 0.0000753703 |
| 627.000 | 0.00811547 | 0.000218185 | 0.0000720910 |
| 628.000 | 0.00594231 | 0.000188520 | 0.0000543400 |
| 629.000 | 0.00366473 | 0.000155320 | 0.0000346563 |
| 630.000 | 0.00231976 | 0.000133717 | 0.0000243558 |
| 631.000 | 0.00171719 | 0.000122359 | 0.0000176051 |
| 632.000 | 0.00128144 | 0.000111631 | 0.0000123713 |
| 633.000 | 0.000885217 | 0.000103698 | 0.00000984742 |
| 634.000 | 0.000575395 | 0.0000946380 | 0.00000762758 |
| 635.000 | 0.000388723 | 0.0000895190 | 0.00000697055 |
| 636.000 | 0.000262419 | 0.0000837352 | 0.00000609480 |
| 637.000 | 0.000178495 | 0.0000797002 | 0.00000606802 |
| 638.000 | 0.000125497 | 0.0000764206 | 0.00000588899 |
| 639.000 | 0.0000946855 | 0.0000715646 | 0.00000553034 |
| 640.000 | 0.0000723191 | 0.0000682853 | 0.00000481812 |
| 641.000 | 0.0000597466 | 0.0000654503 | 0.00000441089 |
| 642.000 | 0.0000488206 | 0.0000633801 | 0.00000563090 |
| 643.000 | 0.0000421611 | 0.0000620622 | 0.00000564721 |

| Wavelenght $\lambda(\mathrm{nm})$ | Primary colourants of the CRT (SMPTE phosphor) | | |
|---|---|---|---|
| | red | green | blue |
| 644.000 | 0.0000380794 | 0.0000594736 | 0.00000503280 |
| 645.000 | 0.0000377663 | 0.0000555376 | 0.00000570312 |
| 646.000 | 0.0000355476 | 0.0000513254 | 0.00000366182 |
| 647.000 | 0.0000345583 | 0.0000499921 | 0.00000386580 |
| 648.000 | 0.0000321224 | 0.0000489710 | 0.00000358381 |
| 649.000 | 0.0000270794 | 0.0000473035 | 0.00000347918 |
| 650.000 | 0.0000245136 | 0.0000443279 | 0.00000443837 |
| 651.000 | 0.0000232966 | 0.0000418087 | 0.00000402065 |
| 652.000 | 0.0000249015 | 0.0000394960 | 0.00000408840 |
| 653.000 | 0.0000321253 | 0.0000399754 | 0.00000462401 |
| 654.000 | 0.0000428726 | 0.0000379999 | 0.00000486171 |
| 655.000 | 0.0000466073 | 0.0000359402 | 0.00000443749 |
| 656.000 | 0.0000453841 | 0.0000346587 | 0.00000474863 |
| 657.000 | 0.0000342508 | 0.0000327808 | 0.00000574175 |
| 658.000 | 0.0000281059 | 0.0000323039 | 0.00000457342 |
| 659.000 | 0.0000257917 | 0.0000314810 | 0.00000468324 |
| 660.000 | 0.0000273537 | 0.0000301412 | 0.00000396468 |
| 661.000 | 0.0000279905 | 0.0000294848 | 0.00000375435 |
| 662.000 | 0.0000266410 | 0.0000264935 | 0.00000401106 |
| 663.000 | 0.0000257743 | 0.0000256763 | 0.00000502172 |
| 664.000 | 0.0000261506 | 0.0000257483 | 0.00000530169 |
| 665.000 | 0.0000263654 | 0.0000235140 | 0.00000426828 |
| 666.000 | 0.0000266721 | 0.0000234992 | 0.00000506100 |
| 667.000 | 0.0000250539 | 0.0000220937 | 0.00000620110 |
| 668.000 | 0.0000260436 | 0.0000225540 | 0.00000627313 |
| 669.000 | 0.0000279301 | 0.0000227470 | 0.00000688306 |
| 670.000 | 0.0000359215 | 0.0000219688 | 0.00000849165 |
| 671.000 | 0.0000501303 | 0.0000208369 | 0.00000751426 |
| 672.000 | 0.0000561861 | 0.0000174659 | 0.00000651492 |
| 673.000 | 0.0000548416 | 0.0000174778 | 0.00000666960 |
| 674.000 | 0.0000493585 | 0.0000163354 | 0.00000568139 |
| 675.000 | 0.0000381444 | 0.0000151375 | 0.00000495973 |
| 676.000 | 0.0000317855 | 0.0000143353 | 0.00000583215 |
| 677.000 | 0.0000298436 | 0.0000135977 | 0.00000508326 |
| 678.000 | 0.0000253100 | 0.0000117706 | 0.00000589904 |
| 679.000 | 0.0000243475 | 0.0000131439 | 0.00000639209 |
| 680.000 | 0.0000246370 | 0.0000140595 | 0.00000652127 |
| 681.000 | 0.0000244868 | 0.0000115590 | 0.00000713376 |
| 682.000 | 0.0000286810 | 0.0000131936 | 0.00000662890 |
| 683.000 | 0.0000393960 | 0.0000121354 | 0.00000498669 |
| 684.000 | 0.0000901538 | 0.0000120281 | 0.00000504569 |
| 685.000 | 0.000197280 | 0.0000135038 | 0.00000592501 |
| 686.000 | 0.000286616 | 0.0000115968 | 0.00000681705 |
| 687.000 | 0.000292530 | 0.0000122039 | 0.00000668806 |

| Wavelenght $\lambda(\mathrm{nm})$ | Primary colourants of the CRT (SMPTE phosphor) | | |
|---|---|---|---|
| | **red** | **green** | **blue** |
| 688.000 | 0.000226149 | 0.0000124365 | 0.00000541787 |
| 689.000 | 0.000134252 | 0.0000111510 | 0.00000554363 |
| 690.000 | 0.0000813556 | 0.0000100557 | 0.00000425541 |
| 691.000 | 0.0000620231 | 0.00000981781 | 0.00000563368 |
| 692.000 | 0.0000577906 | 0.00000884503 | 0.00000577106 |
| 693.000 | 0.0000629943 | 0.00000750604 | 0.00000495310 |
| 694.000 | 0.0000918842 | 0.00000931793 | 0.00000643284 |
| 695.000 | 0.000161249 | 0.0000104925 | 0.00000665922 |
| 696.000 | 0.000212631 | 0.00000885482 | 0.00000670465 |
| 697.000 | 0.000222346 | 0.00000916258 | 0.00000653570 |
| 698.000 | 0.000191747 | 0.00000851202 | 0.00000539056 |
| 699.000 | 0.000151114 | 0.00000896802 | 0.00000453144 |
| 700.000 | 0.000159527 | 0.0000101333 | 0.00000648319 |
| 701.000 | 0.000279593 | 0.00000980155 | 0.00000562886 |
| 702.000 | 0.000723783 | 0.0000116375 | 0.00000933128 |
| 703.000 | 0.00174712 | 0.0000220800 | 0.0000149842 |
| 704.000 | 0.00297334 | 0.0000372015 | 0.0000193111 |
| 705.000 | 0.00399498 | 0.0000464210 | 0.0000289790 |
| 706.000 | 0.00404043 | 0.0000482103 | 0.0000320187 |
| 707.000 | 0.00320595 | 0.0000415980 | 0.0000233136 |
| 708.000 | 0.00204869 | 0.0000293571 | 0.0000170858 |
| 709.000 | 0.00108340 | 0.0000165425 | 0.0000117402 |
| 710.000 | 0.000642964 | 0.0000128429 | 0.00000977148 |
| 711.000 | 0.000455541 | 0.0000115538 | 0.00000864690 |
| 712.000 | 0.000310249 | 0.0000114560 | 0.00000896047 |
| 713.000 | 0.000208454 | 0.0000122685 | 0.00000931731 |
| 714.000 | 0.000142504 | 0.0000105882 | 0.00000930612 |
| 715.000 | 0.0000996280 | 0.00000926055 | 0.00000732829 |
| 716.000 | 0.0000672178 | 0.0000100472 | 0.00000949255 |
| 717.000 | 0.0000484415 | 0.00000975398 | 0.00000922827 |
| 718.000 | 0.0000323541 | 0.0000108569 | 0.00000945270 |
| 719.000 | 0.0000225869 | 0.0000101750 | 0.00000873899 |
| 720.000 | 0.0000168868 | 0.00000967406 | 0.0000104614 |
| 721.000 | 0.0000167878 | 0.0000105840 | 0.00000894656 |
| 722.000 | 0.0000182103 | 0.0000100334 | 0.00000567058 |
| 723.000 | 0.0000190280 | 0.00000932094 | 0.00000846488 |
| 724.000 | 0.0000208167 | 0.0000101575 | 0.00000921969 |
| 725.000 | 0.0000215289 | 0.0000110490 | 0.00000963464 |
| 726.000 | 0.0000212817 | 0.0000119440 | 0.00000914956 |
| 727.000 | 0.0000220822 | 0.00000803853 | 0.00000717598 |
| 728.000 | 0.0000218639 | 0.00000933485 | 0.00000919301 |
| 729.000 | 0.0000202634 | 0.00000953150 | 0.00000960088 |
| 730.000 | 0.0000164873 | 0.0000117336 | 0.00000921318 |
| 731.000 | 0.0000158940 | 0.0000112008 | 0.00000923544 |

| Wavelenght $\lambda(\mathrm{nm})$ | Primary colourants of the CRT (SMPTE phosphor) | | |
|---|---|---|---|
| | red | green | blue |
| 732.000 | 0.0000153315 | 0.0000117738 | 0.0000126685 |
| 733.000 | 0.0000171379 | 0.0000113336 | 0.0000125800 |
| 734.000 | 0.0000150818 | 0.0000104538 | 0.0000115814 |
| 735.000 | 0.0000139547 | 0.0000100777 | 0.0000123395 |
| 736.000 | 0.0000157587 | 0.0000117304 | 0.0000129299 |
| 737.000 | 0.0000179941 | 0.0000119854 | 0.0000104529 |
| 738.000 | 0.0000170578 | 0.0000138858 | 0.0000151047 |
| 739.000 | 0.0000132114 | 0.0000144875 | 0.0000112966 |
| 740.000 | 0.0000162678 | 0.0000126642 | 0.0000104825 |
| 741.000 | 0.0000175562 | 0.0000146471 | 0.0000111031 |
| 742.000 | 0.0000177496 | 0.0000155204 | 0.0000100487 |
| 743.000 | 0.0000147109 | 0.0000145536 | 0.0000111515 |
| 744.000 | 0.0000157476 | 0.0000131282 | 0.0000143650 |
| 745.000 | 0.0000222557 | 0.0000123158 | 0.0000130820 |
| 746.000 | 0.0000193544 | 0.0000146881 | 0.0000103810 |
| 747.000 | 0.0000235783 | 0.0000132738 | 0.0000150659 |
| 748.000 | 0.0000203056 | 0.0000161259 | 0.0000134434 |
| 749.000 | 0.0000176311 | 0.0000148475 | 0.0000137879 |
| 750.000 | 0.0000157417 | 0.0000133586 | 0.0000125601 |
| 751.000 | 0.0000144023 | 0.0000142354 | 0.0000125087 |
| 752.000 | 0.0000121417 | 0.0000126558 | 0.0000121960 |
| 753.000 | 0.0000172017 | 0.0000147300 | 0.0000101052 |
| 754.000 | 0.0000192404 | 0.0000169445 | 0.0000143174 |
| 755.000 | 0.0000173795 | 0.0000202216 | 0.0000151642 |
| 756.000 | 0.0000220906 | 0.0000165187 | 0.0000126676 |
| 757.000 | 0.0000216997 | 0.0000180113 | 0.0000146204 |
| 758.000 | 0.0000263112 | 0.0000176652 | 0.0000160250 |
| 759.000 | 0.0000256306 | 0.0000174671 | 0.0000162882 |
| 760.000 | 0.0000199888 | 0.0000141177 | 0.0000148166 |
| 761.000 | 0.0000220552 | 0.0000155644 | 0.0000135882 |
| 762.000 | 0.0000260944 | 0.0000170421 | 0.0000166694 |
| 763.000 | 0.0000277469 | 0.0000161544 | 0.0000179439 |
| 764.000 | 0.0000273126 | 0.0000204493 | 0.0000191845 |
| 765.000 | 0.0000312502 | 0.0000159428 | 0.0000149200 |
| 766.000 | 0.0000249524 | 0.0000184533 | 0.0000180050 |
| 767.000 | 0.0000191191 | 0.0000179595 | 0.0000183919 |
| 768.000 | 0.0000248310 | 0.0000187512 | 0.0000171301 |
| 769.000 | 0.0000277612 | 0.0000217861 | 0.0000174974 |
| 770.000 | 0.0000275390 | 0.0000170818 | 0.0000218495 |
| 771.000 | 0.0000305619 | 0.0000203897 | 0.0000199994 |
| 772.000 | 0.0000267325 | 0.0000201907 | 0.0000262191 |
| 773.000 | 0.0000275911 | 0.0000231809 | 0.0000197233 |
| 774.000 | 0.0000248323 | 0.0000252888 | 0.0000187867 |
| 775.000 | 0.0000227620 | 0.0000213583 | 0.0000247064 |

| Wavelenght $\lambda(\mathrm{nm})$ | Primary colourants of the CRT (SMPTE phosphor) | | |
|---|---|---|---|
| | **red** | **green** | **blue** |
| 776.000 | 0.0000214582 | 0.0000216812 | 0.0000243092 |
| 777.000 | 0.0000241468 | 0.0000230925 | 0.0000220107 |
| 778.000 | 0.0000229450 | 0.0000224611 | 0.0000252910 |
| 779.000 | 0.0000336130 | 0.0000204684 | 0.0000282486 |
| 780.000 | 0.0000397533 | 0.0000279871 | 0.0000328351 |

*Table 17: Measured SPDs of the BVM-20F1U CRT (SMPTE phosphor).*

## A.2. Spectral radiant power distribution of a Sony BVM-20E1E (EBU phosphor)

$\lambda = 380$ nm to 780 nm at 1 nm interval, measured with Konica Minolta CS-2000 spectroradiometer.

Data is available at: https://github.com/3dmedium/display_calibration_tool/tree/79833b1/datasets/display_primaries/crt_displays

Data is averaged from 100 measurements, 40.000 ms integration time for each.

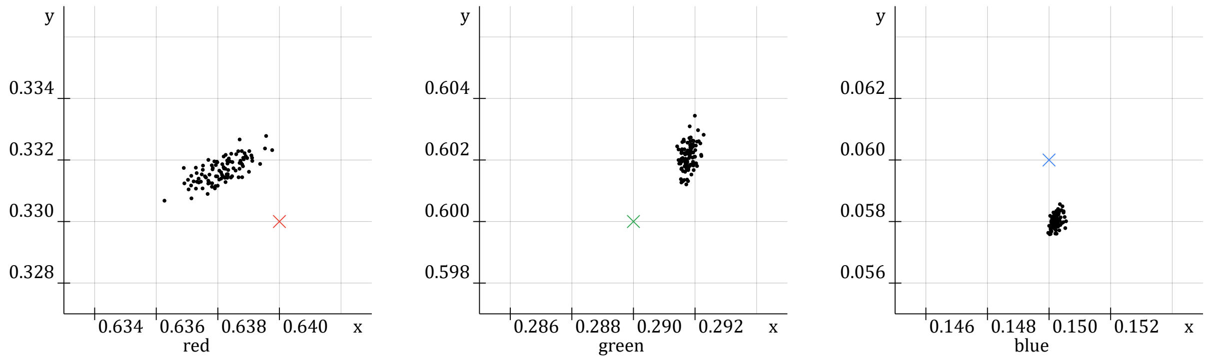


*Figure 25: Deviation of the single measurements in CIE 1931 xy chromaticity diagram, EBU phosphors.*

| Colour | x | | y | |
|---|---|---|---|---|
| | $\bar{x}$ | $\sigma_x$ | $\bar{y}$ | $\sigma_y$ |
| Red | 0.63814 | 0.00065 | 0.33166 | 0.00040 |
| Green | 0.29179 | 0.00018 | 0.60210 | 0.00041 |
| Blue | 0.15022 | 0.00012 | 0.058017 | 0.00020 |

*Figure 26: Averaged chromaticity coordinates and standard deviation, EBU phosphors.*

| Wavelenght $\lambda(\mathrm{nm})$ | primary colourants of the CRT (EBU phosphor) | | |
|---|---|---|---|
| | red | green | blue |
| 380.000 | 0.0000159219 | 0.0000278732 | 0.0000490825 |
| 381.000 | 0.0000176006 | 0.0000303653 | 0.0000519215 |
| 382.000 | 0.0000172267 | 0.0000323370 | 0.0000594729 |
| 383.000 | 0.0000157737 | 0.0000355753 | 0.0000645462 |
| 384.000 | 0.0000185002 | 0.0000353485 | 0.0000735811 |

| Wavelenght $\lambda(\mathrm{nm})$ | primary colourants of the CRT (EBU phosphor) | | |
|---|---|---|---|
| | **red** | **green** | **blue** |
| 385.000 | 0.0000152270 | 0.0000270914 | 0.0000871262 |
| 386.000 | 0.0000101903 | 0.0000199719 | 0.0000975184 |
| 387.000 | 0.0000105290 | 0.0000137053 | 0.000101971 |
| 388.000 | 0.00000882909 | 0.0000113464 | 0.000117657 |
| 389.000 | 0.00000764682 | 0.0000107441 | 0.000128842 |
| 390.000 | 0.00000636828 | 0.00000719089 | 0.000137909 |
| 391.000 | 0.00000652680 | 0.00000651165 | 0.000148765 |
| 392.000 | 0.00000536920 | 0.00000636464 | 0.000162097 |
| 393.000 | 0.00000491333 | 0.00000626468 | 0.000170016 |
| 394.000 | 0.00000534775 | 0.00000540961 | 0.000183204 |
| 395.000 | 0.00000509653 | 0.00000565006 | 0.000194156 |
| 396.000 | 0.00000377212 | 0.00000458978 | 0.000204600 |
| 397.000 | 0.00000441287 | 0.00000650694 | 0.000214836 |
| 398.000 | 0.00000675585 | 0.00000699484 | 0.000232535 |
| 399.000 | 0.00000674434 | 0.00000535204 | 0.000239566 |
| 400.000 | 0.00000612724 | 0.00000402933 | 0.000252308 |
| 401.000 | 0.00000493651 | 0.00000602478 | 0.000275878 |
| 402.000 | 0.00000603734 | 0.00000623636 | 0.000287308 |
| 403.000 | 0.00000534145 | 0.00000466103 | 0.000307148 |
| 404.000 | 0.00000511086 | 0.00000524590 | 0.000325519 |
| 405.000 | 0.00000572049 | 0.00000558926 | 0.000348780 |
| 406.000 | 0.00000558895 | 0.00000536175 | 0.000369840 |
| 407.000 | 0.00000630449 | 0.00000534860 | 0.000393932 |
| 408.000 | 0.00000797288 | 0.00000837279 | 0.000422440 |
| 409.000 | 0.00000643716 | 0.0000121145 | 0.000448957 |
| 410.000 | 0.00000841997 | 0.0000166358 | 0.000480521 |
| 411.000 | 0.0000119404 | 0.0000253815 | 0.000514029 |
| 412.000 | 0.0000143443 | 0.0000349800 | 0.000548058 |
| 413.000 | 0.0000220158 | 0.0000453050 | 0.000585193 |
| 414.000 | 0.0000284989 | 0.0000684429 | 0.000624651 |
| 415.000 | 0.0000346012 | 0.0000823663 | 0.000667352 |
| 416.000 | 0.0000376649 | 0.0000917591 | 0.000713561 |
| 417.000 | 0.0000381082 | 0.000100135 | 0.000761107 |
| 418.000 | 0.0000337731 | 0.0000898645 | 0.000808136 |
| 419.000 | 0.0000297750 | 0.0000723321 | 0.000854430 |
| 420.000 | 0.0000227506 | 0.0000513856 | 0.000901935 |
| 421.000 | 0.0000149833 | 0.0000316014 | 0.000962141 |
| 422.000 | 0.0000131130 | 0.0000246855 | 0.00101565 |
| 423.000 | 0.0000129524 | 0.0000192477 | 0.00106551 |
| 424.000 | 0.0000132732 | 0.0000167202 | 0.00112204 |
| 425.000 | 0.0000147587 | 0.0000204223 | 0.00117602 |
| 426.000 | 0.0000152415 | 0.0000204239 | 0.00123018 |
| 427.000 | 0.0000165987 | 0.0000223161 | 0.00128229 |
| 428.000 | 0.0000170491 | 0.0000237160 | 0.00133580 |

| Wavelenght $\lambda(\mathrm{nm})$ | primary colourants of the CRT (EBU phosphor) | | |
|---|---|---|---|
| | **red** | **green** | **blue** |
| 429.000 | 0.0000183177 | 0.0000252284 | 0.00139541 |
| 430.000 | 0.0000198598 | 0.0000266649 | 0.00144676 |
| 431.000 | 0.0000213701 | 0.0000283139 | 0.00149460 |
| 432.000 | 0.0000240249 | 0.0000310142 | 0.00154442 |
| 433.000 | 0.0000246591 | 0.0000349531 | 0.00159570 |
| 434.000 | 0.0000283273 | 0.0000444526 | 0.00163603 |
| 435.000 | 0.0000319255 | 0.0000571931 | 0.00167591 |
| 436.000 | 0.0000322023 | 0.0000675866 | 0.00171766 |
| 437.000 | 0.0000335353 | 0.0000773885 | 0.00175447 |
| 438.000 | 0.0000351662 | 0.0000816188 | 0.00178861 |
| 439.000 | 0.0000376442 | 0.0000846359 | 0.00182078 |
| 440.000 | 0.0000380745 | 0.0000858675 | 0.00185395 |
| 441.000 | 0.0000376670 | 0.0000804630 | 0.00187516 |
| 442.000 | 0.0000350187 | 0.0000691391 | 0.00189734 |
| 443.000 | 0.0000310905 | 0.0000527456 | 0.00191786 |
| 444.000 | 0.0000288597 | 0.0000453996 | 0.00193104 |
| 445.000 | 0.0000284634 | 0.0000395458 | 0.00194381 |
| 446.000 | 0.0000263710 | 0.0000380012 | 0.00195234 |
| 447.000 | 0.0000260250 | 0.0000394101 | 0.00195997 |
| 448.000 | 0.0000259541 | 0.0000377490 | 0.00196018 |
| 449.000 | 0.0000252504 | 0.0000375089 | 0.00196091 |
| 450.000 | 0.0000244437 | 0.0000404512 | 0.00195403 |
| 451.000 | 0.0000233818 | 0.0000397511 | 0.00193905 |
| 452.000 | 0.0000242409 | 0.0000427494 | 0.00192635 |
| 453.000 | 0.0000246557 | 0.0000447280 | 0.00191571 |
| 454.000 | 0.0000267620 | 0.0000511188 | 0.00189903 |
| 455.000 | 0.0000271968 | 0.0000577322 | 0.00187611 |
| 456.000 | 0.0000290704 | 0.0000626016 | 0.00185217 |
| 457.000 | 0.0000305001 | 0.0000713000 | 0.00182675 |
| 458.000 | 0.0000309063 | 0.0000768595 | 0.00180086 |
| 459.000 | 0.0000302949 | 0.0000776657 | 0.00176566 |
| 460.000 | 0.0000276254 | 0.0000777887 | 0.00173471 |
| 461.000 | 0.0000252012 | 0.0000749729 | 0.00169838 |
| 462.000 | 0.0000233076 | 0.0000750615 | 0.00166368 |
| 463.000 | 0.0000250612 | 0.0000769011 | 0.00161924 |
| 464.000 | 0.0000256584 | 0.0000813148 | 0.00158255 |
| 465.000 | 0.0000240273 | 0.0000877547 | 0.00154320 |
| 466.000 | 0.0000270015 | 0.0000955298 | 0.00150315 |
| 467.000 | 0.0000314944 | 0.000102184 | 0.00146225 |
| 468.000 | 0.0000392389 | 0.000113863 | 0.00141241 |
| 469.000 | 0.0000414055 | 0.000125562 | 0.00137302 |
| 470.000 | 0.0000396343 | 0.000138980 | 0.00133295 |
| 471.000 | 0.0000356640 | 0.000151667 | 0.00128869 |
| 472.000 | 0.0000281472 | 0.000165112 | 0.00124582 |

| Wavelenght $\lambda(\mathrm{nm})$ | primary colourants of the CRT (EBU phosphor) | | |
|---|---|---|---|
| | **red** | **green** | **blue** |
| 473.000 | 0.0000263819 | 0.000178146 | 0.00119682 |
| 474.000 | 0.0000293173 | 0.000195993 | 0.00115510 |
| 475.000 | 0.0000321918 | 0.000217027 | 0.00111491 |
| 476.000 | 0.0000335256 | 0.000236403 | 0.00107397 |
| 477.000 | 0.0000324964 | 0.000251455 | 0.00102761 |
| 478.000 | 0.0000259855 | 0.000260219 | 0.000987938 |
| 479.000 | 0.0000207006 | 0.000273328 | 0.000948680 |
| 480.000 | 0.0000190941 | 0.000293326 | 0.000908797 |
| 481.000 | 0.0000193963 | 0.000317375 | 0.000866571 |
| 482.000 | 0.0000190818 | 0.000343821 | 0.000831979 |
| 483.000 | 0.0000196916 | 0.000371931 | 0.000796116 |
| 484.000 | 0.0000219409 | 0.000401205 | 0.000763044 |
| 485.000 | 0.0000239263 | 0.000428290 | 0.000727890 |
| 486.000 | 0.0000245876 | 0.000456219 | 0.000693014 |
| 487.000 | 0.0000272319 | 0.000484205 | 0.000662748 |
| 488.000 | 0.0000332562 | 0.000521843 | 0.000632841 |
| 489.000 | 0.0000370098 | 0.000561314 | 0.000603035 |
| 490.000 | 0.0000388584 | 0.000600473 | 0.000570121 |
| 491.000 | 0.0000382061 | 0.000633148 | 0.000543759 |
| 492.000 | 0.0000347265 | 0.000662833 | 0.000519683 |
| 493.000 | 0.0000338430 | 0.000693775 | 0.000493999 |
| 494.000 | 0.0000370505 | 0.000728620 | 0.000470580 |
| 495.000 | 0.0000442197 | 0.000762385 | 0.000443698 |
| 496.000 | 0.0000487084 | 0.000790108 | 0.000421735 |
| 497.000 | 0.0000488148 | 0.000822005 | 0.000402283 |
| 498.000 | 0.0000442891 | 0.000857601 | 0.000382181 |
| 499.000 | 0.0000332817 | 0.000896077 | 0.000359511 |
| 500.000 | 0.0000281151 | 0.000933728 | 0.000339919 |
| 501.000 | 0.0000233673 | 0.000972426 | 0.000322844 |
| 502.000 | 0.0000214518 | 0.00101016 | 0.000306577 |
| 503.000 | 0.0000206182 | 0.00104948 | 0.000290779 |
| 504.000 | 0.0000202243 | 0.00109033 | 0.000273544 |
| 505.000 | 0.0000200141 | 0.00112628 | 0.000260162 |
| 506.000 | 0.0000209099 | 0.00116399 | 0.000248049 |
| 507.000 | 0.0000214991 | 0.00120271 | 0.000235345 |
| 508.000 | 0.0000232101 | 0.00123965 | 0.000222777 |
| 509.000 | 0.0000262917 | 0.00127687 | 0.000209187 |
| 510.000 | 0.0000311493 | 0.00131237 | 0.000198757 |
| 511.000 | 0.0000415781 | 0.00134772 | 0.000189122 |
| 512.000 | 0.0000561111 | 0.00138113 | 0.000179537 |
| 513.000 | 0.0000696655 | 0.00141362 | 0.000168725 |
| 514.000 | 0.0000703634 | 0.00144581 | 0.000159559 |
| 515.000 | 0.0000614680 | 0.00147231 | 0.000151683 |
| 516.000 | 0.0000480993 | 0.00149902 | 0.000144102 |

| Wavelenght $\lambda(\mathrm{nm})$ | primary colourants of the CRT (EBU phosphor) | | |
|---|---|---|---|
| | **red** | **green** | **blue** |
| 517.000 | 0.0000372740 | 0.00152676 | 0.000137560 |
| 518.000 | 0.0000316494 | 0.00155218 | 0.000129669 |
| 519.000 | 0.0000293351 | 0.00157444 | 0.000123182 |
| 520.000 | 0.0000280456 | 0.00159472 | 0.000117173 |
| 521.000 | 0.0000268389 | 0.00161383 | 0.000110787 |
| 522.000 | 0.0000257900 | 0.00162861 | 0.000105219 |
| 523.000 | 0.0000261890 | 0.00164609 | 0.0000991057 |
| 524.000 | 0.0000272059 | 0.00165825 | 0.0000940640 |
| 525.000 | 0.0000270328 | 0.00166996 | 0.0000900085 |
| 526.000 | 0.0000275751 | 0.00167890 | 0.0000859121 |
| 527.000 | 0.0000295333 | 0.00168575 | 0.0000800909 |
| 528.000 | 0.0000310436 | 0.00168983 | 0.0000771719 |
| 529.000 | 0.0000317165 | 0.00169638 | 0.0000740675 |
| 530.000 | 0.0000319534 | 0.00169744 | 0.0000696494 |
| 531.000 | 0.0000332825 | 0.00169828 | 0.0000680703 |
| 532.000 | 0.0000336608 | 0.00170039 | 0.0000648160 |
| 533.000 | 0.0000355797 | 0.00169810 | 0.0000591476 |
| 534.000 | 0.0000386701 | 0.00169167 | 0.0000559493 |
| 535.000 | 0.0000448976 | 0.00168629 | 0.0000557434 |
| 536.000 | 0.0000612519 | 0.00168054 | 0.0000517434 |
| 537.000 | 0.0000954545 | 0.00167465 | 0.0000512947 |
| 538.000 | 0.000150444 | 0.00167027 | 0.0000512037 |
| 539.000 | 0.000185362 | 0.00166453 | 0.0000471899 |
| 540.000 | 0.000182847 | 0.00166004 | 0.0000454622 |
| 541.000 | 0.000147962 | 0.00166275 | 0.0000417543 |
| 542.000 | 0.000108843 | 0.00168902 | 0.0000405449 |
| 543.000 | 0.0000960230 | 0.00172579 | 0.0000396058 |
| 544.000 | 0.0000975287 | 0.00174665 | 0.0000384671 |
| 545.000 | 0.0000948098 | 0.00172877 | 0.0000371099 |
| 546.000 | 0.0000823208 | 0.00168069 | 0.0000353475 |
| 547.000 | 0.0000667031 | 0.00162591 | 0.0000341621 |
| 548.000 | 0.0000607573 | 0.00159717 | 0.0000324664 |
| 549.000 | 0.0000585978 | 0.00157725 | 0.0000312782 |
| 550.000 | 0.0000550511 | 0.00154470 | 0.0000304985 |
| 551.000 | 0.0000488732 | 0.00149565 | 0.0000290048 |
| 552.000 | 0.0000438642 | 0.00144339 | 0.0000286833 |
| 553.000 | 0.0000454544 | 0.00140466 | 0.0000270982 |
| 554.000 | 0.0000593443 | 0.00137305 | 0.0000270740 |
| 555.000 | 0.0000772699 | 0.00134449 | 0.0000257288 |
| 556.000 | 0.0000837343 | 0.00131627 | 0.0000250210 |
| 557.000 | 0.0000764557 | 0.00128582 | 0.0000245736 |
| 558.000 | 0.0000574027 | 0.00125847 | 0.0000236959 |
| 559.000 | 0.0000388482 | 0.00122915 | 0.0000226706 |
| 560.000 | 0.0000291251 | 0.00120001 | 0.0000218849 |

| Wavelenght $\lambda(\mathrm{nm})$ | primary colourants of the CRT (EBU phosphor) | | |
|---|---|---|---|
| | **red** | **green** | **blue** |
| 561.000 | 0.0000262902 | 0.00116827 | 0.0000209560 |
| 562.000 | 0.0000268992 | 0.00113877 | 0.0000202457 |
| 563.000 | 0.0000312135 | 0.00111081 | 0.0000195241 |
| 564.000 | 0.0000338147 | 0.00108140 | 0.0000179077 |
| 565.000 | 0.0000333715 | 0.00105115 | 0.0000172448 |
| 566.000 | 0.0000306137 | 0.00102229 | 0.0000164558 |
| 567.000 | 0.0000265204 | 0.000989643 | 0.0000156355 |
| 568.000 | 0.0000250045 | 0.000961888 | 0.0000141920 |
| 569.000 | 0.0000249652 | 0.000932183 | 0.0000134255 |
| 570.000 | 0.0000251009 | 0.000904340 | 0.0000140200 |
| 571.000 | 0.0000238536 | 0.000876202 | 0.0000126371 |
| 572.000 | 0.0000226655 | 0.000848027 | 0.0000121734 |
| 573.000 | 0.0000210022 | 0.000819975 | 0.0000118068 |
| 574.000 | 0.0000213899 | 0.000792024 | 0.0000114179 |
| 575.000 | 0.0000219663 | 0.000766906 | 0.0000108015 |
| 576.000 | 0.0000240415 | 0.000741507 | 0.0000107401 |
| 577.000 | 0.0000274241 | 0.000714677 | 0.0000108073 |
| 578.000 | 0.0000324412 | 0.000689962 | 0.0000106479 |
| 579.000 | 0.0000411521 | 0.000667482 | 0.00000985697 |
| 580.000 | 0.0000728273 | 0.000646028 | 0.00000956750 |
| 581.000 | 0.000159488 | 0.000628321 | 0.0000101392 |
| 582.000 | 0.000263078 | 0.000607073 | 0.0000103738 |
| 583.000 | 0.000290136 | 0.000587318 | 0.0000101578 |
| 584.000 | 0.000269914 | 0.000567540 | 0.0000100466 |
| 585.000 | 0.000242134 | 0.000551741 | 0.00000974949 |
| 586.000 | 0.000259088 | 0.000542293 | 0.0000100175 |
| 587.000 | 0.000302831 | 0.000528441 | 0.0000102165 |
| 588.000 | 0.000310900 | 0.000510933 | 0.00000950109 |
| 589.000 | 0.000266097 | 0.000487354 | 0.00000869793 |
| 590.000 | 0.000215601 | 0.000465304 | 0.00000837641 |
| 591.000 | 0.000197000 | 0.000444481 | 0.00000791964 |
| 592.000 | 0.000274571 | 0.000425663 | 0.00000861027 |
| 593.000 | 0.000592870 | 0.000409196 | 0.00000965469 |
| 594.000 | 0.00103338 | 0.000397146 | 0.0000124013 |
| 595.000 | 0.00131219 | 0.000383743 | 0.0000141485 |
| 596.000 | 0.00127135 | 0.000367614 | 0.0000132994 |
| 597.000 | 0.000932911 | 0.000349951 | 0.0000117299 |
| 598.000 | 0.000535047 | 0.000329650 | 0.00000965432 |
| 599.000 | 0.000280836 | 0.000313299 | 0.00000749750 |
| 600.000 | 0.000183603 | 0.000299589 | 0.00000592544 |
| 601.000 | 0.000140615 | 0.000286910 | 0.00000577855 |
| 602.000 | 0.000112452 | 0.000275069 | 0.00000520971 |
| 603.000 | 0.0000966746 | 0.000264280 | 0.00000503666 |
| 604.000 | 0.0000928202 | 0.000251753 | 0.00000488023 |

| Wavelenght $\lambda(\mathrm{nm})$ | primary colourants of the CRT (EBU phosphor) | | |
|---|---|---|---|
| | **red** | **green** | **blue** |
| 605.000 | 0.0000967444 | 0.000241883 | 0.00000490366 |
| 606.000 | 0.000110451 | 0.000232762 | 0.00000468732 |
| 607.000 | 0.000128063 | 0.000224330 | 0.00000462530 |
| 608.000 | 0.000147415 | 0.000215044 | 0.00000398683 |
| 609.000 | 0.000177263 | 0.000206013 | 0.00000439079 |
| 610.000 | 0.000220035 | 0.000197039 | 0.00000465632 |
| 611.000 | 0.000265704 | 0.000189197 | 0.00000424889 |
| 612.000 | 0.000324570 | 0.000182765 | 0.00000460230 |
| 613.000 | 0.000458365 | 0.000176431 | 0.00000519995 |
| 614.000 | 0.000914441 | 0.000176244 | 0.00000905062 |
| 615.000 | 0.00190619 | 0.000183264 | 0.0000148982 |
| 616.000 | 0.00286959 | 0.000189477 | 0.0000231881 |
| 617.000 | 0.00302333 | 0.000187209 | 0.0000246517 |
| 618.000 | 0.00250909 | 0.000179011 | 0.0000212763 |
| 619.000 | 0.00167238 | 0.000168616 | 0.0000151775 |
| 620.000 | 0.00115440 | 0.000160507 | 0.0000120252 |
| 621.000 | 0.00113644 | 0.000158712 | 0.0000105660 |
| 622.000 | 0.00143645 | 0.000157665 | 0.0000120443 |
| 623.000 | 0.00235679 | 0.000160550 | 0.0000190153 |
| 624.000 | 0.00443786 | 0.000178858 | 0.0000346167 |
| 625.000 | 0.00715998 | 0.000205701 | 0.0000556082 |
| 626.000 | 0.00873607 | 0.000221041 | 0.0000695891 |
| 627.000 | 0.00819397 | 0.000209168 | 0.0000673919 |
| 628.000 | 0.00597446 | 0.000172988 | 0.0000504159 |
| 629.000 | 0.00367877 | 0.000135917 | 0.0000326992 |
| 630.000 | 0.00232934 | 0.000113346 | 0.0000217953 |
| 631.000 | 0.00172763 | 0.000100744 | 0.0000143168 |
| 632.000 | 0.00129336 | 0.0000908377 | 0.0000111164 |
| 633.000 | 0.000895185 | 0.0000814510 | 0.00000931612 |
| 634.000 | 0.000582747 | 0.0000730415 | 0.00000690804 |
| 635.000 | 0.000392274 | 0.0000673394 | 0.00000507931 |
| 636.000 | 0.000265660 | 0.0000625675 | 0.00000395499 |
| 637.000 | 0.000180343 | 0.0000584064 | 0.00000342681 |
| 638.000 | 0.000128405 | 0.0000552121 | 0.00000329999 |
| 639.000 | 0.0000950286 | 0.0000533524 | 0.00000319292 |
| 640.000 | 0.0000741948 | 0.0000511347 | 0.00000296161 |
| 641.000 | 0.0000616973 | 0.0000470829 | 0.00000288738 |
| 642.000 | 0.0000512225 | 0.0000453702 | 0.00000272920 |
| 643.000 | 0.0000440168 | 0.0000443479 | 0.00000256369 |
| 644.000 | 0.0000407689 | 0.0000420188 | 0.00000285713 |
| 645.000 | 0.0000384239 | 0.0000403640 | 0.00000251220 |
| 646.000 | 0.0000363381 | 0.0000402604 | 0.00000207059 |
| 647.000 | 0.0000345515 | 0.0000375053 | 0.00000225319 |
| 648.000 | 0.0000317607 | 0.0000343236 | 0.00000247060 |

| Wavelenght $\lambda(\mathrm{nm})$ | primary colourants of the CRT (EBU phosphor) | | |
|---|---|---|---|
| | red | green | blue |
| 649.000 | 0.0000280150 | 0.0000322576 | 0.00000175066 |
| 650.000 | 0.0000243931 | 0.0000310715 | 0.00000153006 |
| 651.000 | 0.0000234542 | 0.0000291680 | 0.00000154348 |
| 652.000 | 0.0000246311 | 0.0000285128 | 0.00000242481 |
| 653.000 | 0.0000335747 | 0.0000277058 | 0.00000248006 |
| 654.000 | 0.0000428705 | 0.0000274722 | 0.00000277104 |
| 655.000 | 0.0000473921 | 0.0000261941 | 0.00000231790 |
| 656.000 | 0.0000450324 | 0.0000257788 | 0.00000202852 |
| 657.000 | 0.0000376793 | 0.0000242062 | 0.00000238634 |
| 658.000 | 0.0000288818 | 0.0000214975 | 0.00000272906 |
| 659.000 | 0.0000242001 | 0.0000205654 | 0.00000230295 |
| 660.000 | 0.0000237265 | 0.0000190718 | 0.00000291648 |
| 661.000 | 0.0000235927 | 0.0000189917 | 0.00000260820 |
| 662.000 | 0.0000233004 | 0.0000173939 | 0.00000267453 |
| 663.000 | 0.0000212179 | 0.0000156376 | 0.00000302413 |
| 664.000 | 0.0000218485 | 0.0000159163 | 0.00000221776 |
| 665.000 | 0.0000240919 | 0.0000162783 | 0.00000255016 |
| 666.000 | 0.0000237155 | 0.0000162929 | 0.00000260552 |
| 667.000 | 0.0000227185 | 0.0000168824 | 0.00000269129 |
| 668.000 | 0.0000236603 | 0.0000171965 | 0.00000249793 |
| 669.000 | 0.0000273395 | 0.0000171257 | 0.00000182327 |
| 670.000 | 0.0000329405 | 0.0000166084 | 0.00000287165 |
| 671.000 | 0.0000414899 | 0.0000156795 | 0.00000273492 |
| 672.000 | 0.0000469927 | 0.0000151753 | 0.00000317907 |
| 673.000 | 0.0000442964 | 0.0000139011 | 0.00000286011 |
| 674.000 | 0.0000367473 | 0.0000131379 | 0.00000192243 |
| 675.000 | 0.0000305361 | 0.0000120780 | 0.00000228021 |
| 676.000 | 0.0000282811 | 0.0000119817 | 0.00000292819 |
| 677.000 | 0.0000271753 | 0.0000103794 | 0.00000349432 |
| 678.000 | 0.0000243457 | 0.0000103199 | 0.00000360356 |
| 679.000 | 0.0000232785 | 0.0000115691 | 0.00000304095 |
| 680.000 | 0.0000244201 | 0.0000118892 | 0.00000365581 |
| 681.000 | 0.0000258733 | 0.0000126346 | 0.00000338453 |
| 682.000 | 0.0000282925 | 0.0000119273 | 0.00000271491 |
| 683.000 | 0.0000407186 | 0.0000111349 | 0.00000242048 |
| 684.000 | 0.0000921390 | 0.0000115937 | 0.00000333695 |
| 685.000 | 0.000202113 | 0.0000109295 | 0.00000456502 |
| 686.000 | 0.000293546 | 0.0000114122 | 0.00000433277 |
| 687.000 | 0.000298751 | 0.0000121216 | 0.00000474674 |
| 688.000 | 0.000231240 | 0.0000110660 | 0.00000408248 |
| 689.000 | 0.000136181 | 0.00000865473 | 0.00000418830 |
| 690.000 | 0.0000805625 | 0.00000901199 | 0.00000305783 |
| 691.000 | 0.0000651880 | 0.00000953700 | 0.00000255907 |
| 692.000 | 0.0000596997 | 0.00000765772 | 0.00000386177 |

| Wavelenght $\lambda(\mathrm{nm})$ | primary colourants of the CRT (EBU phosphor) | | |
|---|---|---|---|
| | **red** | **green** | **blue** |
| 693.000 | 0.0000637972 | 0.00000748565 | 0.00000325915 |
| 694.000 | 0.0000957726 | 0.00000884732 | 0.00000480682 |
| 695.000 | 0.000168085 | 0.00000847127 | 0.00000530782 |
| 696.000 | 0.000222582 | 0.00000820681 | 0.00000597622 |
| 697.000 | 0.000228096 | 0.00000912200 | 0.00000488439 |
| 698.000 | 0.000197328 | 0.00000873574 | 0.00000493542 |
| 699.000 | 0.000159880 | 0.00000757130 | 0.00000385152 |
| 700.000 | 0.000167255 | 0.00000818844 | 0.00000517476 |
| 701.000 | 0.000296663 | 0.00000982774 | 0.00000646636 |
| 702.000 | 0.000767300 | 0.0000150394 | 0.00000837757 |
| 703.000 | 0.00181942 | 0.0000248551 | 0.0000152755 |
| 704.000 | 0.00307250 | 0.0000411061 | 0.0000217430 |
| 705.000 | 0.00409877 | 0.0000544409 | 0.0000318678 |
| 706.000 | 0.00412369 | 0.0000567416 | 0.0000333194 |
| 707.000 | 0.00326182 | 0.0000492822 | 0.0000261323 |
| 708.000 | 0.00208108 | 0.0000342707 | 0.0000165103 |
| 709.000 | 0.00110425 | 0.0000192360 | 0.0000124750 |
| 710.000 | 0.000658257 | 0.0000166044 | 0.0000108924 |
| 711.000 | 0.000464550 | 0.0000140558 | 0.0000101361 |
| 712.000 | 0.000317020 | 0.0000114543 | 0.00000772115 |
| 713.000 | 0.000215089 | 0.0000110393 | 0.00000621630 |
| 714.000 | 0.000145836 | 0.00000920953 | 0.00000821894 |
| 715.000 | 0.000102103 | 0.00000864577 | 0.00000770131 |
| 716.000 | 0.0000730985 | 0.00000738054 | 0.00000668048 |
| 717.000 | 0.0000539934 | 0.00000910365 | 0.00000453097 |
| 718.000 | 0.0000342328 | 0.00000953764 | 0.00000593781 |
| 719.000 | 0.0000227466 | 0.00000899736 | 0.00000742835 |
| 720.000 | 0.0000171429 | 0.00000704044 | 0.00000719117 |
| 721.000 | 0.0000193189 | 0.00000890212 | 0.00000533144 |
| 722.000 | 0.0000212125 | 0.00000964587 | 0.00000480052 |
| 723.000 | 0.0000207820 | 0.00000695220 | 0.00000510514 |
| 724.000 | 0.0000232517 | 0.00000612496 | 0.00000486374 |
| 725.000 | 0.0000273703 | 0.00000625375 | 0.00000621576 |
| 726.000 | 0.0000256795 | 0.00000774575 | 0.00000593323 |
| 727.000 | 0.0000228037 | 0.00000655846 | 0.00000406792 |
| 728.000 | 0.0000196784 | 0.00000703577 | 0.00000657184 |
| 729.000 | 0.0000159112 | 0.00000920278 | 0.00000750081 |
| 730.000 | 0.0000163851 | 0.00000821030 | 0.00000584622 |
| 731.000 | 0.0000168903 | 0.00000790479 | 0.00000683579 |
| 732.000 | 0.0000163862 | 0.00000980422 | 0.00000850256 |
| 733.000 | 0.0000143075 | 0.00000824405 | 0.00000783277 |
| 734.000 | 0.0000112312 | 0.0000104660 | 0.0000106233 |
| 735.000 | 0.0000124883 | 0.00000868615 | 0.0000100193 |
| 736.000 | 0.0000142867 | 0.00000713831 | 0.00000776653 |

| Wavelenght $\lambda(\mathrm{nm})$ | primary colourants of the CRT (EBU phosphor) | | |
|---|---|---|---|
| | red | green | blue |
| 737.000 | 0.0000142444 | 0.00000704232 | 0.00000679967 |
| 738.000 | 0.0000136736 | 0.00000606049 | 0.0000104639 |
| 739.000 | 0.0000118622 | 0.00000772045 | 0.0000104158 |
| 740.000 | 0.0000148096 | 0.00000686923 | 0.00000574379 |
| 741.000 | 0.0000129298 | 0.00000923463 | 0.00000593791 |
| 742.000 | 0.0000119199 | 0.00000951188 | 0.00000792165 |
| 743.000 | 0.0000124577 | 0.0000117007 | 0.00000877621 |
| 744.000 | 0.0000152185 | 0.00000883547 | 0.00000786907 |
| 745.000 | 0.0000146645 | 0.00000735157 | 0.00000887187 |
| 746.000 | 0.0000152685 | 0.00000794820 | 0.00000672857 |
| 747.000 | 0.0000178670 | 0.00000843617 | 0.00000807977 |
| 748.000 | 0.0000142314 | 0.00000784409 | 0.00000810019 |
| 749.000 | 0.0000149812 | 0.0000114962 | 0.0000102590 |
| 750.000 | 0.0000129756 | 0.00000894350 | 0.00000673610 |
| 751.000 | 0.0000141800 | 0.00000892489 | 0.00000814076 |
| 752.000 | 0.0000153110 | 0.00000991430 | 0.0000112858 |
| 753.000 | 0.0000184308 | 0.0000102881 | 0.0000108163 |
| 754.000 | 0.0000172042 | 0.00000887068 | 0.0000100060 |
| 755.000 | 0.0000170558 | 0.0000106342 | 0.0000126139 |
| 756.000 | 0.0000191307 | 0.00000914525 | 0.0000145463 |
| 757.000 | 0.0000147770 | 0.00000983367 | 0.00000954171 |
| 758.000 | 0.0000162320 | 0.0000105535 | 0.0000112826 |
| 759.000 | 0.0000139507 | 0.00000927447 | 0.00000916071 |
| 760.000 | 0.0000162427 | 0.0000111219 | 0.00000770028 |
| 761.000 | 0.0000151167 | 0.0000112436 | 0.00000660965 |
| 762.000 | 0.0000184696 | 0.0000101309 | 0.00000874925 |
| 763.000 | 0.0000186345 | 0.00000876510 | 0.00000798650 |
| 764.000 | 0.0000188471 | 0.0000127824 | 0.0000114275 |
| 765.000 | 0.0000134755 | 0.0000137761 | 0.0000118050 |
| 766.000 | 0.0000104472 | 0.00000790086 | 0.0000115629 |
| 767.000 | 0.0000175452 | 0.0000132473 | 0.00000969589 |
| 768.000 | 0.0000197418 | 0.0000115039 | 0.0000117126 |
| 769.000 | 0.0000243500 | 0.0000109290 | 0.0000102943 |
| 770.000 | 0.0000176682 | 0.0000140107 | 0.0000108440 |
| 771.000 | 0.0000203375 | 0.0000107420 | 0.00000981559 |
| 772.000 | 0.0000145234 | 0.0000157820 | 0.0000145507 |
| 773.000 | 0.0000149734 | 0.0000129157 | 0.0000105882 |
| 774.000 | 0.0000137314 | 0.0000130483 | 0.0000132443 |
| 775.000 | 0.0000169726 | 0.0000119104 | 0.0000134175 |
| 776.000 | 0.0000130107 | 0.0000126576 | 0.00000876841 |
| 777.000 | 0.0000140500 | 0.0000129585 | 0.0000125214 |
| 778.000 | 0.0000191649 | 0.0000106929 | 0.0000117920 |
| 779.000 | 0.0000165094 | 0.0000178166 | 0.0000148500 |
| 780.000 | 0.0000224912 | 0.0000131453 | 0.0000250094 |

*Table 18: Measured SPDs of the BVM-20F1E CRT (EBU phosphor).*

## A.3. Spectral radiant power distribution of the averaged BT.709 primaries

$\lambda = 380\text{nm to } 780\text{nm at } 1\text{nm intervals}$, this table is created from the measured spectral radiant power distribution seen in Appendix A.1 and Appendix A.2.

Data is available at: https://github.com/3dmedium/display_calibration_tool/tree/79833b1/datasets/display_primaries/crt_displays

| **Wavelenght $\lambda(\mathrm{nm})$** | **primary colourants of the CRT (BT.709)** | | |
|---|---|---|---|
| | **red** | **green** | **blue** |
| 380 | 0.00001592191 | 0.00001883967 | 0.00004908248 |
| 381 | 0.00001760056 | 0.00002140488 | 0.00005192146 |
| 382 | 0.00001722668 | 0.00002322009 | 0.00005947294 |
| 383 | 0.00001577369 | 0.00002417198 | 0.00006454622 |
| 384 | 0.00001850019 | 0.00002286629 | 0.00007358113 |
| 385 | 0.00001522697 | 0.00001835574 | 0.00008712619 |
| 386 | 0.00001019026 | 0.00001460948 | 0.00009751838 |
| 387 | 0.00001052898 | 0.000009985582 | 0.0001019710 |
| 388 | 0.000008829091 | 0.000009447471 | 0.0001176573 |
| 389 | 0.000007646820 | 0.000009708654 | 0.0001288417 |
| 390 | 0.000006368280 | 0.000006171213 | 0.0001379086 |
| 391 | 0.000006526799 | 0.000005737355 | 0.0001487651 |
| 392 | 0.000005369204 | 0.000006229971 | 0.0001620970 |
| 393 | 0.000004913331 | 0.000005354803 | 0.0001700160 |
| 394 | 0.000005347746 | 0.000005374421 | 0.0001832041 |
| 395 | 0.000005096528 | 0.000005418088 | 0.0001941558 |
| 396 | 0.000003772125 | 0.000004365442 | 0.0002045999 |
| 397 | 0.000004412869 | 0.000005964681 | 0.0002148355 |
| 398 | 0.000006755846 | 0.000005963495 | 0.0002325348 |
| 399 | 0.000006744338 | 0.000005512205 | 0.0002395655 |
| 400 | 0.000006127237 | 0.000005397948 | 0.0002523078 |
| 401 | 0.000004936513 | 0.000005464442 | 0.0002758784 |
| 402 | 0.000006037337 | 0.000004783762 | 0.0002873080 |
| 403 | 0.000005341449 | 0.000004258941 | 0.0003071482 |
| 404 | 0.000005110859 | 0.000005017484 | 0.0003255188 |
| 405 | 0.000005720487 | 0.000005704211 | 0.0003487804 |
| 406 | 0.000005588946 | 0.000005287620 | 0.0003698395 |
| 407 | 0.000006304489 | 0.000005403833 | 0.0003939318 |
| 408 | 0.000007972879 | 0.000007833493 | 0.0004224398 |
| 409 | 0.000006437161 | 0.00001011430 | 0.0004489569 |
| 410 | 0.000008419969 | 0.00001270346 | 0.0004805209 |
| 411 | 0.00001194045 | 0.00001882247 | 0.0005140290 |
| 412 | 0.00001434427 | 0.00002549015 | 0.0005480583 |

| Wavelenght $\lambda(\mathrm{nm})$ | primary colourants of the CRT (BT.709) | | |
|---|---|---|---|
| | red | green | blue |
| 413 | 0.00002201581 | 0.00003280945 | 0.0005851932 |
| 414 | 0.00002849886 | 0.00004806996 | 0.0006246510 |
| 415 | 0.00003460124 | 0.00005768089 | 0.0006673516 |
| 416 | 0.00003766492 | 0.00006426757 | 0.0007135615 |
| 417 | 0.00003810817 | 0.00006899885 | 0.0007611070 |
| 418 | 0.00003377308 | 0.00006325742 | 0.0008081360 |
| 419 | 0.00002977500 | 0.00005253291 | 0.0008544297 |
| 420 | 0.00002275065 | 0.00003813152 | 0.0009019346 |
| 421 | 0.00001498326 | 0.00002360396 | 0.0009621406 |
| 422 | 0.00001311299 | 0.00001957769 | 0.001015654 |
| 423 | 0.00001295243 | 0.00001799930 | 0.001065514 |
| 424 | 0.00001327319 | 0.00001721967 | 0.001122040 |
| 425 | 0.00001475870 | 0.00001865743 | 0.001176024 |
| 426 | 0.00001524152 | 0.00001834939 | 0.001230179 |
| 427 | 0.00001659868 | 0.00002001213 | 0.001282287 |
| 428 | 0.00001704908 | 0.00002176337 | 0.001335802 |
| 429 | 0.00001831771 | 0.00002274577 | 0.001395407 |
| 430 | 0.00001985976 | 0.00002355030 | 0.001446763 |
| 431 | 0.00002137011 | 0.00002522036 | 0.001494600 |
| 432 | 0.00002402488 | 0.00002744363 | 0.001544415 |
| 433 | 0.00002465913 | 0.00003044811 | 0.001595704 |
| 434 | 0.00002832729 | 0.00003687845 | 0.001636034 |
| 435 | 0.00003192545 | 0.00004426934 | 0.001675909 |
| 436 | 0.00003220232 | 0.00005108430 | 0.001717656 |
| 437 | 0.00003353530 | 0.00005770848 | 0.001754468 |
| 438 | 0.00003516622 | 0.00006164452 | 0.001788608 |
| 439 | 0.00003764421 | 0.00006515012 | 0.001820785 |
| 440 | 0.00003807453 | 0.00006655660 | 0.001853950 |
| 441 | 0.00003766696 | 0.00006396515 | 0.001875156 |
| 442 | 0.00003501869 | 0.00005622819 | 0.001897340 |
| 443 | 0.00003109048 | 0.00004424027 | 0.001917862 |
| 444 | 0.00002885973 | 0.00003970660 | 0.001931040 |
| 445 | 0.00002846338 | 0.00003628476 | 0.001943811 |
| 446 | 0.00002637097 | 0.00003441320 | 0.001952345 |
| 447 | 0.00002602502 | 0.00003644110 | 0.001959967 |
| 448 | 0.00002595412 | 0.00003678628 | 0.001960183 |
| 449 | 0.00002525041 | 0.00003772655 | 0.001960913 |
| 450 | 0.00002444374 | 0.00003907733 | 0.001954026 |
| 451 | 0.00002338176 | 0.00003993193 | 0.001939048 |
| 452 | 0.00002424093 | 0.00004257846 | 0.001926350 |
| 453 | 0.00002465569 | 0.00004521751 | 0.001915712 |
| 454 | 0.00002676198 | 0.00004985938 | 0.001899025 |
| 455 | 0.00002719678 | 0.00005432697 | 0.001876107 |
| 456 | 0.00002907044 | 0.00005840928 | 0.001852174 |

| Wavelenght $\lambda(\mathrm{nm})$ | primary colourants of the CRT (BT.709) | | |
|---|---|---|---|
| | **red** | **green** | **blue** |
| 457 | 0.00003050014 | 0.00006550217 | 0.001826750 |
| 458 | 0.00003090634 | 0.00007131052 | 0.001800865 |
| 459 | 0.00003029490 | 0.00007239078 | 0.001765659 |
| 460 | 0.00002762537 | 0.00007371371 | 0.001734710 |
| 461 | 0.00002520119 | 0.00007236479 | 0.001698377 |
| 462 | 0.00002330756 | 0.00007241381 | 0.001663680 |
| 463 | 0.00002506122 | 0.00007621023 | 0.001619243 |
| 464 | 0.00002565841 | 0.00008037247 | 0.001582554 |
| 465 | 0.00002402727 | 0.00008746565 | 0.001543199 |
| 466 | 0.00002700149 | 0.00009422995 | 0.001503155 |
| 467 | 0.00003149443 | 0.0001005239 | 0.001462248 |
| 468 | 0.00003923894 | 0.0001116025 | 0.001412406 |
| 469 | 0.00004140548 | 0.0001210263 | 0.001373019 |
| 470 | 0.00003963433 | 0.0001340221 | 0.001332954 |
| 471 | 0.00003566402 | 0.0001453720 | 0.001288691 |
| 472 | 0.00002814716 | 0.0001577149 | 0.001245825 |
| 473 | 0.00002638193 | 0.0001694997 | 0.001196820 |
| 474 | 0.00002931733 | 0.0001857326 | 0.001155101 |
| 475 | 0.00003219175 | 0.0002043919 | 0.001114906 |
| 476 | 0.00003352560 | 0.0002211131 | 0.001073972 |
| 477 | 0.00003249637 | 0.0002363268 | 0.001027615 |
| 478 | 0.00002598553 | 0.0002467030 | 0.0009879378 |
| 479 | 0.00002070059 | 0.0002618222 | 0.0009486803 |
| 480 | 0.00001909411 | 0.0002802832 | 0.0009087968 |
| 481 | 0.00001939632 | 0.0003022997 | 0.0008665708 |
| 482 | 0.00001908176 | 0.0003266697 | 0.0008319790 |
| 483 | 0.00001969156 | 0.0003531535 | 0.0007961164 |
| 484 | 0.00002194092 | 0.0003797476 | 0.0007630436 |
| 485 | 0.00002392632 | 0.0004045575 | 0.0007278903 |
| 486 | 0.00002458757 | 0.0004315269 | 0.0006930145 |
| 487 | 0.00002723190 | 0.0004585767 | 0.0006627476 |
| 488 | 0.00003325615 | 0.0004920974 | 0.0006328414 |
| 489 | 0.00003700984 | 0.0005284224 | 0.0006030351 |
| 490 | 0.00003885844 | 0.0005638934 | 0.0005701208 |
| 491 | 0.00003820613 | 0.0005946511 | 0.0005437595 |
| 492 | 0.00003472654 | 0.0006241271 | 0.0005196831 |
| 493 | 0.00003384301 | 0.0006548827 | 0.0004939986 |
| 494 | 0.00003705050 | 0.0006883756 | 0.0004705797 |
| 495 | 0.00004421971 | 0.0007212943 | 0.0004436978 |
| 496 | 0.00004870841 | 0.0007509193 | 0.0004217352 |
| 497 | 0.00004881484 | 0.0007838902 | 0.0004022828 |
| 498 | 0.00004428905 | 0.0008186805 | 0.0003821810 |
| 499 | 0.00003328167 | 0.0008546903 | 0.0003595107 |
| 500 | 0.00002811510 | 0.0008919351 | 0.0003399186 |

| Wavelenght $\lambda(\mathrm{nm})$ | primary colourants of the CRT (BT.709) | | |
|---|---|---|---|
| | **red** | **green** | **blue** |
| 501 | 0.00002336730 | 0.0009290307 | 0.0003228445 |
| 502 | 0.00002145181 | 0.0009662885 | 0.0003065767 |
| 503 | 0.00002061819 | 0.001004661 | 0.0002907785 |
| 504 | 0.00002022435 | 0.001044236 | 0.0002735442 |
| 505 | 0.00002001408 | 0.001080051 | 0.0002601620 |
| 506 | 0.00002090989 | 0.001116501 | 0.0002480492 |
| 507 | 0.00002149911 | 0.001154389 | 0.0002353451 |
| 508 | 0.00002321011 | 0.001191161 | 0.0002227766 |
| 509 | 0.00002629169 | 0.001227674 | 0.0002091866 |
| 510 | 0.00003114932 | 0.001261637 | 0.0001987571 |
| 511 | 0.00004157810 | 0.001296148 | 0.0001891225 |
| 512 | 0.00005611109 | 0.001328641 | 0.0001795370 |
| 513 | 0.00006966549 | 0.001361742 | 0.0001687253 |
| 514 | 0.00007036340 | 0.001392872 | 0.0001595589 |
| 515 | 0.00006146797 | 0.001420758 | 0.0001516827 |
| 516 | 0.00004809930 | 0.001448114 | 0.0001441016 |
| 517 | 0.00003727398 | 0.001474336 | 0.0001375597 |
| 518 | 0.00003164943 | 0.001500709 | 0.0001296686 |
| 519 | 0.00002933514 | 0.001523767 | 0.0001231823 |
| 520 | 0.00002804556 | 0.001544980 | 0.0001171727 |
| 521 | 0.00002683887 | 0.001563948 | 0.0001107866 |
| 522 | 0.00002579005 | 0.001580996 | 0.0001052192 |
| 523 | 0.00002618896 | 0.001599595 | 0.00009910571 |
| 524 | 0.00002720589 | 0.001612852 | 0.00009406399 |
| 525 | 0.00002703279 | 0.001624761 | 0.00009000848 |
| 526 | 0.00002757511 | 0.001635937 | 0.00008591210 |
| 527 | 0.00002953328 | 0.001643823 | 0.00008009088 |
| 528 | 0.00003104365 | 0.001650724 | 0.00007717187 |
| 529 | 0.00003171645 | 0.001657905 | 0.00007406749 |
| 530 | 0.00003195337 | 0.001661808 | 0.00006964943 |
| 531 | 0.00003328250 | 0.001664180 | 0.00006807034 |
| 532 | 0.00003366083 | 0.001666238 | 0.00006481596 |
| 533 | 0.00003557973 | 0.001666157 | 0.00005914758 |
| 534 | 0.00003867014 | 0.001662662 | 0.00005594928 |
| 535 | 0.00004489759 | 0.001658977 | 0.00005574342 |
| 536 | 0.00006125194 | 0.001655120 | 0.00005174338 |
| 537 | 0.00009545446 | 0.001651152 | 0.00005129474 |
| 538 | 0.0001504440 | 0.001647969 | 0.00005120374 |
| 539 | 0.0001853618 | 0.001644630 | 0.00004718992 |
| 540 | 0.0001828472 | 0.001639239 | 0.00004546225 |
| 541 | 0.0001479624 | 0.001639744 | 0.00004175430 |
| 542 | 0.0001088432 | 0.001654393 | 0.00004054493 |
| 543 | 0.00009602301 | 0.001677292 | 0.00003960581 |
| 544 | 0.00009752874 | 0.001688478 | 0.00003846715 |

| Wavelenght $\lambda(\mathrm{nm})$ | primary colourants of the CRT (BT.709) | | |
|---|---|---|---|
| | **red** | **green** | **blue** |
| 545 | 0.00009480978 | 0.001673309 | 0.00003710991 |
| 546 | 0.00008232081 | 0.001636117 | 0.00003534749 |
| 547 | 0.00006670309 | 0.001593989 | 0.00003416206 |
| 548 | 0.00006075732 | 0.001570468 | 0.00003246638 |
| 549 | 0.00005859778 | 0.001552018 | 0.00003127820 |
| 550 | 0.00005505113 | 0.001525040 | 0.00003049846 |
| 551 | 0.00004887323 | 0.001486412 | 0.00002900476 |
| 552 | 0.00004386423 | 0.001443618 | 0.00002868329 |
| 553 | 0.00004545437 | 0.001413281 | 0.00002709819 |
| 554 | 0.00005934431 | 0.001385078 | 0.00002707396 |
| 555 | 0.00007726991 | 0.001359625 | 0.00002572884 |
| 556 | 0.00008373431 | 0.001332091 | 0.00002502096 |
| 557 | 0.00007645574 | 0.001304796 | 0.00002457364 |
| 558 | 0.00005740275 | 0.001279366 | 0.00002369590 |
| 559 | 0.00003884824 | 0.001252926 | 0.00002267063 |
| 560 | 0.00002912514 | 0.001224445 | 0.00002188489 |
| 561 | 0.00002629021 | 0.001194287 | 0.00002095598 |
| 562 | 0.00002689923 | 0.001166705 | 0.00002024566 |
| 563 | 0.00003121353 | 0.001139887 | 0.00001952406 |
| 564 | 0.00003381469 | 0.001111932 | 0.00001790769 |
| 565 | 0.00003337152 | 0.001082152 | 0.00001724482 |
| 566 | 0.00003061372 | 0.001054803 | 0.00001645579 |
| 567 | 0.00002652036 | 0.001024155 | 0.00001563554 |
| 568 | 0.00002500447 | 0.0009978195 | 0.00001419201 |
| 569 | 0.00002496515 | 0.0009695007 | 0.00001342549 |
| 570 | 0.00002510088 | 0.0009426008 | 0.00001402004 |
| 571 | 0.00002385358 | 0.0009148794 | 0.00001263712 |
| 572 | 0.00002266546 | 0.0008868013 | 0.00001217337 |
| 573 | 0.00002100220 | 0.0008594545 | 0.00001180676 |
| 574 | 0.00002138994 | 0.0008322552 | 0.00001141792 |
| 575 | 0.00002196628 | 0.0008067501 | 0.00001080154 |
| 576 | 0.00002404154 | 0.0007816424 | 0.00001074014 |
| 577 | 0.00002742412 | 0.0007545901 | 0.00001080731 |
| 578 | 0.00003244124 | 0.0007295977 | 0.00001064786 |
| 579 | 0.00004115211 | 0.0007073310 | 0.000009856974 |
| 580 | 0.00007282726 | 0.0006854145 | 0.000009567497 |
| 581 | 0.0001594880 | 0.0006656125 | 0.00001013922 |
| 582 | 0.0002630775 | 0.0006444249 | 0.00001037376 |
| 583 | 0.0002901355 | 0.0006243565 | 0.00001015777 |
| 584 | 0.0002699141 | 0.0006036521 | 0.00001004665 |
| 585 | 0.0002421345 | 0.0005864875 | 0.000009749492 |
| 586 | 0.0002590878 | 0.0005743872 | 0.00001001749 |
| 587 | 0.0003028315 | 0.0005578089 | 0.00001021650 |
| 588 | 0.0003108996 | 0.0005396839 | 0.000009501088 |

| Wavelenght $\lambda(\mathrm{nm})$ | primary colourants of the CRT (BT.709) | | |
|---|---|---|---|
| | red | green | blue |
| 589 | 0.0002660973 | 0.0005171002 | 0.000008697925 |
| 590 | 0.0002156011 | 0.0004953443 | 0.000008376408 |
| 591 | 0.0001970003 | 0.0004753066 | 0.000007919636 |
| 592 | 0.0002745707 | 0.0004574419 | 0.000008610271 |
| 593 | 0.0005928705 | 0.0004414424 | 0.000009654686 |
| 594 | 0.001033379 | 0.0004297537 | 0.00001240126 |
| 595 | 0.001312194 | 0.0004166663 | 0.00001414848 |
| 596 | 0.001271354 | 0.0004009691 | 0.00001329935 |
| 597 | 0.0009329113 | 0.0003824214 | 0.00001172986 |
| 598 | 0.0005350466 | 0.0003630011 | 0.000009654323 |
| 599 | 0.0002808359 | 0.0003454528 | 0.000007497498 |
| 600 | 0.0001836032 | 0.0003316940 | 0.000005925435 |
| 601 | 0.0001406145 | 0.0003188287 | 0.000005778546 |
| 602 | 0.0001124525 | 0.0003070978 | 0.000005209710 |
| 603 | 0.00009667462 | 0.0002952200 | 0.000005036664 |
| 604 | 0.00009282023 | 0.0002821159 | 0.000004880231 |
| 605 | 0.00009674441 | 0.0002715141 | 0.000004903662 |
| 606 | 0.0001104515 | 0.0002618894 | 0.000004687316 |
| 607 | 0.0001280634 | 0.0002529636 | 0.000004625298 |
| 608 | 0.0001474145 | 0.0002429743 | 0.000003986832 |
| 609 | 0.0001772628 | 0.0002329866 | 0.000004390793 |
| 610 | 0.0002200347 | 0.0002238026 | 0.000004656320 |
| 611 | 0.0002657040 | 0.0002152781 | 0.000004248890 |
| 612 | 0.0003245697 | 0.0002084572 | 0.000004602296 |
| 613 | 0.0004583650 | 0.0002018629 | 0.000005199952 |
| 614 | 0.0009144406 | 0.0001999347 | 0.000009050621 |
| 615 | 0.001906185 | 0.0002052194 | 0.00001489818 |
| 616 | 0.002869586 | 0.0002101308 | 0.00002318811 |
| 617 | 0.003023331 | 0.0002066833 | 0.00002465169 |
| 618 | 0.002509091 | 0.0001964957 | 0.00002127626 |
| 619 | 0.001672381 | 0.0001835292 | 0.00001517751 |
| 620 | 0.001154401 | 0.0001746529 | 0.00001202516 |
| 621 | 0.001136441 | 0.0001704566 | 0.00001056595 |
| 622 | 0.001436453 | 0.0001685890 | 0.00001204433 |
| 623 | 0.002356790 | 0.0001713234 | 0.00001901528 |
| 624 | 0.004437858 | 0.0001887232 | 0.00003461670 |
| 625 | 0.007159983 | 0.0002149622 | 0.00005560820 |
| 626 | 0.008736074 | 0.0002298045 | 0.00006958906 |
| 627 | 0.008193975 | 0.0002180740 | 0.00006739191 |
| 628 | 0.005974465 | 0.0001845539 | 0.00005041594 |
| 629 | 0.003678770 | 0.0001487490 | 0.00003269916 |
| 630 | 0.002329343 | 0.0001262267 | 0.00002179526 |
| 631 | 0.001727630 | 0.0001140177 | 0.00001431678 |
| 632 | 0.001293363 | 0.0001034844 | 0.00001111642 |

| Wavelenght $\lambda(\mathrm{nm})$ | primary colourants of the CRT (BT.709) | | |
|---|---|---|---|
| | **red** | **green** | **blue** |
| 633 | 0.0008951852 | 0.00009466478 | 0.000009316118 |
| 634 | 0.0005827470 | 0.00008574723 | 0.000006908038 |
| 635 | 0.0003922739 | 0.00008023354 | 0.000005079309 |
| 636 | 0.0002656598 | 0.00007483908 | 0.000003954988 |
| 637 | 0.0001803428 | 0.00007065971 | 0.000003426813 |
| 638 | 0.0001284055 | 0.00006735664 | 0.000003299988 |
| 639 | 0.00009502863 | 0.00006390095 | 0.000003192924 |
| 640 | 0.00007419476 | 0.00006108633 | 0.000002961612 |
| 641 | 0.00006169729 | 0.00005758579 | 0.000002887385 |
| 642 | 0.00005122254 | 0.00005565260 | 0.000002729198 |
| 643 | 0.00004401682 | 0.00005445599 | 0.000002563689 |
| 644 | 0.00004076889 | 0.00005194491 | 0.000002857131 |
| 645 | 0.00003842391 | 0.00004907023 | 0.000002512199 |
| 646 | 0.00003633811 | 0.00004682740 | 0.000002070591 |
| 647 | 0.00003455147 | 0.00004475628 | 0.000002253187 |
| 648 | 0.00003176072 | 0.00004263435 | 0.000002470596 |
| 649 | 0.00002801502 | 0.00004073397 | 0.000001750658 |
| 650 | 0.00002439315 | 0.00003859312 | 0.000001530062 |
| 651 | 0.00002345418 | 0.00003633104 | 0.000001543475 |
| 652 | 0.00002463113 | 0.00003480048 | 0.000002424808 |
| 653 | 0.00003357468 | 0.00003464629 | 0.000002480061 |
| 654 | 0.00004287051 | 0.00003350197 | 0.000002771041 |
| 655 | 0.00004739213 | 0.00003179157 | 0.000002317904 |
| 656 | 0.00004503237 | 0.00003091735 | 0.000002028523 |
| 657 | 0.00003767925 | 0.00002915423 | 0.000002386340 |
| 658 | 0.00002888178 | 0.00002755176 | 0.000002729057 |
| 659 | 0.00002420006 | 0.00002665771 | 0.000002302948 |
| 660 | 0.00002372645 | 0.00002521403 | 0.000002916479 |
| 661 | 0.00002359273 | 0.00002483256 | 0.000002608196 |
| 662 | 0.00002330043 | 0.00002247768 | 0.000002674534 |
| 663 | 0.00002121792 | 0.00002117443 | 0.000003024126 |
| 664 | 0.00002184848 | 0.00002135123 | 0.000002217757 |
| 665 | 0.00002409188 | 0.00002037011 | 0.000002550159 |
| 666 | 0.00002371546 | 0.00002036967 | 0.000002605522 |
| 667 | 0.00002271847 | 0.00001993339 | 0.000002691287 |
| 668 | 0.00002366029 | 0.00002032983 | 0.000002497928 |
| 669 | 0.00002733947 | 0.00002039483 | 0.000001823269 |
| 670 | 0.00003294046 | 0.00001973140 | 0.000002871649 |
| 671 | 0.00004148988 | 0.00001867818 | 0.000002734924 |
| 672 | 0.00004699272 | 0.00001667263 | 0.000003179067 |
| 673 | 0.00004429641 | 0.00001604171 | 0.000002860111 |
| 674 | 0.00003674733 | 0.00001506590 | 0.000001922427 |
| 675 | 0.00003053606 | 0.00001391287 | 0.000002280214 |
| 676 | 0.00002828106 | 0.00001344742 | 0.000002928191 |

| Wavelenght $\lambda(\mathrm{nm})$ | primary colourants of the CRT (BT.709) | | |
|---|---|---|---|
| | red | green | blue |
| 677 | 0.00002717527 | 0.00001226262 | 0.000003494319 |
| 678 | 0.00002434566 | 0.00001128253 | 0.000003603563 |
| 679 | 0.00002327847 | 0.00001262141 | 0.000003040954 |
| 680 | 0.00002442015 | 0.00001325772 | 0.000003655812 |
| 681 | 0.00002587327 | 0.00001232977 | 0.000003384527 |
| 682 | 0.00002829253 | 0.00001282637 | 0.000002714909 |
| 683 | 0.00004071862 | 0.00001187975 | 0.000002420476 |
| 684 | 0.00009213904 | 0.00001205330 | 0.000003336954 |
| 685 | 0.0002021130 | 0.00001248882 | 0.000004565019 |
| 686 | 0.0002935456 | 0.00001173827 | 0.000004332769 |
| 687 | 0.0002987515 | 0.00001240873 | 0.000004746741 |
| 688 | 0.0002312398 | 0.00001200192 | 0.000004082478 |
| 689 | 0.0001361813 | 0.00001012763 | 0.000004188305 |
| 690 | 0.00008056246 | 0.000009736545 | 0.000003057833 |
| 691 | 0.00006518796 | 0.000009875286 | 0.000002559075 |
| 692 | 0.00005969973 | 0.000008429654 | 0.000003861766 |
| 693 | 0.00006379719 | 0.000007647135 | 0.000003259152 |
| 694 | 0.00009577264 | 0.000009270434 | 0.000004806822 |
| 695 | 0.0001680851 | 0.000009693392 | 0.000005307819 |
| 696 | 0.0002225817 | 0.000008709290 | 0.000005976218 |
| 697 | 0.0002280957 | 0.000009326965 | 0.000004884389 |
| 698 | 0.0001973284 | 0.000008795443 | 0.000004935424 |
| 699 | 0.0001598798 | 0.000008450418 | 0.000003851517 |
| 700 | 0.0001672553 | 0.000009365105 | 0.000005174761 |
| 701 | 0.0002966630 | 0.00001001220 | 0.000006466357 |
| 702 | 0.0007673004 | 0.00001357304 | 0.000008377571 |
| 703 | 0.001819424 | 0.00002391261 | 0.00001527554 |
| 704 | 0.003072501 | 0.00003990361 | 0.00002174299 |
| 705 | 0.004098773 | 0.00005136661 | 0.00003186780 |
| 706 | 0.004123688 | 0.00005344768 | 0.00003331944 |
| 707 | 0.003261816 | 0.00004627855 | 0.00002613233 |
| 708 | 0.002081077 | 0.00003240564 | 0.00001651033 |
| 709 | 0.001104250 | 0.00001822265 | 0.00001247495 |
| 710 | 0.0006582575 | 0.00001498248 | 0.00001089242 |
| 711 | 0.0004645496 | 0.00001303767 | 0.00001013614 |
| 712 | 0.0003170196 | 0.00001168605 | 0.000007721147 |
| 713 | 0.0002150886 | 0.00001190116 | 0.000006216299 |
| 714 | 0.0001458364 | 0.00001011229 | 0.000008218942 |
| 715 | 0.0001021027 | 0.000009139815 | 0.000007701314 |
| 716 | 0.00007309849 | 0.000008916395 | 0.000006680481 |
| 717 | 0.00005399345 | 0.000009625407 | 0.000004530971 |
| 718 | 0.00003423282 | 0.00001041611 | 0.000005937809 |
| 719 | 0.00002274661 | 0.000009791282 | 0.000007428347 |
| 720 | 0.00001714294 | 0.000008552233 | 0.000007191166 |

| Wavelenght $\lambda(\mathrm{nm})$ | primary colourants of the CRT (BT.709) | | |
|---|---|---|---|
| | red | green | blue |
| 721 | 0.00001931894 | 0.000009956399 | 0.000005331439 |
| 722 | 0.00002121247 | 0.00001004188 | 0.000004800524 |
| 723 | 0.00002078200 | 0.000008324438 | 0.000005105140 |
| 724 | 0.00002325165 | 0.000008345954 | 0.000004863744 |
| 725 | 0.00002737028 | 0.000008874068 | 0.000006215756 |
| 726 | 0.00002567953 | 0.00001008563 | 0.000005933233 |
| 727 | 0.00002280374 | 0.000007460518 | 0.000004067918 |
| 728 | 0.00001967840 | 0.000008373459 | 0.000006571845 |
| 729 | 0.00001591120 | 0.000009559248 | 0.000007500808 |
| 730 | 0.00001638507 | 0.00001020847 | 0.000005846219 |
| 731 | 0.00001689032 | 0.000009778568 | 0.000006835792 |
| 732 | 0.00001638618 | 0.00001102633 | 0.000008502557 |
| 733 | 0.00001430747 | 0.00001001725 | 0.000007832765 |
| 734 | 0.00001123124 | 0.00001067058 | 0.00001062327 |
| 735 | 0.00001248835 | 0.000009585070 | 0.00001001927 |
| 736 | 0.00001428675 | 0.000009670768 | 0.000007766532 |
| 737 | 0.00001424439 | 0.000009755452 | 0.000006799673 |
| 738 | 0.00001367363 | 0.00001025301 | 0.00001046395 |
| 739 | 0.00001186220 | 0.00001139598 | 0.00001041580 |
| 740 | 0.00001480956 | 0.00001002199 | 0.000005743785 |
| 741 | 0.00001292981 | 0.00001223610 | 0.000005937906 |
| 742 | 0.00001191995 | 0.00001282895 | 0.000007921646 |
| 743 | 0.00001245769 | 0.00001342046 | 0.000008776209 |
| 744 | 0.00001521850 | 0.00001124645 | 0.000007869074 |
| 745 | 0.00001466447 | 0.00001008190 | 0.000008871873 |
| 746 | 0.00001526854 | 0.00001161421 | 0.000006728574 |
| 747 | 0.00001786695 | 0.00001112251 | 0.000008079767 |
| 748 | 0.00001423139 | 0.00001231002 | 0.000008100188 |
| 749 | 0.00001498124 | 0.00001347109 | 0.00001025904 |
| 750 | 0.00001297559 | 0.00001142028 | 0.000006736103 |
| 751 | 0.00001418004 | 0.00001186705 | 0.000008140755 |
| 752 | 0.00001531097 | 0.00001154012 | 0.00001128583 |
| 753 | 0.00001843076 | 0.00001280591 | 0.00001081632 |
| 754 | 0.00001720419 | 0.00001324910 | 0.00001000599 |
| 755 | 0.00001705584 | 0.00001583544 | 0.00001261390 |
| 756 | 0.00001913068 | 0.00001316490 | 0.00001454630 |
| 757 | 0.00001477695 | 0.00001428551 | 0.000009541713 |
| 758 | 0.00001623195 | 0.00001446542 | 0.00001128257 |
| 759 | 0.00001395069 | 0.00001372284 | 0.000009160707 |
| 760 | 0.00001624265 | 0.00001290431 | 0.000007700283 |
| 761 | 0.00001511667 | 0.00001371772 | 0.000006609647 |
| 762 | 0.00001846960 | 0.00001392999 | 0.000008749249 |
| 763 | 0.00001863449 | 0.00001278538 | 0.000007986500 |
| 764 | 0.00001884707 | 0.00001702802 | 0.00001142753 |

| Wavelenght $\lambda(\mathrm{nm})$ | primary colourants of the CRT (BT.709) | | |
|---|---|---|---|
| | **red** | **green** | **blue** |
| 765 | 0.00001347552 | 0.00001518078 | 0.00001180497 |
| 766 | 0.00001044722 | 0.00001354904 | 0.00001156287 |
| 767 | 0.00001754516 | 0.00001596541 | 0.000009695890 |
| 768 | 0.00001974178 | 0.00001550547 | 0.00001171262 |
| 769 | 0.00002434999 | 0.00001679668 | 0.00001029434 |
| 770 | 0.00001766815 | 0.00001589059 | 0.00001084403 |
| 771 | 0.00002033749 | 0.00001597682 | 0.000009815585 |
| 772 | 0.00001452338 | 0.00001839334 | 0.00001455073 |
| 773 | 0.00001497339 | 0.00001851552 | 0.00001058817 |
| 774 | 0.00001373139 | 0.00001967827 | 0.00001324435 |
| 775 | 0.00001697261 | 0.00001706483 | 0.00001341754 |
| 776 | 0.00001301074 | 0.00001760639 | 0.000008768412 |
| 777 | 0.00001405000 | 0.00001849091 | 0.00001252137 |
| 778 | 0.00001916490 | 0.00001702974 | 0.00001179201 |
| 779 | 0.00001650935 | 0.00001955503 | 0.00001485002 |
| 780 | 0.00002249120 | 0.00002113028 | 0.00002500940 |

*Table 19: Measured SPDs of the virtual BT.709 CRT.*

## A.4. CIE illuminant series D spectral power distributions

The SPD of the CIE standard illuminant D65 $S_{D65}(\lambda)$ is given as a table by ISO/CIE 11664-2:2022 [CIE D65].

The mean spectral radiant power distribution $S_0(\lambda)$ and the first two eigenvectors $S_1(\lambda)$, $S_2(\lambda)$ used for calculating CIE daylight illuminants SPD [Wyszecki & Stiles, 2000, p. 762] is given in 10nm steps. For using these values in the maths in this thesis, the values are linearly interpolated to 1nm.

| **Wavelenght** | **CIE illuminant series D** | | | |
|---|---|---|---|---|
| $\lambda$(nm) | $S_{D65}(\lambda)$ | $S_0(\lambda)$ | $S_1(\lambda)$ | $S_2(\lambda)$ |
| 300 | 0.0341 | 0.04 | 0.02 | 0.00 |
| 301 | 0.36014 | 0.64 | 0.47 | 0.20 |
| 302 | 0.68618 | 1.23 | 0.92 | 0.40 |
| 303 | 1.01222 | 1.83 | 1.36 | 0.60 |
| 304 | 1.33826 | 2.42 | 1.81 | 0.80 |
| 305 | 1.6643 | 3.02 | 2.26 | 1.00 |
| 306 | 1.99034 | 3.62 | 2.71 | 1.20 |
| 307 | 2.31638 | 4.21 | 3.16 | 1.40 |
| 308 | 2.64242 | 4.81 | 3.60 | 1.60 |
| 309 | 2.96846 | 5.40 | 4.05 | 1.80 |
| 310 | 3.2945 | 6.00 | 4.50 | 2.00 |
| 311 | 4.98865 | 8.36 | 6.29 | 2.20 |
| 312 | 6.6828 | 10.72 | 8.08 | 2.40 |
| 313 | 8.37695 | 13.08 | 9.87 | 2.60 |
| 314 | 10.0711 | 15.44 | 11.66 | 2.80 |
| 315 | 11.7652 | 17.80 | 13.45 | 3.00 |
| 316 | 13.4594 | 20.16 | 15.24 | 3.20 |
| 317 | 15.1535 | 22.52 | 17.03 | 3.40 |
| 318 | 16.8477 | 24.88 | 18.82 | 3.60 |
| 319 | 18.5418 | 27.24 | 20.61 | 3.80 |
| 320 | 20.236 | 29.60 | 22.40 | 4.00 |
| 321 | 21.9177 | 32.17 | 24.36 | 4.45 |
| 322 | 23.5995 | 34.74 | 26.32 | 4.90 |
| 323 | 25.2812 | 37.31 | 28.28 | 5.35 |
| 324 | 26.963 | 39.88 | 30.24 | 5.80 |
| 325 | 28.6447 | 42.45 | 32.20 | 6.25 |
| 326 | 30.3265 | 45.02 | 34.16 | 6.70 |
| 327 | 32.0082 | 47.59 | 36.12 | 7.15 |
| 328 | 33.69 | 50.16 | 38.08 | 7.60 |
| 329 | 35.3717 | 52.73 | 40.04 | 8.05 |
| 330 | 37.0535 | 55.30 | 42.00 | 8.50 |
| 331 | 37.343 | 55.50 | 41.86 | 8.43 |
| 332 | 37.6326 | 55.70 | 41.72 | 8.36 |

| Wavelenght $\lambda$(nm) | CIE illuminant series D | | | |
|---|---|---|---|---|
| | $S_{D65}(\lambda)$ | $S_0(\lambda)$ | $S_1(\lambda)$ | $S_2(\lambda)$ |
| 333 | 37.9221 | 55.90 | 41.58 | 8.29 |
| 334 | 38.2116 | 56.10 | 41.44 | 8.22 |
| 335 | 38.5011 | 56.30 | 41.30 | 8.15 |
| 336 | 38.7907 | 56.50 | 41.16 | 8.08 |
| 337 | 39.0802 | 56.70 | 41.02 | 8.01 |
| 338 | 39.3697 | 56.90 | 40.88 | 7.94 |
| 339 | 39.6593 | 57.10 | 40.74 | 7.87 |
| 340 | 39.9488 | 57.30 | 40.60 | 7.80 |
| 341 | 40.4451 | 57.75 | 40.70 | 7.69 |
| 342 | 40.9414 | 58.20 | 40.80 | 7.58 |
| 343 | 41.4377 | 58.65 | 40.90 | 7.47 |
| 344 | 41.934 | 59.10 | 41.00 | 7.36 |
| 345 | 42.4302 | 59.55 | 41.10 | 7.25 |
| 346 | 42.9265 | 60.00 | 41.20 | 7.14 |
| 347 | 43.4228 | 60.45 | 41.30 | 7.03 |
| 348 | 43.9191 | 60.90 | 41.40 | 6.92 |
| 349 | 44.4154 | 61.35 | 41.50 | 6.81 |
| 350 | 44.9117 | 61.80 | 41.60 | 6.70 |
| 351 | 45.0844 | 61.77 | 41.24 | 6.56 |
| 352 | 45.257 | 61.74 | 40.88 | 6.42 |
| 353 | 45.4297 | 61.71 | 40.52 | 6.28 |
| 354 | 45.6023 | 61.68 | 40.16 | 6.14 |
| 355 | 45.775 | 61.65 | 39.80 | 6.00 |
| 356 | 45.9477 | 61.62 | 39.44 | 5.86 |
| 357 | 46.1203 | 61.59 | 39.08 | 5.72 |
| 358 | 46.293 | 61.56 | 38.72 | 5.58 |
| 359 | 46.4656 | 61.53 | 38.36 | 5.44 |
| 360 | 46.6383 | 61.50 | 38.00 | 5.30 |
| 361 | 47.1834 | 62.23 | 38.44 | 5.38 |
| 362 | 47.7285 | 62.96 | 38.88 | 5.46 |
| 363 | 48.2735 | 63.69 | 39.32 | 5.54 |
| 364 | 48.8186 | 64.42 | 39.76 | 5.62 |
| 365 | 49.3637 | 65.15 | 40.20 | 5.70 |
| 366 | 49.9088 | 65.88 | 40.64 | 5.78 |
| 367 | 50.4539 | 66.61 | 41.08 | 5.86 |
| 368 | 50.9989 | 67.34 | 41.52 | 5.94 |
| 369 | 51.544 | 68.07 | 41.96 | 6.02 |
| 370 | 52.0891 | 68.80 | 42.40 | 6.10 |
| 371 | 51.8777 | 68.26 | 42.01 | 5.79 |
| 372 | 51.6664 | 67.72 | 41.62 | 5.48 |
| 373 | 51.455 | 67.18 | 41.23 | 5.17 |
| 374 | 51.2437 | 66.64 | 40.84 | 4.86 |
| 375 | 51.0323 | 66.10 | 40.45 | 4.55 |
| 376 | 50.8209 | 65.56 | 40.06 | 4.24 |

| Wavelenght $\lambda(\mathrm{nm})$ | CIE illuminant series D | | | |
|---|---|---|---|---|
| | $S_{D65}(\lambda)$ | $S_0(\lambda)$ | $S_1(\lambda)$ | $S_2(\lambda)$ |
| 377 | 50.6096 | 65.02 | 39.67 | 3.93 |
| 378 | 50.3982 | 64.48 | 39.28 | 3.62 |
| 379 | 50.1869 | 63.94 | 38.89 | 3.31 |
| 380 | 49.9755 | 63.40 | 38.50 | 3.00 |
| 381 | 50.4428 | 63.64 | 38.15 | 2.82 |
| 382 | 50.91 | 63.88 | 37.80 | 2.64 |
| 383 | 51.3773 | 64.12 | 37.45 | 2.46 |
| 384 | 51.8446 | 64.36 | 37.10 | 2.28 |
| 385 | 52.3118 | 64.60 | 36.75 | 2.10 |
| 386 | 52.7791 | 64.84 | 36.40 | 1.92 |
| 387 | 53.2464 | 65.08 | 36.05 | 1.74 |
| 388 | 53.7137 | 65.32 | 35.70 | 1.56 |
| 389 | 54.1809 | 65.56 | 35.35 | 1.38 |
| 390 | 54.6482 | 65.80 | 35.00 | 1.20 |
| 391 | 57.4589 | 68.70 | 35.84 | 0.97 |
| 392 | 60.2695 | 71.60 | 36.68 | 0.74 |
| 393 | 63.0802 | 74.50 | 37.52 | 0.51 |
| 394 | 65.8909 | 77.40 | 38.36 | 0.28 |
| 395 | 68.7015 | 80.30 | 39.20 | 0.05 |
| 396 | 71.5122 | 83.20 | 40.04 | -0.18 |
| 397 | 74.3229 | 86.10 | 40.88 | -0.41 |
| 398 | 77.1336 | 89.00 | 41.72 | -0.64 |
| 399 | 79.9442 | 91.90 | 42.56 | -0.87 |
| 400 | 82.7549 | 94.80 | 43.40 | -1.10 |
| 401 | 83.628 | 95.80 | 43.69 | -1.04 |
| 402 | 84.5011 | 96.80 | 43.98 | -0.98 |
| 403 | 85.3742 | 97.80 | 44.27 | -0.92 |
| 404 | 86.2473 | 98.80 | 44.56 | -0.86 |
| 405 | 87.1204 | 99.80 | 44.85 | -0.80 |
| 406 | 87.9936 | 100.80 | 45.14 | -0.74 |
| 407 | 88.8667 | 101.80 | 45.43 | -0.68 |
| 408 | 89.7398 | 102.80 | 45.72 | -0.62 |
| 409 | 90.6129 | 103.80 | 46.01 | -0.56 |
| 410 | 91.486 | 104.80 | 46.30 | -0.50 |
| 411 | 91.6806 | 104.91 | 46.06 | -0.52 |
| 412 | 91.8752 | 105.02 | 45.82 | -0.54 |
| 413 | 92.0697 | 105.13 | 45.58 | -0.56 |
| 414 | 92.2643 | 105.24 | 45.34 | -0.58 |
| 415 | 92.4589 | 105.35 | 45.10 | -0.60 |
| 416 | 92.6535 | 105.46 | 44.86 | -0.62 |
| 417 | 92.8481 | 105.57 | 44.62 | -0.64 |
| 418 | 93.0426 | 105.68 | 44.38 | -0.66 |
| 419 | 93.2372 | 105.79 | 44.14 | -0.68 |
| 420 | 93.4318 | 105.90 | 43.90 | -0.70 |

| Wavelenght $\lambda$(nm) | CIE illuminant series D | | | |
|---|---|---|---|---|
| | $S_{D65}(\lambda)$ | $S_0(\lambda)$ | $S_1(\lambda)$ | $S_2(\lambda)$ |
| 421 | 92.7568 | 104.99 | 43.22 | -0.75 |
| 422 | 92.0819 | 104.08 | 42.54 | -0.80 |
| 423 | 91.4069 | 103.17 | 41.86 | -0.85 |
| 424 | 90.732 | 102.26 | 41.18 | -0.90 |
| 425 | 90.057 | 101.35 | 40.50 | -0.95 |
| 426 | 89.3821 | 100.44 | 39.82 | -1.00 |
| 427 | 88.7071 | 99.53 | 39.14 | -1.05 |
| 428 | 88.0322 | 98.62 | 38.46 | -1.10 |
| 429 | 87.3572 | 97.71 | 37.78 | -1.15 |
| 430 | 86.6823 | 96.80 | 37.10 | -1.20 |
| 431 | 88.5006 | 98.51 | 37.06 | -1.34 |
| 432 | 90.3188 | 100.22 | 37.02 | -1.48 |
| 433 | 92.1371 | 101.93 | 36.98 | -1.62 |
| 434 | 93.9554 | 103.64 | 36.94 | -1.76 |
| 435 | 95.7736 | 105.35 | 36.90 | -1.90 |
| 436 | 97.5919 | 107.06 | 36.86 | -2.04 |
| 437 | 99.4102 | 108.77 | 36.82 | -2.18 |
| 438 | 101.228 | 110.48 | 36.78 | -2.32 |
| 439 | 103.047 | 112.19 | 36.74 | -2.46 |
| 440 | 104.865 | 113.90 | 36.70 | -2.60 |
| 441 | 106.079 | 115.07 | 36.62 | -2.63 |
| 442 | 107.294 | 116.24 | 36.54 | -2.66 |
| 443 | 108.508 | 117.41 | 36.46 | -2.69 |
| 444 | 109.722 | 118.58 | 36.38 | -2.72 |
| 445 | 110.936 | 119.75 | 36.30 | -2.75 |
| 446 | 112.151 | 120.92 | 36.22 | -2.78 |
| 447 | 113.365 | 122.09 | 36.14 | -2.81 |
| 448 | 114.579 | 123.26 | 36.06 | -2.84 |
| 449 | 115.794 | 124.43 | 35.98 | -2.87 |
| 450 | 117.008 | 125.60 | 35.90 | -2.90 |
| 451 | 117.088 | 125.59 | 35.57 | -2.89 |
| 452 | 117.169 | 125.58 | 35.24 | -2.88 |
| 453 | 117.249 | 125.57 | 34.91 | -2.87 |
| 454 | 117.33 | 125.56 | 34.58 | -2.86 |
| 455 | 117.41 | 125.55 | 34.25 | -2.85 |
| 456 | 117.49 | 125.54 | 33.92 | -2.84 |
| 457 | 117.571 | 125.53 | 33.59 | -2.83 |
| 458 | 117.651 | 125.52 | 33.26 | -2.82 |
| 459 | 117.732 | 125.51 | 32.93 | -2.81 |
| 460 | 117.812 | 125.50 | 32.60 | -2.80 |
| 461 | 117.517 | 125.08 | 32.13 | -2.78 |
| 462 | 117.222 | 124.66 | 31.66 | -2.76 |
| 463 | 116.927 | 124.24 | 31.19 | -2.74 |
| 464 | 116.632 | 123.82 | 30.72 | -2.72 |

| Wavelenght $\lambda$(nm) | CIE illuminant series D | | | |
|---|---|---|---|---|
| | $S_{D65}(\lambda)$ | $S_0(\lambda)$ | $S_1(\lambda)$ | $S_2(\lambda)$ |
| 465 | 116.336 | 123.40 | 30.25 | -2.70 |
| 466 | 116.041 | 122.98 | 29.78 | -2.68 |
| 467 | 115.746 | 122.56 | 29.31 | -2.66 |
| 468 | 115.451 | 122.14 | 28.84 | -2.64 |
| 469 | 115.156 | 121.72 | 28.37 | -2.62 |
| 470 | 114.861 | 121.30 | 27.90 | -2.60 |
| 471 | 114.967 | 121.30 | 27.54 | -2.60 |
| 472 | 115.073 | 121.30 | 27.18 | -2.60 |
| 473 | 115.18 | 121.30 | 26.82 | -2.60 |
| 474 | 115.286 | 121.30 | 26.46 | -2.60 |
| 475 | 115.392 | 121.30 | 26.10 | -2.60 |
| 476 | 115.498 | 121.30 | 25.74 | -2.60 |
| 477 | 115.604 | 121.30 | 25.38 | -2.60 |
| 478 | 115.711 | 121.30 | 25.02 | -2.60 |
| 479 | 115.817 | 121.30 | 24.66 | -2.60 |
| 480 | 115.923 | 121.30 | 24.30 | -2.60 |
| 481 | 115.212 | 120.52 | 23.88 | -2.52 |
| 482 | 114.501 | 119.74 | 23.46 | -2.44 |
| 483 | 113.789 | 118.96 | 23.04 | -2.36 |
| 484 | 113.078 | 118.18 | 22.62 | -2.28 |
| 485 | 112.367 | 117.40 | 22.20 | -2.20 |
| 486 | 111.656 | 116.62 | 21.78 | -2.12 |
| 487 | 110.945 | 115.84 | 21.36 | -2.04 |
| 488 | 110.233 | 115.06 | 20.94 | -1.96 |
| 489 | 109.522 | 114.28 | 20.52 | -1.88 |
| 490 | 108.811 | 113.50 | 20.10 | -1.80 |
| 491 | 108.865 | 113.46 | 19.71 | -1.77 |
| 492 | 108.92 | 113.42 | 19.32 | -1.74 |
| 493 | 108.974 | 113.38 | 18.93 | -1.71 |
| 494 | 109.028 | 113.34 | 18.54 | -1.68 |
| 495 | 109.082 | 113.30 | 18.15 | -1.65 |
| 496 | 109.137 | 113.26 | 17.76 | -1.62 |
| 497 | 109.191 | 113.22 | 17.37 | -1.59 |
| 498 | 109.245 | 113.18 | 16.98 | -1.56 |
| 499 | 109.3 | 113.14 | 16.59 | -1.53 |
| 500 | 109.354 | 113.10 | 16.20 | -1.50 |
| 501 | 109.199 | 112.87 | 15.90 | -1.48 |
| 502 | 109.044 | 112.64 | 15.60 | -1.46 |
| 503 | 108.888 | 112.41 | 15.30 | -1.44 |
| 504 | 108.733 | 112.18 | 15.00 | -1.42 |
| 505 | 108.578 | 111.95 | 14.70 | -1.40 |
| 506 | 108.423 | 111.72 | 14.40 | -1.38 |
| 507 | 108.268 | 111.49 | 14.10 | -1.36 |
| 508 | 108.112 | 111.26 | 13.80 | -1.34 |

| Wavelenght $\lambda(\mathrm{nm})$ | CIE illuminant series D | | | |
|---|---|---|---|---|
| | $S_{D65}(\lambda)$ | $S_0(\lambda)$ | $S_1(\lambda)$ | $S_2(\lambda)$ |
| 509 | 107.957 | 111.03 | 13.50 | -1.32 |
| 510 | 107.802 | 110.80 | 13.20 | -1.30 |
| 511 | 107.501 | 110.37 | 12.74 | -1.29 |
| 512 | 107.2 | 109.94 | 12.28 | -1.28 |
| 513 | 106.898 | 109.51 | 11.82 | -1.27 |
| 514 | 106.597 | 109.08 | 11.36 | -1.26 |
| 515 | 106.296 | 108.65 | 10.90 | -1.25 |
| 516 | 105.995 | 108.22 | 10.44 | -1.24 |
| 517 | 105.694 | 107.79 | 9.98 | -1.23 |
| 518 | 105.392 | 107.36 | 9.52 | -1.22 |
| 519 | 105.091 | 106.93 | 9.06 | -1.21 |
| 520 | 104.79 | 106.50 | 8.60 | -1.20 |
| 521 | 105.08 | 106.73 | 8.35 | -1.18 |
| 522 | 105.37 | 106.96 | 8.10 | -1.16 |
| 523 | 105.66 | 107.19 | 7.85 | -1.14 |
| 524 | 105.95 | 107.42 | 7.60 | -1.12 |
| 525 | 106.239 | 107.65 | 7.35 | -1.10 |
| 526 | 106.529 | 107.88 | 7.10 | -1.08 |
| 527 | 106.819 | 108.11 | 6.85 | -1.06 |
| 528 | 107.109 | 108.34 | 6.60 | -1.04 |
| 529 | 107.399 | 108.57 | 6.35 | -1.02 |
| 530 | 107.689 | 108.80 | 6.10 | -1.00 |
| 531 | 107.361 | 108.45 | 5.91 | -0.95 |
| 532 | 107.032 | 108.10 | 5.72 | -0.90 |
| 533 | 106.704 | 107.75 | 5.53 | -0.85 |
| 534 | 106.375 | 107.40 | 5.34 | -0.80 |
| 535 | 106.047 | 107.05 | 5.15 | -0.75 |
| 536 | 105.719 | 106.70 | 4.96 | -0.70 |
| 537 | 105.39 | 106.35 | 4.77 | -0.65 |
| 538 | 105.062 | 106.00 | 4.58 | -0.60 |
| 539 | 104.733 | 105.65 | 4.39 | -0.55 |
| 540 | 104.405 | 105.30 | 4.20 | -0.50 |
| 541 | 104.369 | 105.21 | 3.97 | -0.48 |
| 542 | 104.333 | 105.12 | 3.74 | -0.46 |
| 543 | 104.297 | 105.03 | 3.51 | -0.44 |
| 544 | 104.261 | 104.94 | 3.28 | -0.42 |
| 545 | 104.225 | 104.85 | 3.05 | -0.40 |
| 546 | 104.19 | 104.76 | 2.82 | -0.38 |
| 547 | 104.154 | 104.67 | 2.59 | -0.36 |
| 548 | 104.118 | 104.58 | 2.36 | -0.34 |
| 549 | 104.082 | 104.49 | 2.13 | -0.32 |
| 550 | 104.046 | 104.40 | 1.90 | -0.30 |
| 551 | 103.641 | 103.96 | 1.71 | -0.27 |
| 552 | 103.237 | 103.52 | 1.52 | -0.24 |

| **Wavelenght** $\lambda(\mathrm{nm})$ | **CIE illuminant series D** | | | |
|---|---|---|---|---|
| | $S_{D65}(\lambda)$ | $S_0(\lambda)$ | $S_1(\lambda)$ | $S_2(\lambda)$ |
| 553 | 102.832 | 103.08 | 1.33 | -0.21 |
| 554 | 102.428 | 102.64 | 1.14 | -0.18 |
| 555 | 102.023 | 102.20 | 0.95 | -0.15 |
| 556 | 101.618 | 101.76 | 0.76 | -0.12 |
| 557 | 101.214 | 101.32 | 0.57 | -0.09 |
| 558 | 100.809 | 100.88 | 0.38 | -0.06 |
| 559 | 100.405 | 100.44 | 0.19 | -0.03 |
| 560 | 100 | 100.00 | 0.00 | 0.00 |
| 561 | 99.6334 | 99.60 | -0.16 | 0.02 |
| 562 | 99.2668 | 99.20 | -0.32 | 0.04 |
| 563 | 98.9003 | 98.80 | -0.48 | 0.06 |
| 564 | 98.5337 | 98.40 | -0.64 | 0.08 |
| 565 | 98.1671 | 98.00 | -0.80 | 0.10 |
| 566 | 97.8005 | 97.60 | -0.96 | 0.12 |
| 567 | 97.4339 | 97.20 | -1.12 | 0.14 |
| 568 | 97.0674 | 96.80 | -1.28 | 0.16 |
| 569 | 96.7008 | 96.40 | -1.44 | 0.18 |
| 570 | 96.3342 | 96.00 | -1.60 | 0.20 |
| 571 | 96.2796 | 95.91 | -1.79 | 0.23 |
| 572 | 96.225 | 95.82 | -1.98 | 0.26 |
| 573 | 96.1703 | 95.73 | -2.17 | 0.29 |
| 574 | 96.1157 | 95.64 | -2.36 | 0.32 |
| 575 | 96.0611 | 95.55 | -2.55 | 0.35 |
| 576 | 96.0065 | 95.46 | -2.74 | 0.38 |
| 577 | 95.9519 | 95.37 | -2.93 | 0.41 |
| 578 | 95.8972 | 95.28 | -3.12 | 0.44 |
| 579 | 95.8426 | 95.19 | -3.31 | 0.47 |
| 580 | 95.788 | 95.10 | -3.50 | 0.50 |
| 581 | 95.0778 | 94.50 | -3.50 | 0.66 |
| 582 | 94.3675 | 93.90 | -3.50 | 0.82 |
| 583 | 93.6573 | 93.30 | -3.50 | 0.98 |
| 584 | 92.947 | 92.70 | -3.50 | 1.14 |
| 585 | 92.2368 | 92.10 | -3.50 | 1.30 |
| 586 | 91.5266 | 91.50 | -3.50 | 1.46 |
| 587 | 90.8163 | 90.90 | -3.50 | 1.62 |
| 588 | 90.1061 | 90.30 | -3.50 | 1.78 |
| 589 | 89.3958 | 89.70 | -3.50 | 1.94 |
| 590 | 88.6856 | 89.10 | -3.50 | 2.10 |
| 591 | 88.8177 | 89.24 | -3.73 | 2.21 |
| 592 | 88.9497 | 89.38 | -3.96 | 2.32 |
| 593 | 89.0818 | 89.52 | -4.19 | 2.43 |
| 594 | 89.2138 | 89.66 | -4.42 | 2.54 |
| 595 | 89.3459 | 89.80 | -4.65 | 2.65 |
| 596 | 89.478 | 89.94 | -4.88 | 2.76 |

| **Wavelenght** | **CIE illuminant series D** | | | |
|---|---|---|---|---|
| $\lambda(\mathrm{nm})$ | $S_{D65}(\lambda)$ | $S_0(\lambda)$ | $S_1(\lambda)$ | $S_2(\lambda)$ |
| 597 | 89.61 | 90.08 | -5.11 | 2.87 |
| 598 | 89.7421 | 90.22 | -5.34 | 2.98 |
| 599 | 89.8741 | 90.36 | -5.57 | 3.09 |
| 600 | 90.0062 | 90.50 | -5.80 | 3.20 |
| 601 | 89.9655 | 90.48 | -5.94 | 3.29 |
| 602 | 89.9248 | 90.46 | -6.08 | 3.38 |
| 603 | 89.8841 | 90.44 | -6.22 | 3.47 |
| 604 | 89.8434 | 90.42 | -6.36 | 3.56 |
| 605 | 89.8026 | 90.40 | -6.50 | 3.65 |
| 606 | 89.7619 | 90.38 | -6.64 | 3.74 |
| 607 | 89.7212 | 90.36 | -6.78 | 3.83 |
| 608 | 89.6805 | 90.34 | -6.92 | 3.92 |
| 609 | 89.6398 | 90.32 | -7.06 | 4.01 |
| 610 | 89.5991 | 90.30 | -7.20 | 4.10 |
| 611 | 89.4091 | 90.11 | -7.34 | 4.16 |
| 612 | 89.219 | 89.92 | -7.48 | 4.22 |
| 613 | 89.029 | 89.73 | -7.62 | 4.28 |
| 614 | 88.8389 | 89.54 | -7.76 | 4.34 |
| 615 | 88.6489 | 89.35 | -7.90 | 4.40 |
| 616 | 88.4589 | 89.16 | -8.04 | 4.46 |
| 617 | 88.2688 | 88.97 | -8.18 | 4.52 |
| 618 | 88.0788 | 88.78 | -8.32 | 4.58 |
| 619 | 87.8887 | 88.59 | -8.46 | 4.64 |
| 620 | 87.6987 | 88.40 | -8.60 | 4.70 |
| 621 | 87.2577 | 87.96 | -8.69 | 4.74 |
| 622 | 86.8167 | 87.52 | -8.78 | 4.78 |
| 623 | 86.3757 | 87.08 | -8.87 | 4.82 |
| 624 | 85.9347 | 86.64 | -8.96 | 4.86 |
| 625 | 85.4936 | 86.20 | -9.05 | 4.90 |
| 626 | 85.0526 | 85.76 | -9.14 | 4.94 |
| 627 | 84.6116 | 85.32 | -9.23 | 4.98 |
| 628 | 84.1706 | 84.88 | -9.32 | 5.02 |
| 629 | 83.7296 | 84.44 | -9.41 | 5.06 |
| 630 | 83.2886 | 84.00 | -9.50 | 5.10 |
| 631 | 83.3297 | 84.11 | -9.64 | 5.26 |
| 632 | 83.3707 | 84.22 | -9.78 | 5.42 |
| 633 | 83.4118 | 84.33 | -9.92 | 5.58 |
| 634 | 83.4528 | 84.44 | -10.06 | 5.74 |
| 635 | 83.4939 | 84.55 | -10.20 | 5.90 |
| 636 | 83.535 | 84.66 | -10.34 | 6.06 |
| 637 | 83.576 | 84.77 | -10.48 | 6.22 |
| 638 | 83.6171 | 84.88 | -10.62 | 6.38 |
| 639 | 83.6581 | 84.99 | -10.76 | 6.54 |
| 640 | 83.6992 | 85.10 | -10.90 | 6.70 |

| Wavelenght | CIE illuminant series D | | | |
|---|---|---|---|---|
| $\lambda$(nm) | $S_{D65}(\lambda)$ | $S_0(\lambda)$ | $S_1(\lambda)$ | $S_2(\lambda)$ |
| 641 | 83.332 | 84.78 | -10.88 | 6.76 |
| 642 | 82.9647 | 84.46 | -10.86 | 6.82 |
| 643 | 82.5975 | 84.14 | -10.84 | 6.88 |
| 644 | 82.2302 | 83.82 | -10.82 | 6.94 |
| 645 | 81.863 | 83.50 | -10.80 | 7.00 |
| 646 | 81.4958 | 83.18 | -10.78 | 7.06 |
| 647 | 81.1285 | 82.86 | -10.76 | 7.12 |
| 648 | 80.7613 | 82.54 | -10.74 | 7.18 |
| 649 | 80.394 | 82.22 | -10.72 | 7.24 |
| 650 | 80.0268 | 81.90 | -10.70 | 7.30 |
| 651 | 80.0456 | 81.97 | -10.83 | 7.43 |
| 652 | 80.0644 | 82.04 | -10.96 | 7.56 |
| 653 | 80.0831 | 82.11 | -11.09 | 7.69 |
| 654 | 80.1019 | 82.18 | -11.22 | 7.82 |
| 655 | 80.1207 | 82.25 | -11.35 | 7.95 |
| 656 | 80.1395 | 82.32 | -11.48 | 8.08 |
| 657 | 80.1583 | 82.39 | -11.61 | 8.21 |
| 658 | 80.177 | 82.46 | -11.74 | 8.34 |
| 659 | 80.1958 | 82.53 | -11.87 | 8.47 |
| 660 | 80.2146 | 82.60 | -12.00 | 8.60 |
| 661 | 80.4209 | 82.83 | -12.20 | 8.72 |
| 662 | 80.6272 | 83.06 | -12.40 | 8.84 |
| 663 | 80.8336 | 83.29 | -12.60 | 8.96 |
| 664 | 81.0399 | 83.52 | -12.80 | 9.08 |
| 665 | 81.2462 | 83.75 | -13.00 | 9.20 |
| 666 | 81.4525 | 83.98 | -13.20 | 9.32 |
| 667 | 81.6588 | 84.21 | -13.40 | 9.44 |
| 668 | 81.8652 | 84.44 | -13.60 | 9.56 |
| 669 | 82.0715 | 84.67 | -13.80 | 9.68 |
| 670 | 82.2778 | 84.90 | -14.00 | 9.80 |
| 671 | 81.8784 | 84.54 | -13.96 | 9.84 |
| 672 | 81.4791 | 84.18 | -13.92 | 9.88 |
| 673 | 81.0797 | 83.82 | -13.88 | 9.92 |
| 674 | 80.6804 | 83.46 | -13.84 | 9.96 |
| 675 | 80.281 | 83.10 | -13.80 | 10.00 |
| 676 | 79.8816 | 82.74 | -13.76 | 10.04 |
| 677 | 79.4823 | 82.38 | -13.72 | 10.08 |
| 678 | 79.0829 | 82.02 | -13.68 | 10.12 |
| 679 | 78.6836 | 81.66 | -13.64 | 10.16 |
| 680 | 78.2842 | 81.30 | -13.60 | 10.20 |
| 681 | 77.4279 | 80.36 | -13.44 | 10.01 |
| 682 | 76.5716 | 79.42 | -13.28 | 9.82 |
| 683 | 75.7153 | 78.48 | -13.12 | 9.63 |
| 684 | 74.859 | 77.54 | -12.96 | 9.44 |

| Wavelenght $\lambda$(nm) | CIE illuminant series D | | | |
|---|---|---|---|---|
| | $S_{D65}(\lambda)$ | $S_0(\lambda)$ | $S_1(\lambda)$ | $S_2(\lambda)$ |
| 685 | 74.0027 | 76.60 | -12.80 | 9.25 |
| 686 | 73.1465 | 75.66 | -12.64 | 9.06 |
| 687 | 72.2902 | 74.72 | -12.48 | 8.87 |
| 688 | 71.4339 | 73.78 | -12.32 | 8.68 |
| 689 | 70.5776 | 72.84 | -12.16 | 8.49 |
| 690 | 69.7213 | 71.90 | -12.00 | 8.30 |
| 691 | 69.9101 | 72.14 | -12.13 | 8.43 |
| 692 | 70.0989 | 72.38 | -12.26 | 8.56 |
| 693 | 70.2876 | 72.62 | -12.39 | 8.69 |
| 694 | 70.4764 | 72.86 | -12.52 | 8.82 |
| 695 | 70.6652 | 73.10 | -12.65 | 8.95 |
| 696 | 70.854 | 73.34 | -12.78 | 9.08 |
| 697 | 71.0428 | 73.58 | -12.91 | 9.21 |
| 698 | 71.2315 | 73.82 | -13.04 | 9.34 |
| 699 | 71.4203 | 74.06 | -13.17 | 9.47 |
| 700 | 71.6091 | 74.30 | -13.30 | 9.60 |
| 701 | 71.8831 | 74.51 | -13.26 | 9.49 |
| 702 | 72.1571 | 74.72 | -13.22 | 9.38 |
| 703 | 72.4311 | 74.93 | -13.18 | 9.27 |
| 704 | 72.7051 | 75.14 | -13.14 | 9.16 |
| 705 | 72.979 | 75.35 | -13.10 | 9.05 |
| 706 | 73.253 | 75.56 | -13.06 | 8.94 |
| 707 | 73.527 | 75.77 | -13.02 | 8.83 |
| 708 | 73.801 | 75.98 | -12.98 | 8.72 |
| 709 | 74.075 | 76.19 | -12.94 | 8.61 |
| 710 | 74.349 | 76.40 | -12.90 | 8.50 |
| 711 | 73.0745 | 75.09 | -12.67 | 8.35 |
| 712 | 71.8 | 73.78 | -12.44 | 8.20 |
| 713 | 70.5255 | 72.47 | -12.21 | 8.05 |
| 714 | 69.251 | 71.16 | -11.98 | 7.90 |
| 715 | 67.9765 | 69.85 | -11.75 | 7.75 |
| 716 | 66.702 | 68.54 | -11.52 | 7.60 |
| 717 | 65.4275 | 67.23 | -11.29 | 7.45 |
| 718 | 64.153 | 65.92 | -11.06 | 7.30 |
| 719 | 62.8785 | 64.61 | -10.83 | 7.15 |
| 720 | 61.604 | 63.30 | -10.60 | 7.00 |
| 721 | 62.4322 | 64.14 | -10.70 | 7.06 |
| 722 | 63.2603 | 64.98 | -10.80 | 7.12 |
| 723 | 64.0885 | 65.82 | -10.90 | 7.18 |
| 724 | 64.9166 | 66.66 | -11.00 | 7.24 |
| 725 | 65.7448 | 67.50 | -11.10 | 7.30 |
| 726 | 66.573 | 68.34 | -11.20 | 7.36 |
| 727 | 67.4011 | 69.18 | -11.30 | 7.42 |
| 728 | 68.2293 | 70.02 | -11.40 | 7.48 |

| Wavelenght $\lambda$(nm) | CIE illuminant series D | | | |
|---|---|---|---|---|
| | $S_{D65}(\lambda)$ | $S_0(\lambda)$ | $S_1(\lambda)$ | $S_2(\lambda)$ |
| 729 | 69.0574 | 70.86 | -11.50 | 7.54 |
| 730 | 69.8856 | 71.70 | -11.60 | 7.60 |
| 731 | 70.4057 | 72.23 | -11.66 | 7.64 |
| 732 | 70.9259 | 72.76 | -11.72 | 7.68 |
| 733 | 71.446 | 73.29 | -11.78 | 7.72 |
| 734 | 71.9662 | 73.82 | -11.84 | 7.76 |
| 735 | 72.4863 | 74.35 | -11.90 | 7.80 |
| 736 | 73.0064 | 74.88 | -11.96 | 7.84 |
| 737 | 73.5266 | 75.41 | -12.02 | 7.88 |
| 738 | 74.0467 | 75.94 | -12.08 | 7.92 |
| 739 | 74.5669 | 76.47 | -12.14 | 7.96 |
| 740 | 75.087 | 77.00 | -12.20 | 8.00 |
| 741 | 73.9376 | 75.82 | -12.00 | 7.87 |
| 742 | 72.7881 | 74.64 | -11.80 | 7.74 |
| 743 | 71.6387 | 73.46 | -11.60 | 7.61 |
| 744 | 70.4893 | 72.28 | -11.40 | 7.48 |
| 745 | 69.3398 | 71.10 | -11.20 | 7.35 |
| 746 | 68.1904 | 69.92 | -11.00 | 7.22 |
| 747 | 67.041 | 68.74 | -10.80 | 7.09 |
| 748 | 65.8916 | 67.56 | -10.60 | 6.96 |
| 749 | 64.7421 | 66.38 | -10.40 | 6.83 |
| 750 | 63.5927 | 65.20 | -10.20 | 6.70 |
| 751 | 61.8752 | 63.45 | -9.96 | 6.55 |
| 752 | 60.1578 | 61.70 | -9.72 | 6.40 |
| 753 | 58.4403 | 59.95 | -9.48 | 6.25 |
| 754 | 56.7229 | 58.20 | -9.24 | 6.10 |
| 755 | 55.0054 | 56.45 | -9.00 | 5.95 |
| 756 | 53.288 | 54.70 | -8.76 | 5.80 |
| 757 | 51.5705 | 52.95 | -8.52 | 5.65 |
| 758 | 49.8531 | 51.20 | -8.28 | 5.50 |
| 759 | 48.1356 | 49.45 | -8.04 | 5.35 |
| 760 | 46.4182 | 47.70 | -7.80 | 5.20 |
| 761 | 48.4569 | 49.79 | -8.14 | 5.42 |
| 762 | 50.4956 | 51.88 | -8.48 | 5.64 |
| 763 | 52.5344 | 53.97 | -8.82 | 5.86 |
| 764 | 54.5731 | 56.06 | -9.16 | 6.08 |
| 765 | 56.6118 | 58.15 | -9.50 | 6.30 |
| 766 | 58.6505 | 60.24 | -9.84 | 6.52 |
| 767 | 60.6892 | 62.33 | -10.18 | 6.74 |
| 768 | 62.728 | 64.42 | -10.52 | 6.96 |
| 769 | 64.7667 | 66.51 | -10.86 | 7.18 |
| 770 | 66.8054 | 68.60 | -11.20 | 7.40 |
| 771 | 66.4631 | 68.24 | -11.12 | 7.34 |
| 772 | 66.1209 | 67.88 | -11.04 | 7.28 |

| Wavelenght $\lambda(\text{nm})$ | CIE illuminant series D | | | |
|---|---|---|---|---|
| | $S_{D65}(\lambda)$ | $S_0(\lambda)$ | $S_1(\lambda)$ | $S_2(\lambda)$ |
| 773 | 65.7786 | 67.52 | -10.96 | 7.22 |
| 774 | 65.4364 | 67.16 | -10.88 | 7.16 |
| 775 | 65.0941 | 66.80 | -10.80 | 7.10 |
| 776 | 64.7518 | 66.44 | -10.72 | 7.04 |
| 777 | 64.4096 | 66.08 | -10.64 | 6.98 |
| 778 | 64.0673 | 65.72 | -10.56 | 6.92 |
| 779 | 63.7251 | 65.36 | -10.48 | 6.86 |
| 780 | 63.3828 | 65.00 | -10.40 | 6.80 |
| 781 | 63.4749 | 65.10 | -10.42 | 6.82 |
| 782 | 63.567 | 65.20 | -10.44 | 6.84 |
| 783 | 63.6592 | 65.30 | -10.46 | 6.86 |
| 784 | 63.7513 | 65.40 | -10.48 | 6.88 |
| 785 | 63.8434 | 65.50 | -10.50 | 6.90 |
| 786 | 63.9355 | 65.60 | -10.52 | 6.92 |
| 787 | 64.0276 | 65.70 | -10.54 | 6.94 |
| 788 | 64.1198 | 65.80 | -10.56 | 6.96 |
| 789 | 64.2119 | 65.90 | -10.58 | 6.98 |
| 790 | 64.304 | 66.00 | -10.60 | 7.00 |
| 791 | 63.8188 | 65.50 | -10.51 | 6.94 |
| 792 | 63.3336 | 65.00 | -10.42 | 6.88 |
| 793 | 62.8484 | 64.50 | -10.33 | 6.82 |
| 794 | 62.3632 | 64.00 | -10.24 | 6.76 |
| 795 | 61.8779 | 63.50 | -10.15 | 6.70 |
| 796 | 61.3927 | 63.00 | -10.06 | 6.64 |
| 797 | 60.9075 | 62.50 | -9.97 | 6.58 |
| 798 | 60.4223 | 62.00 | -9.88 | 6.52 |
| 799 | 59.9371 | 61.50 | -9.79 | 6.46 |
| 800 | 59.4519 | 61.00 | -9.70 | 6.40 |
| 801 | 58.7026 | 60.23 | -9.56 | 6.31 |
| 802 | 57.9533 | 59.46 | -9.42 | 6.22 |
| 803 | 57.204 | 58.69 | -9.28 | 6.13 |
| 804 | 56.4547 | 57.92 | -9.14 | 6.04 |
| 805 | 55.7054 | 57.15 | -9.00 | 5.95 |
| 806 | 54.9562 | 56.38 | -8.86 | 5.86 |
| 807 | 54.2069 | 55.61 | -8.72 | 5.77 |
| 808 | 53.4576 | 54.84 | -8.58 | 5.68 |
| 809 | 52.7083 | 54.07 | -8.44 | 5.59 |
| 810 | 51.959 | 53.30 | -8.30 | 5.50 |
| 811 | 52.5072 | 53.86 | -8.40 | 5.56 |
| 812 | 53.0553 | 54.42 | -8.50 | 5.62 |
| 813 | 53.6035 | 54.98 | -8.60 | 5.68 |
| 814 | 54.1516 | 55.54 | -8.70 | 5.74 |
| 815 | 54.6998 | 56.10 | -8.80 | 5.80 |
| 816 | 55.248 | 56.66 | -8.90 | 5.86 |

| **Wavelenght** | **CIE illuminant series D** | | | |
|---|---|---|---|---|
| $\lambda(\mathrm{nm})$ | $S_{D65}(\lambda)$ | $S_0(\lambda)$ | $S_1(\lambda)$ | $S_2(\lambda)$ |
| 817 | 55.7961 | 57.22 | -9.00 | 5.92 |
| 818 | 56.3443 | 57.78 | -9.10 | 5.98 |
| 819 | 56.8924 | 58.34 | -9.20 | 6.04 |
| 820 | 57.4406 | 58.90 | -9.30 | 6.10 |
| 821 | 57.7278 | 59.20 | -9.35 | 6.14 |
| 822 | 58.015 | 59.50 | -9.40 | 6.18 |
| 823 | 58.3022 | 59.80 | -9.45 | 6.22 |
| 824 | 58.5894 | 60.10 | -9.50 | 6.26 |
| 825 | 58.8765 | 60.40 | -9.55 | 6.30 |
| 826 | 59.1637 | 60.70 | -9.60 | 6.34 |
| 827 | 59.4509 | 61.00 | -9.65 | 6.38 |
| 828 | 59.7381 | 61.30 | -9.70 | 6.42 |
| 829 | 60.0253 | 61.60 | -9.75 | 6.46 |
| 830 | 60.3125 | 61.90 | -9.80 | 6.50 |

*Table 20: CIE illuminant series D spectral power distributions.*

## A.5. Colour-matching functions and corresponding chromaticity coordinates of the CIE 1931 standard colourimetric system

*CIE 1931 colour-matching functions, 2 degree observer*, International Commission on Illumination (CIE), 2019. Available at: https://doi.org/10.25039/CIE.DS.xvudnb9b

| Wavelenght | CIE 1931 2° colour-matching functions | | | chromaticity coordinates | |
|---|---|---|---|---|---|
| $\lambda(\text{nm})$ | $\bar{x}(\lambda)$ | $\bar{y}(\lambda)$ | $\bar{z}(\lambda)$ | $x(\lambda)$ | $y(\lambda)$ |
| 360 | 0.000129900000 | 0.000003917000 | 0.000606100000 | 0.175560 | 0.00529384 |
| 361 | 0.000145847000 | 0.000004393581 | 0.000680879200 | 0.175483 | 0.00528634 |
| 362 | 0.000163802100 | 0.000004929604 | 0.000765145600 | 0.175400 | 0.00527864 |
| 363 | 0.000184003700 | 0.000005532136 | 0.000860012400 | 0.175317 | 0.00527097 |
| 364 | 0.000206690200 | 0.000006208245 | 0.000966592800 | 0.175237 | 0.00526349 |
| 365 | 0.000232100000 | 0.000006965000 | 0.001086000000 | 0.175161 | 0.00525635 |
| 366 | 0.000260728000 | 0.000007813219 | 0.001220586000 | 0.175088 | 0.00524684 |
| 367 | 0.000293075000 | 0.000008767336 | 0.001372729000 | 0.175015 | 0.00523557 |
| 368 | 0.000329388000 | 0.000009839844 | 0.001543579000 | 0.174945 | 0.00522616 |
| 369 | 0.000369914000 | 0.000011043230 | 0.001734286000 | 0.174880 | 0.00522078 |
| 370 | 0.000414900000 | 0.000012390000 | 0.001946000000 | 0.174821 | 0.00522060 |
| 371 | 0.000464158700 | 0.000013886410 | 0.002177777000 | 0.174770 | 0.00522867 |
| 372 | 0.000518986000 | 0.000015557280 | 0.002435809000 | 0.174722 | 0.00523752 |
| 373 | 0.000581854000 | 0.000017442960 | 0.002731953000 | 0.174665 | 0.00523616 |
| 374 | 0.000655234700 | 0.000019583750 | 0.003078064000 | 0.174595 | 0.00521832 |
| 375 | 0.000741600000 | 0.000022020000 | 0.003486000000 | 0.174510 | 0.00518164 |
| 376 | 0.000845029600 | 0.000024839650 | 0.003975227000 | 0.174409 | 0.00512676 |
| 377 | 0.000964526800 | 0.000028041260 | 0.004540880000 | 0.174308 | 0.00506759 |
| 378 | 0.001094949000 | 0.000031531040 | 0.005158320000 | 0.174222 | 0.00501703 |
| 379 | 0.001231154000 | 0.000035215210 | 0.005802907000 | 0.174156 | 0.00498144 |
| 380 | 0.001368000000 | 0.000039000000 | 0.006450001000 | 0.174112 | 0.00496373 |
| 381 | 0.001502050000 | 0.000042826400 | 0.007083216000 | 0.174088 | 0.00496360 |
| 382 | 0.001642328000 | 0.000046914600 | 0.007745488000 | 0.174073 | 0.00497254 |
| 383 | 0.001802382000 | 0.000051589600 | 0.008501152000 | 0.174057 | 0.00498204 |
| 384 | 0.001995757000 | 0.000057176400 | 0.009414544000 | 0.174036 | 0.00498596 |
| 385 | 0.002236000000 | 0.000064000000 | 0.010549990000 | 0.174008 | 0.00498055 |
| 386 | 0.002535385000 | 0.000072344210 | 0.011965800000 | 0.173972 | 0.00496408 |
| 387 | 0.002892603000 | 0.000082212240 | 0.013655870000 | 0.173932 | 0.00494341 |
| 388 | 0.003300829000 | 0.000093508160 | 0.015588050000 | 0.173889 | 0.00492605 |
| 389 | 0.003753236000 | 0.000106136100 | 0.017730150000 | 0.173845 | 0.00491609 |
| 390 | 0.004243000000 | 0.000120000000 | 0.020050010000 | 0.173801 | 0.00491541 |
| 391 | 0.004762389000 | 0.000134984000 | 0.022511360000 | 0.173754 | 0.00492485 |
| 392 | 0.005330048000 | 0.000151492000 | 0.025202880000 | 0.173705 | 0.00493710 |
| 393 | 0.005978712000 | 0.000170208000 | 0.028279720000 | 0.173655 | 0.00494379 |
| 394 | 0.006741117000 | 0.000191816000 | 0.031897040000 | 0.173606 | 0.00493990 |
| 395 | 0.007650000000 | 0.000217000000 | 0.036210000000 | 0.173560 | 0.00492320 |

| Wavelenght $\lambda(\mathrm{nm})$ | CIE 1931 2° colour-matching functions | | | chromaticity coordinates | |
|---|---|---|---|---|---|
| | $\bar{x}(\lambda)$ | $\bar{y}(\lambda)$ | $\bar{z}(\lambda)$ | $x(\lambda)$ | $y(\lambda)$ |
| 396 | 0.008751373000 | 0.000246906700 | 0.041437710000 | 0.173514 | 0.00489545 |
| 397 | 0.010028880000 | 0.000281240000 | 0.047503720000 | 0.173468 | 0.00486458 |
| 398 | 0.011421700000 | 0.000318520000 | 0.054119880000 | 0.173424 | 0.00483631 |
| 399 | 0.012869010000 | 0.000357266700 | 0.060998030000 | 0.173380 | 0.00481334 |
| 400 | 0.014310000000 | 0.000396000000 | 0.067850010000 | 0.173337 | 0.00479674 |
| 401 | 0.015704430000 | 0.000433714700 | 0.074486320000 | 0.173291 | 0.00478585 |
| 402 | 0.017147440000 | 0.000473024000 | 0.081361560000 | 0.173238 | 0.00477889 |
| 403 | 0.018781220000 | 0.000517876000 | 0.089153640000 | 0.173174 | 0.00477513 |
| 404 | 0.020748010000 | 0.000572218700 | 0.098540480000 | 0.173101 | 0.00477403 |
| 405 | 0.023190000000 | 0.000640000000 | 0.110200000000 | 0.173021 | 0.00477505 |
| 406 | 0.026207360000 | 0.000724560000 | 0.124613300000 | 0.172934 | 0.00478115 |
| 407 | 0.029782480000 | 0.000825500000 | 0.141701700000 | 0.172843 | 0.00479079 |
| 408 | 0.033880920000 | 0.000941160000 | 0.161303500000 | 0.172751 | 0.00479876 |
| 409 | 0.038468240000 | 0.001069880000 | 0.183256800000 | 0.172662 | 0.00480208 |
| 410 | 0.043510000000 | 0.001210000000 | 0.207400000000 | 0.172577 | 0.00479930 |
| 411 | 0.048995600000 | 0.001362091000 | 0.233692100000 | 0.172489 | 0.00479525 |
| 412 | 0.055022600000 | 0.001530752000 | 0.262611400000 | 0.172396 | 0.00479612 |
| 413 | 0.061718800000 | 0.001720368000 | 0.294774600000 | 0.172296 | 0.00480263 |
| 414 | 0.069212000000 | 0.001935323000 | 0.330798500000 | 0.172192 | 0.00481489 |
| 415 | 0.077630000000 | 0.002180000000 | 0.371300000000 | 0.172087 | 0.00483252 |
| 416 | 0.086958110000 | 0.002454800000 | 0.416209100000 | 0.171982 | 0.00485501 |
| 417 | 0.097176720000 | 0.002764000000 | 0.465464200000 | 0.171871 | 0.00488853 |
| 418 | 0.108406300000 | 0.003117800000 | 0.519694800000 | 0.171741 | 0.00493933 |
| 419 | 0.120767200000 | 0.003526400000 | 0.579530300000 | 0.171587 | 0.00501034 |
| 420 | 0.134380000000 | 0.004000000000 | 0.645600000000 | 0.171407 | 0.00510217 |
| 421 | 0.149358200000 | 0.004546240000 | 0.718483800000 | 0.171206 | 0.00521126 |
| 422 | 0.165395700000 | 0.005159320000 | 0.796713300000 | 0.170993 | 0.00533391 |
| 423 | 0.181983100000 | 0.005829280000 | 0.877845900000 | 0.170771 | 0.00547012 |
| 424 | 0.198611000000 | 0.006546160000 | 0.959439000000 | 0.170541 | 0.00562097 |
| 425 | 0.214770000000 | 0.007300000000 | 1.039050100000 | 0.170301 | 0.00578850 |
| 426 | 0.230186800000 | 0.008086507000 | 1.115367300000 | 0.170050 | 0.00597390 |
| 427 | 0.244879700000 | 0.008908720000 | 1.188497100000 | 0.169786 | 0.00617681 |
| 428 | 0.258777300000 | 0.009767680000 | 1.258123300000 | 0.169505 | 0.00639804 |
| 429 | 0.271807900000 | 0.010664430000 | 1.323929600000 | 0.169203 | 0.00663871 |
| 430 | 0.283900000000 | 0.011600000000 | 1.385600000000 | 0.168878 | 0.00690024 |
| 431 | 0.294943800000 | 0.012573170000 | 1.442635200000 | 0.168525 | 0.00718404 |
| 432 | 0.304896500000 | 0.013582720000 | 1.494803500000 | 0.168146 | 0.00749068 |
| 433 | 0.313787300000 | 0.014629680000 | 1.542190300000 | 0.167746 | 0.00782082 |
| 434 | 0.321645400000 | 0.015715090000 | 1.584880700000 | 0.167328 | 0.00817540 |
| 435 | 0.328500000000 | 0.016840000000 | 1.622960000000 | 0.166895 | 0.00855561 |
| 436 | 0.334351300000 | 0.018007360000 | 1.656404800000 | 0.166446 | 0.00896440 |
| 437 | 0.339210100000 | 0.019214480000 | 1.685295900000 | 0.165977 | 0.00940172 |
| 438 | 0.343121300000 | 0.020453920000 | 1.709874500000 | 0.165483 | 0.00986468 |
| 439 | 0.346129600000 | 0.021718240000 | 1.730382100000 | 0.164963 | 0.0103507 |

| Wavelenght $\lambda$(nm) | CIE 1931 2° colour-matching functions | | | chromaticity coordinates | |
|---|---|---|---|---|---|
| | $\bar{x}(\lambda)$ | $\bar{y}(\lambda)$ | $\bar{z}(\lambda)$ | $x(\lambda)$ | $y(\lambda)$ |
| 440 | 0.348280000000 | 0.023000000000 | 1.747060000000 | 0.164412 | 0.0108576 |
| 441 | 0.349599900000 | 0.024294610000 | 1.760044600000 | 0.163828 | 0.0113849 |
| 442 | 0.350147400000 | 0.025610240000 | 1.769623300000 | 0.163210 | 0.0119374 |
| 443 | 0.350013000000 | 0.026958570000 | 1.776263700000 | 0.162552 | 0.0125200 |
| 444 | 0.349287000000 | 0.028351250000 | 1.780433400000 | 0.161851 | 0.0131373 |
| 445 | 0.348060000000 | 0.029800000000 | 1.782600000000 | 0.161105 | 0.0137934 |
| 446 | 0.346373300000 | 0.031310830000 | 1.782968200000 | 0.160310 | 0.0144914 |
| 447 | 0.344262400000 | 0.032883680000 | 1.781699800000 | 0.159466 | 0.0152321 |
| 448 | 0.341808800000 | 0.034521120000 | 1.779198200000 | 0.158573 | 0.0160152 |
| 449 | 0.339094100000 | 0.036225710000 | 1.775867100000 | 0.157631 | 0.0168399 |
| 450 | 0.336200000000 | 0.038000000000 | 1.772110000000 | 0.156641 | 0.0177048 |
| 451 | 0.333197700000 | 0.039846670000 | 1.768258900000 | 0.155605 | 0.0186086 |
| 452 | 0.330041100000 | 0.041768000000 | 1.764039000000 | 0.154525 | 0.0195557 |
| 453 | 0.326635700000 | 0.043766000000 | 1.758943800000 | 0.153397 | 0.0205537 |
| 454 | 0.322886800000 | 0.045842670000 | 1.752466300000 | 0.152219 | 0.0216117 |
| 455 | 0.318700000000 | 0.048000000000 | 1.744100000000 | 0.150985 | 0.0227402 |
| 456 | 0.314025100000 | 0.050243680000 | 1.733559500000 | 0.149691 | 0.0239503 |
| 457 | 0.308884000000 | 0.052573040000 | 1.720858100000 | 0.148337 | 0.0252474 |
| 458 | 0.303290400000 | 0.054980560000 | 1.705936900000 | 0.146928 | 0.0266352 |
| 459 | 0.297257900000 | 0.057458720000 | 1.688737200000 | 0.145468 | 0.0281184 |
| 460 | 0.290800000000 | 0.060000000000 | 1.669200000000 | 0.143960 | 0.0297030 |
| 461 | 0.283970100000 | 0.062601970000 | 1.647528700000 | 0.142405 | 0.0313936 |
| 462 | 0.276721400000 | 0.065277520000 | 1.623412700000 | 0.140796 | 0.0332132 |
| 463 | 0.268917800000 | 0.068042080000 | 1.596022300000 | 0.139121 | 0.0352006 |
| 464 | 0.260422700000 | 0.070911090000 | 1.564528000000 | 0.137364 | 0.0374031 |
| 465 | 0.251100000000 | 0.073900000000 | 1.528100000000 | 0.135503 | 0.0398791 |
| 466 | 0.240847500000 | 0.077016000000 | 1.486111400000 | 0.133509 | 0.0426924 |
| 467 | 0.229851200000 | 0.080266400000 | 1.439521500000 | 0.131371 | 0.0458760 |
| 468 | 0.218407200000 | 0.083666800000 | 1.389879900000 | 0.129086 | 0.0494498 |
| 469 | 0.206811500000 | 0.087232800000 | 1.338736200000 | 0.126662 | 0.0534259 |
| 470 | 0.195360000000 | 0.090980000000 | 1.287640000000 | 0.124118 | 0.0578025 |
| 471 | 0.184213600000 | 0.094917550000 | 1.237422300000 | 0.121469 | 0.0625877 |
| 472 | 0.173327300000 | 0.099045840000 | 1.187824300000 | 0.118701 | 0.0678304 |
| 473 | 0.162688100000 | 0.103367400000 | 1.138761100000 | 0.115807 | 0.0735807 |
| 474 | 0.152283300000 | 0.107884600000 | 1.090148000000 | 0.112776 | 0.0798958 |
| 475 | 0.142100000000 | 0.112600000000 | 1.041900000000 | 0.109594 | 0.0868425 |
| 476 | 0.132178600000 | 0.117532000000 | 0.994197600000 | 0.106261 | 0.0944861 |
| 477 | 0.122569600000 | 0.122674400000 | 0.947347300000 | 0.102776 | 0.102864 |
| 478 | 0.113275200000 | 0.127992800000 | 0.901453100000 | 0.0991276 | 0.112007 |
| 479 | 0.104297900000 | 0.133452800000 | 0.856619300000 | 0.0953041 | 0.121945 |
| 480 | 0.095640000000 | 0.139020000000 | 0.812950100000 | 0.0912935 | 0.132702 |
| 481 | 0.087299550000 | 0.144676400000 | 0.770517300000 | 0.0870824 | 0.144317 |
| 482 | 0.079308040000 | 0.150469300000 | 0.729444800000 | 0.0826795 | 0.156866 |
| 483 | 0.071717760000 | 0.156461900000 | 0.689913600000 | 0.0781160 | 0.170420 |

| Wavelenght $\lambda(\mathrm{nm})$ | CIE 1931 2° colour-matching functions | | | chromaticity coordinates | |
|---|---|---|---|---|---|
| | $\bar{x}(\lambda)$ | $\bar{y}(\lambda)$ | $\bar{z}(\lambda)$ | $x(\lambda)$ | $y(\lambda)$ |
| 484 | 0.064580990000 | 0.162717700000 | 0.652104900000 | 0.0734373 | 0.185032 |
| 485 | 0.057950010000 | 0.169300000000 | 0.616200000000 | 0.0687059 | 0.200723 |
| 486 | 0.051862110000 | 0.176243100000 | 0.582328600000 | 0.0639930 | 0.217468 |
| 487 | 0.046281520000 | 0.183558100000 | 0.550416200000 | 0.0593158 | 0.235254 |
| 488 | 0.041150880000 | 0.191273500000 | 0.520337600000 | 0.0546665 | 0.254096 |
| 489 | 0.036412830000 | 0.199418000000 | 0.491967300000 | 0.0500315 | 0.274002 |
| 490 | 0.032010000000 | 0.208020000000 | 0.465180000000 | 0.0453907 | 0.294976 |
| 491 | 0.027917200000 | 0.217119900000 | 0.439924600000 | 0.0407573 | 0.316981 |
| 492 | 0.024144400000 | 0.226734500000 | 0.416183600000 | 0.0361951 | 0.339900 |
| 493 | 0.020687000000 | 0.236857100000 | 0.393882200000 | 0.0317565 | 0.363598 |
| 494 | 0.017540400000 | 0.247481200000 | 0.372945900000 | 0.0274942 | 0.387921 |
| 495 | 0.014700000000 | 0.258600000000 | 0.353300000000 | 0.0234599 | 0.412703 |
| 496 | 0.012161790000 | 0.270184900000 | 0.334857800000 | 0.0197046 | 0.437756 |
| 497 | 0.009919960000 | 0.282293900000 | 0.317552100000 | 0.0162685 | 0.462955 |
| 498 | 0.007967240000 | 0.295050500000 | 0.301337500000 | 0.0131830 | 0.488207 |
| 499 | 0.006296346000 | 0.308578000000 | 0.286168600000 | 0.0104757 | 0.513404 |
| 500 | 0.004900000000 | 0.323000000000 | 0.272000000000 | 0.00816803 | 0.538423 |
| 501 | 0.003777173000 | 0.338402100000 | 0.258817100000 | 0.00628485 | 0.563068 |
| 502 | 0.002945320000 | 0.354685800000 | 0.246483800000 | 0.00487543 | 0.587116 |
| 503 | 0.002424880000 | 0.371698600000 | 0.234771800000 | 0.00398243 | 0.610447 |
| 504 | 0.002236293000 | 0.389287500000 | 0.223453300000 | 0.00363638 | 0.633011 |
| 505 | 0.002400000000 | 0.407300000000 | 0.212300000000 | 0.00385852 | 0.654823 |
| 506 | 0.002925520000 | 0.425629900000 | 0.201169200000 | 0.00464571 | 0.675898 |
| 507 | 0.003836560000 | 0.444309600000 | 0.190119600000 | 0.00601091 | 0.696120 |
| 508 | 0.005174840000 | 0.463394400000 | 0.179225400000 | 0.00798840 | 0.715342 |
| 509 | 0.006982080000 | 0.482939500000 | 0.168560800000 | 0.0106033 | 0.733413 |
| 510 | 0.009300000000 | 0.503000000000 | 0.158200000000 | 0.0138702 | 0.750186 |
| 511 | 0.012149490000 | 0.523569300000 | 0.148138300000 | 0.0177661 | 0.765612 |
| 512 | 0.015535880000 | 0.544512000000 | 0.138375800000 | 0.0222442 | 0.779630 |
| 513 | 0.019477520000 | 0.565690000000 | 0.128994200000 | 0.0272733 | 0.792104 |
| 514 | 0.023992770000 | 0.586965300000 | 0.120075100000 | 0.0328204 | 0.802926 |
| 515 | 0.029100000000 | 0.608200000000 | 0.111700000000 | 0.0388518 | 0.812016 |
| 516 | 0.034814850000 | 0.629345600000 | 0.103904800000 | 0.0453280 | 0.819391 |
| 517 | 0.041120160000 | 0.650306800000 | 0.096667480000 | 0.0521767 | 0.825164 |
| 518 | 0.047985040000 | 0.670875200000 | 0.089982720000 | 0.0593255 | 0.829426 |
| 519 | 0.055378610000 | 0.690842400000 | 0.083845310000 | 0.0667159 | 0.832274 |
| 520 | 0.063270000000 | 0.710000000000 | 0.078249990000 | 0.0743024 | 0.833803 |
| 521 | 0.071635010000 | 0.728185200000 | 0.073208990000 | 0.0820534 | 0.834090 |
| 522 | 0.080462240000 | 0.745463600000 | 0.068678160000 | 0.0899417 | 0.833289 |
| 523 | 0.089739960000 | 0.761969400000 | 0.064567840000 | 0.0979398 | 0.831593 |
| 524 | 0.099456450000 | 0.777836800000 | 0.060788350000 | 0.106021 | 0.829178 |
| 525 | 0.109600000000 | 0.793200000000 | 0.057250010000 | 0.114161 | 0.826207 |
| 526 | 0.120167400000 | 0.808110400000 | 0.053904350000 | 0.122347 | 0.822770 |
| 527 | 0.131114500000 | 0.822496200000 | 0.050746640000 | 0.130546 | 0.818928 |

| Wavelenght $\lambda(\mathrm{nm})$ | CIE 1931 2° colour-matching functions | | | chromaticity coordinates | |
|---|---|---|---|---|---|
| | $\bar{x}(\lambda)$ | $\bar{y}(\lambda)$ | $\bar{z}(\lambda)$ | $x(\lambda)$ | $y(\lambda)$ |
| 528 | 0.142367900000 | 0.836306800000 | 0.047752760000 | 0.138702 | 0.814774 |
| 529 | 0.153854200000 | 0.849491600000 | 0.044898590000 | 0.146773 | 0.810395 |
| 530 | 0.165500000000 | 0.862000000000 | 0.042160000000 | 0.154722 | 0.805864 |
| 531 | 0.177257100000 | 0.873810800000 | 0.039507280000 | 0.162535 | 0.801238 |
| 532 | 0.189140000000 | 0.884962400000 | 0.036935640000 | 0.170237 | 0.796519 |
| 533 | 0.201169400000 | 0.895493600000 | 0.034458360000 | 0.177850 | 0.791687 |
| 534 | 0.213365800000 | 0.905443200000 | 0.032088720000 | 0.185391 | 0.786728 |
| 535 | 0.225749900000 | 0.914850100000 | 0.029840000000 | 0.192876 | 0.781629 |
| 536 | 0.238320900000 | 0.923734800000 | 0.027711810000 | 0.200309 | 0.776399 |
| 537 | 0.251066800000 | 0.932092400000 | 0.025694440000 | 0.207690 | 0.771055 |
| 538 | 0.263992200000 | 0.939922600000 | 0.023787160000 | 0.215030 | 0.765595 |
| 539 | 0.277101700000 | 0.947225200000 | 0.021989250000 | 0.222337 | 0.760020 |
| 540 | 0.290400000000 | 0.954000000000 | 0.020300000000 | 0.229620 | 0.754329 |
| 541 | 0.303891200000 | 0.960256100000 | 0.018718050000 | 0.236885 | 0.748524 |
| 542 | 0.317572600000 | 0.966007400000 | 0.017240360000 | 0.244133 | 0.742614 |
| 543 | 0.331438400000 | 0.971260600000 | 0.015863640000 | 0.251363 | 0.736606 |
| 544 | 0.345482800000 | 0.976022500000 | 0.014584610000 | 0.258578 | 0.730507 |
| 545 | 0.359700000000 | 0.980300000000 | 0.013400000000 | 0.265775 | 0.724324 |
| 546 | 0.374083900000 | 0.984092400000 | 0.012307230000 | 0.272958 | 0.718062 |
| 547 | 0.388639600000 | 0.987418200000 | 0.011301880000 | 0.280129 | 0.711725 |
| 548 | 0.403378400000 | 0.990312800000 | 0.010377920000 | 0.287292 | 0.705316 |
| 549 | 0.418311500000 | 0.992811600000 | 0.009529306000 | 0.294450 | 0.698842 |
| 550 | 0.433449900000 | 0.994950100000 | 0.008749999000 | 0.301604 | 0.692308 |
| 551 | 0.448795300000 | 0.996710800000 | 0.008035200000 | 0.308760 | 0.685712 |
| 552 | 0.464336000000 | 0.998098300000 | 0.007381600000 | 0.315914 | 0.679063 |
| 553 | 0.480064000000 | 0.999112000000 | 0.006785400000 | 0.323066 | 0.672367 |
| 554 | 0.495971300000 | 0.999748200000 | 0.006242800000 | 0.330216 | 0.665628 |
| 555 | 0.512050100000 | 1.000000000000 | 0.005749999000 | 0.337363 | 0.658848 |
| 556 | 0.528295900000 | 0.999856700000 | 0.005303600000 | 0.344513 | 0.652028 |
| 557 | 0.544691600000 | 0.999304600000 | 0.004899800000 | 0.351664 | 0.645172 |
| 558 | 0.561209400000 | 0.998325500000 | 0.004534200000 | 0.358814 | 0.638287 |
| 559 | 0.577821500000 | 0.996898700000 | 0.004202400000 | 0.365959 | 0.631379 |
| 560 | 0.594500000000 | 0.995000000000 | 0.003900000000 | 0.373102 | 0.624451 |
| 561 | 0.611220900000 | 0.992600500000 | 0.003623200000 | 0.380244 | 0.617502 |
| 562 | 0.627975800000 | 0.989742600000 | 0.003370600000 | 0.387379 | 0.610542 |
| 563 | 0.644760200000 | 0.986444400000 | 0.003141400000 | 0.394507 | 0.603571 |
| 564 | 0.661569700000 | 0.982724100000 | 0.002934800000 | 0.401626 | 0.596592 |
| 565 | 0.678400000000 | 0.978600000000 | 0.002749999000 | 0.408736 | 0.589607 |
| 566 | 0.695239200000 | 0.974083700000 | 0.002585200000 | 0.415836 | 0.582618 |
| 567 | 0.712058600000 | 0.969171200000 | 0.002438600000 | 0.422921 | 0.575631 |
| 568 | 0.728828400000 | 0.963856800000 | 0.002309400000 | 0.429989 | 0.568649 |
| 569 | 0.745518800000 | 0.958134900000 | 0.002196800000 | 0.437036 | 0.561676 |
| 570 | 0.762100000000 | 0.952000000000 | 0.002100000000 | 0.444062 | 0.554714 |
| 571 | 0.778543200000 | 0.945450400000 | 0.002017733000 | 0.451065 | 0.547766 |

| Wavelenght $\lambda(\text{nm})$ | CIE 1931 2° colour-matching functions | | | chromaticity coordinates | |
|---|---|---|---|---|---|
| | $\bar{x}(\lambda)$ | $\bar{y}(\lambda)$ | $\bar{z}(\lambda)$ | $x(\lambda)$ | $y(\lambda)$ |
| 572 | 0.794825600000 | 0.938499200000 | 0.001948200000 | 0.458041 | 0.540837 |
| 573 | 0.810926400000 | 0.931162800000 | 0.001889800000 | 0.464986 | 0.533930 |
| 574 | 0.826824800000 | 0.923457600000 | 0.001840933000 | 0.471899 | 0.527051 |
| 575 | 0.842500000000 | 0.915400000000 | 0.001800000000 | 0.478775 | 0.520202 |
| 576 | 0.857932500000 | 0.907006400000 | 0.001766267000 | 0.485612 | 0.513389 |
| 577 | 0.873081600000 | 0.898277200000 | 0.001737800000 | 0.492405 | 0.506615 |
| 578 | 0.887894400000 | 0.889204800000 | 0.001711200000 | 0.499151 | 0.499887 |
| 579 | 0.902318100000 | 0.879781600000 | 0.001683067000 | 0.505845 | 0.493211 |
| 580 | 0.916300000000 | 0.870000000000 | 0.001650001000 | 0.512486 | 0.486591 |
| 581 | 0.929799500000 | 0.859861300000 | 0.001610133000 | 0.519073 | 0.480029 |
| 582 | 0.942798400000 | 0.849392000000 | 0.001564400000 | 0.525600 | 0.473527 |
| 583 | 0.955277600000 | 0.838622000000 | 0.001513600000 | 0.532066 | 0.467091 |
| 584 | 0.967217900000 | 0.827581300000 | 0.001458533000 | 0.538463 | 0.460725 |
| 585 | 0.978600000000 | 0.816300000000 | 0.001400000000 | 0.544787 | 0.454434 |
| 586 | 0.989385600000 | 0.804794700000 | 0.001336667000 | 0.551031 | 0.448225 |
| 587 | 0.999548800000 | 0.793082000000 | 0.001270000000 | 0.557193 | 0.442099 |
| 588 | 1.009089200000 | 0.781192000000 | 0.001205000000 | 0.563269 | 0.436058 |
| 589 | 1.018006400000 | 0.769154700000 | 0.001146667000 | 0.569257 | 0.430102 |
| 590 | 1.026300000000 | 0.757000000000 | 0.001100000000 | 0.575151 | 0.424232 |
| 591 | 1.033982700000 | 0.744754100000 | 0.001068800000 | 0.580953 | 0.418447 |
| 592 | 1.040986000000 | 0.732422400000 | 0.001049400000 | 0.586650 | 0.412758 |
| 593 | 1.047188000000 | 0.720003600000 | 0.001035600000 | 0.592225 | 0.407190 |
| 594 | 1.052466700000 | 0.707496500000 | 0.001021200000 | 0.597658 | 0.401762 |
| 595 | 1.056700000000 | 0.694900000000 | 0.001000000000 | 0.602933 | 0.396497 |
| 596 | 1.059794400000 | 0.682219200000 | 0.000968640000 | 0.608035 | 0.391409 |
| 597 | 1.061799200000 | 0.669471600000 | 0.000929920000 | 0.612977 | 0.386486 |
| 598 | 1.062806800000 | 0.656674400000 | 0.000886880000 | 0.617779 | 0.381706 |
| 599 | 1.062909600000 | 0.643844800000 | 0.000842560000 | 0.622459 | 0.377047 |
| 600 | 1.062200000000 | 0.631000000000 | 0.000800000000 | 0.627037 | 0.372491 |
| 601 | 1.060735200000 | 0.618155500000 | 0.000760960000 | 0.631521 | 0.368026 |
| 602 | 1.058443600000 | 0.605314400000 | 0.000723680000 | 0.635900 | 0.363665 |
| 603 | 1.055224400000 | 0.592475600000 | 0.000685920000 | 0.640156 | 0.359428 |
| 604 | 1.050976800000 | 0.579637900000 | 0.000645440000 | 0.644273 | 0.355331 |
| 605 | 1.045600000000 | 0.566800000000 | 0.000600000000 | 0.648233 | 0.351395 |
| 606 | 1.039036900000 | 0.553961100000 | 0.000547866700 | 0.652028 | 0.347628 |
| 607 | 1.031360800000 | 0.541137200000 | 0.000491600000 | 0.655669 | 0.344018 |
| 608 | 1.022666200000 | 0.528352800000 | 0.000435400000 | 0.659166 | 0.340553 |
| 609 | 1.013047700000 | 0.515632300000 | 0.000383466700 | 0.662528 | 0.337221 |
| 610 | 1.002600000000 | 0.503000000000 | 0.000340000000 | 0.665764 | 0.334011 |
| 611 | 0.991367500000 | 0.490468800000 | 0.000307253300 | 0.668874 | 0.330919 |
| 612 | 0.979331400000 | 0.478030400000 | 0.000283160000 | 0.671859 | 0.327947 |
| 613 | 0.966491600000 | 0.465677600000 | 0.000265440000 | 0.674720 | 0.325095 |
| 614 | 0.952847900000 | 0.453403200000 | 0.000251813300 | 0.677459 | 0.322362 |
| 615 | 0.938400000000 | 0.441200000000 | 0.000240000000 | 0.680079 | 0.319747 |

| Wavelenght $\lambda(\text{nm})$ | CIE 1931 2° colour-matching functions | | | chromaticity coordinates | |
|---|---|---|---|---|---|
| | $\bar{x}(\lambda)$ | $\bar{y}(\lambda)$ | $\bar{z}(\lambda)$ | $x(\lambda)$ | $y(\lambda)$ |
| 616 | 0.923194000000 | 0.429080000000 | 0.000229546700 | 0.682582 | 0.317249 |
| 617 | 0.907244000000 | 0.417036000000 | 0.000220640000 | 0.684971 | 0.314863 |
| 618 | 0.890502000000 | 0.405032000000 | 0.000211960000 | 0.687250 | 0.312586 |
| 619 | 0.872920000000 | 0.393032000000 | 0.000202186700 | 0.689426 | 0.310414 |
| 620 | 0.854449900000 | 0.381000000000 | 0.000190000000 | 0.691504 | 0.308342 |
| 621 | 0.835084000000 | 0.368918400000 | 0.000174213300 | 0.693490 | 0.306366 |
| 622 | 0.814946000000 | 0.356827200000 | 0.000155640000 | 0.695389 | 0.304479 |
| 623 | 0.794186000000 | 0.344776800000 | 0.000135960000 | 0.697206 | 0.302675 |
| 624 | 0.772954000000 | 0.332817600000 | 0.000116853300 | 0.698944 | 0.300950 |
| 625 | 0.751400000000 | 0.321000000000 | 0.000100000000 | 0.700606 | 0.299301 |
| 626 | 0.729583600000 | 0.309338100000 | 0.000086133330 | 0.702193 | 0.297725 |
| 627 | 0.707588800000 | 0.297850400000 | 0.000074600000 | 0.703709 | 0.296217 |
| 628 | 0.685602200000 | 0.286593600000 | 0.000065000000 | 0.705163 | 0.294770 |
| 629 | 0.663810400000 | 0.275624500000 | 0.000056933330 | 0.706563 | 0.293376 |
| 630 | 0.642400000000 | 0.265000000000 | 0.000049999990 | 0.707918 | 0.292027 |
| 631 | 0.621514900000 | 0.254763200000 | 0.000044160000 | 0.709231 | 0.290719 |
| 632 | 0.601113800000 | 0.244889600000 | 0.000039480000 | 0.710500 | 0.289453 |
| 633 | 0.581105200000 | 0.235334400000 | 0.000035720000 | 0.711724 | 0.288232 |
| 634 | 0.561397700000 | 0.226052800000 | 0.000032640000 | 0.712901 | 0.287057 |
| 635 | 0.541900000000 | 0.217000000000 | 0.000030000000 | 0.714032 | 0.285929 |
| 636 | 0.522599500000 | 0.208161600000 | 0.000027653330 | 0.715117 | 0.284845 |
| 637 | 0.503546400000 | 0.199548800000 | 0.000025560000 | 0.716159 | 0.283804 |
| 638 | 0.484743600000 | 0.191155200000 | 0.000023640000 | 0.717159 | 0.282806 |
| 639 | 0.466193900000 | 0.182974400000 | 0.000021813330 | 0.718116 | 0.281850 |
| 640 | 0.447900000000 | 0.175000000000 | 0.000020000000 | 0.719033 | 0.280935 |
| 641 | 0.429861300000 | 0.167223500000 | 0.000018133330 | 0.719912 | 0.280058 |
| 642 | 0.412098000000 | 0.159646400000 | 0.000016200000 | 0.720753 | 0.279219 |
| 643 | 0.394644000000 | 0.152277600000 | 0.000014200000 | 0.721555 | 0.278420 |
| 644 | 0.377533300000 | 0.145125900000 | 0.000012133330 | 0.722315 | 0.277662 |
| 645 | 0.360800000000 | 0.138200000000 | 0.000010000000 | 0.723032 | 0.276948 |
| 646 | 0.344456300000 | 0.131500300000 | 0.000007733333 | 0.723702 | 0.276282 |
| 647 | 0.328516800000 | 0.125024800000 | 0.000005400000 | 0.724328 | 0.275660 |
| 648 | 0.313019200000 | 0.118779200000 | 0.000003200000 | 0.724914 | 0.275078 |
| 649 | 0.298001100000 | 0.112769100000 | 0.000001333333 | 0.725467 | 0.274530 |
| 650 | 0.283500000000 | 0.107000000000 | 0.000000000000 | 0.725992 | 0.274008 |
| 651 | 0.269544800000 | 0.101476200000 | 0.000000000000 | 0.726495 | 0.273505 |
| 652 | 0.256118400000 | 0.096188640000 | 0.000000000000 | 0.726975 | 0.273025 |
| 653 | 0.243189600000 | 0.091122960000 | 0.000000000000 | 0.727432 | 0.272568 |
| 654 | 0.230727200000 | 0.086264850000 | 0.000000000000 | 0.727864 | 0.272136 |
| 655 | 0.218700000000 | 0.081600000000 | 0.000000000000 | 0.728272 | 0.271728 |
| 656 | 0.207097100000 | 0.077120640000 | 0.000000000000 | 0.728656 | 0.271344 |
| 657 | 0.195923200000 | 0.072825520000 | 0.000000000000 | 0.729020 | 0.270980 |
| 658 | 0.185170800000 | 0.068710080000 | 0.000000000000 | 0.729361 | 0.270639 |
| 659 | 0.174832300000 | 0.064769760000 | 0.000000000000 | 0.729678 | 0.270322 |

| Wavelenght $\lambda$(nm) | CIE 1931 2° colour-matching functions | | | chromaticity coordinates | |
|---|---|---|---|---|---|
| | $\bar{x}(\lambda)$ | $\bar{y}(\lambda)$ | $\bar{z}(\lambda)$ | $x(\lambda)$ | $y(\lambda)$ |
| 660 | 0.164900000000 | 0.061000000000 | 0.000000000000 | 0.729969 | 0.270031 |
| 661 | 0.155366700000 | 0.057396210000 | 0.000000000000 | 0.730234 | 0.269766 |
| 662 | 0.146230000000 | 0.053955040000 | 0.000000000000 | 0.730474 | 0.269526 |
| 663 | 0.137490000000 | 0.050673760000 | 0.000000000000 | 0.730693 | 0.269307 |
| 664 | 0.129146700000 | 0.047549650000 | 0.000000000000 | 0.730896 | 0.269104 |
| 665 | 0.121200000000 | 0.044580000000 | 0.000000000000 | 0.731089 | 0.268911 |
| 666 | 0.113639700000 | 0.041758720000 | 0.000000000000 | 0.731280 | 0.268720 |
| 667 | 0.106465000000 | 0.039084960000 | 0.000000000000 | 0.731467 | 0.268533 |
| 668 | 0.099690440000 | 0.036563840000 | 0.000000000000 | 0.731650 | 0.268350 |
| 669 | 0.093330610000 | 0.034200480000 | 0.000000000000 | 0.731826 | 0.268174 |
| 670 | 0.087400000000 | 0.032000000000 | 0.000000000000 | 0.731993 | 0.268007 |
| 671 | 0.081900960000 | 0.029962610000 | 0.000000000000 | 0.732150 | 0.267850 |
| 672 | 0.076804280000 | 0.028076640000 | 0.000000000000 | 0.732300 | 0.267700 |
| 673 | 0.072077120000 | 0.026329360000 | 0.000000000000 | 0.732443 | 0.267557 |
| 674 | 0.067686640000 | 0.024708050000 | 0.000000000000 | 0.732581 | 0.267419 |
| 675 | 0.063600000000 | 0.023200000000 | 0.000000000000 | 0.732719 | 0.267281 |
| 676 | 0.059806850000 | 0.021800770000 | 0.000000000000 | 0.732859 | 0.267141 |
| 677 | 0.056282160000 | 0.020501120000 | 0.000000000000 | 0.733000 | 0.267000 |
| 678 | 0.052971040000 | 0.019281080000 | 0.000000000000 | 0.733142 | 0.266858 |
| 679 | 0.049818610000 | 0.018120690000 | 0.000000000000 | 0.733281 | 0.266719 |
| 680 | 0.046770000000 | 0.017000000000 | 0.000000000000 | 0.733417 | 0.266583 |
| 681 | 0.043784050000 | 0.015903790000 | 0.000000000000 | 0.733551 | 0.266449 |
| 682 | 0.040875360000 | 0.014837180000 | 0.000000000000 | 0.733683 | 0.266317 |
| 683 | 0.038072640000 | 0.013810680000 | 0.000000000000 | 0.733813 | 0.266187 |
| 684 | 0.035404610000 | 0.012834780000 | 0.000000000000 | 0.733936 | 0.266064 |
| 685 | 0.032900000000 | 0.011920000000 | 0.000000000000 | 0.734047 | 0.265953 |
| 686 | 0.030564190000 | 0.011068310000 | 0.000000000000 | 0.734143 | 0.265857 |
| 687 | 0.028380560000 | 0.010273390000 | 0.000000000000 | 0.734221 | 0.265779 |
| 688 | 0.026344840000 | 0.009533311000 | 0.000000000000 | 0.734286 | 0.265714 |
| 689 | 0.024452750000 | 0.008846157000 | 0.000000000000 | 0.734341 | 0.265659 |
| 690 | 0.022700000000 | 0.008210000000 | 0.000000000000 | 0.734390 | 0.265610 |
| 691 | 0.021084290000 | 0.007623781000 | 0.000000000000 | 0.734438 | 0.265562 |
| 692 | 0.019599880000 | 0.007085424000 | 0.000000000000 | 0.734482 | 0.265518 |
| 693 | 0.018237320000 | 0.006591476000 | 0.000000000000 | 0.734523 | 0.265477 |
| 694 | 0.016987170000 | 0.006138485000 | 0.000000000000 | 0.734560 | 0.265440 |
| 695 | 0.015840000000 | 0.005723000000 | 0.000000000000 | 0.734592 | 0.265408 |
| 696 | 0.014790640000 | 0.005343059000 | 0.000000000000 | 0.734621 | 0.265379 |
| 697 | 0.013831320000 | 0.004995796000 | 0.000000000000 | 0.734649 | 0.265351 |
| 698 | 0.012948680000 | 0.004676404000 | 0.000000000000 | 0.734673 | 0.265327 |
| 699 | 0.012129200000 | 0.004380075000 | 0.000000000000 | 0.734690 | 0.265310 |
| 700 | 0.011359160000 | 0.004102000000 | 0.000000000000 | 0.734690 | 0.265310 |
| 701 | 0.010629350000 | 0.003838453000 | 0.000000000000 | 0.734690 | 0.265310 |
| 702 | 0.009938846000 | 0.003589099000 | 0.000000000000 | 0.734690 | 0.265310 |
| 703 | 0.009288422000 | 0.003354219000 | 0.000000000000 | 0.734690 | 0.265310 |

| Wavelenght $\lambda(\mathrm{nm})$ | CIE 1931 2° colour-matching functions | | | chromaticity coordinates | |
|---|---|---|---|---|---|
| | $\bar{x}(\lambda)$ | $\bar{y}(\lambda)$ | $\bar{z}(\lambda)$ | $x(\lambda)$ | $y(\lambda)$ |
| 704 | 0.008678854000 | 0.003134093000 | 0.000000000000 | 0.734690 | 0.265310 |
| 705 | 0.008110916000 | 0.002929000000 | 0.000000000000 | 0.734690 | 0.265310 |
| 706 | 0.007582388000 | 0.002738139000 | 0.000000000000 | 0.734690 | 0.265310 |
| 707 | 0.007088746000 | 0.002559876000 | 0.000000000000 | 0.734690 | 0.265310 |
| 708 | 0.006627313000 | 0.002393244000 | 0.000000000000 | 0.734690 | 0.265310 |
| 709 | 0.006195408000 | 0.002237275000 | 0.000000000000 | 0.734690 | 0.265310 |
| 710 | 0.005790346000 | 0.002091000000 | 0.000000000000 | 0.734690 | 0.265310 |
| 711 | 0.005409826000 | 0.001953587000 | 0.000000000000 | 0.734690 | 0.265310 |
| 712 | 0.005052583000 | 0.001824580000 | 0.000000000000 | 0.734690 | 0.265310 |
| 713 | 0.004717512000 | 0.001703580000 | 0.000000000000 | 0.734690 | 0.265310 |
| 714 | 0.004403507000 | 0.001590187000 | 0.000000000000 | 0.734690 | 0.265310 |
| 715 | 0.004109457000 | 0.001484000000 | 0.000000000000 | 0.734690 | 0.265310 |
| 716 | 0.003833913000 | 0.001384496000 | 0.000000000000 | 0.734690 | 0.265310 |
| 717 | 0.003575748000 | 0.001291268000 | 0.000000000000 | 0.734690 | 0.265310 |
| 718 | 0.003334342000 | 0.001204092000 | 0.000000000000 | 0.734690 | 0.265310 |
| 719 | 0.003109075000 | 0.001122744000 | 0.000000000000 | 0.734690 | 0.265310 |
| 720 | 0.002899327000 | 0.001047000000 | 0.000000000000 | 0.734690 | 0.265310 |
| 721 | 0.002704348000 | 0.000976589600 | 0.000000000000 | 0.734690 | 0.265310 |
| 722 | 0.002523020000 | 0.000911108800 | 0.000000000000 | 0.734690 | 0.265310 |
| 723 | 0.002354168000 | 0.000850133200 | 0.000000000000 | 0.734690 | 0.265310 |
| 724 | 0.002196616000 | 0.000793238400 | 0.000000000000 | 0.734690 | 0.265310 |
| 725 | 0.002049190000 | 0.000740000000 | 0.000000000000 | 0.734690 | 0.265310 |
| 726 | 0.001910960000 | 0.000690082700 | 0.000000000000 | 0.734690 | 0.265310 |
| 727 | 0.001781438000 | 0.000643310000 | 0.000000000000 | 0.734690 | 0.265310 |
| 728 | 0.001660110000 | 0.000599496000 | 0.000000000000 | 0.734690 | 0.265310 |
| 729 | 0.001546459000 | 0.000558454700 | 0.000000000000 | 0.734690 | 0.265310 |
| 730 | 0.001439971000 | 0.000520000000 | 0.000000000000 | 0.734690 | 0.265310 |
| 731 | 0.001340042000 | 0.000483913600 | 0.000000000000 | 0.734690 | 0.265310 |
| 732 | 0.001246275000 | 0.000450052800 | 0.000000000000 | 0.734690 | 0.265310 |
| 733 | 0.001158471000 | 0.000418345200 | 0.000000000000 | 0.734690 | 0.265310 |
| 734 | 0.001076430000 | 0.000388718400 | 0.000000000000 | 0.734690 | 0.265310 |
| 735 | 0.000999949300 | 0.000361100000 | 0.000000000000 | 0.734690 | 0.265310 |
| 736 | 0.000928735800 | 0.000335383500 | 0.000000000000 | 0.734690 | 0.265310 |
| 737 | 0.000862433200 | 0.000311440400 | 0.000000000000 | 0.734690 | 0.265310 |
| 738 | 0.000800750300 | 0.000289165600 | 0.000000000000 | 0.734690 | 0.265310 |
| 739 | 0.000743396000 | 0.000268453900 | 0.000000000000 | 0.734690 | 0.265310 |
| 740 | 0.000690078600 | 0.000249200000 | 0.000000000000 | 0.734690 | 0.265310 |
| 741 | 0.000640515600 | 0.000231301900 | 0.000000000000 | 0.734690 | 0.265310 |
| 742 | 0.000594502100 | 0.000214685600 | 0.000000000000 | 0.734690 | 0.265310 |
| 743 | 0.000551864600 | 0.000199288400 | 0.000000000000 | 0.734690 | 0.265310 |
| 744 | 0.000512429000 | 0.000185047500 | 0.000000000000 | 0.734690 | 0.265310 |
| 745 | 0.000476021300 | 0.000171900000 | 0.000000000000 | 0.734690 | 0.265310 |
| 746 | 0.000442453600 | 0.000159778100 | 0.000000000000 | 0.734690 | 0.265310 |
| 747 | 0.000411511700 | 0.000148604400 | 0.000000000000 | 0.734690 | 0.265310 |

| Wavelenght $\lambda$(nm) | CIE 1931 2° colour-matching functions | | | chromaticity coordinates | |
|---|---|---|---|---|---|
| | $\bar{x}(\lambda)$ | $\bar{y}(\lambda)$ | $\bar{z}(\lambda)$ | $x(\lambda)$ | $y(\lambda)$ |
| 748 | 0.000382981400 | 0.000138301600 | 0.000000000000 | 0.734690 | 0.265310 |
| 749 | 0.000356649100 | 0.000128792500 | 0.000000000000 | 0.734690 | 0.265310 |
| 750 | 0.000332301100 | 0.000120000000 | 0.000000000000 | 0.734690 | 0.265310 |
| 751 | 0.000309758600 | 0.000111859500 | 0.000000000000 | 0.734690 | 0.265310 |
| 752 | 0.000288887100 | 0.000104322400 | 0.000000000000 | 0.734690 | 0.265310 |
| 753 | 0.000269539400 | 0.000097335600 | 0.000000000000 | 0.734690 | 0.265310 |
| 754 | 0.000251568200 | 0.000090845870 | 0.000000000000 | 0.734690 | 0.265310 |
| 755 | 0.000234826100 | 0.000084800000 | 0.000000000000 | 0.734690 | 0.265310 |
| 756 | 0.000219171000 | 0.000079146670 | 0.000000000000 | 0.734690 | 0.265310 |
| 757 | 0.000204525800 | 0.000073858000 | 0.000000000000 | 0.734690 | 0.265310 |
| 758 | 0.000190840500 | 0.000068916000 | 0.000000000000 | 0.734690 | 0.265310 |
| 759 | 0.000178065400 | 0.000064302670 | 0.000000000000 | 0.734690 | 0.265310 |
| 760 | 0.000166150500 | 0.000060000000 | 0.000000000000 | 0.734690 | 0.265310 |
| 761 | 0.000155023600 | 0.000055981870 | 0.000000000000 | 0.734690 | 0.265310 |
| 762 | 0.000144621900 | 0.000052225600 | 0.000000000000 | 0.734690 | 0.265310 |
| 763 | 0.000134909800 | 0.000048718400 | 0.000000000000 | 0.734690 | 0.265310 |
| 764 | 0.000125852000 | 0.000045447470 | 0.000000000000 | 0.734690 | 0.265310 |
| 765 | 0.000117413000 | 0.000042400000 | 0.000000000000 | 0.734690 | 0.265310 |
| 766 | 0.000109551500 | 0.000039561040 | 0.000000000000 | 0.734690 | 0.265310 |
| 767 | 0.000102224500 | 0.000036915120 | 0.000000000000 | 0.734690 | 0.265310 |
| 768 | 0.000095394450 | 0.000034448680 | 0.000000000000 | 0.734690 | 0.265310 |
| 769 | 0.000089023900 | 0.000032148160 | 0.000000000000 | 0.734690 | 0.265310 |
| 770 | 0.000083075270 | 0.000030000000 | 0.000000000000 | 0.734690 | 0.265310 |
| 771 | 0.000077512690 | 0.000027991250 | 0.000000000000 | 0.734690 | 0.265310 |
| 772 | 0.000072313040 | 0.000026113560 | 0.000000000000 | 0.734690 | 0.265310 |
| 773 | 0.000067457780 | 0.000024360240 | 0.000000000000 | 0.734690 | 0.265310 |
| 774 | 0.000062928440 | 0.000022724610 | 0.000000000000 | 0.734690 | 0.265310 |
| 775 | 0.000058706520 | 0.000021200000 | 0.000000000000 | 0.734690 | 0.265310 |
| 776 | 0.000054770280 | 0.000019778550 | 0.000000000000 | 0.734690 | 0.265310 |
| 777 | 0.000051099180 | 0.000018452850 | 0.000000000000 | 0.734690 | 0.265310 |
| 778 | 0.000047676540 | 0.000017216870 | 0.000000000000 | 0.734690 | 0.265310 |
| 779 | 0.000044485670 | 0.000016064590 | 0.000000000000 | 0.734690 | 0.265310 |
| 780 | 0.000041509940 | 0.000014990000 | 0.000000000000 | 0.734690 | 0.265310 |
| 781 | 0.000038733240 | 0.000013987280 | 0.000000000000 | 0.734690 | 0.265310 |
| 782 | 0.000036142030 | 0.000013051550 | 0.000000000000 | 0.734690 | 0.265310 |
| 783 | 0.000033723520 | 0.000012178180 | 0.000000000000 | 0.734690 | 0.265310 |
| 784 | 0.000031464870 | 0.000011362540 | 0.000000000000 | 0.734690 | 0.265310 |
| 785 | 0.000029353260 | 0.000010600000 | 0.000000000000 | 0.734690 | 0.265310 |
| 786 | 0.000027375730 | 0.000009885877 | 0.000000000000 | 0.734690 | 0.265310 |
| 787 | 0.000025524330 | 0.000009217304 | 0.000000000000 | 0.734690 | 0.265310 |
| 788 | 0.000023793760 | 0.000008592362 | 0.000000000000 | 0.734690 | 0.265310 |
| 789 | 0.000022178700 | 0.000008009133 | 0.000000000000 | 0.734690 | 0.265310 |
| 790 | 0.000020673830 | 0.000007465700 | 0.000000000000 | 0.734690 | 0.265310 |
| 791 | 0.000019272260 | 0.000006959567 | 0.000000000000 | 0.734690 | 0.265310 |

| Wavelenght $\lambda(\mathrm{nm})$ | CIE 1931 2° colour-matching functions | | | chromaticity coordinates | |
|---|---|---|---|---|---|
| | $\bar{x}(\lambda)$ | $\bar{y}(\lambda)$ | $\bar{z}(\lambda)$ | $x(\lambda)$ | $y(\lambda)$ |
| 792 | 0.000017966400 | 0.000006487995 | 0.000000000000 | 0.734690 | 0.265310 |
| 793 | 0.000016749910 | 0.000006048699 | 0.000000000000 | 0.734690 | 0.265310 |
| 794 | 0.000015616480 | 0.000005639396 | 0.000000000000 | 0.734690 | 0.265310 |
| 795 | 0.000014559770 | 0.000005257800 | 0.000000000000 | 0.734690 | 0.265310 |
| 796 | 0.000013573870 | 0.000004901771 | 0.000000000000 | 0.734690 | 0.265310 |
| 797 | 0.000012654360 | 0.000004569720 | 0.000000000000 | 0.734690 | 0.265310 |
| 798 | 0.000011797230 | 0.000004260194 | 0.000000000000 | 0.734690 | 0.265310 |
| 799 | 0.000010998440 | 0.000003971739 | 0.000000000000 | 0.734690 | 0.265310 |
| 800 | 0.000010253980 | 0.000003702900 | 0.000000000000 | 0.734690 | 0.265310 |
| 801 | 0.000009559646 | 0.000003452163 | 0.000000000000 | 0.734690 | 0.265310 |
| 802 | 0.000008912044 | 0.000003218302 | 0.000000000000 | 0.734690 | 0.265310 |
| 803 | 0.000008308358 | 0.000003000300 | 0.000000000000 | 0.734690 | 0.265310 |
| 804 | 0.000007745769 | 0.000002797139 | 0.000000000000 | 0.734690 | 0.265310 |
| 805 | 0.000007221456 | 0.000002607800 | 0.000000000000 | 0.734690 | 0.265310 |
| 806 | 0.000006732475 | 0.000002431220 | 0.000000000000 | 0.734690 | 0.265310 |
| 807 | 0.000006276423 | 0.000002266531 | 0.000000000000 | 0.734690 | 0.265310 |
| 808 | 0.000005851304 | 0.000002113013 | 0.000000000000 | 0.734690 | 0.265310 |
| 809 | 0.000005455118 | 0.000001969943 | 0.000000000000 | 0.734690 | 0.265310 |
| 810 | 0.000005085868 | 0.000001836600 | 0.000000000000 | 0.734690 | 0.265310 |
| 811 | 0.000004741466 | 0.000001712230 | 0.000000000000 | 0.734690 | 0.265310 |
| 812 | 0.000004420236 | 0.000001596228 | 0.000000000000 | 0.734690 | 0.265310 |
| 813 | 0.000004120783 | 0.000001488090 | 0.000000000000 | 0.734690 | 0.265310 |
| 814 | 0.000003841716 | 0.000001387314 | 0.000000000000 | 0.734690 | 0.265310 |
| 815 | 0.000003581652 | 0.000001293400 | 0.000000000000 | 0.734690 | 0.265310 |
| 816 | 0.000003339127 | 0.000001205820 | 0.000000000000 | 0.734690 | 0.265310 |
| 817 | 0.000003112949 | 0.000001124143 | 0.000000000000 | 0.734690 | 0.265310 |
| 818 | 0.000002902121 | 0.000001048009 | 0.000000000000 | 0.734690 | 0.265310 |
| 819 | 0.000002705645 | 0.000000977058 | 0.000000000000 | 0.734690 | 0.265310 |
| 820 | 0.000002522525 | 0.000000910930 | 0.000000000000 | 0.734690 | 0.265310 |
| 821 | 0.000002351726 | 0.000000849251 | 0.000000000000 | 0.734690 | 0.265310 |
| 822 | 0.000002192415 | 0.000000791721 | 0.000000000000 | 0.734690 | 0.265310 |
| 823 | 0.000002043902 | 0.000000738090 | 0.000000000000 | 0.734690 | 0.265310 |
| 824 | 0.000001905497 | 0.000000688110 | 0.000000000000 | 0.734690 | 0.265310 |
| 825 | 0.000001776509 | 0.000000641530 | 0.000000000000 | 0.734690 | 0.265310 |
| 826 | 0.000001656215 | 0.000000598090 | 0.000000000000 | 0.734690 | 0.265310 |
| 827 | 0.000001544022 | 0.000000557575 | 0.000000000000 | 0.734690 | 0.265310 |
| 828 | 0.000001439440 | 0.000000519808 | 0.000000000000 | 0.734690 | 0.265310 |
| 829 | 0.000001341977 | 0.000000484612 | 0.000000000000 | 0.734690 | 0.265310 |
| 830 | 0.000001251141 | 0.000000451810 | 0.000000000000 | 0.734690 | 0.265310 |

*Table 21: CIE 1931 standard observer properties.*

## A.6. Colour-matching functions and corresponding chromaticity coordinates of the CIE 2015 standard colourimetric system

*CIE cone-fundamental-based spectral tristimulus values for 2 degree field size*, International Commission on Illumination (CIE), 2015. Available at: https://doi.org/10.25039/CIE.DS.548rw69q

| Wavelenght | CIE 2015 2° colour-matching functions | | | chromaticity coordinates | |
|---|---|---|---|---|---|
| $\lambda(\mathrm{nm})$ | $\bar{x}(\lambda)$ | $\bar{y}(\lambda)$ | $\bar{z}(\lambda)$ | $x(\lambda)$ | $y(\lambda)$ |
| 390 | 3.769647E-03 | 4.146161E-04 | 1.847260E-02 | 0.166380 | 0.0182998 |
| 391 | 4.532416E-03 | 5.028333E-04 | 2.221101E-02 | 0.166350 | 0.0184551 |
| 392 | 5.446553E-03 | 6.084991E-04 | 2.669819E-02 | 0.166290 | 0.0185783 |
| 393 | 6.538868E-03 | 7.344436E-04 | 3.206937E-02 | 0.166203 | 0.0186679 |
| 394 | 7.839699E-03 | 8.837389E-04 | 3.847832E-02 | 0.166089 | 0.0187226 |
| 395 | 9.382967E-03 | 1.059646E-03 | 4.609784E-02 | 0.165951 | 0.0187414 |
| 396 | 1.120608E-02 | 1.265532E-03 | 5.511953E-02 | 0.165792 | 0.0187233 |
| 397 | 1.334965E-02 | 1.504753E-03 | 6.575257E-02 | 0.165614 | 0.0186678 |
| 398 | 1.585690E-02 | 1.780493E-03 | 7.822113E-02 | 0.165420 | 0.0185742 |
| 399 | 1.877286E-02 | 2.095572E-03 | 9.276013E-02 | 0.165213 | 0.0184423 |
| 400 | 2.214302E-02 | 2.452194E-03 | 1.096090E-01 | 0.164995 | 0.0182721 |
| 401 | 2.601285E-02 | 2.852216E-03 | 1.290077E-01 | 0.164771 | 0.0180665 |
| 402 | 3.043036E-02 | 3.299115E-03 | 1.512047E-01 | 0.164547 | 0.0178394 |
| 403 | 3.544325E-02 | 3.797466E-03 | 1.764441E-01 | 0.164329 | 0.0176066 |
| 404 | 4.109640E-02 | 4.352768E-03 | 2.049517E-01 | 0.164122 | 0.0173832 |
| 405 | 4.742986E-02 | 4.971717E-03 | 2.369246E-01 | 0.163932 | 0.0171838 |
| 406 | 5.447394E-02 | 5.661014E-03 | 2.725123E-01 | 0.163759 | 0.0170181 |
| 407 | 6.223612E-02 | 6.421615E-03 | 3.117820E-01 | 0.163590 | 0.0168795 |
| 408 | 7.070048E-02 | 7.250312E-03 | 3.547064E-01 | 0.163410 | 0.0167576 |
| 409 | 7.982513E-02 | 8.140173E-03 | 4.011473E-01 | 0.163204 | 0.0166427 |
| 410 | 8.953803E-02 | 9.079860E-03 | 4.508369E-01 | 0.162958 | 0.0165252 |
| 411 | 9.974848E-02 | 1.005608E-02 | 5.034164E-01 | 0.162663 | 0.0163988 |
| 412 | 1.104019E-01 | 1.106456E-02 | 5.586361E-01 | 0.162331 | 0.0162690 |
| 413 | 1.214566E-01 | 1.210522E-02 | 6.162734E-01 | 0.161978 | 0.0161438 |
| 414 | 1.328741E-01 | 1.318014E-02 | 6.760982E-01 | 0.161617 | 0.0160313 |
| 415 | 1.446214E-01 | 1.429377E-02 | 7.378822E-01 | 0.161264 | 0.0159387 |
| 416 | 1.566468E-01 | 1.545004E-02 | 8.013019E-01 | 0.160928 | 0.0158723 |
| 417 | 1.687901E-01 | 1.664093E-02 | 8.655573E-01 | 0.160601 | 0.0158336 |
| 418 | 1.808328E-01 | 1.785302E-02 | 9.295791E-01 | 0.160275 | 0.0158234 |
| 419 | 1.925216E-01 | 1.907018E-02 | 9.921293E-01 | 0.159939 | 0.0158427 |
| 420 | 2.035729E-01 | 2.027369E-02 | 1.051821E+00 | 0.159581 | 0.0158926 |
| 421 | 2.137531E-01 | 2.144805E-02 | 1.107509E+00 | 0.159195 | 0.0159737 |
| 422 | 2.231348E-01 | 2.260041E-02 | 1.159527E+00 | 0.158785 | 0.0160827 |
| 423 | 2.319245E-01 | 2.374789E-02 | 1.208869E+00 | 0.158360 | 0.0162152 |
| 424 | 2.403892E-01 | 2.491247E-02 | 1.256834E+00 | 0.157929 | 0.0163668 |
| 425 | 2.488523E-01 | 2.612106E-02 | 1.305008E+00 | 0.157503 | 0.0165325 |

| Wavelenght $\lambda(\mathrm{nm})$ | CIE 2015 2° colour-matching functions | | | chromaticity coordinates | |
|---|---|---|---|---|---|
| | $\bar{x}(\lambda)$ | $\bar{y}(\lambda)$ | $\bar{z}(\lambda)$ | $x(\lambda)$ | $y(\lambda)$ |
| 426 | 2.575896E-01 | 2.739923E-02 | 1.354758E+00 | 0.157091 | 0.0167094 |
| 427 | 2.664991E-01 | 2.874993E-02 | 1.405594E+00 | 0.156686 | 0.0169033 |
| 428 | 2.753532E-01 | 3.016909E-02 | 1.456414E+00 | 0.156279 | 0.0171227 |
| 429 | 2.838921E-01 | 3.165145E-02 | 1.505960E+00 | 0.155856 | 0.0173766 |
| 430 | 2.918246E-01 | 3.319038E-02 | 1.552826E+00 | 0.155404 | 0.0176748 |
| 431 | 2.989200E-01 | 3.477912E-02 | 1.595902E+00 | 0.154913 | 0.0180240 |
| 432 | 3.052993E-01 | 3.641495E-02 | 1.635768E+00 | 0.154388 | 0.0184148 |
| 433 | 3.112031E-01 | 3.809569E-02 | 1.673573E+00 | 0.153842 | 0.0188325 |
| 434 | 3.169047E-01 | 3.981843E-02 | 1.710604E+00 | 0.153292 | 0.0192608 |
| 435 | 3.227087E-01 | 4.157940E-02 | 1.748280E+00 | 0.152757 | 0.0196819 |
| 436 | 3.288194E-01 | 4.337098E-02 | 1.787504E+00 | 0.152253 | 0.0200820 |
| 437 | 3.349242E-01 | 4.517180E-02 | 1.826609E+00 | 0.151776 | 0.0204702 |
| 438 | 3.405452E-01 | 4.695420E-02 | 1.863108E+00 | 0.151313 | 0.0208629 |
| 439 | 3.451688E-01 | 4.868718E-02 | 1.894332E+00 | 0.150848 | 0.0212776 |
| 440 | 3.482554E-01 | 5.033657E-02 | 1.917479E+00 | 0.150365 | 0.0217336 |
| 441 | 3.494153E-01 | 5.187611E-02 | 1.930529E+00 | 0.149847 | 0.0222470 |
| 442 | 3.489075E-01 | 5.332218E-02 | 1.934819E+00 | 0.149294 | 0.0228160 |
| 443 | 3.471746E-01 | 5.470603E-02 | 1.932650E+00 | 0.148713 | 0.0234334 |
| 444 | 3.446705E-01 | 5.606335E-02 | 1.926395E+00 | 0.148110 | 0.0240912 |
| 445 | 3.418483E-01 | 5.743393E-02 | 1.918437E+00 | 0.147493 | 0.0247804 |
| 446 | 3.390240E-01 | 5.885107E-02 | 1.910430E+00 | 0.146871 | 0.0254954 |
| 447 | 3.359926E-01 | 6.030809E-02 | 1.901224E+00 | 0.146241 | 0.0262492 |
| 448 | 3.324276E-01 | 6.178644E-02 | 1.889000E+00 | 0.145596 | 0.0270612 |
| 449 | 3.280157E-01 | 6.326570E-02 | 1.871996E+00 | 0.144930 | 0.0279531 |
| 450 | 3.224637E-01 | 6.472352E-02 | 1.848545E+00 | 0.144232 | 0.0289496 |
| 451 | 3.156225E-01 | 6.614749E-02 | 1.817792E+00 | 0.143493 | 0.0300730 |
| 452 | 3.078201E-01 | 6.757256E-02 | 1.781627E+00 | 0.142706 | 0.0313268 |
| 453 | 2.994771E-01 | 6.904928E-02 | 1.742514E+00 | 0.141862 | 0.0327086 |
| 454 | 2.909776E-01 | 7.063280E-02 | 1.702749E+00 | 0.140953 | 0.0342154 |
| 455 | 2.826646E-01 | 7.238339E-02 | 1.664439E+00 | 0.139969 | 0.0358425 |
| 456 | 2.747962E-01 | 7.435960E-02 | 1.629207E+00 | 0.138901 | 0.0375864 |
| 457 | 2.674312E-01 | 7.659383E-02 | 1.597360E+00 | 0.137753 | 0.0394532 |
| 458 | 2.605847E-01 | 7.911436E-02 | 1.568896E+00 | 0.136532 | 0.0414516 |
| 459 | 2.542749E-01 | 8.195345E-02 | 1.543823E+00 | 0.135249 | 0.0435911 |
| 460 | 2.485254E-01 | 8.514816E-02 | 1.522157E+00 | 0.133916 | 0.0458814 |
| 461 | 2.433039E-01 | 8.872657E-02 | 1.503611E+00 | 0.132544 | 0.0483355 |
| 462 | 2.383414E-01 | 9.266008E-02 | 1.486673E+00 | 0.131124 | 0.0509773 |
| 463 | 2.333253E-01 | 9.689723E-02 | 1.469595E+00 | 0.129638 | 0.0538373 |
| 464 | 2.279619E-01 | 1.013746E-01 | 1.450709E+00 | 0.128065 | 0.0569506 |
| 465 | 2.219781E-01 | 1.060145E-01 | 1.428440E+00 | 0.126380 | 0.0603579 |
| 466 | 2.151735E-01 | 1.107377E-01 | 1.401587E+00 | 0.124558 | 0.0641029 |
| 467 | 2.075619E-01 | 1.155111E-01 | 1.370094E+00 | 0.122588 | 0.0682219 |
| 468 | 1.992183E-01 | 1.203122E-01 | 1.334220E+00 | 0.120465 | 0.0727511 |
| 469 | 1.902290E-01 | 1.251161E-01 | 1.294275E+00 | 0.118183 | 0.0777302 |

| Wavelenght $\lambda(\mathrm{nm})$ | CIE 2015 2° colour-matching functions | | | chromaticity coordinates | |
|---|---|---|---|---|---|
| | $\bar{x}(\lambda)$ | $\bar{y}(\lambda)$ | $\bar{z}(\lambda)$ | $x(\lambda)$ | $y(\lambda)$ |
| 470 | 1.806905E-01 | 1.298957E-01 | 1.250610E+00 | 0.115738 | 0.0832027 |
| 471 | 1.707154E-01 | 1.346299E-01 | 1.203696E+00 | 0.113128 | 0.0892155 |
| 472 | 1.604471E-01 | 1.393309E-01 | 1.154316E+00 | 0.110342 | 0.0958197 |
| 473 | 1.500244E-01 | 1.440235E-01 | 1.103284E+00 | 0.107365 | 0.103070 |
| 474 | 1.395705E-01 | 1.487372E-01 | 1.051347E+00 | 0.104184 | 0.111027 |
| 475 | 1.291920E-01 | 1.535066E-01 | 9.991789E-01 | 0.100783 | 0.119751 |
| 476 | 1.189859E-01 | 1.583644E-01 | 9.473958E-01 | 0.0971515 | 0.129304 |
| 477 | 1.090615E-01 | 1.633199E-01 | 8.966222E-01 | 0.0932944 | 0.139709 |
| 478 | 9.951424E-02 | 1.683761E-01 | 8.473981E-01 | 0.0892274 | 0.150971 |
| 479 | 9.041850E-02 | 1.735365E-01 | 8.001576E-01 | 0.0849708 | 0.163081 |
| 480 | 8.182895E-02 | 1.788048E-01 | 7.552379E-01 | 0.0805505 | 0.176011 |
| 481 | 7.376817E-02 | 1.841819E-01 | 7.127879E-01 | 0.0759918 | 0.189734 |
| 482 | 6.619477E-02 | 1.896559E-01 | 6.725198E-01 | 0.0713021 | 0.204289 |
| 483 | 5.906380E-02 | 1.952101E-01 | 6.340976E-01 | 0.0664855 | 0.219739 |
| 484 | 5.234242E-02 | 2.008259E-01 | 5.972433E-01 | 0.0615495 | 0.236151 |
| 485 | 4.600865E-02 | 2.064828E-01 | 5.617313E-01 | 0.0565062 | 0.253595 |
| 486 | 4.006154E-02 | 2.121826E-01 | 5.274921E-01 | 0.0513783 | 0.272121 |
| 487 | 3.454373E-02 | 2.180279E-01 | 4.948809E-01 | 0.0462153 | 0.291695 |
| 488 | 2.949091E-02 | 2.241586E-01 | 4.642586E-01 | 0.0410789 | 0.312239 |
| 489 | 2.492140E-02 | 2.307302E-01 | 4.358841E-01 | 0.0360378 | 0.333649 |
| 490 | 2.083981E-02 | 2.379160E-01 | 4.099313E-01 | 0.0311653 | 0.355796 |
| 491 | 1.723591E-02 | 2.458706E-01 | 3.864261E-01 | 0.0265359 | 0.378535 |
| 492 | 1.407924E-02 | 2.546023E-01 | 3.650566E-01 | 0.0222162 | 0.401747 |
| 493 | 1.134516E-02 | 2.640760E-01 | 3.454812E-01 | 0.0182721 | 0.425310 |
| 494 | 9.019658E-03 | 2.742490E-01 | 3.274095E-01 | 0.0147699 | 0.449089 |
| 495 | 7.097731E-03 | 2.850680E-01 | 3.105939E-01 | 0.0117754 | 0.472938 |
| 496 | 5.571145E-03 | 2.964837E-01 | 2.948102E-01 | 0.00933401 | 0.496735 |
| 497 | 4.394566E-03 | 3.085010E-01 | 2.798194E-01 | 0.00741430 | 0.520488 |
| 498 | 3.516303E-03 | 3.211393E-01 | 2.654100E-01 | 0.00595917 | 0.544243 |
| 499 | 2.887638E-03 | 3.344175E-01 | 2.514084E-01 | 0.00490500 | 0.568048 |
| 500 | 2.461588E-03 | 3.483536E-01 | 2.376753E-01 | 0.00418288 | 0.591944 |
| 501 | 2.206348E-03 | 3.629601E-01 | 2.241211E-01 | 0.00374409 | 0.615930 |
| 502 | 2.149559E-03 | 3.782275E-01 | 2.107484E-01 | 0.00363638 | 0.639843 |
| 503 | 2.337091E-03 | 3.941359E-01 | 1.975839E-01 | 0.00393412 | 0.663465 |
| 504 | 2.818931E-03 | 4.106582E-01 | 1.846574E-01 | 0.00471287 | 0.686565 |
| 505 | 3.649178E-03 | 4.277595E-01 | 1.720018E-01 | 0.00604759 | 0.708903 |
| 506 | 4.891359E-03 | 4.453993E-01 | 1.596918E-01 | 0.00801885 | 0.730184 |
| 507 | 6.629364E-03 | 4.635396E-01 | 1.479415E-01 | 0.0107252 | 0.749930 |
| 508 | 8.942902E-03 | 4.821376E-01 | 1.369428E-01 | 0.0142398 | 0.767707 |
| 509 | 1.190224E-02 | 5.011430E-01 | 1.268279E-01 | 0.0186009 | 0.783191 |
| 510 | 1.556989E-02 | 5.204972E-01 | 1.176796E-01 | 0.0238164 | 0.796176 |
| 511 | 1.997668E-02 | 5.401387E-01 | 1.094970E-01 | 0.0298332 | 0.806644 |
| 512 | 2.504698E-02 | 5.600208E-01 | 1.020943E-01 | 0.0364499 | 0.814976 |
| 513 | 3.067530E-02 | 5.800972E-01 | 9.527993E-02 | 0.0434462 | 0.821606 |

| Wavelenght $\lambda(\mathrm{nm})$ | CIE 2015 2° colour-matching functions | | | chromaticity coordinates | |
|---|---|---|---|---|---|
| | $\bar{x}(\lambda)$ | $\bar{y}(\lambda)$ | $\bar{z}(\lambda)$ | $x(\lambda)$ | $y(\lambda)$ |
| 514 | 3.674999E-02 | 6.003172E-01 | 8.890075E-02 | 0.0506221 | 0.826920 |
| 515 | 4.315171E-02 | 6.206256E-01 | 8.283548E-02 | 0.0577966 | 0.831255 |
| 516 | 4.978584E-02 | 6.409398E-01 | 7.700982E-02 | 0.0648476 | 0.834845 |
| 517 | 5.668554E-02 | 6.610772E-01 | 7.144001E-02 | 0.0718263 | 0.837652 |
| 518 | 6.391651E-02 | 6.808134E-01 | 6.615436E-02 | 0.0788232 | 0.839594 |
| 519 | 7.154352E-02 | 6.999044E-01 | 6.117199E-02 | 0.0859258 | 0.840605 |
| 520 | 7.962917E-02 | 7.180890E-01 | 5.650407E-02 | 0.0932183 | 0.840635 |
| 521 | 8.821473E-02 | 7.351593E-01 | 5.215121E-02 | 0.100756 | 0.839678 |
| 522 | 9.726978E-02 | 7.511821E-01 | 4.809566E-02 | 0.108494 | 0.837861 |
| 523 | 1.067504E-01 | 7.663143E-01 | 4.431720E-02 | 0.116364 | 0.835327 |
| 524 | 1.166192E-01 | 7.807352E-01 | 4.079734E-02 | 0.124307 | 0.832206 |
| 525 | 1.268468E-01 | 7.946448E-01 | 3.751912E-02 | 0.132268 | 0.828609 |
| 526 | 1.374060E-01 | 8.082074E-01 | 3.446846E-02 | 0.140198 | 0.824633 |
| 527 | 1.482471E-01 | 8.213817E-01 | 3.163764E-02 | 0.148060 | 0.820343 |
| 528 | 1.593076E-01 | 8.340701E-01 | 2.901901E-02 | 0.155818 | 0.815799 |
| 529 | 1.705181E-01 | 8.461711E-01 | 2.660364E-02 | 0.163442 | 0.811058 |
| 530 | 1.818026E-01 | 8.575799E-01 | 2.438164E-02 | 0.170905 | 0.806175 |
| 531 | 1.931090E-01 | 8.682408E-01 | 2.234097E-02 | 0.178196 | 0.801189 |
| 532 | 2.045085E-01 | 8.783061E-01 | 2.046415E-02 | 0.185364 | 0.796087 |
| 533 | 2.161166E-01 | 8.879907E-01 | 1.873456E-02 | 0.192473 | 0.790842 |
| 534 | 2.280650E-01 | 8.975211E-01 | 1.713788E-02 | 0.199580 | 0.785422 |
| 535 | 2.405015E-01 | 9.071347E-01 | 1.566174E-02 | 0.206741 | 0.779796 |
| 536 | 2.535441E-01 | 9.169947E-01 | 1.429644E-02 | 0.213991 | 0.773943 |
| 537 | 2.671300E-01 | 9.269295E-01 | 1.303702E-02 | 0.221300 | 0.767900 |
| 538 | 2.811351E-01 | 9.366731E-01 | 1.187897E-02 | 0.228623 | 0.761717 |
| 539 | 2.954164E-01 | 9.459482E-01 | 1.081725E-02 | 0.235921 | 0.755440 |
| 540 | 3.098117E-01 | 9.544675E-01 | 9.846470E-03 | 0.243156 | 0.749116 |
| 541 | 3.241678E-01 | 9.619834E-01 | 8.960687E-03 | 0.250301 | 0.742780 |
| 542 | 3.384319E-01 | 9.684390E-01 | 8.152811E-03 | 0.257358 | 0.736442 |
| 543 | 3.525786E-01 | 9.738289E-01 | 7.416025E-03 | 0.264337 | 0.730103 |
| 544 | 3.665839E-01 | 9.781519E-01 | 6.744115E-03 | 0.271246 | 0.723764 |
| 545 | 3.804244E-01 | 9.814106E-01 | 6.131421E-03 | 0.278095 | 0.717423 |
| 546 | 3.940988E-01 | 9.836669E-01 | 5.572778E-03 | 0.284890 | 0.711082 |
| 547 | 4.076972E-01 | 9.852081E-01 | 5.063463E-03 | 0.291635 | 0.704743 |
| 548 | 4.213484E-01 | 9.863813E-01 | 4.599169E-03 | 0.298336 | 0.698408 |
| 549 | 4.352003E-01 | 9.875357E-01 | 4.175971E-03 | 0.304994 | 0.692079 |
| 550 | 4.494206E-01 | 9.890228E-01 | 3.790291E-03 | 0.311614 | 0.685758 |
| 551 | 4.641616E-01 | 9.910811E-01 | 3.438952E-03 | 0.318206 | 0.679436 |
| 552 | 4.794395E-01 | 9.934913E-01 | 3.119341E-03 | 0.324812 | 0.673074 |
| 553 | 4.952180E-01 | 9.959172E-01 | 2.829038E-03 | 0.331479 | 0.666627 |
| 554 | 5.114395E-01 | 9.980205E-01 | 2.565722E-03 | 0.338248 | 0.660055 |
| 555 | 5.280233E-01 | 9.994608E-01 | 2.327186E-03 | 0.345156 | 0.653323 |
| 556 | 5.448696E-01 | 9.999930E-01 | 2.111280E-03 | 0.352216 | 0.646419 |
| 557 | 5.618898E-01 | 9.997557E-01 | 1.915766E-03 | 0.359365 | 0.639409 |

| Wavelenght $\lambda(\mathrm{nm})$ | CIE 2015 2° colour-matching functions | | | chromaticity coordinates | |
|---|---|---|---|---|---|
| | $\bar{x}(\lambda)$ | $\bar{y}(\lambda)$ | $\bar{z}(\lambda)$ | $x(\lambda)$ | $y(\lambda)$ |
| 558 | 5.790137E-01 | 9.989839E-01 | 1.738589E-03 | 0.366526 | 0.632374 |
| 559 | 5.961882E-01 | 9.979123E-01 | 1.577920E-03 | 0.373627 | 0.625384 |
| 560 | 6.133784E-01 | 9.967737E-01 | 1.432128E-03 | 0.380606 | 0.618505 |
| 561 | 6.305897E-01 | 9.957356E-01 | 1.299781E-03 | 0.387429 | 0.611772 |
| 562 | 6.479223E-01 | 9.947115E-01 | 1.179667E-03 | 0.394158 | 0.605124 |
| 563 | 6.654866E-01 | 9.935534E-01 | 1.070694E-03 | 0.400869 | 0.598486 |
| 564 | 6.833782E-01 | 9.921156E-01 | 9.718623E-04 | 0.407630 | 0.591790 |
| 565 | 7.016774E-01 | 9.902549E-01 | 8.822531E-04 | 0.414503 | 0.584975 |
| 566 | 7.204110E-01 | 9.878596E-01 | 8.010231E-04 | 0.421522 | 0.578009 |
| 567 | 7.394495E-01 | 9.849324E-01 | 7.273884E-04 | 0.428639 | 0.570939 |
| 568 | 7.586285E-01 | 9.815036E-01 | 6.606347E-04 | 0.435795 | 0.563826 |
| 569 | 7.777885E-01 | 9.776035E-01 | 6.001146E-04 | 0.442934 | 0.556724 |
| 570 | 7.967750E-01 | 9.732611E-01 | 5.452416E-04 | 0.450008 | 0.549684 |
| 571 | 8.154530E-01 | 9.684764E-01 | 4.954847E-04 | 0.456984 | 0.542739 |
| 572 | 8.337389E-01 | 9.631369E-01 | 4.503642E-04 | 0.463877 | 0.535872 |
| 573 | 8.515493E-01 | 9.571062E-01 | 4.094455E-04 | 0.470712 | 0.529061 |
| 574 | 8.687862E-01 | 9.502540E-01 | 3.723345E-04 | 0.477509 | 0.522286 |
| 575 | 8.853376E-01 | 9.424569E-01 | 3.386739E-04 | 0.484285 | 0.515530 |
| 576 | 9.011588E-01 | 9.336897E-01 | 3.081396E-04 | 0.491053 | 0.508779 |
| 577 | 9.165278E-01 | 9.242893E-01 | 2.804370E-04 | 0.497816 | 0.502032 |
| 578 | 9.318245E-01 | 9.146707E-01 | 2.552996E-04 | 0.504575 | 0.495287 |
| 579 | 9.474524E-01 | 9.052333E-01 | 2.324859E-04 | 0.511330 | 0.488545 |
| 580 | 9.638388E-01 | 8.963613E-01 | 2.117772E-04 | 0.518078 | 0.481808 |
| 581 | 9.812596E-01 | 8.883069E-01 | 1.929758E-04 | 0.524805 | 0.475092 |
| 582 | 9.992953E-01 | 8.808462E-01 | 1.759024E-04 | 0.531450 | 0.468456 |
| 583 | 1.017343E+00 | 8.736445E-01 | 1.603947E-04 | 0.537950 | 0.461965 |
| 584 | 1.034790E+00 | 8.663755E-01 | 1.463059E-04 | 0.544251 | 0.455672 |
| 585 | 1.051011E+00 | 8.587203E-01 | 1.335031E-04 | 0.550306 | 0.449624 |
| 586 | 1.065522E+00 | 8.504295E-01 | 1.218660E-04 | 0.556097 | 0.443840 |
| 587 | 1.078421E+00 | 8.415047E-01 | 1.112857E-04 | 0.561667 | 0.438275 |
| 588 | 1.089944E+00 | 8.320109E-01 | 1.016634E-04 | 0.567072 | 0.432875 |
| 589 | 1.100320E+00 | 8.220154E-01 | 9.291003E-05 | 0.572359 | 0.427592 |
| 590 | 1.109767E+00 | 8.115868E-01 | 8.494468E-05 | 0.577571 | 0.422385 |
| 591 | 1.118438E+00 | 8.007874E-01 | 7.769425E-05 | 0.582731 | 0.417228 |
| 592 | 1.126266E+00 | 7.896515E-01 | 7.109247E-05 | 0.587825 | 0.412138 |
| 593 | 1.133138E+00 | 7.782053E-01 | 6.507936E-05 | 0.592829 | 0.407137 |
| 594 | 1.138952E+00 | 7.664733E-01 | 5.960061E-05 | 0.597723 | 0.402246 |
| 595 | 1.143620E+00 | 7.544785E-01 | 5.460706E-05 | 0.602491 | 0.397480 |
| 596 | 1.147095E+00 | 7.422473E-01 | 5.005417E-05 | 0.607124 | 0.392850 |
| 597 | 1.149464E+00 | 7.298229E-01 | 4.590157E-05 | 0.611634 | 0.388341 |
| 598 | 1.150838E+00 | 7.172525E-01 | 4.211268E-05 | 0.616037 | 0.383941 |
| 599 | 1.151326E+00 | 7.045818E-01 | 3.865437E-05 | 0.620344 | 0.379635 |
| 600 | 1.151033E+00 | 6.918553E-01 | 3.549661E-05 | 0.624569 | 0.375412 |
| 601 | 1.150002E+00 | 6.791009E-01 | 3.261220E-05 | 0.628713 | 0.371269 |

| Wavelenght $\lambda(\mathrm{nm})$ | CIE 2015 2° colour-matching functions | | | chromaticity coordinates | |
|---|---|---|---|---|---|
| | $\bar{x}(\lambda)$ | $\bar{y}(\lambda)$ | $\bar{z}(\lambda)$ | $x(\lambda)$ | $y(\lambda)$ |
| 602 | 1.148061E+00 | 6.662846E-01 | 2.997643E-05 | 0.632758 | 0.367225 |
| 603 | 1.144998E+00 | 6.533595E-01 | 2.756693E-05 | 0.636681 | 0.363303 |
| 604 | 1.140622E+00 | 6.402807E-01 | 2.536339E-05 | 0.640465 | 0.359521 |
| 605 | 1.134757E+00 | 6.270066E-01 | 2.334738E-05 | 0.644094 | 0.355892 |
| 606 | 1.127298E+00 | 6.135148E-01 | 2.150221E-05 | 0.647562 | 0.352426 |
| 607 | 1.118342E+00 | 5.998494E-01 | 1.981268E-05 | 0.650876 | 0.349113 |
| 608 | 1.108033E+00 | 5.860682E-01 | 1.826500E-05 | 0.654047 | 0.345943 |
| 609 | 1.096515E+00 | 5.722261E-01 | 1.684667E-05 | 0.657085 | 0.342905 |
| 610 | 1.083928E+00 | 5.583746E-01 | 1.554631E-05 | 0.659999 | 0.339992 |
| 611 | 1.070387E+00 | 5.445535E-01 | 1.435360E-05 | 0.662797 | 0.337194 |
| 612 | 1.055934E+00 | 5.307673E-01 | 1.325915E-05 | 0.665485 | 0.334507 |
| 613 | 1.040592E+00 | 5.170130E-01 | 1.225443E-05 | 0.668067 | 0.331926 |
| 614 | 1.024385E+00 | 5.032889E-01 | 1.133169E-05 | 0.670547 | 0.329445 |
| 615 | 1.007344E+00 | 4.895950E-01 | 1.048387E-05 | 0.672931 | 0.327062 |
| 616 | 9.895268E-01 | 4.759442E-01 | 0.000000E+00 | 0.675228 | 0.324772 |
| 617 | 9.711213E-01 | 4.623958E-01 | 0.000000E+00 | 0.677440 | 0.322560 |
| 618 | 9.523257E-01 | 4.490154E-01 | 0.000000E+00 | 0.679582 | 0.320418 |
| 619 | 9.333248E-01 | 4.358622E-01 | 0.000000E+00 | 0.681663 | 0.318337 |
| 620 | 9.142877E-01 | 4.229897E-01 | 0.000000E+00 | 0.683693 | 0.316307 |
| 621 | 8.952798E-01 | 4.104152E-01 | 0.000000E+00 | 0.685673 | 0.314327 |
| 622 | 8.760157E-01 | 3.980356E-01 | 0.000000E+00 | 0.687583 | 0.312417 |
| 623 | 8.561607E-01 | 3.857300E-01 | 0.000000E+00 | 0.689401 | 0.310599 |
| 624 | 8.354235E-01 | 3.733907E-01 | 0.000000E+00 | 0.691110 | 0.308890 |
| 625 | 8.135565E-01 | 3.609245E-01 | 0.000000E+00 | 0.692694 | 0.307306 |
| 626 | 7.904565E-01 | 3.482860E-01 | 0.000000E+00 | 0.694149 | 0.305851 |
| 627 | 7.664364E-01 | 3.355702E-01 | 0.000000E+00 | 0.695492 | 0.304508 |
| 628 | 7.418777E-01 | 3.228963E-01 | 0.000000E+00 | 0.696747 | 0.303253 |
| 629 | 7.171219E-01 | 3.103704E-01 | 0.000000E+00 | 0.697934 | 0.302066 |
| 630 | 6.924717E-01 | 2.980865E-01 | 0.000000E+00 | 0.699072 | 0.300928 |
| 631 | 6.681600E-01 | 2.861160E-01 | 0.000000E+00 | 0.700175 | 0.299825 |
| 632 | 6.442697E-01 | 2.744822E-01 | 0.000000E+00 | 0.701244 | 0.298756 |
| 633 | 6.208450E-01 | 2.631953E-01 | 0.000000E+00 | 0.702281 | 0.297719 |
| 634 | 5.979243E-01 | 2.522628E-01 | 0.000000E+00 | 0.703286 | 0.296714 |
| 635 | 5.755410E-01 | 2.416902E-01 | 0.000000E+00 | 0.704257 | 0.295743 |
| 636 | 5.537296E-01 | 2.314809E-01 | 0.000000E+00 | 0.705199 | 0.294801 |
| 637 | 5.325412E-01 | 2.216378E-01 | 0.000000E+00 | 0.706120 | 0.293880 |
| 638 | 5.120218E-01 | 2.121622E-01 | 0.000000E+00 | 0.707033 | 0.292967 |
| 639 | 4.922070E-01 | 2.030542E-01 | 0.000000E+00 | 0.707945 | 0.292055 |
| 640 | 4.731224E-01 | 1.943124E-01 | 0.000000E+00 | 0.708867 | 0.291133 |
| 641 | 4.547417E-01 | 1.859227E-01 | 0.000000E+00 | 0.709797 | 0.290203 |
| 642 | 4.368719E-01 | 1.778274E-01 | 0.000000E+00 | 0.710708 | 0.289292 |
| 643 | 4.193121E-01 | 1.699654E-01 | 0.000000E+00 | 0.711570 | 0.288430 |
| 644 | 4.018980E-01 | 1.622841E-01 | 0.000000E+00 | 0.712355 | 0.287645 |
| 645 | 3.844986E-01 | 1.547397E-01 | 0.000000E+00 | 0.713040 | 0.286960 |

| Wavelenght $\lambda(\mathrm{nm})$ | CIE 2015 2° colour-matching functions | | | chromaticity coordinates | |
|---|---|---|---|---|---|
| | $\bar{x}(\lambda)$ | $\bar{y}(\lambda)$ | $\bar{z}(\lambda)$ | $x(\lambda)$ | $y(\lambda)$ |
| 646 | 3.670592E-01 | 1.473081E-01 | 0.000000E+00 | 0.713613 | 0.286387 |
| 647 | 3.497167E-01 | 1.400169E-01 | 0.000000E+00 | 0.714096 | 0.285904 |
| 648 | 3.326305E-01 | 1.329013E-01 | 0.000000E+00 | 0.714517 | 0.285483 |
| 649 | 3.159341E-01 | 1.259913E-01 | 0.000000E+00 | 0.714904 | 0.285096 |
| 650 | 2.997374E-01 | 1.193120E-01 | 0.000000E+00 | 0.715279 | 0.284721 |
| 651 | 2.841189E-01 | 1.128820E-01 | 0.000000E+00 | 0.715663 | 0.284337 |
| 652 | 2.691053E-01 | 1.067113E-01 | 0.000000E+00 | 0.716055 | 0.283945 |
| 653 | 2.547077E-01 | 1.008052E-01 | 0.000000E+00 | 0.716451 | 0.283549 |
| 654 | 2.409319E-01 | 9.516653E-02 | 0.000000E+00 | 0.716849 | 0.283151 |
| 655 | 2.277792E-01 | 8.979594E-02 | 0.000000E+00 | 0.717245 | 0.282755 |
| 656 | 2.152431E-01 | 8.469044E-02 | 0.000000E+00 | 0.717636 | 0.282364 |
| 657 | 2.033010E-01 | 7.984009E-02 | 0.000000E+00 | 0.718020 | 0.281980 |
| 658 | 1.919276E-01 | 7.523372E-02 | 0.000000E+00 | 0.718396 | 0.281604 |
| 659 | 1.810987E-01 | 7.086061E-02 | 0.000000E+00 | 0.718762 | 0.281238 |
| 660 | 1.707914E-01 | 6.671045E-02 | 0.000000E+00 | 0.719116 | 0.280884 |
| 661 | 1.609842E-01 | 6.277360E-02 | 0.000000E+00 | 0.719457 | 0.280543 |
| 662 | 1.516577E-01 | 5.904179E-02 | 0.000000E+00 | 0.719782 | 0.280218 |
| 663 | 1.427936E-01 | 5.550703E-02 | 0.000000E+00 | 0.720086 | 0.279914 |
| 664 | 1.343737E-01 | 5.216139E-02 | 0.000000E+00 | 0.720367 | 0.279633 |
| 665 | 1.263808E-01 | 4.899699E-02 | 0.000000E+00 | 0.720620 | 0.279380 |
| 666 | 1.187979E-01 | 4.600578E-02 | 0.000000E+00 | 0.720845 | 0.279155 |
| 667 | 1.116088E-01 | 4.317885E-02 | 0.000000E+00 | 0.721045 | 0.278955 |
| 668 | 1.047975E-01 | 4.050755E-02 | 0.000000E+00 | 0.721224 | 0.278776 |
| 669 | 9.834835E-02 | 3.798376E-02 | 0.000000E+00 | 0.721388 | 0.278612 |
| 670 | 9.224597E-02 | 3.559982E-02 | 0.000000E+00 | 0.721541 | 0.278459 |
| 671 | 8.647506E-02 | 3.334856E-02 | 0.000000E+00 | 0.721686 | 0.278314 |
| 672 | 8.101986E-02 | 3.122332E-02 | 0.000000E+00 | 0.721824 | 0.278176 |
| 673 | 7.586514E-02 | 2.921780E-02 | 0.000000E+00 | 0.721955 | 0.278045 |
| 674 | 7.099633E-02 | 2.732601E-02 | 0.000000E+00 | 0.722077 | 0.277923 |
| 675 | 6.639960E-02 | 2.554223E-02 | 0.000000E+00 | 0.722191 | 0.277809 |
| 676 | 6.206225E-02 | 2.386121E-02 | 0.000000E+00 | 0.722297 | 0.277703 |
| 677 | 5.797409E-02 | 2.227859E-02 | 0.000000E+00 | 0.722394 | 0.277606 |
| 678 | 5.412533E-02 | 2.079020E-02 | 0.000000E+00 | 0.722485 | 0.277515 |
| 679 | 5.050600E-02 | 1.939185E-02 | 0.000000E+00 | 0.722569 | 0.277431 |
| 680 | 4.710606E-02 | 1.807939E-02 | 0.000000E+00 | 0.722647 | 0.277353 |
| 681 | 4.391411E-02 | 1.684817E-02 | 0.000000E+00 | 0.722720 | 0.277280 |
| 682 | 4.091411E-02 | 1.569188E-02 | 0.000000E+00 | 0.722788 | 0.277212 |
| 683 | 3.809067E-02 | 1.460446E-02 | 0.000000E+00 | 0.722850 | 0.277150 |
| 684 | 3.543034E-02 | 1.358062E-02 | 0.000000E+00 | 0.722906 | 0.277094 |
| 685 | 3.292138E-02 | 1.261573E-02 | 0.000000E+00 | 0.722957 | 0.277043 |
| 686 | 3.055672E-02 | 1.170696E-02 | 0.000000E+00 | 0.723002 | 0.276998 |
| 687 | 2.834146E-02 | 1.085608E-02 | 0.000000E+00 | 0.723042 | 0.276958 |
| 688 | 2.628033E-02 | 1.006476E-02 | 0.000000E+00 | 0.723078 | 0.276922 |
| 689 | 2.437465E-02 | 9.333376E-03 | 0.000000E+00 | 0.723111 | 0.276889 |

| Wavelenght $\lambda(\mathrm{nm})$ | CIE 2015 2° colour-matching functions | | | chromaticity coordinates | |
|---|---|---|---|---|---|
| | $\bar{x}(\lambda)$ | $\bar{y}(\lambda)$ | $\bar{z}(\lambda)$ | $x(\lambda)$ | $y(\lambda)$ |
| 690 | 2.262306E-02 | 8.661284E-03 | 0.000000E+00 | 0.723143 | 0.276857 |
| 691 | 2.101935E-02 | 8.046048E-03 | 0.000000E+00 | 0.723174 | 0.276826 |
| 692 | 1.954647E-02 | 7.481130E-03 | 0.000000E+00 | 0.723204 | 0.276796 |
| 693 | 1.818727E-02 | 6.959987E-03 | 0.000000E+00 | 0.723231 | 0.276769 |
| 694 | 1.692727E-02 | 6.477070E-03 | 0.000000E+00 | 0.723253 | 0.276747 |
| 695 | 1.575417E-02 | 6.027677E-03 | 0.000000E+00 | 0.723271 | 0.276729 |
| 696 | 1.465854E-02 | 5.608169E-03 | 0.000000E+00 | 0.723282 | 0.276718 |
| 697 | 1.363571E-02 | 5.216691E-03 | 0.000000E+00 | 0.723288 | 0.276712 |
| 698 | 1.268205E-02 | 4.851785E-03 | 0.000000E+00 | 0.723290 | 0.276710 |
| 699 | 1.179394E-02 | 4.512008E-03 | 0.000000E+00 | 0.723291 | 0.276709 |
| 700 | 1.096778E-02 | 4.195941E-03 | 0.000000E+00 | 0.723291 | 0.276709 |
| 701 | 1.019964E-02 | 3.902057E-03 | 0.000000E+00 | 0.723292 | 0.276708 |
| 702 | 9.484317E-03 | 3.628371E-03 | 0.000000E+00 | 0.723293 | 0.276707 |
| 703 | 8.816851E-03 | 3.373005E-03 | 0.000000E+00 | 0.723294 | 0.276706 |
| 704 | 8.192921E-03 | 3.134315E-03 | 0.000000E+00 | 0.723294 | 0.276706 |
| 705 | 7.608750E-03 | 2.910864E-03 | 0.000000E+00 | 0.723292 | 0.276708 |
| 706 | 7.061391E-03 | 2.701528E-03 | 0.000000E+00 | 0.723287 | 0.276713 |
| 707 | 6.549509E-03 | 2.505796E-03 | 0.000000E+00 | 0.723279 | 0.276721 |
| 708 | 6.071970E-03 | 2.323231E-03 | 0.000000E+00 | 0.723267 | 0.276733 |
| 709 | 5.627476E-03 | 2.153333E-03 | 0.000000E+00 | 0.723251 | 0.276749 |
| 710 | 5.214608E-03 | 1.995557E-03 | 0.000000E+00 | 0.723230 | 0.276770 |
| 711 | 4.831848E-03 | 1.849316E-03 | 0.000000E+00 | 0.723205 | 0.276795 |
| 712 | 4.477579E-03 | 1.713976E-03 | 0.000000E+00 | 0.723175 | 0.276825 |
| 713 | 4.150166E-03 | 1.588899E-03 | 0.000000E+00 | 0.723143 | 0.276857 |
| 714 | 3.847988E-03 | 1.473453E-03 | 0.000000E+00 | 0.723110 | 0.276890 |
| 715 | 3.569452E-03 | 1.367022E-03 | 0.000000E+00 | 0.723077 | 0.276923 |
| 716 | 3.312857E-03 | 1.268954E-03 | 0.000000E+00 | 0.723045 | 0.276955 |
| 717 | 3.076022E-03 | 1.178421E-03 | 0.000000E+00 | 0.723014 | 0.276986 |
| 718 | 2.856894E-03 | 1.094644E-03 | 0.000000E+00 | 0.722983 | 0.277017 |
| 719 | 2.653681E-03 | 1.016943E-03 | 0.000000E+00 | 0.722951 | 0.277049 |
| 720 | 2.464821E-03 | 9.447269E-04 | 0.000000E+00 | 0.722917 | 0.277083 |
| 721 | 2.289060E-03 | 8.775171E-04 | 0.000000E+00 | 0.722881 | 0.277119 |
| 722 | 2.125694E-03 | 8.150438E-04 | 0.000000E+00 | 0.722844 | 0.277156 |
| 723 | 1.974121E-03 | 7.570755E-04 | 0.000000E+00 | 0.722804 | 0.277196 |
| 724 | 1.833723E-03 | 7.033755E-04 | 0.000000E+00 | 0.722764 | 0.277236 |
| 725 | 1.703876E-03 | 6.537050E-04 | 0.000000E+00 | 0.722722 | 0.277278 |
| 726 | 1.583904E-03 | 6.078048E-04 | 0.000000E+00 | 0.722680 | 0.277320 |
| 727 | 1.472939E-03 | 5.653435E-04 | 0.000000E+00 | 0.722637 | 0.277363 |
| 728 | 1.370151E-03 | 5.260046E-04 | 0.000000E+00 | 0.722594 | 0.277406 |
| 729 | 1.274803E-03 | 4.895061E-04 | 0.000000E+00 | 0.722551 | 0.277449 |
| 730 | 1.186238E-03 | 4.555970E-04 | 0.000000E+00 | 0.722507 | 0.277493 |
| 731 | 1.103871E-03 | 4.240548E-04 | 0.000000E+00 | 0.722464 | 0.277536 |
| 732 | 1.027194E-03 | 3.946860E-04 | 0.000000E+00 | 0.722420 | 0.277580 |
| 733 | 9.557493E-04 | 3.673178E-04 | 0.000000E+00 | 0.722374 | 0.277626 |

| Wavelenght $\lambda$(nm) | CIE 2015 2° colour-matching functions | | | chromaticity coordinates | |
|---|---|---|---|---|---|
| | $\bar{x}(\lambda)$ | $\bar{y}(\lambda)$ | $\bar{z}(\lambda)$ | $x(\lambda)$ | $y(\lambda)$ |
| 734 | 8.891262E-04 | 3.417941E-04 | 0.000000E+00 | 0.722326 | 0.277674 |
| 735 | 8.269535E-04 | 3.179738E-04 | 0.000000E+00 | 0.722276 | 0.277724 |
| 736 | 7.689351E-04 | 2.957441E-04 | 0.000000E+00 | 0.722222 | 0.277778 |
| 737 | 7.149425E-04 | 2.750558E-04 | 0.000000E+00 | 0.722165 | 0.277835 |
| 738 | 6.648590E-04 | 2.558640E-04 | 0.000000E+00 | 0.722105 | 0.277895 |
| 739 | 6.185421E-04 | 2.381142E-04 | 0.000000E+00 | 0.722042 | 0.277958 |
| 740 | 5.758303E-04 | 2.217445E-04 | 0.000000E+00 | 0.721977 | 0.278023 |
| 741 | 5.365046E-04 | 2.066711E-04 | 0.000000E+00 | 0.721908 | 0.278092 |
| 742 | 5.001842E-04 | 1.927474E-04 | 0.000000E+00 | 0.721838 | 0.278162 |
| 743 | 4.665005E-04 | 1.798315E-04 | 0.000000E+00 | 0.721766 | 0.278234 |
| 744 | 4.351386E-04 | 1.678023E-04 | 0.000000E+00 | 0.721694 | 0.278306 |
| 745 | 4.058303E-04 | 1.565566E-04 | 0.000000E+00 | 0.721621 | 0.278379 |
| 746 | 3.783733E-04 | 1.460168E-04 | 0.000000E+00 | 0.721549 | 0.278451 |
| 747 | 3.526892E-04 | 1.361535E-04 | 0.000000E+00 | 0.721478 | 0.278522 |
| 748 | 3.287199E-04 | 1.269451E-04 | 0.000000E+00 | 0.721407 | 0.278593 |
| 749 | 3.063998E-04 | 1.183671E-04 | 0.000000E+00 | 0.721336 | 0.278664 |
| 750 | 2.856577E-04 | 1.103928E-04 | 0.000000E+00 | 0.721266 | 0.278734 |
| 751 | 2.664108E-04 | 1.029908E-04 | 0.000000E+00 | 0.721196 | 0.278804 |
| 752 | 2.485462E-04 | 9.611836E-05 | 0.000000E+00 | 0.721125 | 0.278875 |
| 753 | 2.319529E-04 | 8.973323E-05 | 0.000000E+00 | 0.721053 | 0.278947 |
| 754 | 2.165300E-04 | 8.379694E-05 | 0.000000E+00 | 0.720981 | 0.279019 |
| 755 | 2.021853E-04 | 7.827442E-05 | 0.000000E+00 | 0.720907 | 0.279093 |
| 756 | 1.888338E-04 | 7.313312E-05 | 0.000000E+00 | 0.720831 | 0.279169 |
| 757 | 1.763935E-04 | 6.834142E-05 | 0.000000E+00 | 0.720753 | 0.279247 |
| 758 | 1.647895E-04 | 6.387035E-05 | 0.000000E+00 | 0.720675 | 0.279325 |
| 759 | 1.539542E-04 | 5.969389E-05 | 0.000000E+00 | 0.720597 | 0.279403 |
| 760 | 1.438270E-04 | 5.578862E-05 | 0.000000E+00 | 0.720520 | 0.279480 |
| 761 | 1.343572E-04 | 5.213509E-05 | 0.000000E+00 | 0.720444 | 0.279556 |
| 762 | 1.255141E-04 | 4.872179E-05 | 0.000000E+00 | 0.720369 | 0.279631 |
| 763 | 1.172706E-04 | 4.553845E-05 | 0.000000E+00 | 0.720295 | 0.279705 |
| 764 | 1.095983E-04 | 4.257443E-05 | 0.000000E+00 | 0.720223 | 0.279777 |
| 765 | 1.024685E-04 | 3.981884E-05 | 0.000000E+00 | 0.720152 | 0.279848 |
| 766 | 9.584715E-05 | 3.725877E-05 | 0.000000E+00 | 0.720082 | 0.279918 |
| 767 | 8.968316E-05 | 3.487467E-05 | 0.000000E+00 | 0.720012 | 0.279988 |
| 768 | 8.392734E-05 | 3.264765E-05 | 0.000000E+00 | 0.719943 | 0.280057 |
| 769 | 7.853708E-05 | 3.056140E-05 | 0.000000E+00 | 0.719873 | 0.280127 |
| 770 | 7.347551E-05 | 2.860175E-05 | 0.000000E+00 | 0.719803 | 0.280197 |
| 771 | 6.871576E-05 | 2.675841E-05 | 0.000000E+00 | 0.719731 | 0.280269 |
| 772 | 6.425257E-05 | 2.502943E-05 | 0.000000E+00 | 0.719659 | 0.280341 |
| 773 | 6.008292E-05 | 2.341373E-05 | 0.000000E+00 | 0.719585 | 0.280415 |
| 774 | 5.620098E-05 | 2.190914E-05 | 0.000000E+00 | 0.719510 | 0.280490 |
| 775 | 5.259870E-05 | 2.051259E-05 | 0.000000E+00 | 0.719433 | 0.280567 |
| 776 | 4.926279E-05 | 1.921902E-05 | 0.000000E+00 | 0.719356 | 0.280644 |
| 777 | 4.616623E-05 | 1.801796E-05 | 0.000000E+00 | 0.719277 | 0.280723 |

| Wavelenght $\lambda$(nm) | CIE 2015 2° colour-matching functions | | | chromaticity coordinates | |
|---|---|---|---|---|---|
| | $\bar{x}(\lambda)$ | $\bar{y}(\lambda)$ | $\bar{z}(\lambda)$ | $x(\lambda)$ | $y(\lambda)$ |
| 778 | 4.328212E-05 | 1.689899E-05 | 0.000000E+00 | 0.719198 | 0.280802 |
| 779 | 4.058715E-05 | 1.585309E-05 | 0.000000E+00 | 0.719117 | 0.280883 |
| 780 | 3.806114E-05 | 1.487243E-05 | 0.000000E+00 | 0.719036 | 0.280964 |
| 781 | 3.568818E-05 | 1.395085E-05 | 0.000000E+00 | 0.718954 | 0.281046 |
| 782 | 3.346023E-05 | 1.308528E-05 | 0.000000E+00 | 0.718871 | 0.281129 |
| 783 | 3.137090E-05 | 1.227327E-05 | 0.000000E+00 | 0.718788 | 0.281212 |
| 784 | 2.941371E-05 | 1.151233E-05 | 0.000000E+00 | 0.718704 | 0.281296 |
| 785 | 2.758222E-05 | 1.080001E-05 | 0.000000E+00 | 0.718620 | 0.281380 |
| 786 | 2.586951E-05 | 1.013364E-05 | 0.000000E+00 | 0.718535 | 0.281465 |
| 787 | 2.426701E-05 | 9.509919E-06 | 0.000000E+00 | 0.718449 | 0.281551 |
| 788 | 2.276639E-05 | 8.925630E-06 | 0.000000E+00 | 0.718363 | 0.281637 |
| 789 | 2.136009E-05 | 8.377852E-06 | 0.000000E+00 | 0.718277 | 0.281723 |
| 790 | 2.004122E-05 | 7.863920E-06 | 0.000000E+00 | 0.718191 | 0.281809 |
| 791 | 1.880380E-05 | 7.381539E-06 | 0.000000E+00 | 0.718104 | 0.281896 |
| 792 | 1.764358E-05 | 6.929096E-06 | 0.000000E+00 | 0.718016 | 0.281984 |
| 793 | 1.655671E-05 | 6.505136E-06 | 0.000000E+00 | 0.717926 | 0.282074 |
| 794 | 1.553939E-05 | 6.108221E-06 | 0.000000E+00 | 0.717834 | 0.282166 |
| 795 | 1.458792E-05 | 5.736935E-06 | 0.000000E+00 | 0.717738 | 0.282262 |
| 796 | 1.369853E-05 | 5.389831E-06 | 0.000000E+00 | 0.717638 | 0.282362 |
| 797 | 1.286705E-05 | 5.065269E-06 | 0.000000E+00 | 0.717534 | 0.282466 |
| 798 | 1.208947E-05 | 4.761667E-06 | 0.000000E+00 | 0.717428 | 0.282572 |
| 799 | 1.136207E-05 | 4.477561E-06 | 0.000000E+00 | 0.717319 | 0.282681 |
| 800 | 1.068141E-05 | 4.211597E-06 | 0.000000E+00 | 0.717210 | 0.282790 |
| 801 | 1.004411E-05 | 3.962457E-06 | 0.000000E+00 | 0.717100 | 0.282900 |
| 802 | 9.446399E-06 | 3.728674E-06 | 0.000000E+00 | 0.716990 | 0.283010 |
| 803 | 8.884754E-06 | 3.508881E-06 | 0.000000E+00 | 0.716880 | 0.283120 |
| 804 | 8.356050E-06 | 3.301868E-06 | 0.000000E+00 | 0.716770 | 0.283230 |
| 805 | 7.857521E-06 | 3.106561E-06 | 0.000000E+00 | 0.716660 | 0.283340 |
| 806 | 7.386996E-06 | 2.922119E-06 | 0.000000E+00 | 0.716550 | 0.283450 |
| 807 | 6.943576E-06 | 2.748208E-06 | 0.000000E+00 | 0.716439 | 0.283561 |
| 808 | 6.526548E-06 | 2.584560E-06 | 0.000000E+00 | 0.716329 | 0.283671 |
| 809 | 6.135087E-06 | 2.430867E-06 | 0.000000E+00 | 0.716218 | 0.283782 |
| 810 | 5.768284E-06 | 2.286786E-06 | 0.000000E+00 | 0.716106 | 0.283894 |
| 811 | 5.425069E-06 | 2.151905E-06 | 0.000000E+00 | 0.715994 | 0.284006 |
| 812 | 5.103974E-06 | 2.025656E-06 | 0.000000E+00 | 0.715882 | 0.284118 |
| 813 | 4.803525E-06 | 1.907464E-06 | 0.000000E+00 | 0.715770 | 0.284230 |
| 814 | 4.522350E-06 | 1.796794E-06 | 0.000000E+00 | 0.715659 | 0.284341 |
| 815 | 4.259166E-06 | 1.693147E-06 | 0.000000E+00 | 0.715548 | 0.284452 |
| 816 | 4.012715E-06 | 1.596032E-06 | 0.000000E+00 | 0.715439 | 0.284561 |
| 817 | 3.781597E-06 | 1.504903E-06 | 0.000000E+00 | 0.715331 | 0.284669 |
| 818 | 3.564496E-06 | 1.419245E-06 | 0.000000E+00 | 0.715225 | 0.284775 |
| 819 | 3.360236E-06 | 1.338600E-06 | 0.000000E+00 | 0.715121 | 0.284879 |
| 820 | 3.167765E-06 | 1.262556E-06 | 0.000000E+00 | 0.715019 | 0.284981 |
| 821 | 2.986206E-06 | 1.190771E-06 | 0.000000E+00 | 0.714920 | 0.285080 |

| **Wavelenght** $\lambda(\mathrm{nm})$ | **CIE 2015 2° colour-matching functions** | | | **chromaticity coordinates** | |
|---|---|---|---|---|---|
| | $\bar{x}(\lambda)$ | $\bar{y}(\lambda)$ | $\bar{z}(\lambda)$ | $x(\lambda)$ | $y(\lambda)$ |
| 822 | 2.814999E-06 | 1.123031E-06 | 0.000000E+00 | 0.714824 | 0.285176 |
| 823 | 2.653663E-06 | 1.059151E-06 | 0.000000E+00 | 0.714731 | 0.285269 |
| 824 | 2.501725E-06 | 9.989507E-07 | 0.000000E+00 | 0.714641 | 0.285359 |
| 825 | 2.358723E-06 | 9.422514E-07 | 0.000000E+00 | 0.714554 | 0.285446 |
| 826 | 2.224206E-06 | 8.888804E-07 | 0.000000E+00 | 0.714470 | 0.285530 |
| 827 | 2.097737E-06 | 8.386690E-07 | 0.000000E+00 | 0.714389 | 0.285611 |
| 828 | 1.978894E-06 | 7.914539E-07 | 0.000000E+00 | 0.714312 | 0.285688 |
| 829 | 1.867268E-06 | 7.470770E-07 | 0.000000E+00 | 0.714239 | 0.285761 |
| 830 | 1.762465E-06 | 7.053860E-07 | 0.000000E+00 | 0.714170 | 0.285830 |

*Table 22: CIE 1931 standard observer properties.*

## *Declaration of Authenticity*

## Eigenständigkeitserklärung

Hiermit versichere ich, dass ich die vorliegende Bachelorarbeit mit dem Titel:

**Redefinition of current display colour spaces**
**based on CIE 2015 colour-matching functions**

selbständig und nur mit den angegebenen Hilfsmitteln verfasst habe. Alle Passagen, die ich wörtlich aus der Literatur oder aus anderen Quellen wie z. B. Internetseiten übernommen habe, habe ich deutlich als Zitat mit Angabe der Quelle kenntlich gemacht.

Hamburg, Februar 2026 Johannes Grieb